This is to certify that the

dissertation entitled

SYNTHESIS AND CHARACTERIZATION
OF SUBSTITUTED POLYLACTIDES

presented by

MAO YIN

has been accepted towards fulfillment
of the requirements for

DOCTOR degree in PHILOSOPHY

Major professor

Date 13 June 2000

SYNTHESIS AND CHARACTERIZATION OF SUBSTITUTED POLYLACTIDES

By

Mao Yin

A DISSERTATION

Submitted to
Michigan State University
in partial fulfillment of the requirements
for the degree of

DOCTOR OF PHILOSOPHY

Department of Chemistry

2000

ABSTRACT

SYNTHESIS AND CHARACTERIZATION OF SUBSTITUTED POLYLACTIDES

By

Mao Yin

Because of their biocompatibility and environmental degradability, polymers derived from lactic acid have long been important materials for medical applications. Once used primarily as sutures and implants, polylactide materials are now entering high volume areas such as packaging. To be successful in these new applications, polylactides must be available that exhibit a broad spectrum of physical properties while retaining the degradability of the parent polymers. This objective can be achieved by altering the substituents on the polylactide chains.

A variety of substituted lactides were synthesized and polymerized to high molecular weight polymers using solution and bulk polymerization. The polymers show a wide range of physical properties: glass transition temperatures range from –37 °C to 85 °C, hydrolytic degradation rates are 2-3 times slower than polylactide's, and degradation temperatures are around 350 °C. We established the relationship between the pendant group and the physical properties of the polymers.

The kinetics and mechanism of lactide polymerization was studied. Lactide polymerizations are first-order reactions in both solution and bulk

polymeriza

size of s

polymeriz

follow the

different

lactide p

when in

molecula

W

polymer

racemic

monom

optical

The a

groups

substi

synthe

polymerization. In bulk polymerization, polymerization rates follow the order of size of substituted group, the bigger the substituted group, the slower the polymerization rate. In solution polymerizations, the polymerization rates do not follow the order of size of substituted group, which is probably caused by different rate-determining steps for the polymerizations. We proposed that lactide polymerization mechanism is similar to "atom-transfer polymerization" when initiated by $Sn(Oct)_2$. Using it as guide, we achieved control of the molecular weights and molecular weight distributions of the polymers.

We studied the influence of stereochemistry on the kinetics of polymerizations and the physical properties of the polymers. We found that racemic monomers polymerize faster than either of the optically pure monomers. The racemic polymers are usually amorphous polymers and optically pure polymers are usually crystalline polymers.

Copolymerization of lactide with substituted lactides were investigated. The architectures of polymers depend on the size difference of substituted groups between the lactide and substituted lactide. By controlling the size of substituted group, random, block and alternating copolymers can be synthesized.

To my wife Tianle

ACKNOWLEDGEMENTS

I wish to express my deep appreciation to Professor Gregory L. Baker for his guidance, assistance and constant encouragement throughout the course of this research. A work such as this would not be possible without his assistance. It has been my privilege to have him as my mentor.

I would also like to thank professor James Jackson, Milton Smith, Gary Blanchard, and Thomas Pinnavaia for their guidance and assistance. My thanks go to all Baker group members: Jun Qiao, Jun Hou, Jingpin, Yiyan, Gao, Corey, Susan, Tara, Tianqi, J, B,, Kirk, Fadi and all the friends in Michigan State University, for making my stay an enjoyable one

Finally, I want to thank my wife Tianle for her love and sacrifices. I thank my parents and sister for their love and encouragement.

TABLE OF CONTENTS

3.2

4 M

4.1

4.2

4.3

5 D

5.1.

5.2.

RESUL

1. M

2 E

2.1

2.2

3. S

3.1

3.2

3.3

Poly

3.4.

3.4

3.4

3.5.

Poly

LIST OF TABLES

LIST OF FIGURES

Figure 4

Figure 4

Figure

Figure

Figure

Figure

Figure

Figure

Figure

Figure

Figure

Figure

Figure

Figure

Figure

Figure

LIST OF SCHEMES

Scheme 1

Scheme 2

Scheme 2

Scheme

Scheme

Scheme

Scheme

Scheme

Scheme

Scheme

Scheme

Scheme

Scheme

Scheme

Scheme

Scheme

Scheme

1. Applic

1.1 Medic

Bec

polyglycol

in Figure

repair ar

applicatio

surgical c

The biore

and futur

the polyg

by Davis

copolym

Th

develope

A porou

FDA fo

membra

compar

nonbioc

INTRODUCTION

1. Applications

1.1 Medical application

Because of their biodegradability and biocompatibility, polylactide, polyglycolide and polylactones (monomer and polymer structures are displayed in **Figure 1**) have been used in medical applications for wound closure,[1] tissue repair and regeneration,[2-4] and drug delivery.[5-7] The most successful application has been wound closure, where biodegradable surgical sutures and surgical clips have been made using polylactide, polyglycolide and polylactones. The bioresorption of sutures eliminates the possibility of foreign-body reactions and future infection. Some commercially available biodegradable sutures such as the polyglyconate sutures (glycolide/trimethylene carbonate copolymer) marketed by Davis & Geck as Maxon and polyglecaprone 25 (glycolide/caprolactone copolymer) have been used successfully in clinics.

Tissue repair and regeneration and drug delivery applications are less developed than wound closure, but there has been exciting progress in the field. A porous biodegradable membrane made from DL-PLA was approved by the FDA for periodontal use. Clinical results show that the new biodegradable membrane, marketed in the U. S. as Guidor by the Butler Company, gives comparable if not better periodontal tissue regeneration than the nonbiodegradable Gore-Tex products made from poly(tetrafluoroethylene). Many

degradable products have been developed to deliver a variety of drugs, such as anti-cancer agents, narcotic antagonists, antibiotics, fertility drugs and vaccines. Some products have been marketed such as Lupron Depot, an injectable microcapsule system marketed by Takeda-Abbot using a 70:30 DL-lactide/glycolide copolymer to deliver leuprorelin (anti-cancer drug). However, the majority of products are still in the evaluation stage and more research needs to be done.

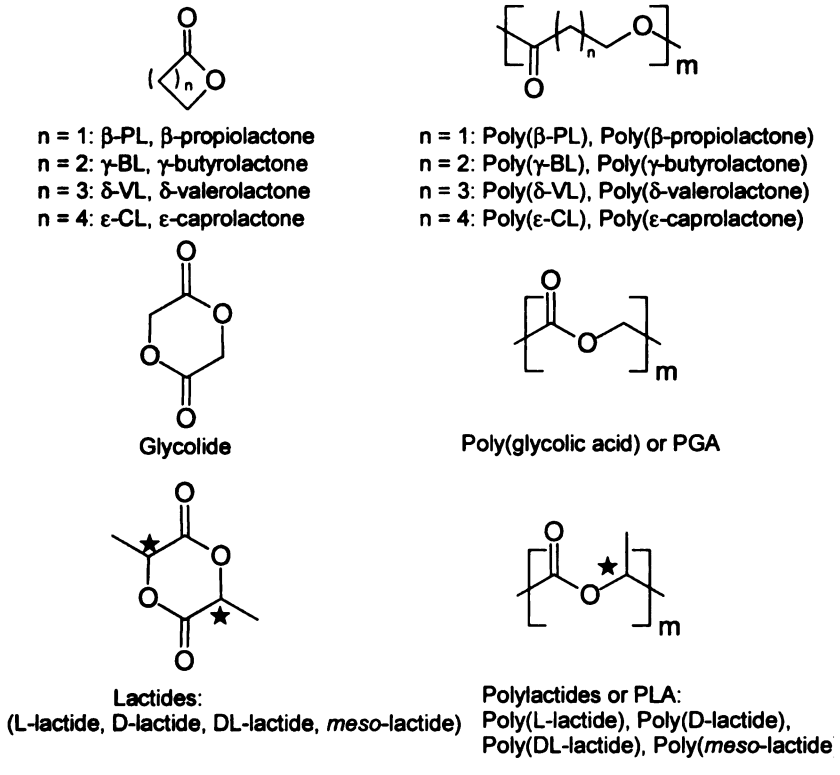

Figure 1. Structures and abbreviations of monomers and degradable polymers

1.2 Bio

T

an answ

U S p

plastics

become

life Mo

mamm

concer

will ha

compri

waste

time

therm

100 p

sever

after

soil o

water

mate

Packa

1.2 Biodegradable Packaging Thermoplastics

There is a need for an environmentally benign packaging thermoplastic as an answer to the tremendous amounts of discarded plastic packaging materials. U. S. plastic sales in 1997 were 74.0 billion pounds of which 29% were listed as plastics in packaging.[8] A significant amount of this plastic is discarded and becomes a plastic pollutant that is a blot on the landscape and a threat to marine life. Mortality estimates range as high as 1-2 million seabirds and 100,000 marine mammals per year. A further problem with disposal plastic packaging is the concern for dwindling landfill space. It has been estimated that most major cities will have used up available landfills for solid waste disposal very soon. Plastics comprise approximately 3 percent by weight and 6 percent of the volume of solid waste.[9]

The polymers and copolymers of lactic acid have been known for some time as unique materials since they are biodegradable, biocompatible and thermoplastic. These polymers are well-behaved thermoplastics,[10,11] and are 100 percent biodegradable in an animal body via hydrolysis over a time period of several months to a year. In a wet environment they begin to show degradation after several weeks and disappear in about a year's time when left on or in the soil or seawater. The degradation products are lactic acid, carbon dioxide and water, all of which are harmless.

Conventional plastics have good reasons for their success as packaging materials. They provide appealing aesthetic qualities in the form of attractive packages, which can be quickly fabricated and filled, with specified units of

products

desirable

polymers

better p

copolym

are very

selected

contain

is very

temper

poly(la

some a

plastici

reactor

compo

well a

provid

for var

and po

a rang

products. The packages maintain cleanliness, good mechanical properties and desirable qualities such as transparency for inspection of contents. If lactic acid polymers are to compete with conventional plastics, they should have similar or better properties.[12] **Table 1** comparies the properties of unplasticized 90/10 copolymer of L and DL-lactide and polystyrene. Unplasticized poly(lactic acid)s are very stiff with tensile properties similar to PS. The 90/10 copolymer is selected because of property and processing advantages. Poly(lactic acid)s containing 98 to 100% of the L-lactic acid have very high crystallinity. Fabrication is very difficult because of crazing, and need for processing at very high temperatures causes discoloration and loss of molecular weight.

By using monomer, lactide, or lactide oligmer as plasticizers, flexible poly(lactic acid)s can be made. Using monomer and oligmer as plasticizers has some advantages. First, they are perfectly safe. Second, their incorporation as plasticizers during polymerization allows shorter cycle times in the polymerization reactor, lowers the melt viscosity during reactor handling and during compounding, thereby easing melt processing and preventing discoloration as well as maintaining molecular weight. The plasticization of poly(lactic acid)s provides a systematic attenuation of properties and a broad rang of compounds for various application. The basic tensile physical properties of a poly(lactic acid) and polyethylene are compared in **Table 2**. Both materials can be fine toned over a range of values for specific packaging applications.

Tabl

P
Ultim
De
[a] 90

Table 1. Some Basic Physical Properties Comparisons of Poly(lactic acid) and Polystyrene

Physical properties	Poly(lactic acid) [a]		Polystyrene [b]	
	Oriented	Unoriented	Oriented	Unoriented
Ultimate Tensile Strength[c]				
psi	14,700	6,900	7,400	7,015
MPa	101	48	51	48
Elastic Modulus	564,000	221,000	450,000	240,000
psi	3,889	1,524	3,103	1,655
MPa	15.4	5.8	4.0	-
Impact Strength				
Ft-lb/in	-	0.44	0.4	0.24
MN/m	-	23	21	13
Deflection temperature				
°F	181	127	200	-
°C	83	53	93	-
Specific Gravity	1.25	1.25	1.05	1.05
Melt Flow Rate				
200°C	-	46	-	3.5
155°C	-	2	-	-

[a] 90/10 L-lactide/DL-lactide copolymer. [b] Crystal PS, Amoco R3. [c] ASTM D882

Table 2. Comparison of Polyethylene to Poly(lactic acid)

Properties	Low density polyethylene	Poly(lactic acid) [a]
Tensile Strength:		
Kpsi	2.18	3.19
MPa	15	22
Elongation, %	261	280
Tangent modulus		
Kpsi	54.9	36.6
MPa	379	252
100% modulus:		
kpsi	1.77	0.74
MPa	12	5
200% modulus		
kpsi	1.82	1.2
MPa	13	8
HDT		
264 psi, °F	95	122
1.82 Mpa, °C	35	50

[a] L-Lactide plasticizer equals 19.5 wt%

for larg

solvent

these f

$1.00 "

the cos

are lim

polyme

process

biodegr

biodegr

costs t

legislati

biodegr

develop

polymer

2. Syn

P

polycond

hydroxy

without

The poly(lactic acid)s have some deficiencies that inhibit their acceptance for large-scale applications.[13,14] These deficiencies include high price, poor solvent resistance, insufficient physical properties, and various combinations of these factors. The selling prices of lactic acid polymers have been estimated at $1.00/lb. Compared to $0.30-0.60 for polystyrene, poly(lactic acid)s are 2-3 times the cost of the conventional plastics. The major deficiencies of poly(lactic acid)s are limited physical properties. The technological development of biodegradable polymers is restricted presently by the range of these polymers that can fulfill processing and property requirements for many applications in which biodegradability would be an important materials property. Acceptance of biodegradable polymers will depend on five unknowns: (1) customer response to costs that are considerably higher than conventional polymers; (2) possible legislation (particularly water-soluble polymers); (3) the achievement of total biodegradability; (4) wider range of available physical properties; and (5) the development of an infrastructure to collect, accept, and process biodegradable polymers as a generally available option for waste disposal.

2. Synthesis of Biodegradable Polyesters

Polyesters such as poly(lactic acid) can be synthesized by polycondensation from the hydroxy acid (**Scheme 1**). The polycondensation of hydroxy acids is generally performed by removal of water by distillation, with or without catalyst, and application of vacuum as the temperature is progressively

increase

weight (

molecula

polyconc

using

distanno

ether cat

have not

A

opening

low mole

ring-oper

This is th

of this me

Inc. using

Ri

of these

much fas

monomer

high temp

concentra

the system

increased.[6,15] This rather simple step leads to oligomers with low molecular weight (<5,000 Daltons, M_w/M_n close to 2). There have been reports that high molecular weight poly(lactic acids) have been synthesized using polycondensation. The methods include postcondensation in organic solvents using dicyclohexylcarbodiimide (DCC),[16] condensation catalyzed by distannoxane,[17] and refluxing in high boiling point solvents such as diphenyl ether catalyzed by various metals and protonic acids.[18] However, these methods have not been developed industrially.

A better way to make high molecular weight polyesters is through ring-opening polymerization. As shown in **Scheme 1**, lactic acid was condensed to low molecular weight oligomers, the oligomer was cracked to the lactide, and ring-opening polymerization of lactide produced high molecular weight polymers. This is the method used to make poly(lactic acid) commercially.[19] The drawback of this method is its high cost, which has been reduced tremendously by Cargill, Inc. using continuous processes to manufacture poly(lactic acid)s.[20]

Ring-opening polymerization can be carried out in bulk or in solution. Both of these methods have advantages and disadvantages. Bulk polymerization is much faster than solution polymerization because of the higher concentration of monomers and higher reaction temperature. High monomer concentration and high temperature also cause some problems. Because of high monomer concentration, a bulk polymerization system has a high viscosity, which makes the system difficult to stir. Because of concerns about viscosity and melting point

of the

causes

solution

solution

problem

very lo

provide

distribu

such a

amoun

an indu

of their

to mak

of the monomers, bulk polymerizations are conducted around 200 °C, which causes some side reactions such as transesterification and discoloration. In solution polymerization, the monomers are dissolved in organic solvents, so solution polymerizations do not have the same viscosity and melting point problems as bulk polymerizations. Solution polymerizations can be conducted at very low temperature. Compared to bulk polymerization, solution polymerizations provide much better control over molecular weight and molecular weight distribution. However, solution polymerization uses large amounts of solvent such as toluene. Not only the solvents are expensive, but also dealing with large amounts of waste solvent is an environmental problem and costs money. From an industrial point of view, solution polymerizations are not economical because of their slow rates and the high cost of solvents. Thus, most industrial processes to make poly(lactic acid) use bulk polymerization.

Scheme 1. Synthetic route for poly(lactic acid)

Polycondensation:

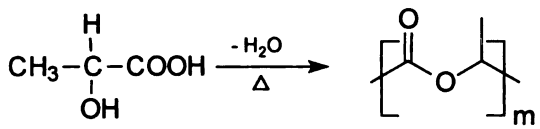

Ring-opening Polymerization

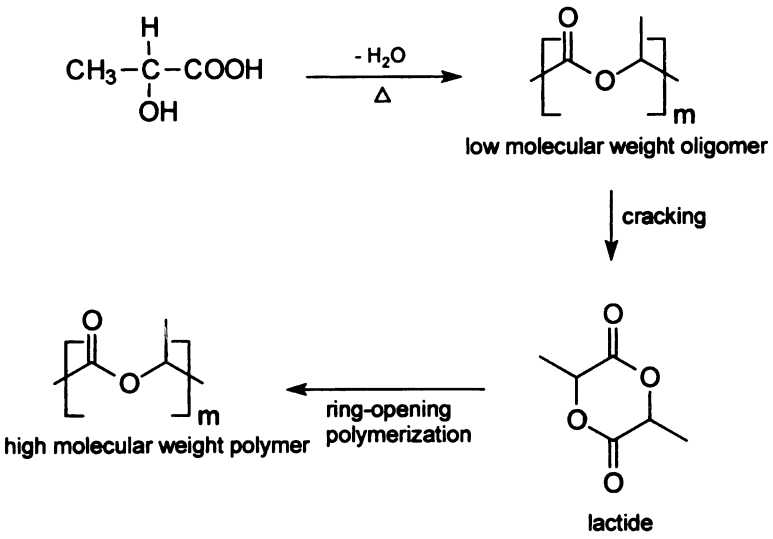

3. R

3.1 R

mus

have

lacti

mon

thes

resu

poly

For

JG

poly

exa

for p

not

com

with

of th

for 3

incre

3. Ring-opening polymerization of lactides and lactones

3.1 Polymerizability

For the ring-opening polymerization of lactides and lactones, one question must first be answered: are the monomers polymerizable or not? Many attempts have been made to correlate the ring-opening polymerizability of lactones and lactides with some basic parameter, such as ring strain, hydrolysis rate, or monomer basicity. No acceptable clear correlation has been found to date, but these attempts provide some insight into the polymerization process, and as a result some generalizations can be made.

Whether a cyclic monomer can be polymerized to high molecular weight polymer depends on thermodynamic and kinetic factors of the polymerization. For a cyclic monomer to be polymerizable, the free energy of the polymerization ΔG must be negative under the conditions used. The effect of ring size on ΔG of polymerization can be readily illustrated by the use of the cycloalkanes as an example. The substitution of a heteroatom for CH_2 does not significantly alter ΔG for polymerization as shown for various cycloalkanes, provided the heteroatom is not too dissimilar in size and bond angle, such as for O or N.[21] **Table 3** [22] compares the heats of combustion per methylene group in these ring compounds with that of a methylene in an open chain alkane. This yields a general measure of the thermodynamic stabilities of rings of different sizes. The strain is very high for 3- and 4- membered rings, decreases sharply for 5-, 6-, 7- membered rings, increases for 8- to 11- membered rings, and then decreases again for larger

rings. Of course, while the presence of strain in a ring compound does not necessarily make it polymerizable, within a given class, the higher the strain, the more exothermic the polymerization, the more likely it is to be polymerizable. The thermodynamic feasibility does not guarantee the actual polymerization of lactones. Polymerization requires that there be a kinetic pathway for the ring to open and undergo reaction at a reasonable rate. **Table 4** lists the experimental results for the polymerizability of a large number of lactones. It shows that none of the 5-membered lactones investigated polymerized, and that substitution rendered some of the 6-membered lactones unpolymerizable; however, nearly all of the 4-, 7-, and 8-, membered lactones were polymerizable.

Hall and coworkers[23] investigated the postulate of Carothers that hydrolysis rate and polymerization tendencies should correspond with each other.[24] However, they found this suggestion not to be generally valid for alkaline hydrolysis because β-propiolactone and γ-butyrolactone hydrolyzed at comparable rates, while the former polymerized and the latter did not. The attempt to relate polymerizability of lactones with basicities of lactones by Lundberg and Cox[25] also did not produce satisfactory results.

Table 3. Heats of combustion and Strains of Cycloalkanes per Methylene group

n-member cycloalkanes	Heat of combustion per methylene group (KJ/mole)	Strain per methylene group (KJ/mole)
3	697.6	38.6
4	686.7	27.7
5	664.5	5.5
6	659.0	0.0
7	662.8	3.8
8	664.1	5.1
9	664.9	5.9
10	664.1	5.1
11	663.2	4.2
12	660.3	1.3
13	660.7	1.7
14	659.0	0.0
15	659.5	0.5
16	659.5	0.5

Table 4. Polymerizability of cyclic ester monomers

Compound	Ring size	Polymerizability
β-propiolactone	4	+
β-butyrolactone	4	+
γ-butyrolactone	5	-
γ-valerolactone	5	-
δ-valerolactone	6	+
glycolide	6	+
lactide	6	+
α-*n*-propyl-δ-valerolactone	6	-
tetramethylglycolide	6	-
ε-caprolactone	7	+
3-oxa-ε-caprolactone	7	+
cis-disalicylide	8	+
di-*o*-cresotide	8	+
trisalicylide	12	+

+ represents polymerizable, - represents unpolymerizable.

3.2 Po

3.2.1

3.2.1.

lacton

RSO$_2$

(stabi

(e.g.

precu

phosp

into t

menti

react

The

acce

oxyg

form

anal

3),

3.2 Polymerization Mechanism

3.2.1 Cationic Polymerization

3.2.1.1 Lactones

The main cationic initiators used in ring-opening polymerization (ROP) of lactones can be divided into four subgroups: (a) protonic acids (HCl, RCOOH, RSO_3H, etc.), (b) Lewis acids ($AlCl_3$, BF_3, $FeCl_3$, etc.), (c) alkylating agents (stabilized carbocations, e.g. $CF_3SO_3CH_3$, Et_3OBF_4), and (d) acylating agents (e.g. CH_3COOCl_3).[26] In addition to these traditional acids and electrophiles, precursors of carbocations have also been considered, e.g., ammonium or phosphonium salts stabilized by complex counterions,[27] which are transformed into the active species by thermal or photochemical processes. It is also worth mentioning diaryliodonium salts, which release an active cationic species upon reaction with a reducing agent.[28]

Many mechanisms have been proposed for the different cationic initiators. The polymerization mechanism proposed by Cherdron *et al.*[29] (**Scheme 2**) was accepted for a long time. It consists of an electrophilic attack on the endocyclic oxygen of the lactone and the subsequent rupture of the acyl-oxygen bond with formation of an acyl carbonium ion prone to propagate.

Penczek *et al.* questioned Cherdron`s mechanism. From chain-end analyses and kinetics data, they proposed another mechanism[30,31] (**Scheme 3**), in which the electrophilic attack was on the exocyclic oxygen of lactone.

Kricheldorf *et al.*[32] and Okamoto[33] also proposed mechanisms for cationic polymerization, which are very similar to what Penczek has proposed.

Scheme 2 Cherdron`s cationic polymerization mechanism

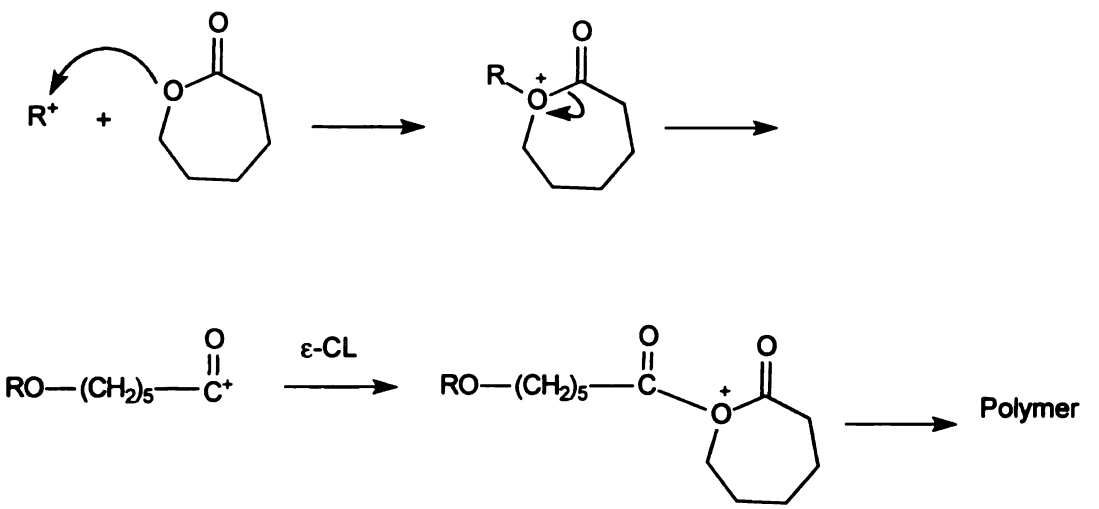

3.2.1.2. Lactides

The secondary carbon atom in lactide is less sensitive to nucleophilic attack compared to the primary carbon atom in lactones. At present, only triflic acid and methyl triflate initiate controlled cationic lactide polymerizations; HBr and HCl also initiate cationic lactide polymerizations, but yield low molecular weight polymers. There also are reports where Sn(II) and Sn(IV) halogenides were used to polymerize lactides, but it is believed that the actual initiating species are HBr and HCl, which are generated by Sn(II) and Sn(IV) halogenides reacting with hydroxyl-containing impurities.

Scheme 3. The cationic polymerization mechanism proposed by Penczek.

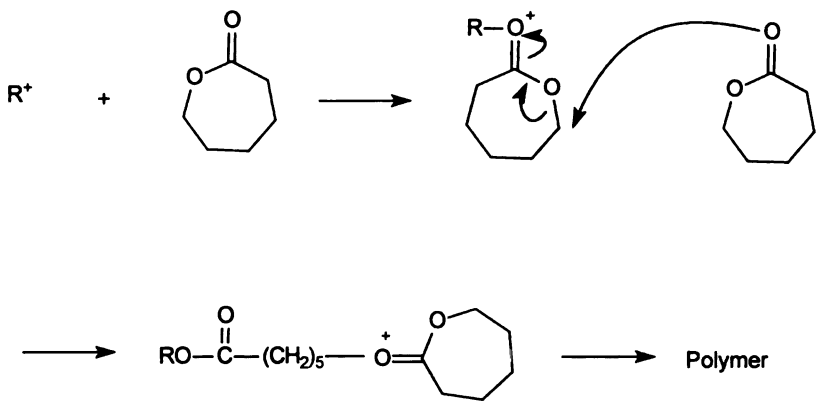

A mechanism proposed by Kohn[34] for the initiation and polymerization of lactide with strong acids such as HBr and HCl is depicted in **Scheme 4**. Protonation at one of the two available carbonyl oxygens on lactide is followed by a proton shift and an S_N2-type transesterification reaction. In my opinion, this mechanism has flaws. The exocyclic oxygen is more nucleophilic than the endocyclic oxygen, so it is more reasonable that it should the exocyclic oxygen that attacks the carbonyl group, and not the endocyclic oxygen.

Methyl triflate gives very interesting results in lactide polymerization. Kricheldorf found that the polymerization of L-lactide gave polylactide that was 100% optically pure. If the polymerization proceeded with complete Walden inversion like traditional cationic polymerizations (**Scheme 5**), the resulting polymer must contain 50% D- and 50% L- units. The polymers should not be

Scheme 4. Cationic polymerization of lactide initiated by protonic acids

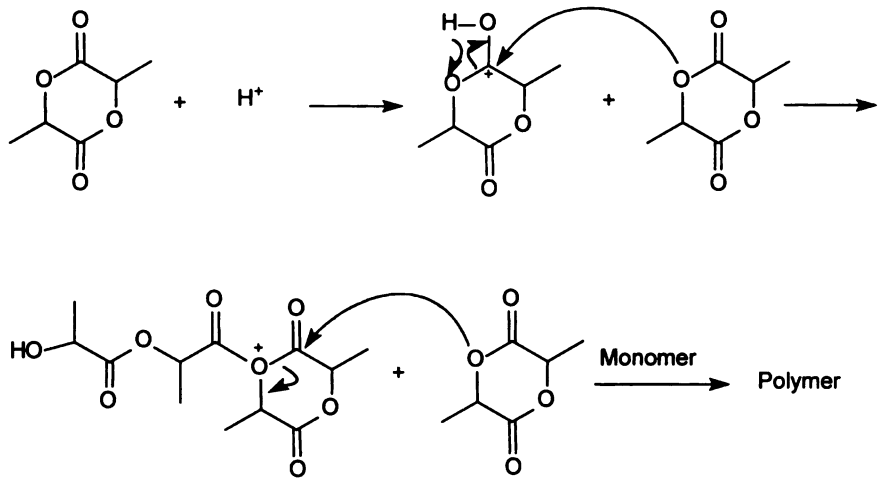

optically active. Kricheldorf proposed a different mechanism[35] (**Scheme 6**) for the methyl triflate initiated polymerization. The initially formed positively charged lactide ring is opened by an S_N2 attack of triflate anion accompanied by Walden inversion. The triflate ester end-group reacts with another lactide again in an S_N2 fashion, so that a second Walden inversion occurs. The net result is perfect retention of the original configuration.

Scheme 5. Polymerization of lactide initiated by methyl triflate (traditional cationic mechanism)

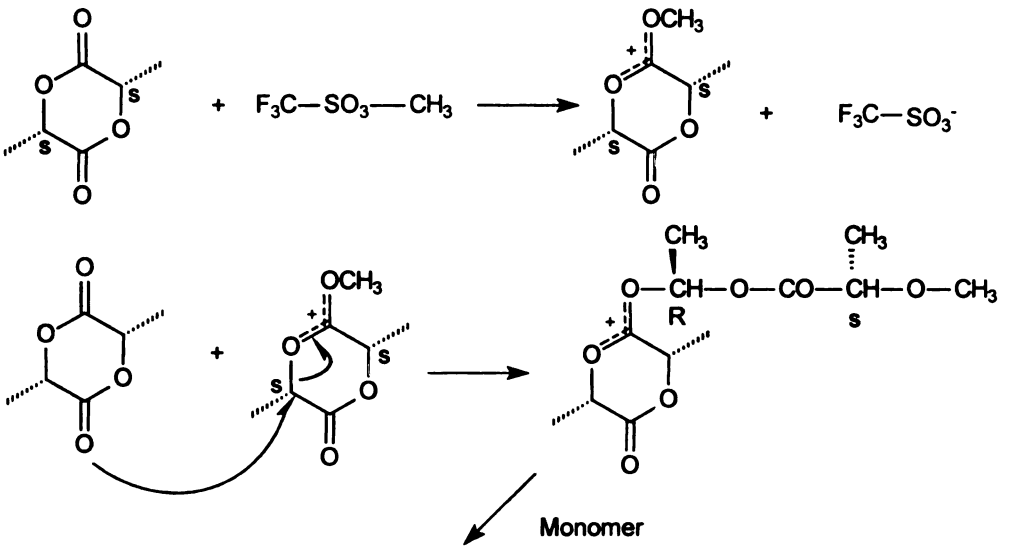

Scheme 6. Polymerization of lactide initiated by methyl triflate

(mechanism proposed by Kricheldorf)

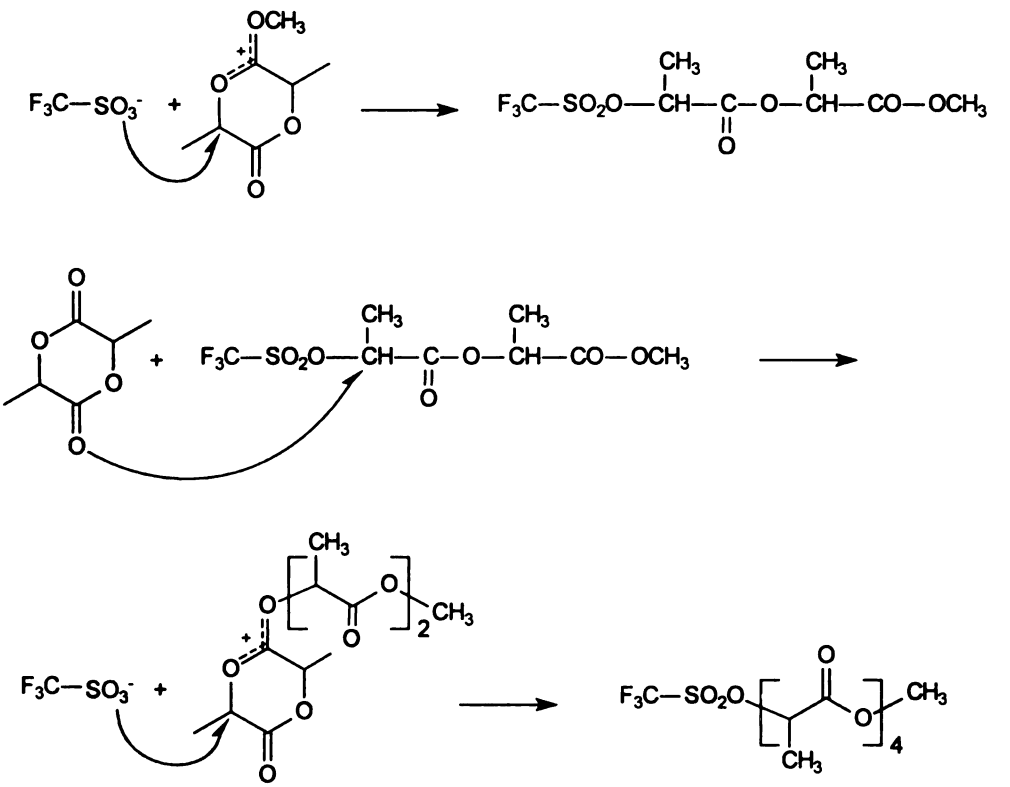

3.2.2 Anionic Polymerization

3.2.2.1 Lactones

Many kinds of anionic initiators have been used in the ring-opening polymerization of lactones. The most commonly used initiators are alkali metal alkoxides, such as potassium methoxide, and potassium butoxide. To improve the solubility and efficiency of the alkali alkoxides, mixtures of alkali alkoxides and crown ethers have been used as initiators. In addition to alkali alkoxides,[36-38] metal carboxylates,[36] alkali metals, and cyclopentadienyl sodium[39] also have been considered as initiators.

The mechanism of anionic polymerization of lactones depends on the ring size and substituents. There are two possible propagation routes in the anionic polymerization of lactones (**Scheme 7**): (A) propagation with alkyl-oxygen bond scission, resulting in an active carboxylate center or (B) propagation with acyl-oxygen bond scission leading to an active alcoholate cente.

ε-Caprolactone (ε-CL) polymerization is initiated exclusively by alcoholates. In the case of β-propiolactone (β-PL), the situation is much more complicated. According to Penzek *et. al.*, β-PL can be initiated by alcoholates or carboxylates. When β-PL is initiated by carboxylate, the carboxylate ion is the only initiation species. When initiated by alcoholate ion, both carboxylate and alcoholate ions were produced. The two ions coexist during the initial period of polymerization. The carboxylate ions reproduce themselves every propagation step, but 50% of the alcoholate ions were changed to carboxylate ions at every

propagation step. After several steps, almost all the alcoholate ion vanished (**Scheme 8**).

Scheme 7. Propagation routes for anionic polymerization of lactones

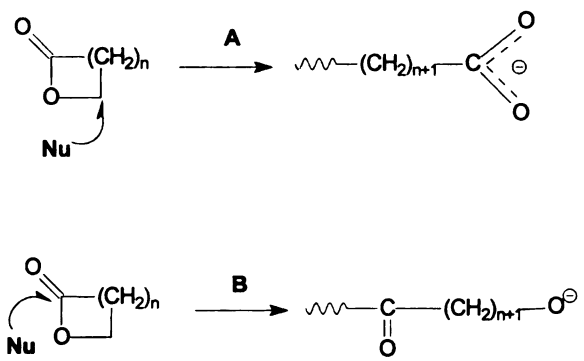

Scheme 8. Polymerization mechanism of β-PL.

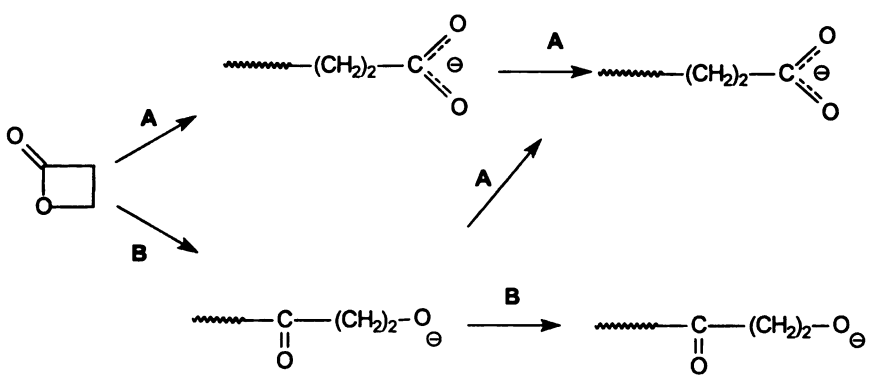

Alcoholate anions are much stronger nucleophiles than carboxylate anions. ε-CL (ΔH_p = -13.9 KJ/mol) is less strained than β-PL (ΔH_p = -82.3 KJ/mol), so carboxylate anions only initiate polymerization of β-PL and can not initiate polymerization of ε-CL. The alcoholate anions are stronger and smaller sized nucleophiles. Thus they initiate polymerization of both ε-CL and β-PL, but are less discriminating. They attack at the carbonyl carbon and the carbon next to the endo-oxygen on the ring and thus both alcoholate and carboxylate ions exist during the polymerization of β-PL.

Penczek's mechanism[37] seems to explain the experimental data well, but Jedlinski[38,40] gave a different account about how the polymerization of β-PL proceeds. During the polymerization of β-PL, Jedlinski found unsaturated double bonds as the end groups and no traces of the initiator in the resulting polymers. This finding was supported by data from Dale and Kricheldorf[41]. From his data, Jedlinski proposed the mechanism shown in **Scheme 9**.

The results above are very confusing. Both authors used the same initiator system, potassium methoxide to polymerize β-PL, but their results were totally different. The only difference in the experimental protocol was the solvent. Penczek used DMF and Jedlinski used THF. Maybe the polarity of solvents can explain the difference in the initiation of polymerization.

Scheme 9. The polymerization mechanism of PL proposed by Jedlinski

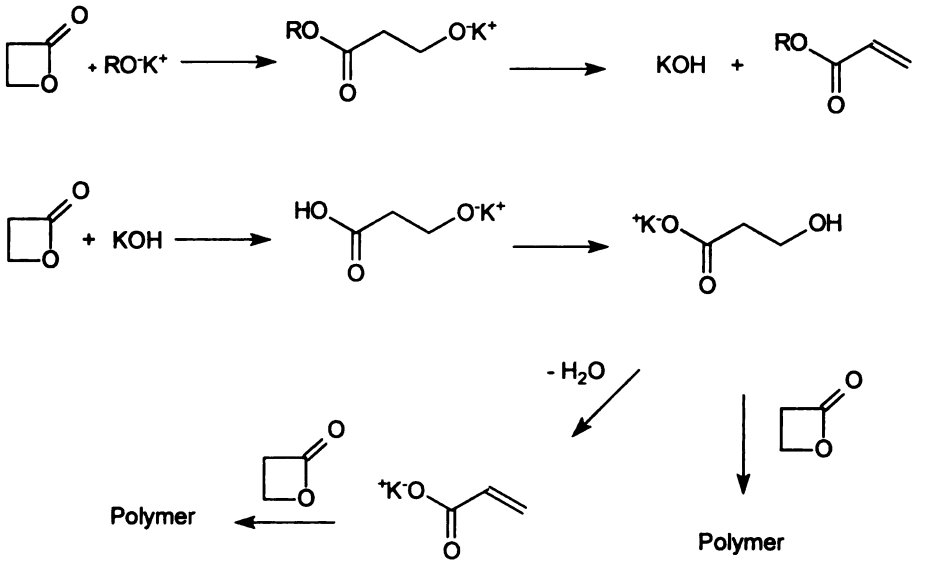

3.2.2.2 Lactide

The mechanism of anionic polymerization of lactide is very complex. The polymerization conditions, such as structures of initiators, counterion, temperature, and solvent, have a large influence on the mechanism of polymerization.

Krichedorf and Krieser-Saunders[42] found that only strong bases such as potassium *tert*-butoxide (pK_a = 18) and butyllithium polymerize lactide and weak bases such as the benzoate ion (pK_a = 5.7), and phenoxide ion (pK_a = 9.5) were not able to initiate polymerization. In addition, polymer was racemized regardless

of the initiator, temperature and solvent. They also were unable to find the initiator fragment in the isolated polymer chain. From these facts, they proposed that initiation mainly involves deprotonation of lactide (**Scheme 10**).

Jedlinski *et al.*[43] used potassium methoxide to initiate the polymerization of lactide. They found the initiator fragment in the polylactide and very little racemization. Thus, they proposed a different mechanism (**Scheme 11**). The methoxide anion attacks the carbonyl carbon in the monomer, with acyl-oxygen bond scission and formation of the methyl ester end group and the active

Scheme 10. Anionic polymerization of lactide through deprotonation

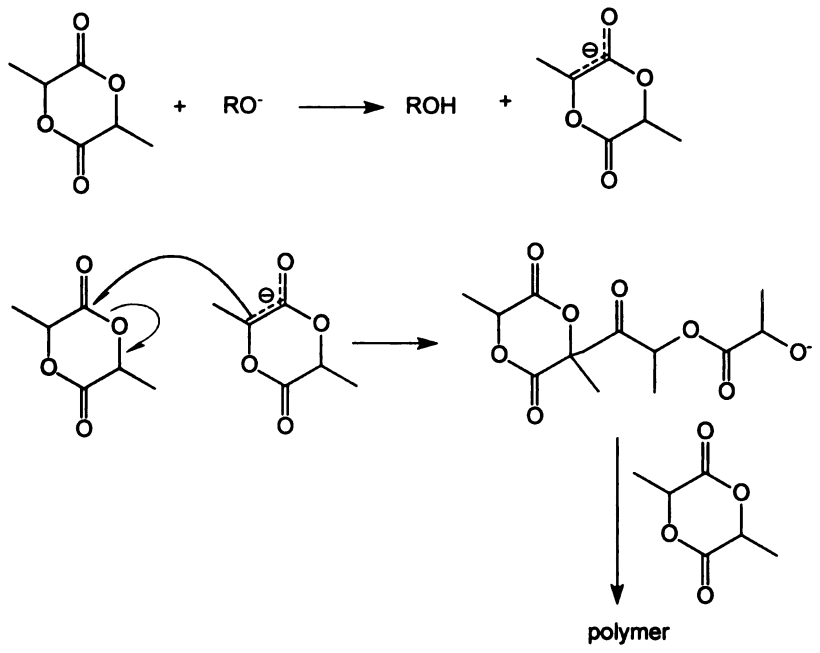

alcoholate center. Propagation proceeds via acyl-oxygen bond scission and regeneration of alcoholate anion each propagation step.

Scheme 11. Anionic polymerization of lactide

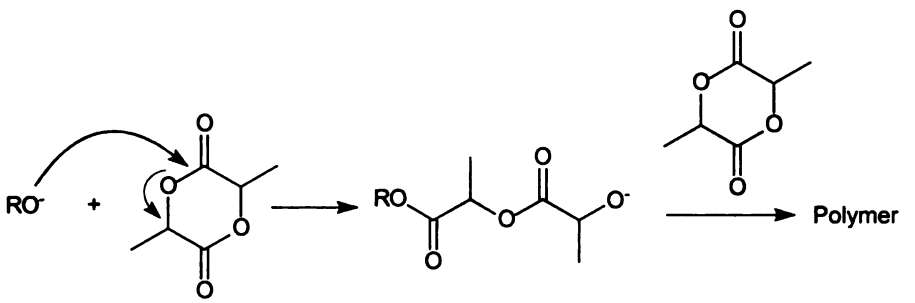

The contradictory results above may be caused by the polymerization conditions. Krichedolf *et al.* used a tertiary alkoxide (potassium *tert*-butoxide) and Jedlinski used a primary alkoxide (potassium methoxide). The difference in the nuclephilicity of anions might explain the difference in the initiation mechanism. The groups also used different solvents. The polarity of solvent might play a role in the initiation mechanism.

Anionic polymerizations of lactides and lactones are very fast processes, but side reactions such as racemization and back-biting make it difficult to obtain high molecular weight polymer with desired properties. It is unlikely that anionic polymerization of lactides and lactones will have important industrial applications.

3.2.3 Coordination Polymerization

As previous discussed, the anionic polymerization of lactide and lactones have side reactions such as transesterification and racemization. These undesired side reactions result from the high reactivity of the alcoholate. A decrease in the reactivity, e.g. by modification of the counterion, is a possible way to eliminate, or at least delay these side reactions.

During the last several decades, many research groups have worked on initiating polymerization using the alkoxides and organometallic derivative of different metals, aluminum,[44,45] tin,[46,47] zinc,[48,49] iron[50] and some rare earth metals such as yttrium,[51] lanthanum.[52] The most frequently used metals are aluminum and tin.

3.2.3.1 Aluminum Derivatives

The most widely used aluminum initiators are aluminum triisopropoxide[37], and soluble bimetallic μ-oxo-alcoholates, expecially zinc and aluminum[53] **(Figure 2)**.

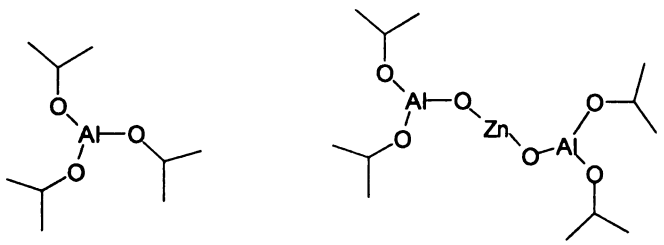

Figure 2. Structure of Al initiators

Aluminum alkoxides polymerize lactide and lactones through a "coordination-insertion" mechanism,[54-56] which involves coordination of initiator with the exo-oxygen of the monomer and insertion of the monomer into an Al-O bond of the initiator, follwed by cleavage of the acyl-oxygen bond of the cyclic monomer (**Scheme 12**).

Scheme 12 Mechanism of lactide polymerization using Al alkoxides

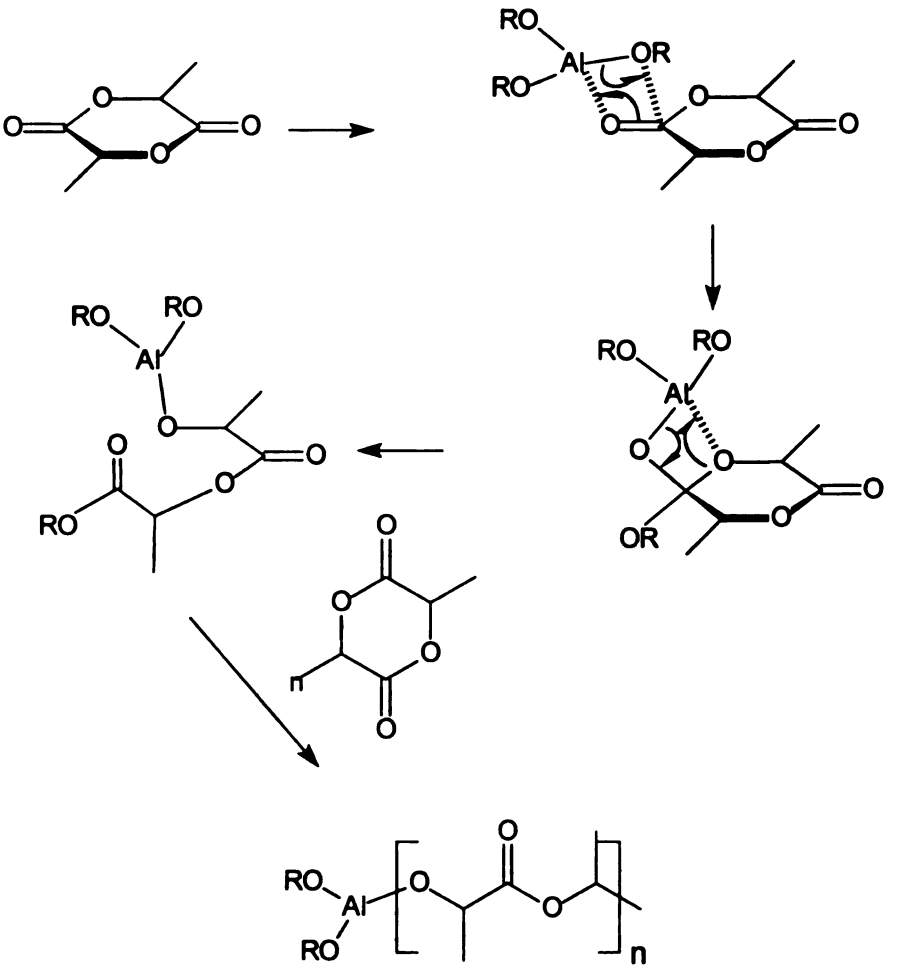

The polymerization of lactide and lactones using Al alkoxides is a living polymerization. If all impurities are excluded, there is no termination reaction and the molecular weight of polymer increases linearly with increases in the conversion of monomer to polymer. The polymerization is first order in concentration of monomer and concentration of initiator, and has the kinetic expression shown below.

$$-\frac{d[M]}{dt} = k_p[M][I]$$

Polymerization kinetics are influenced by polymerization conditions such as monomer and solvent.[57] When using aluminum triisopropoxide to polymerize ε-caprolactone (ε-CL), only one of three alkoxide groups initiates polymerization. In polymerization of lactide (LA), all three alkoxide groups initiate polymerization. This difference is caused by aggregation of the $Al(OiPr)_3$ in the solvent. $Al(OiPr)_3$ has two aggregation states in nonpolar solvents: a tetramer and a trimer, called A_4 and A_3 respectively.[58-62](**Figure 3**) The exchange rate between the tetramer and trimer is small, and almost can be neglected. The two aggregates react with ε-CL with different rates. Therefore, when a mixture of A_4 and A_3 is used to initiate the polymerization ε-CL, A_3 is consumed completely whereas A_4 remains unreacted. This observation explains why it is assumed that only one alkoxide group from $Al(OiPr)_3$ participates in the polymerization of ε-CL. Actually, an A_3/A_4 mixture was used in such a ratio that on average, one alkoxide of the initial amount of $Al(OiPr)_3$ initiates polymerization. A_3 provides all of the alkoxide groups, while A_4 is inactive. Lactide is less reactive than ε-CL, which gives A_4

enough time to dissociate before the monomer polymerizes completely. Furthermore, monomer addition causes the aggregated alkoxides to dissociate to a trisolvated six-coordinate "Al(O*i*Pr)$_3$ • monomer" complex. The only difference between ε-CL and lactide polymerization is that for ε-CL, only A_3 dissociates and for lactide, both A_3 and A_4 dissociate (**Scheme 13**).

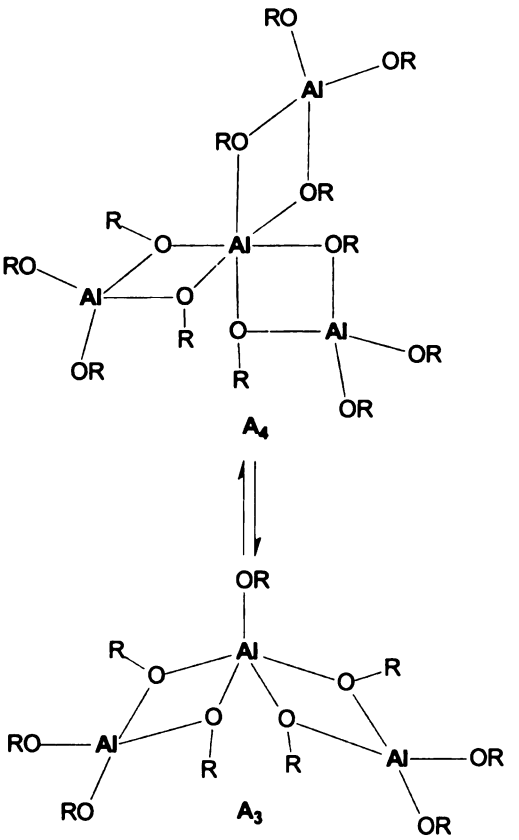

Figure 3 Aggregation states for Al alkoxides

Scheme 13. Dissociation of the Al alkoxide aggregates

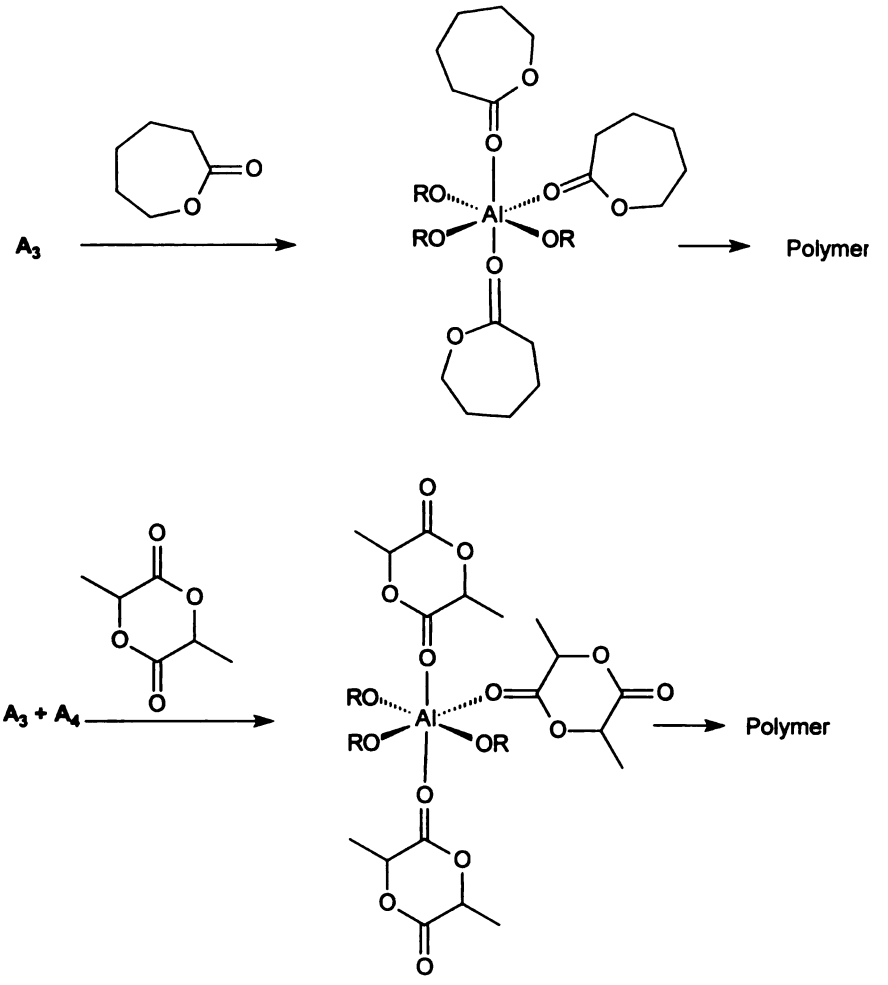

The use of different solvents does not modify the average number of active alkoxide groups per Al, but according to Teyssie,[63] the polymerization rate in THF is significantly smaller than that in toluene. When ε-CL is polymerized, the half polymerization time ($t_{1/2}$) is 3.5 min in toluene and 8.7 min in THF ([ε-CL]=1 mol/L, $[M]_0/[I]_0$=200 and T = 0°C).

The reason for the rate decrease is that THF is a much better solvating agent than toluene. The ether oxygen of THF is able to compete with the carbonyl group of lactones and lactide for coordination to aluminum. Because the ether oxygen on THF is more nucleophilic than the carbonyl group, it makes the formation of $Al(OiPr)_3$•$(lactone)_3$ unfavorable.

$Al(OiPr)_3$ is a very clean initiator for lactones. The molecular weight increases linearly with conversion and the molecular weight distribution is very narrow. But this linearity is not observed at very high conversions, or at high polymerization temperatures. The deviation from linearity is caused by transesterification reactions.[55] Transesterification reactions can be intramolecular ("back-biting" **Scheme 14**) or intermolecular. Backbiting produces a shorter polymer chain and a cyclic oligomer from original polymer chain, and is responsible for the broadening of the molecular weight distribution and for the decrease in the number-average molecular weight. Intermolecular transesterification (**Scheme 15**) does not change the number-average molecular weight of the polymer, but it does increase the polydispersity of the polymer.

Scheme 14. Intramolecular transesterification

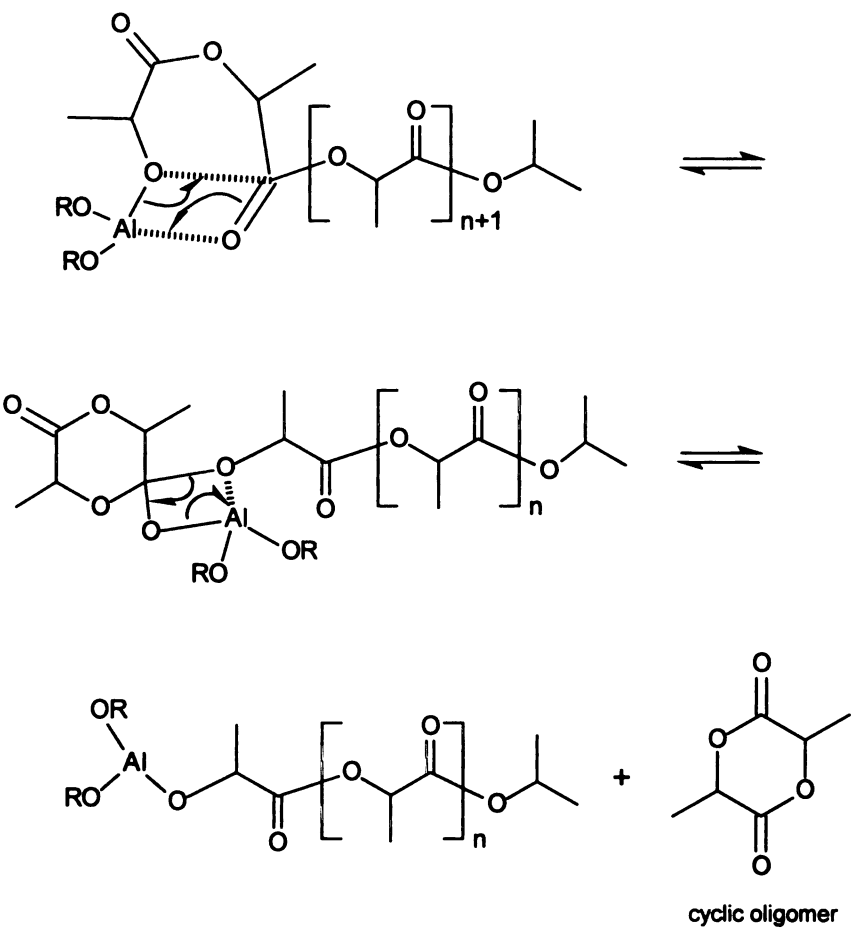

Scheme 15. Intermolecular transesterification

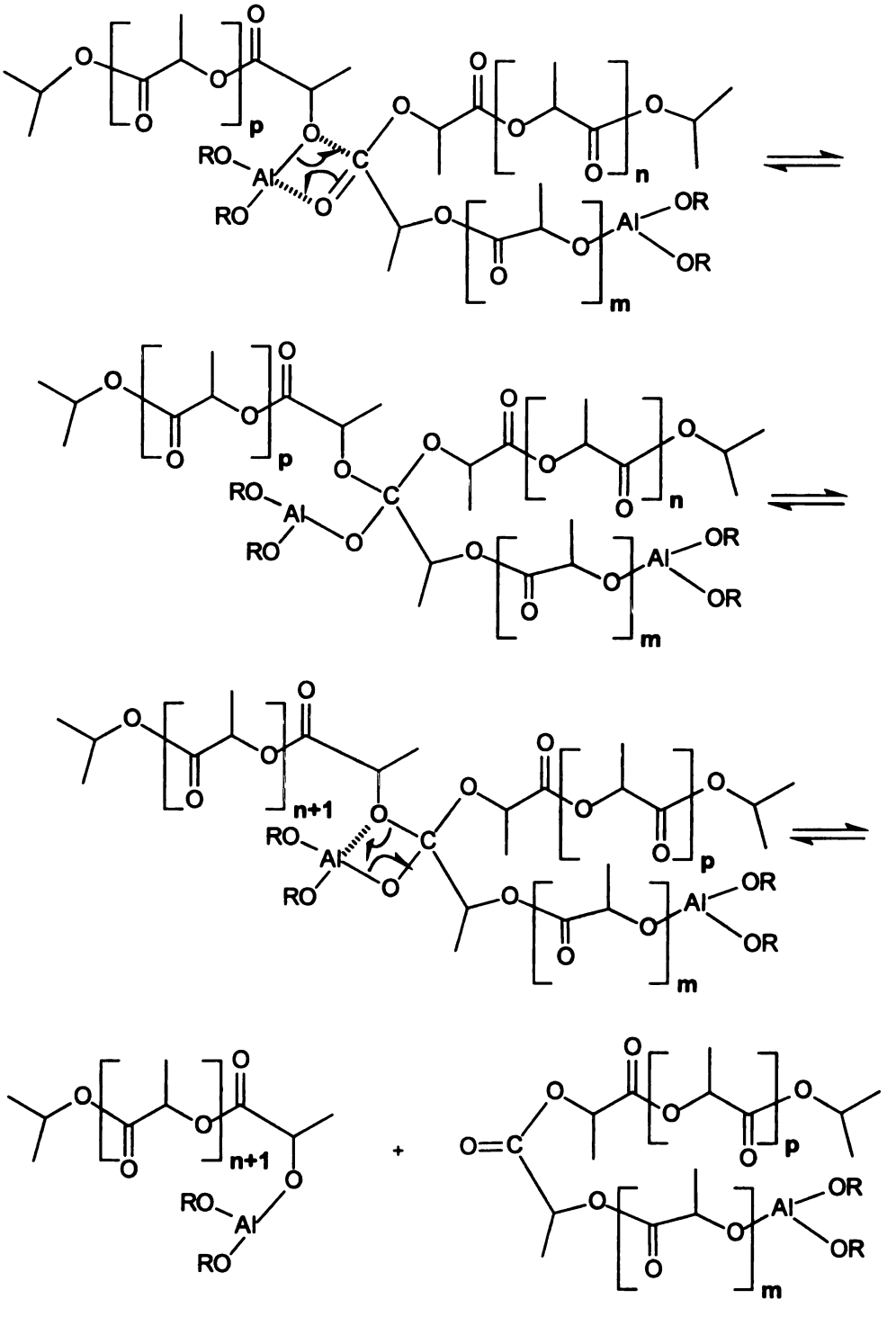

The rate of transesterification depends on the temperature, and the kind of metal center in the initiator. Kricheldorf *et al.*[64] compared the transesterification activity of different kinds of metal alkoxides. He found that aluminum alkoxides are least likely to cause transesterification and the tin alkoxides are most likely to cause transesterification. The order for transesterification activity is $Al(O\textit{i}Pr)_3$ < $Zr(O\textit{n}Pr)_4$ < $Ti(O\textit{n}Bu)_4$ < Bu_3SnOMe < $Bu_2Sn(OMe)_2$.

Polymerizations of lactide and lactones initiated by aluminum alkoxides are perfect living polymerizations and the alkoxide groups are the end-groups of the polymers. If the alkoxide group contains some functionality, the polymers will have a functional end-group. Halogens, tertiary amines, carbon-carbon double bonds, and methacrylates are typical example of functional groups that can be placed at the chain end. The initiators are easy to synthesize by mixing $Al(Et)_3$ with the corresponding alcohol (**Scheme 16**). By controlling the amount of

Scheme 16. Preparation of end-functioned Al initiators

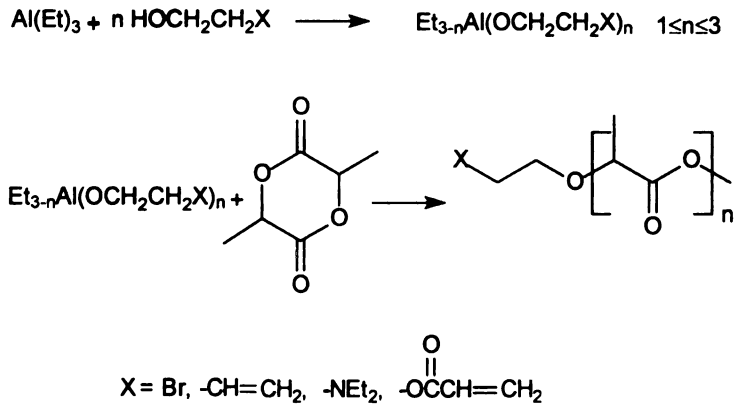

alcohol, the structures of the initiators can be controlled. End-functionalized polylactides and polylactones have been used in many fields. Teyssie *et al.*[65-69] used them to synthesize crosslinkable polylactides and polylactones, graft copolymers and star-branched polyesters. The great versatility of end-functionalized aluminum alkoxides opens the way to the macromolecular engineering of polylactides and polylactones. This approach will dramatically increase the range of the physical properties for polylactide and polylactones.

Inoue *et al.* reported that derivatives of tetraphenylporphinato–aluminum are efficient and versatile initiators for the living polymerization of lactones and lactide. The polymerization mechanism agrees with a "coordination-insertion" mechanism that involves acyl-oxygen cleavage. The polymerization rate can be remarkably increased by addition of sterically hindered Lewis acids. Coordination of the Lewis acid to the carbonyl oxygen of lactone or lactide monomers makes them prone to nucleophilic attack. These porphyrin derivatives polymerize not only lactones and lactide (**Figure 4**, X=OR),[70-72] but also epoxide [73,74](X=Cl), methacrylates,[75] and methacylonitrile[76] (X=SR, R=alkyl). The corresponding copper and iron complexes were investigated by Kricheldorf *et al.*[77] The iron or copper porphrin complexes polymerize lactide but produce relatively low molecular weight polymer in low yield.

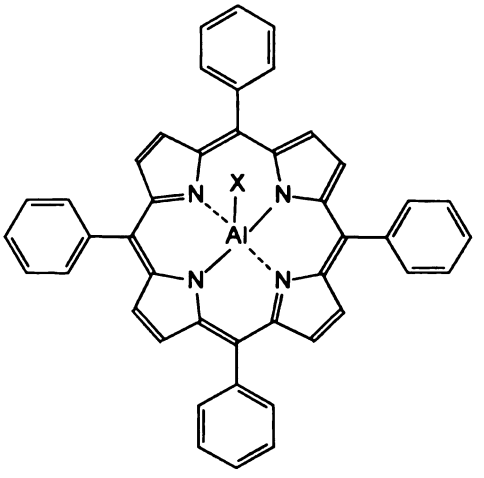

X = OR, Cl, Alkyl, SR, O_2CR

Figure 4. The structure of porphyrin initiators

3.2.3.2 Tin Derivatives.

Many kinds of tin compounds have been used in the polymerization of lactide and lactones such as SnO,[78] SnO_2,[79] SnX_4, SnX_2 (X = Br, Cl),[80-82] $Sn(OR)_2$, $Sn(OR)_4$,[83-86] and $(RCOO^-)_2Sn$.[46,47,87-89] The mechanism for polymerization using tin compounds is very controversial, and anionic, cationic and coordination mechanisms have all been proposed. Because of a lack of experimental evidence, none of the mechanism is very convincing.

Kricheldorf[90,91] investigated tin oxides and oxides of many other metals such as Mg, Sb, Pb and Ge for L-lactide polymerization. These catalysts are heterogeneous, so the repeatability of polymerization is poor. Also, these catalysts cause monomer racemization and transesterification. There is no detailed mechanisric study of the metal oxide catalyzed polymerizations, but people believe that hydroxyl-containing impurities such as water and alcohol initiate the polymerization.

Tin alkoxides perform just like aluminum alkoxides. The polymerization mechanism involves monomer coordination to the tin alkoxide, followed by insertion of monomer into the Sn-O bond (**Scheme 17**). Tin alkoxides are very efficient initiators. They do not cause racemization of monomer up to 150 °C, but since tin alkoxides are good transesterification catalysts for noncyclic ester groups, they may cause extensive back-biting degradation of polylactones and polylactide at elevated temperatures. The loss of molecular weight control is the reason that tin alkoxides are not as widely used as the aluminum alkoxides.

Scheme 17. Mechanism for tin alkoxide initiated polymerization lactides

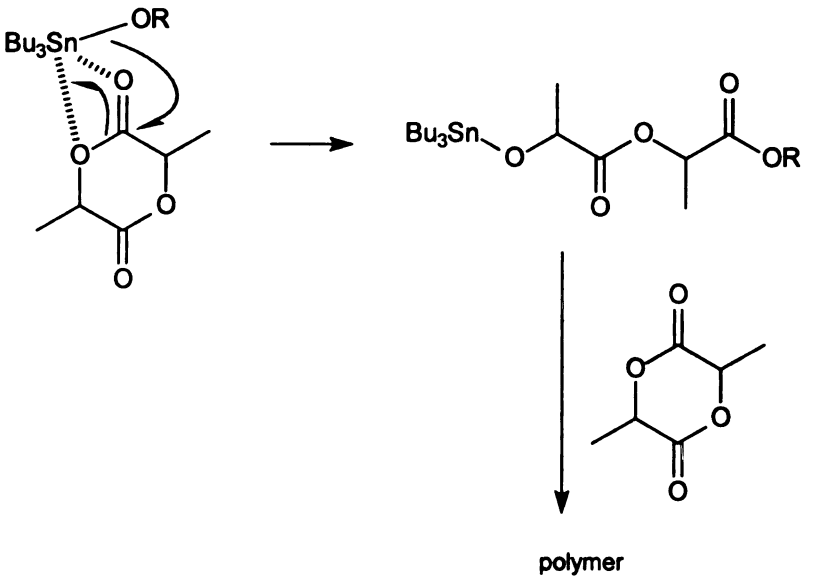

Tin halides such as $SnCl_2$ and $SnBr_2$ are very good catalysts, and high molecular weight polylactide and polylactones have been obtained using tin halide catalysts. Because they are not soluble in organic solvents and monomers, the repeatability problem still exists. The proposed mechanisms for lactone and lactide polymerization using tin halides are very different. The mechanism of lactone polymerization is shown in **Scheme 18**. It includes coordination of acidic tin halides with the carbonyl oxygen, ring-opening by transfer of a halide atom from the catalyst to the ω-carbon, followed by cleavage of the alkyl-oxygen bond. The propagation can proceed through two routes: through the carboxylate (**A**) or through alcoholate (**B**). The exact propagation species has not been identified. Lactide polymerization using tin halides acts much different. Unlike lactone polymerizations, halide end groups have not been found by NMR and elemental analysis. Lactide polymerization is not initiated by

transfer of halide atoms, probably because the secondary carbon on the lactide is less sensitive to nucleophilic attack than the primary carbon of a lactone. Based on the above observations, Kricheldorf proposed that tin halides react with impurities such as alcohol or water to first form tin alkoxides, which then follow the coordination-insertion polymerization mechanism.

Scheme 18. Mechanism for tin halide initiated polymerization of caprolactone

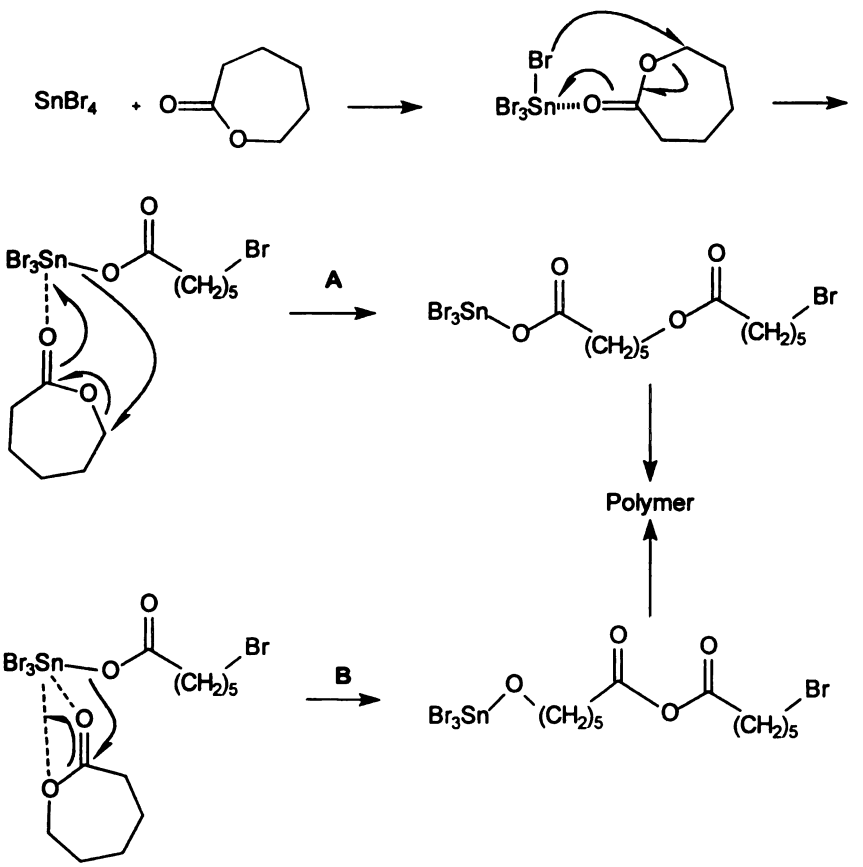

Tin(II) 2-ethylhexanoate ($Sn(Oct)_2$) is the most widely used catalyst for lactide polymerization. Commercial polylactide is synthesized using this catalyst since it provides high reaction rates, high conversions, and high molecular weights even under rather mild polymerization conditions. There are extensive studies of this catalyst system, but the mechanism is still unclear. Nijenhuis *et al.*[92,93] proposed the cationic polymerization mechanism shown in **Scheme 19**.

This is a complicated mechanism, but it is unlikely that the polymerization follows this path. First, the dissociation of $Sn(Oct)_2$ in a non-polar environment is not energetically favorable. Second, formation of an eight membered ring during polymerization should also be unfavorable. Finally, the strong interaction between Sn and lactide prior to reaction with the OH group is energetically unfavorable. To date, there is no spectroscopic evidence for any of the intermediates in the mechanism.

Scheme 19. Mechanism for polymerization of lactide initiated by Sn(2-ethylhexanoate)$_2$ as proposed by Nijenhuis *et al.*

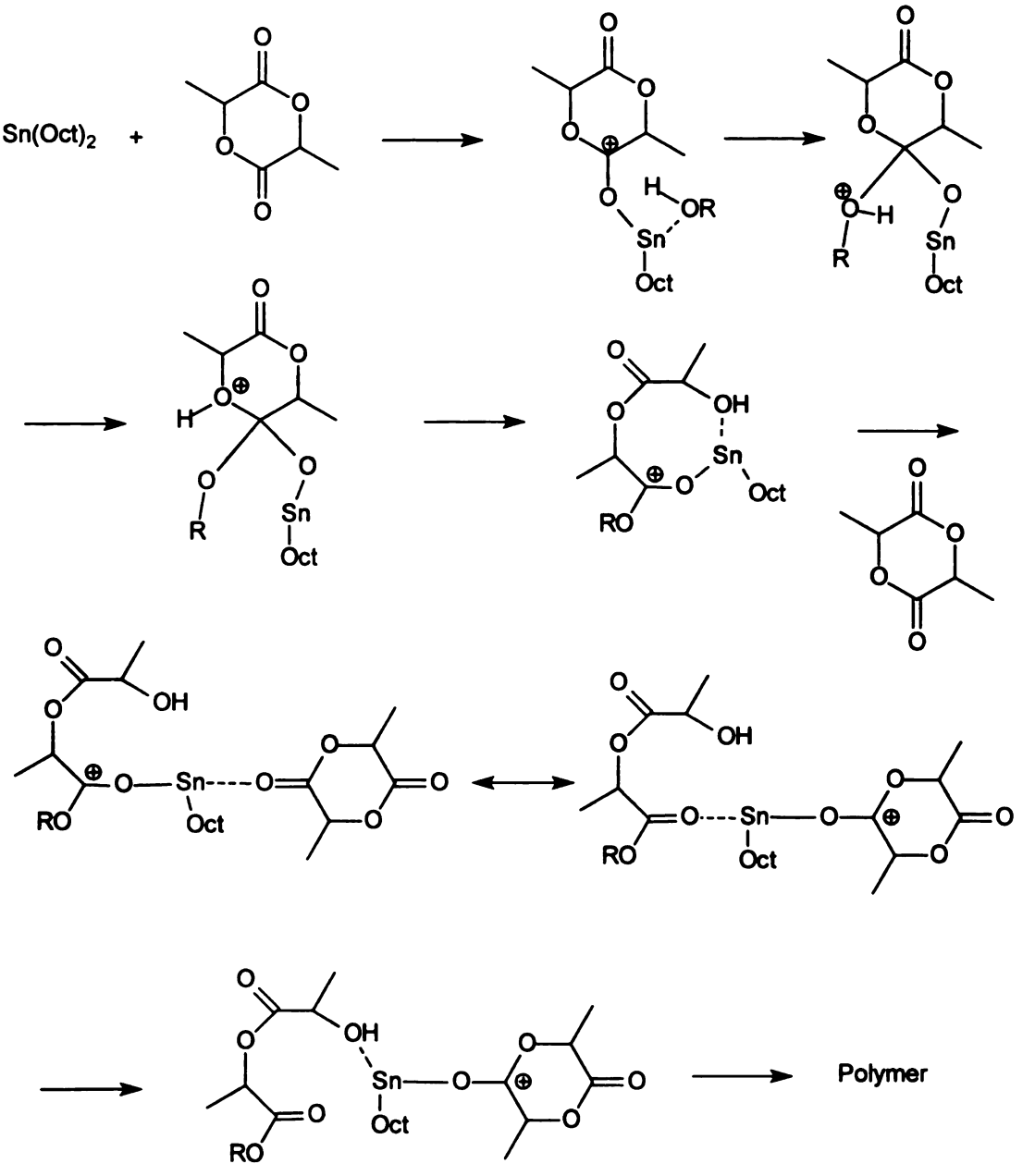

Kricheldorf *et al.*[94] proposed the mechanism shown in **Scheme 20**. The first step consists of coordination of alcohol or water to $Sn(Oct)_2$. The complexation of lactide to the intermediate polarizes its carbonyl group, making it susceptible to nucleophilic attack from alcohol. This mechanism also has a shortcoming. Based on the assumption that the tin catalyst is active via free sp^3d^2 orbitals, $Sn(Oct)_2$ can coordinate with both alcohol and lactide. But this mechanism can not explain the activity of $Bu_2Sn(Oct)_2$, which is six coordinate and should not be active. In past, $Bu_2Sn(Oct)_2$ polymerizes lactide, though not as well as $Sn(Oct)_2$. The authors rationalized their results by treating the Oct group as a monodentate ligand, but it is well known[92] that Oct is a bidentate ligand, and $Sn(Oct)_2$ and $Bu_2Sn(Oct)_2$ have the structure shown in **Figure 5**.

Penczek *et al.*[95] proposed that Sn(II) alkoxide species initiated the lactide and lactone polymerizations shown in **Scheme 21**. In their work, they identified intermediates such as $RO[M]_nOSnOct$. This mechanism is very similar to what we propose based on our experimental work. The details will be discussed later.

Sch

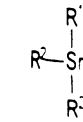

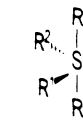

Scheme 20. Mechanism for polymerization of lactide initiated by Sn(2-ethylhexanoate)$_2$ as proposed by Kricheldorf

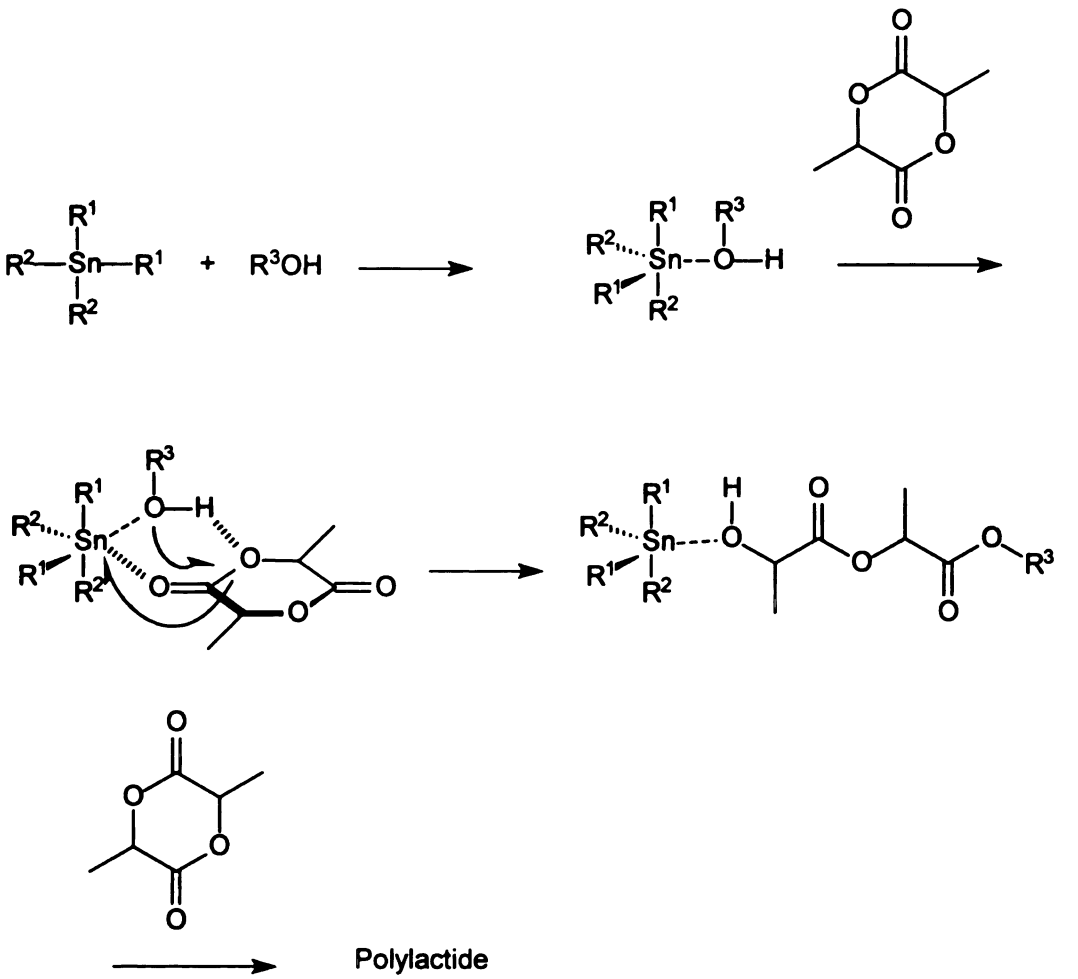

Scheme 21 Mechansim for lactide polymerization initiated by Sn(2-ethylhexanoate)$_2$ as proposed by Penczek *et al.*

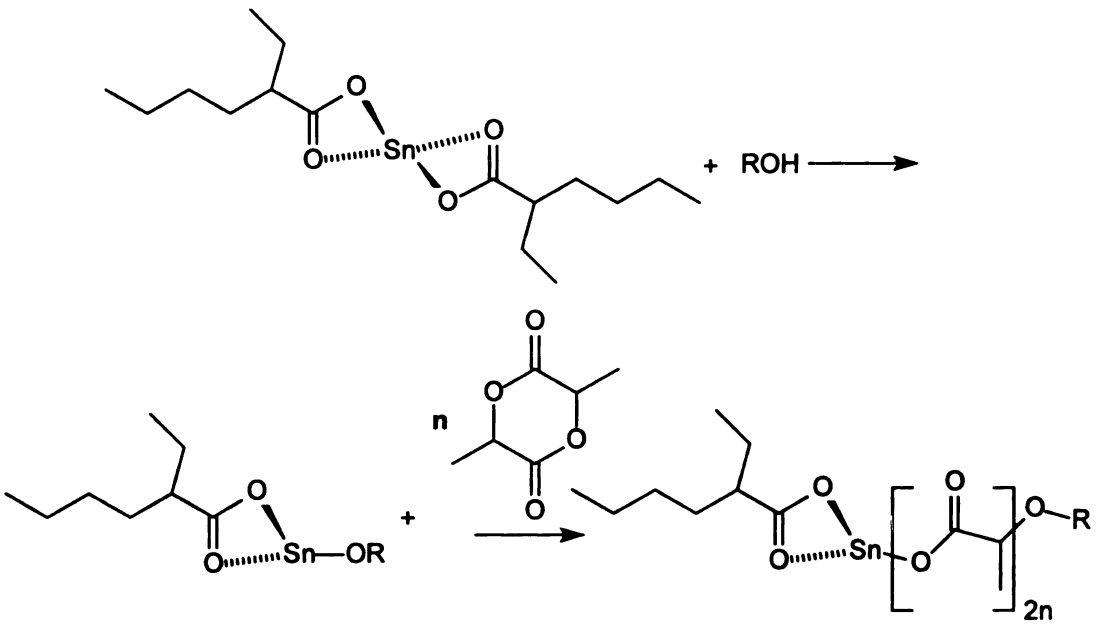

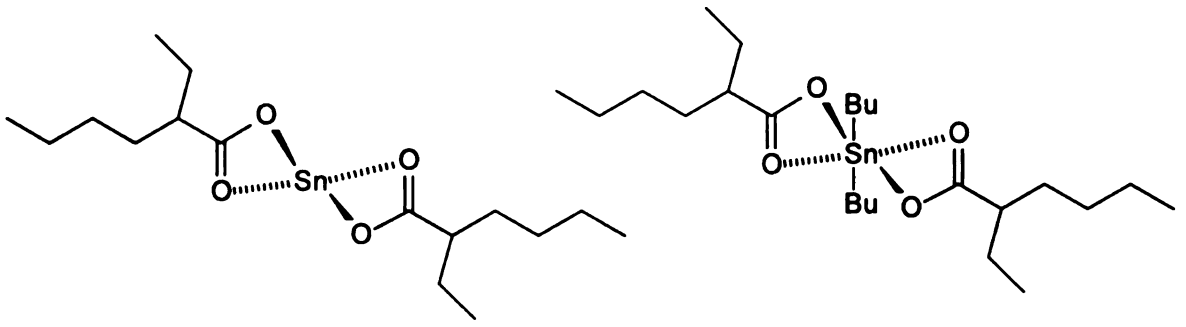

$Sn(Oct)_2$ $Bu_2Sn(Oct)_2$

Figure 5. Structure of $Sn(Oct)_2$ and $Bu_2Sn(Oct)_2$

There are some other proposed mechanism when Sn(2-ethylhexanoate)$_2$ is used as catalyst such as the one by Vert et al[89]., but there is no published mechanism that can explain every experimental fact. More research is needed to fully understand this reaction.

3.2.3.3 Rare Earth Metal Compounds

The 15 lanthanide elements (La, Ce, Pr, Nd, Pm, Sm, Eu, Gd, Tb, Py, Ho, Er, Tm, Yb, and Lu) together with Sc and Y elements are called rare earth elements. They prefer tri-valent oxidation states in complex formation. Rare earth metal complexes are known to initiate the living polymerization of methyl methacrylate over a wide range of polymerization temperatures to give high molecular weight syndiotactic polymers with extremely narrow molecular weight distributions. Lactones and lactide have also been successfully polymerized

using rare earth halide systems and rare earth complex systems. Yasuda *et al.*[96-98] used $[SmH(C_5Me_5)_2]_2$ and $LnMe(C_5Me_5)_2(THF)$ (Ln=Sm, Yb, Y, Lu) to polymerize lactide and lactones. Also, Feijen[99,100] thoroughly studied the polymerization of lactide and lactone using yttrium alkoxides. These catalysts initiate polymerization via a "coordination-insertion" reaction. The mechanism (**Scheme 22**) is very similar to that of the aluminum alkoxides and tin alkoxides. Shen *et al.*[101-106] found that rare earth halides can be used to polymerize lactide and lactones. He also found that the polymerization rate was dramatically increased by adding epoxides. The halides first react with expoxide to form the alkoxides, (**Scheme 23**) which are much better initiators than halides. Because of their high activity and few side reactions, rare earth catalysts will have a bright future in lactide polymerization.

Scheme 22. Polymerization of lactide initiated by rare earth catalysts.

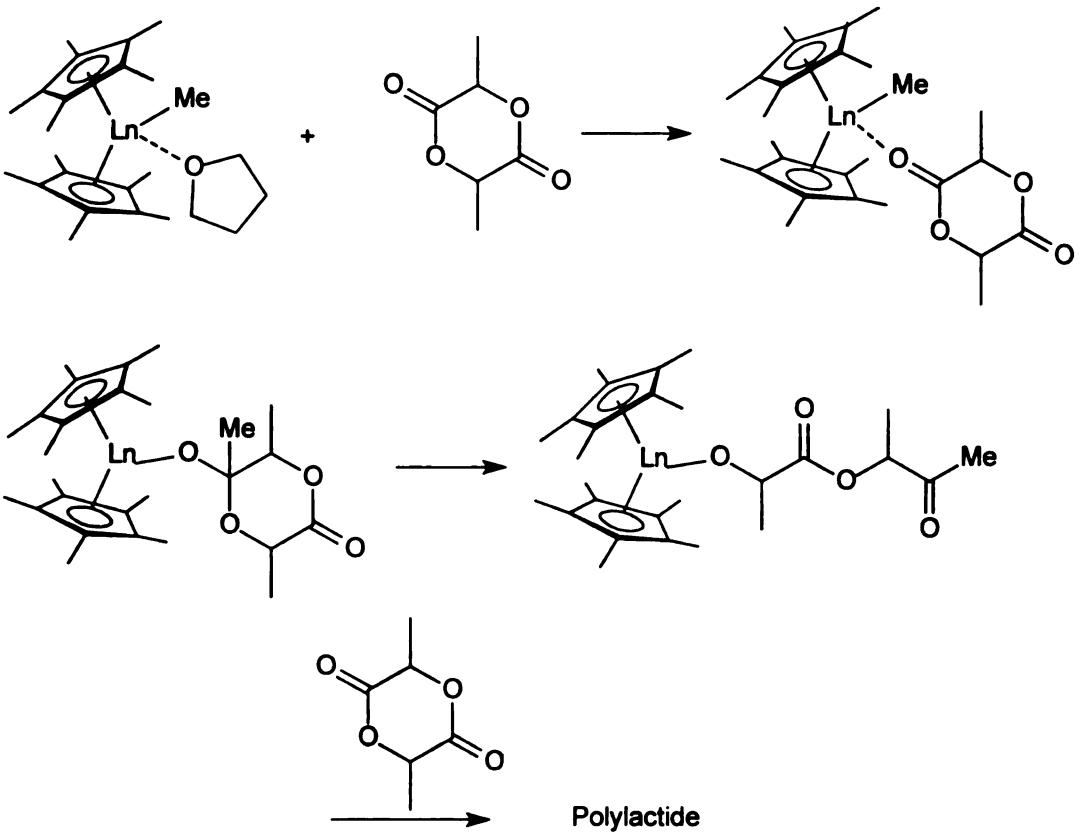

Scheme 23. Initiators made from epoxides and rare earth halides

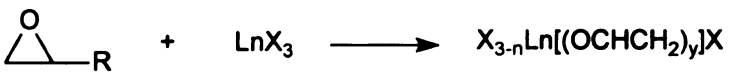

X = Cl, Br, I; R = H, CH_3, CH_2Cl, $CH_2OCH_2CH{=}CH_2$

3.2.4 Other Polymerization methods

In addition to the polymerization methods mentioned above, other polymerization methods such as free-radical polymerization, active hydrogen polymerization and zwitterionic polymerization have been used with lactide and lactones. Free radicals are usually ineffective for the polymerization of lactones and lactide. Molecular weights are often low, and monomer conversion limited,[107] so there are few examples of radical polymerization of lactones. The polymerizations of lactones and lactide initiated by active hydrogen compounds, e.g., amines or alcohols, are relatively slow processes, and usually produce polyesters of low molecular weight.[108] There are examples of the polymerization of lactones initiated by ethanolamine or ethylene glycol, but polymerizations typically need 3-4 days to reach high conversion even at 180 °C.

In contrast to the slow polymerization of lactones initiated with active hydrogen compounds, zwitterionic polymerizations are fast processes that give high yields and high molecular weight polymers. Wilson and Beaman[109] showed that polymerization of pivalolactone initiated with strained cyclic amines is a zwitterionic process (**Scheme 24**). Initiation corresponds to formation of a zwitterion as a result of nucleophilic attack by the amine at the lactone methylene group. The carboxylate anion of the zwitterion is the propagating species. Zwitterionic polymerization usually only occurs with very strained lactones, such as β-PL. There are also some claims that the polymerization of ε-CL proceeds through a zwitterionic mechanism when initiated with aniline in the presence of a protic acid.

Scheme 24. Zwitterionic polymerization mechanism

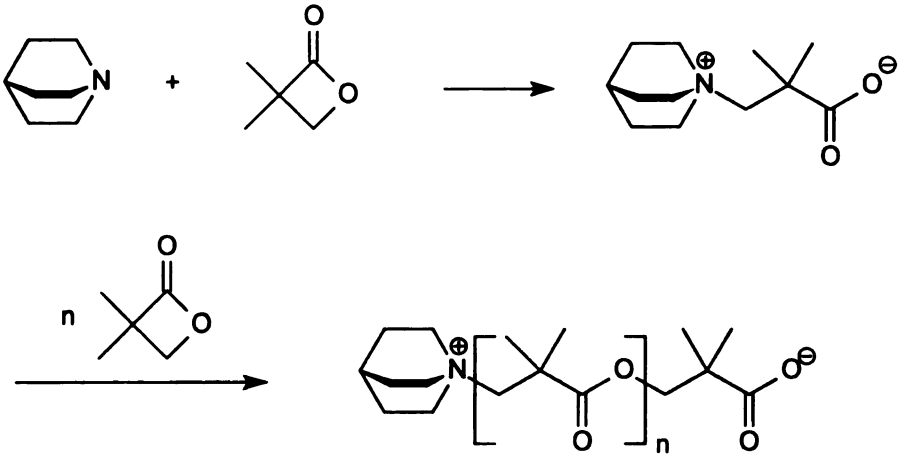

4. Modification of Polylactide Properties

To be successful in areas such as packaging, polylactides must be available that exhibit a broad spectrum of physical properties while retaining the degradability of the parent polymer. Typical approaches used to modify the physical properties of polylactides include manipulation of stereochemistry, copolymerization and formation of blends.

4.1 Manipulation of stereochemistry.

Lactide exists as three diastereomers: SS, RR, and RS (**Figure 6**). The SS diastereomer is referred to as L-lactide, the RR as D-lactide and the RS as *meso*-lactide. An equimolar ratio of L-lactide and R-lactide is referred to as *rac* or D, L-lactide.

Polymers prepared from different lactides have very different physical properties. Polymers of high purity L-lactide or D-lactide are crystalline with melting points around 180 °C. The polymers of *rac*-lactide are amorphous with a glass transition temperature ranging from 22-65 °C.[110] The different properties are related to the tacticity of the polymers. The polymer can have three limiting kinds of tacticity: atactic, isotactic and syndiotactic (**Figure 7**). If all the stereocenters on the polymer chain have the same configuration such as RRRRRRRRR or SSSSSSSS, the polymer is called isotactic. A syndiotactic polymer structure occurs when the configurations of the sterecenters alternate

from one repeating unit to the next such as RSRSRSRSRS. If successive stereocenters are randomly distributed, the polymer is called atactic.

L-lactide and D-lactide are known to polymerize to isotactic crystalline polymers while *rac*-lactide polymerizes to atactic amphours polymer. By manipulating the stereochemistry of polymer, the properties of the polymer can be altered. For example, poly(L-lactide) degrades slowly because of its highly crystallinity; by copolymerizing a small amount of *rac*-lactide with L-lactide, the degradation rate of the resulting polymer is much faster.[111,112] The added *rac*-lactide introduces R stereocenters into the polymer backbone, which act as defects and interrupt the crystallinity of the polymer. Thus, the degree of crystallinity of the polymer is smaller, which results in a faster degradation rate. By controlling the amount of *rac*-lactide added to L-lactide, the rate of degradation can be controlled. Poly(L-lactide) has a melting point around 180 °C, which makes poly(L-lactide) very hard to process without discolorization and loss of molecular weight. To solve this problem, a small amount of *rac*-lactide is often copolymerized with L-lactide to decrease the melting point.

Tsuji *et al.*[113-122] found that mixing an equimolar amount of poly(L-lactide) and poly(D-lactide) produces a polymer with a melting temperature and crystal structure different from poly(L-lactide) and poly(D-lactide) homopolymer. For example, the homopolymer of poly(L-lactide) has a melting point of about 180 °C, but the mixture melts near 230 °C. The mixture of poly(L-lactide) and poly(D-lactide) is termed a stereocomplex. The crystal structure of the stereocomplex has poly(L-lactide) and poly(D-lactide) chains packed side by side

in a 1:1 ratio of D and L monomer units. Because poly(L-lactide) and poly(D-lactide) pack better together than either packs with itself, the racemic crystallites are more stable than crystallites from the homopolymer.

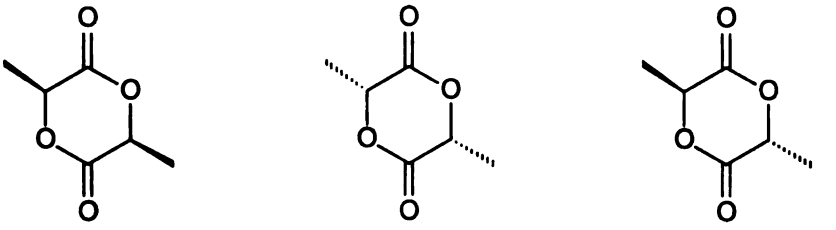

Figure 6. Stereochemistry of lactide

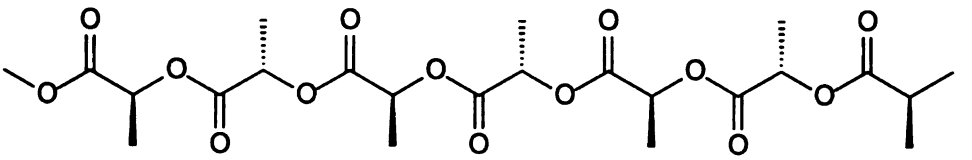

isotactic

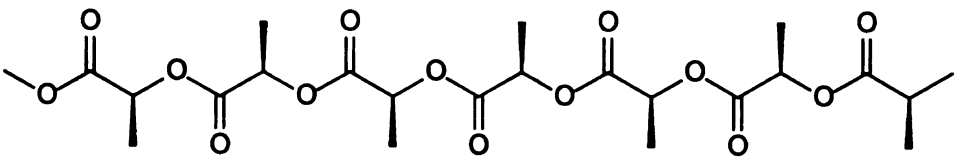

syndiotactic

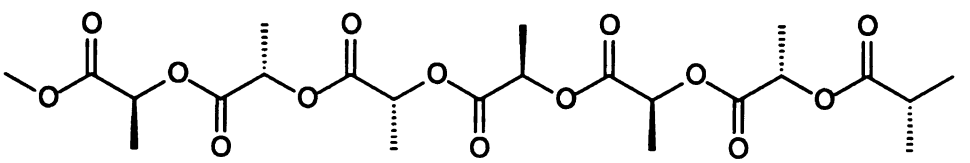

atactic

Figure 7. Tacticity of polylactide

4.2 Copolymerization

Copolymerization is the most important method for modifying the properties of polymers and adjusting them to fit the needs of a particular application. For example, poly(ε-caprolactone) (PCL) is a biodegradable polymer with a half-life *in vivo* of one year and that is permeable to many drugs. In contrast, PLA is hardly permeable to most drugs, and its half-life time is much shorter, a few weeks *in vivo*. Thus, combining the permeability of PCL and the rapid biodegradation of PLA may lead to a wide range of drug delivery devices with adjustable properties such as permeability, hydrophilicity and degradation rate. As shown in **Figure 8,** copolymers can be divided into three groups: random copolymers, block copolymers and graft copolymers.

In random copolymers, the different repeating units are randomly distributed along the copolymer chain. Random copolymers are usually synthesized by initiating a polymerization in a mixture of comonomers and catalyst. The randomness of the copolymer is controlled by many factors such as temperature, nature of the initiators, reactivity of the monomers and ratio of the comonomers in the monomer pool. For example, the reactivities of lactide and ε-caprolactone are very different. When copolymerized, lactide prefers to add to itself and less than 50% of caprolactone has reacted by the time almost all of the lactide monomer is polymerized. Thus poly(ε-caprolactone-co-DL-lactide) has a blocky structure.[123-126] When ε-caprolactone copolymerizes with ε-methyl-ε-caprolactone,[127] the distribution of the monomers in the copolymer are nearly perfectly random because of the similar reactivity of the monomers. The

randomness of the copolymer is also controlled by initiators. Shen *et al.*[102] found that poly(ε-caprolactone-*co*-DL-lactide) produced using the $NdCl_3$-propylene oxide catalyst system is much more random than poly(ε-caprolactone-*co*-DL-lactide) produced using $Sn(Oct)_2$ and $Al(OiPr)_3$. By choosing a high polymerization temperature, ordered copolymers can be randomized by transesterification reactions.[128]

Random copolymers usually have properties intermediate between those of the parent homopolymers and are usually amorphous polymers with a single

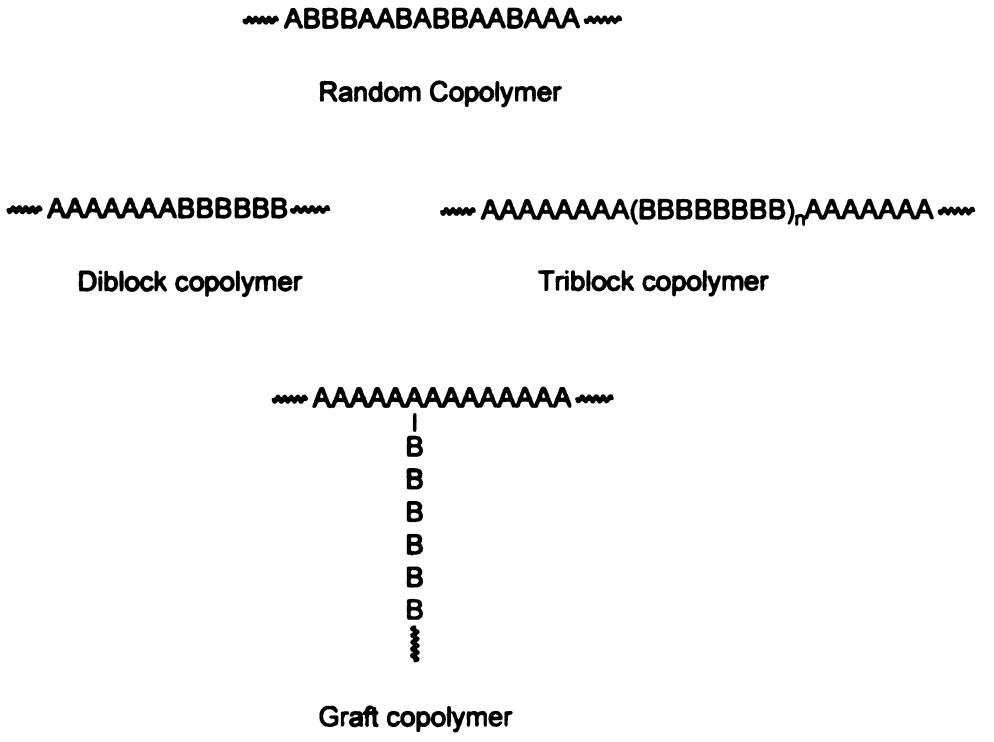

Figure 8. Copolymer architectures

glass transition temperature. The glass transition temperature can be predicted using the Fox equation.

$$\left(\frac{1}{T_g}\right)=\left(\frac{w_1}{T_{g1}}\right)+\left(\frac{w_2}{T_{g2}}\right)$$

where T_g is the glass transition temperature of the copolymer, T_{g1} and T_{g2} are the glass transition temperatures of the pure homopolymer of components 1 and 2, and w_1 and w_2 are the corresponding weight fractions.

By altering the ratio of the comonomers, the properties of the copolymer can be easily controlled. Besides ε-caprolactone, lactide has been copolymerized with monomers such as glycolide,[7,129] δ-valerolactone,[130,131] carbonates,[132,133] and ethylene glycol.[78] These copolymers greatly widen the scope of the physical properties of polylactides.

The most progress has been made in block copolymers of lactide and lactones. Block copolymers have been made with different architectures such as diblock,[40,134,135] triblock,[78,136,137] star-block,[138-140] and multiblock.[141] In contrast to random copolymers, block copolymers are usually multiphase materials. They can form multi-crystalline phases when blocks in the copolymer crystallize separately, alternating crystalline and amorphous phases if some blocks crystallize and some blocks stay amorphous, and a mixture of amorphous phases if none of the block crystallize. The different morphologies of block copolymers provide a wide range of physical properties that can be selected for different applications.

There are several ways to synthesize block copolymers. The first is to take advantage of the living nature of Al-initiated polymerization of lactide and lactones.[142-145] As shown in **Scheme 25**, the comonomers are polymerized sequentially. First, ε-caprolactone is polymerized to form a poly(ε-caprolactone) block. Because there is no termination reaction, the blocks remain active toward polymerization. Lactide monomer is then added, and a polylactide block grows from the end of polylactone block to form the diblock copolymer. There are some problems with this method. The first is the polymerization order. To make poly(lactide-*bloc*-ε-caprolactone), the lactone monomer has to be polymerized first. If lactide is polymerized first, the lactone monomer will not polymerize at all, due to the different cross-propagation rates. The PCL active chain ends react with LA monomers 2.0×10^5 times faster than PLA active chain ends react with CL monomers. Thus, it is very important to know the correct order to add monomer. The second problem is the number of chains initiated by an initiator. For $Al(OiPr)_3$, only one alkoxide group is active if the monomer is ε-caprolactone, but all three alkoxide groups are active when lactide is the monomer. This difference leads to a mixture of the block copolymer of lactide and lactone and the homopolymer of lactide. This problem can be solved by using initiators such as $(Bu)_2AlOiPr$ that initiate only one chain for both lactide and ε-caprolactone.

The second way to make block copolymer is to use macroinitiators. As shown in **Scheme 26**, there are two ways to use macroinitiators. In the first, a polymer with a hydroxyl end-group such as poly(ethylene glycol) monomethyl ether is reacted with $Al(Me)_3$ to produce the macroinitiator.[146-148] Polymerization of lactide using this initiator produces block copolymer. The second route uses $Sn(Oct)_2$ and a polymer with hydroxyl end-groups as the initiator.[93,138,149] This route is very flexible. Triblock and multiblock copolymers can be synthesized using this method.

Scheme 25. Synthesis of diblock copolymers

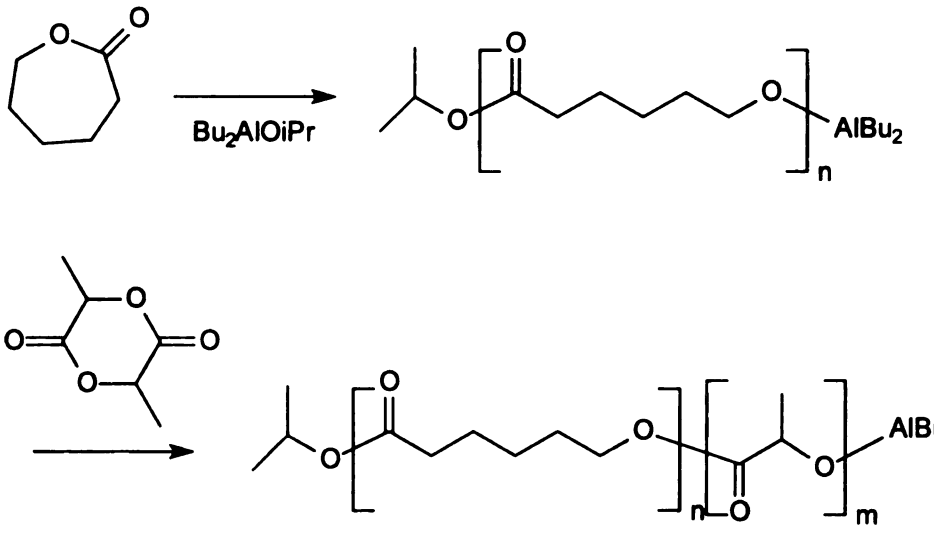

Scheme 26. Synthesis of ABA triblock copolymers

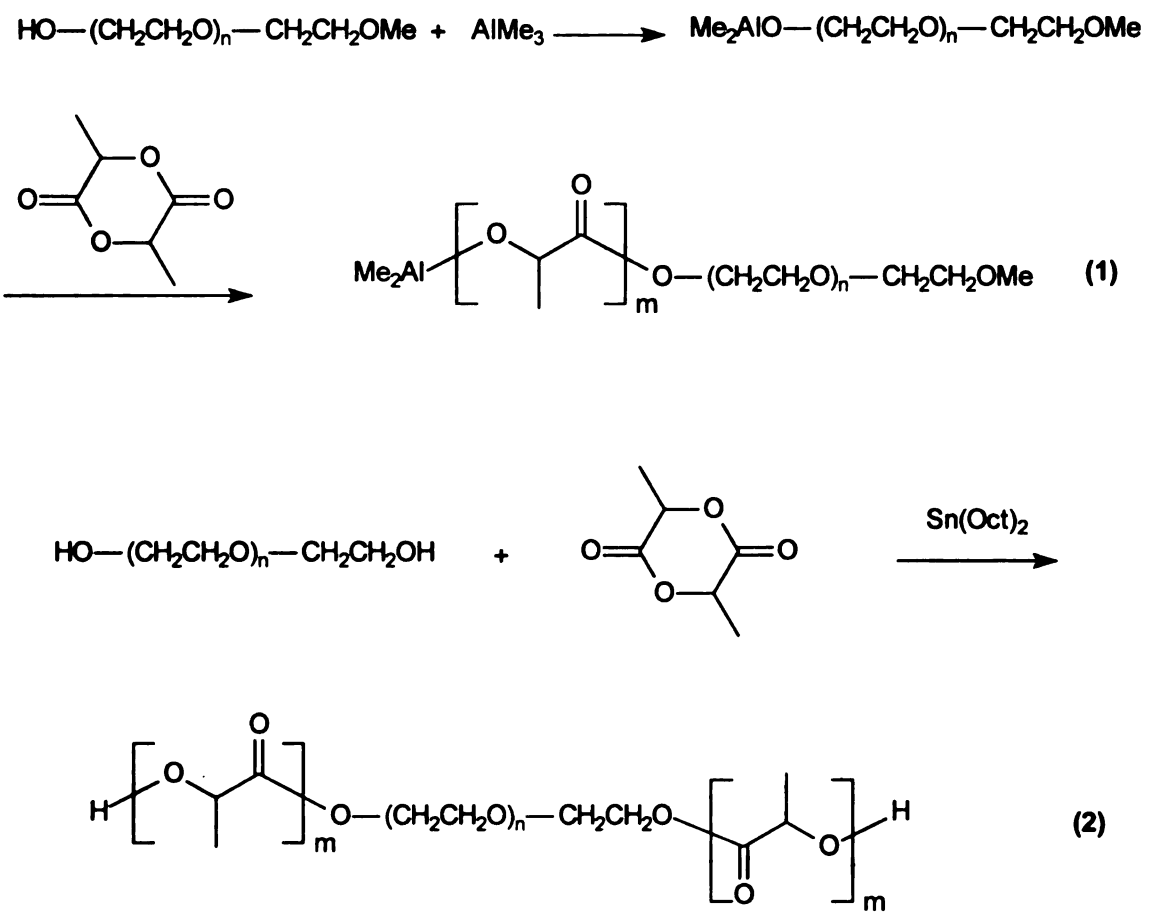

Graft copolymers of lactide and lactones are rare compared to random copolymers and block copolymers. People mainly focus on using polyols such as poly(vinyl alcohol),[150] and polysaccharides (pullulan, amylose)[151,152] as initiators to polymerize lactide and lactones. Polyols are hydrophilic, and polylactide and polylactones are hydrophobic. Combining these two segments in

a copolymer will provide materials very special properties such as micelle formation in solvents, which can be used to make drug delivery devices.

In addition to synthesizing copolymers, the crosslinking of homopolymers and copolymers of linear polylactides and polylactones can be used to modify the physical and mechanical properties of these materials. By introducing crosslinks into polylactide, physical properties such as the crystallinity, the melting point and the glass transition temperature will be influenced. The characteristics of the degradation by hydrolysis of these biodegradable polymers will also be influenced. Three methods that have been used to crosslink polylactide and polylactones: high-energy electron beams, peroxide-induced radical crosslinking and copolymerization of functional lactide and lactone oligomers with a multifunctional monomer.

High-energy electron beams significantly degrade polylactide and polylactones, so it is not a suitable technique for crosslinked polylactide and polylactones. Peroxide crosslinking of polylactide and polylactones appears to be an effective method for affecting the thermal as well as the mechanical properties. However, in terms of the potential biomedical application of these materials, the method has two disadvantages. First, peroxides modified polylactide and polylactone chains may have undesirable degradation products. Secondly, many peroxide compounds are toxic, so crosslinked materials will need to be thoroughly extracted to remove peroxides, which is very costly.[153]

Copolymerization of functional lactide and lactone prepolymers with other monomers is the most successful cross-linking method. As shown in **Scheme 27**, the multifunctional prepolymers with end-groups such as methacylate were synthesized and cured with monomers such as styrene and methyl methacrylate to form networks.[154-158]

Scheme 27. Synthesis of cross-linkable copolymers

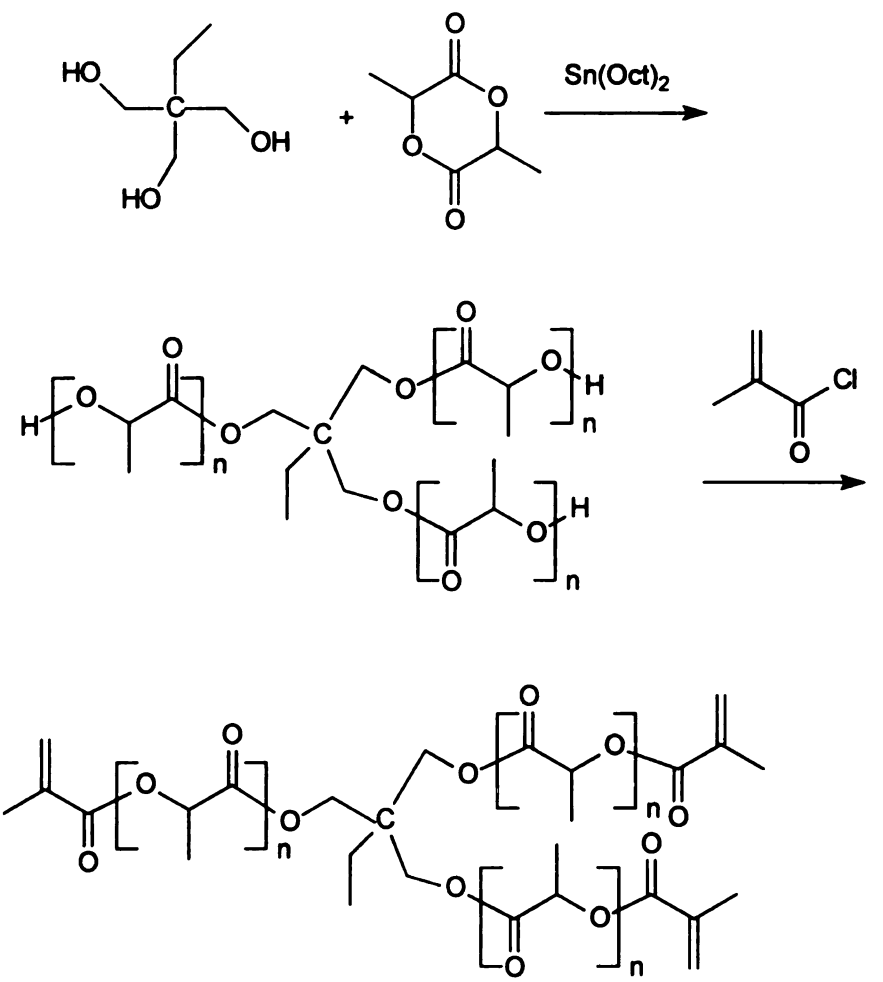

4.3 Blending

Copolymerization is an effective way to modify the properties of the polymers. However, copolymers are often hard to make and are very expensive. Blending of polymers might offer a more cost-effective way to modify polymer properties compared to copolymerization. Blends oftem have inferior properties compared to copolymers, but their ready availability and low-cost are very attractive.

Blends can be made through thermal mixing and solvent mixing. In thermal mixing, the components of the blend are melted, and mixed thoroughly to make blends. In solvent mixing, the components of the blend are dissolved in a common solvent, and evaporation of the solvent yields the blend.

Macroscopic properties such as impact and tensile strength, and degradation behavior can be modified by a reasonable choice of the blend components. The final properties will depend not only on the chemical composition of the blend but also on its physical characteristics, such as glass transition temperature, crystallinity and morphology, which, in turn, are a direct consequence of the compatibility between the components in the blend. The miscibility is the single most important factor for blends. If the components are miscible, the blend is a homogeneous system. If the components are immiscible, the blend will form a two-phase or multi-phase system. Most blends are phase-separated, which hinders applications of the blends.

There are many reports of blends of biodegradable polymers. For instance, Langer *et al.*[159] used poly(lactide)/pluronic blends as protein-releasing

matrices. Eguiburu *et al.*[160] blended amorphous and crystalline polylactides with poly(methyl methyacrylate) and poly(methyl acrylate). The resulting blends are miscible, and have interesting thermal properties. Poly(L-lactide) has also been blended with poly(ε-caprolactone) and other polymers.[161-165]

5. Degradation of the polylactide and polylactones

There are two ways to degrade polylactide and polylactones. They can be degraded thermally, and they can be degraded environmentally which includes hydrolytic and enzymatic degradation.

5.1. Thermal degradation

Understanding thermal degradation is very important for polymer processing and polymer recycling. Poly(L-lactide) has a high melting point, so processing steps such as injection molding and extrusion must be done at around 200 °C, a temperature where polylactide and polylactone begin to degrade. Degradation can be prevented if we understand the mechanism for thermal degradation. Polylactide and polylactones also can be recycled by selecting favorable thermal degradation pathways.

Transesterification, cis-elimination and radical reactions[166-172] have been proposed as thermal degradation mechanisms. The transesterification reaction was discussed earlier. The intra-molecular transesterification reaction generates volatile low molecular weight oligomers, which causes the polymer to degrade. The mechanism of the cis-elimination reaction is shown in **Scheme 28**. The elimination of a proton from methyl group produces 1-alkenes and carboxylic acids. The carboxylic acids also accelerate the degradation of the polymer. The proton on the methyl group is not very labile, so the cis-elimination reaction is lilely only at high temperatures, Usually the cis-elimination reaction cannot compete with the thermal degradation of polylactides by transesterification. Radical reactions (**Scheme 29**) can start with either alkyl-oxygen or acyl-oxygen homolysis. Several types of oxygen and carbon-centered macroradicals may be formed. From the radicals, a varietiy of volatile compounds can form, such as carbon dioxide, carbon monoxide and aldehydes. The thermal degradation can be influenced by many factors such as residual metal compounds and unreacted monomers. Residual metal and monomers increase the degradation rate greatly.

Scheme 28. Thermal degradation via *cis*-elimination

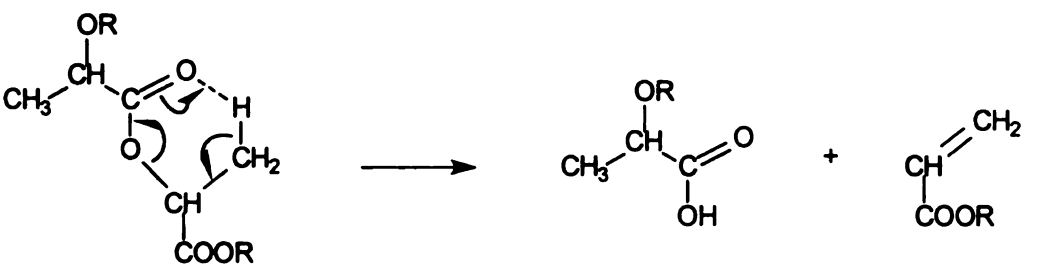

Scheme 29. Radical thermal degradation

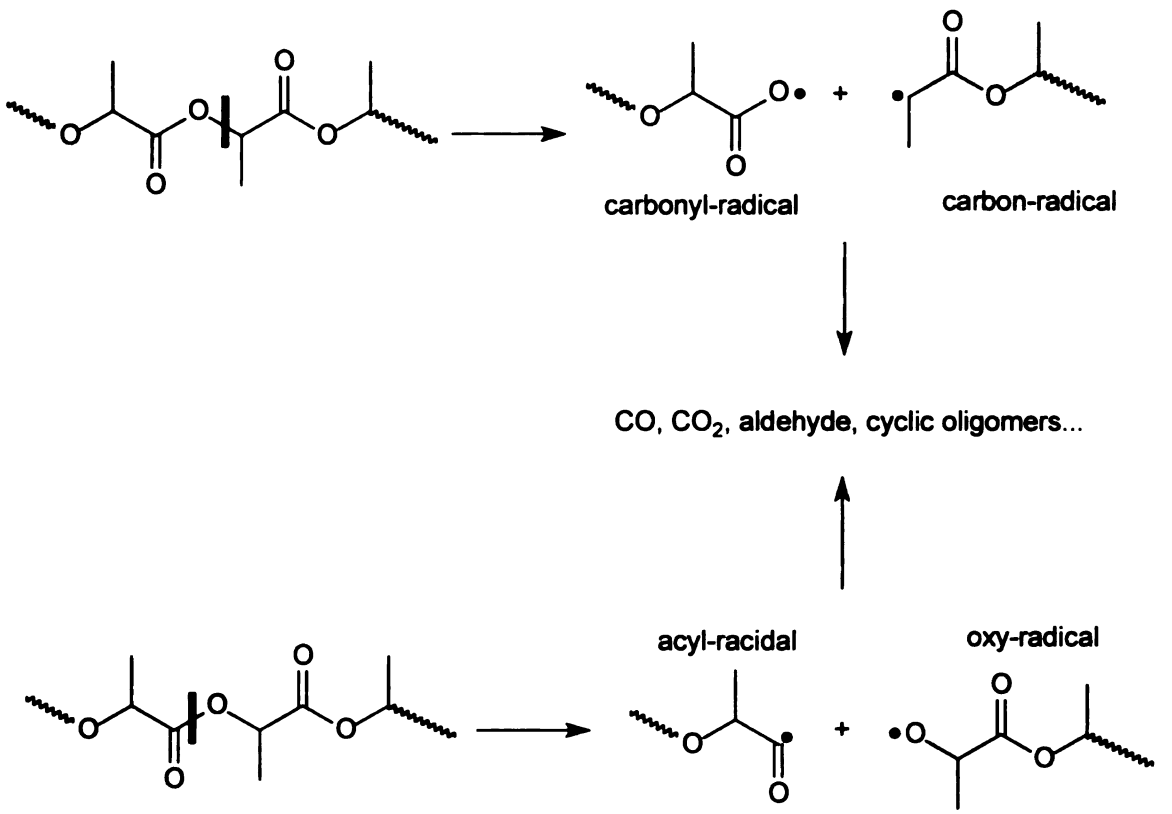

5.2. Biodegradation

Biodegradation mechanisms for lactide include hydrolytic degradation[129,136,173-175] and enzymatic degradation.[176-178] The two degradation processes are very different as shown schematically in **Figure 9**. Enzymes are high molecular weight molecules, so it is very difficult for enzymes to diffuse into polymers. Thus, enzymatic degradation almost always happens at the surface of the polymer. The top half of the **Figure 9** shows the weight loss

and molecular weight loss as a function of time for enzymatic degradation. Because degradation is limited to the surface of the polymer, the surface of the polymer is eroded, but interior of the polymer is unchanged. The weight of polymer drops as polymer chains on the surface are degraded to soluble oligomers, but the molecular weight of the polymer remains almost constant until most of the polymer weight is lost. In contrast to enzymatic degradation, the

Figure 9. Degradation models

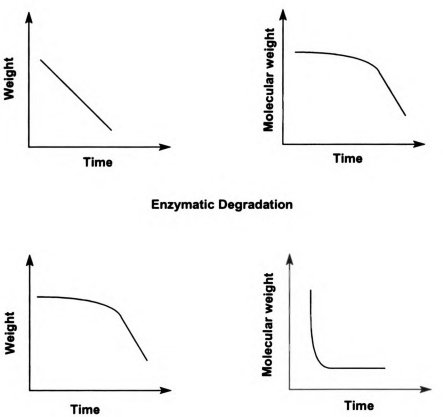

molecular weight drops continually and the polymer weight remains constant during hydrolytic degradation. Hydrolytic degradation ocurrs in the bulk of the polymer. Water molecules diffuse into polymer and hydrolyze the ester bonds of polylactide, causing the molecular weight of the polylactide to drop. When the molecular weight drops to where the polymer becomes soluble, the weight of polymer begin to drop. Hydrolysis of the ester bond produces a carboxylic acid, which catalyzes further degradation of the polylmers. This phenomenon is called autocatalysis.

Temperature, pH of the degradation medium, the stereochemistry of the polymer, the morphology of the polymer and the physical size of the polymer all influence the degradation rate of the polymer. Because water diffuse at a slower rate in crystalline polymers, and has a lower solubility due to the higher density of chains in crystalline polymers, crystalline polylactide degrades slower than amorphous polylactide. Enzymatic degradation is sensitive to the stereochemistry of the polymer, and enzymes often selectively degrade one isomer. The degradation process is complicated, and there are many controversial conclusions. Many people question the role of enzymes in polylactide degradation, since hydrolytic degradation always accompanies the enzymatic degradation. Much work needs to be done in order to fully understand the degradation process.

RESULTS AND DISCUSSION

1. Monomer synthesis

In order to synthesize substituted polylactides through ring-opening polymerization, a series of substituted glycolides, shown in **Figure 10,** were prepared. For simplicity, we used the glycolide structure as a template to name these compounds. Substituted glycolides have been known for over a century, with the synthesis of ethylglycolide via the dimerization of the sodium salt of 2-bromobutyric acid reported as early as 1893.[179] We prepared substituted glycolides using the two routes outlined in **Scheme 30**. The first route mirrors the standard method used to prepare the lactide dimer. The appropriate α-hydroxy acid was first condensed in toluene to give low molecular weight oligomers, and cracking the oligomers under reduced pressure in the presence of a transesterification catalyst such as ZnO directly yielded the volatile dimer. This method has been used industrially to produce polylactide.[19] In the second route, an α-bromo acyl bromide was condensed with an α-hydroxy acid to form an ester,[180] followed by ring closure to give the cyclic dimer. In this method, it is very important to remove the $N(Et)_3$ in the work-up. Even trace amount of $N(Et)_3$ can change dimers to low molecular weight oligomers in a short period of time. Because $N(Et)_3$ is not nucleophilic, it is likely that Et_3NHBr caused the polymerization. The first method gives the dimer in higher yield, but the second method offers more flexibility in synthesis and can be used to synthesize unsymmetrical dimers, which are discussed in a later section.

Both synthetic methods yield a mixture of diastereomers. Thermal cracking of oligomers consistently yields a near-statistical mixture of the R,S and R,R/S,S diastereomers. ^{1}H NMR of a representative example, that of ethylglycolide, is shown in **Figure 11**. The methine protons of the 3,6-disubstituted glycolide ring appear as a doublet of doublets near δ 4.85. The signal for R,S isomer appears at 4.88, while that from the R,R and S,S isomer is at 4.83. The near equal intensities of the peaks confirms the 1:1 mixture of R,R/S,S and R,S diastereomers. Similar results were obtained for isobutylglycolide and hexyglycolide prepared by the thermal cracking route.

Non-statistical mixtures were obtained when the second route was used. The R,R/S,S isomers are about 70% of the total and the R,S isomer is about 30%, which is probably is related to the kinetics of diastereomer formation. It is likely that the R,R/S,S isomers form faster than the R,S isomer. In addition, ring-closing competes with oligomerization to form the linear dimer, trimer and tetramer. Because of the slower rate for forming the R,S isomer, oligomerization is probably favored to form linear oligomers rather than S,R glycolides.

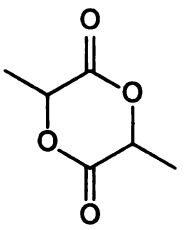

Lactide

3,6-dimethyl-1,4-dioxane-2,5-dione

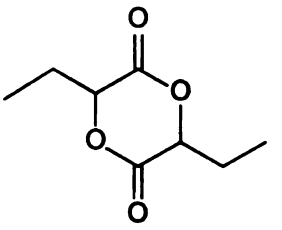

Ethylglycolide

3,6-diethyl-1,4-dioxane-2,5-dione

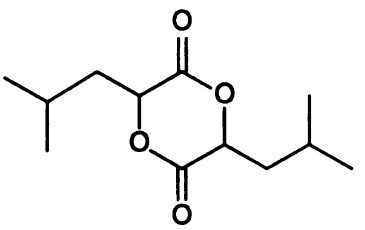

Isobutylglycolide

3,6-diisobutyl-1,4-dioxane-2,5-dione

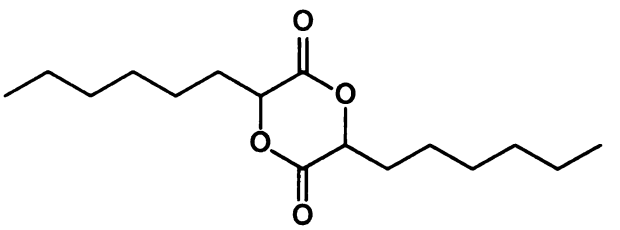

Hexylglycolide

3,6-dihexyl-1,4-dioxane-2,5-dione

Figure 10. The structures of substituted glycolides

Scheme 30. The synthetic route to substituted glycolides

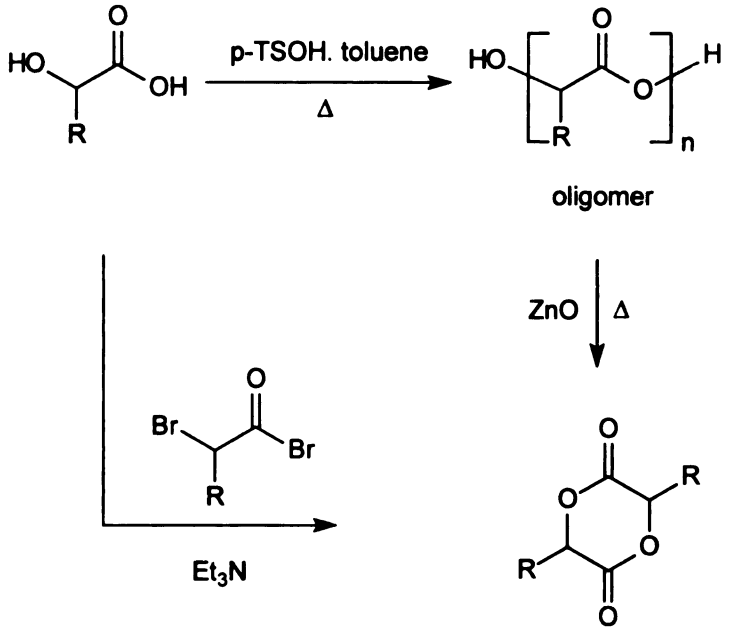

R = CH_3, CH_2CH_3, $CH_2CH(CH_3)_2$
$(CH_2)_5CH_3$

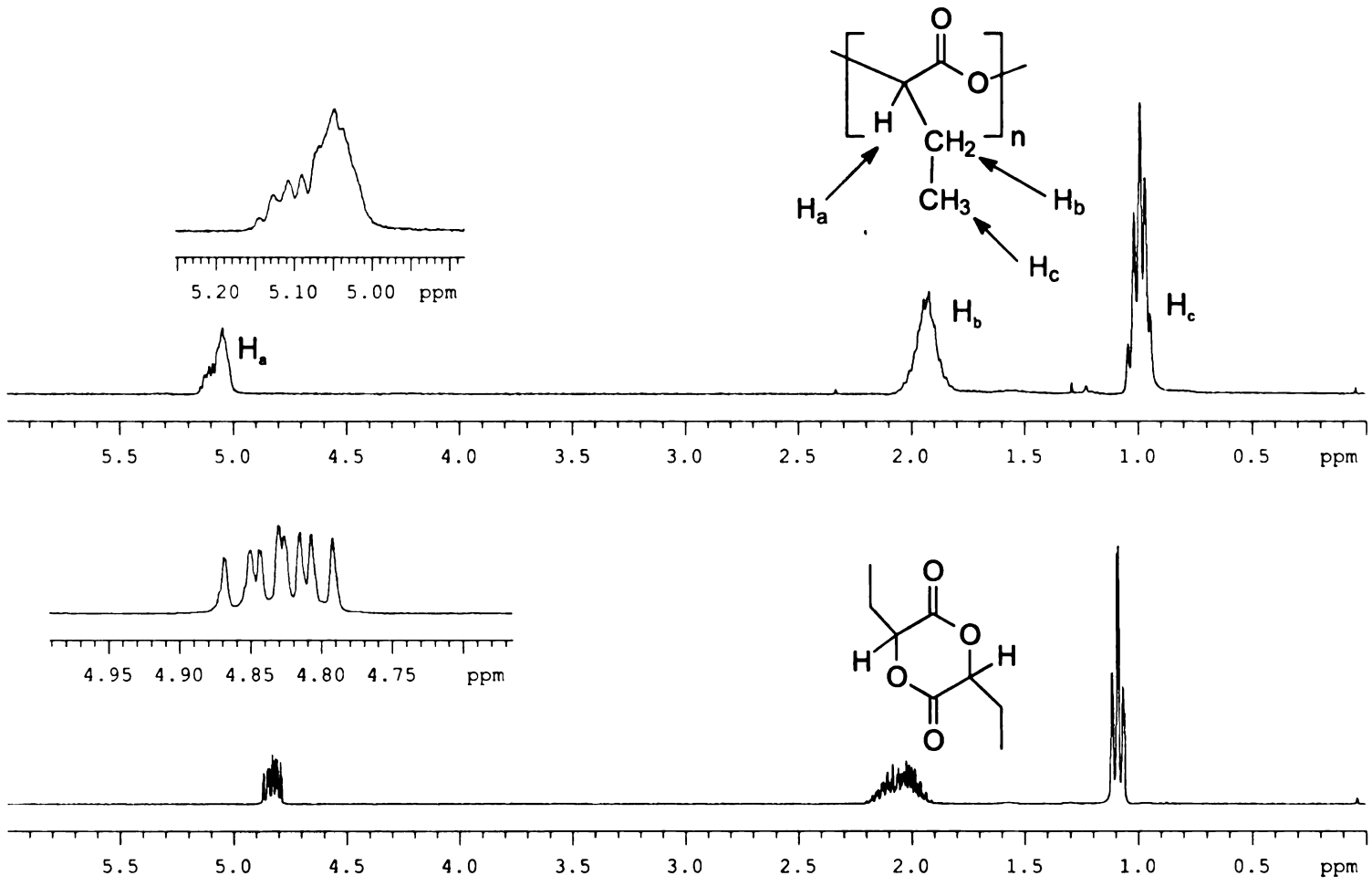

Figure 11. ^{1}H NMR of ethylglycolide and poly(ethylglycolide)

2. Bulk polymerization of substituted lactides

Bulk polymerizations are solvent-free polymerizations, which are usually run at temperatures higher than the melting point of the monomer. Because of the high concentration of the monomer and high polymerization temperature typically found in bulk polymerizations, the bulk polymerization rate and polymer yield is very high. However, because of the high polymerization temperature, bulk polymerizations are usually accompanied by side reactions which limit control of the polymerization. In contrast, in solution polymerization the monomers are dissolved in organic solvents and the polymerization can be conducted at very low temperatures. Compared to bulk polymerization, solution polymerization provides better control over molecular weight and molecular weight distribution. For example, lactide has been polymerized using both bulk polymerization and solution polymerization. The bulk polymerizations are usually run from 110 °C to 180 °C and polymerizations finish within several hours. Side reactions such as transesterification, racemization and discoloration always accompany polymerization, and thus the control over molecular weight and molecular weight distribution is poor. Solution polymerizations are usually run from 50 °C to 90 °C and polymerizations may take days to finish. Solution polymerization provides excellent control over the molecular weight and molecular weight distribution of the polymers.

2.1 Initi

lactide

oxides

variety

provid

shown

broad

polym

show

hexyl

often

conv

syste

mole

26,0

mor

poly

Me

ave

fro

17,

2.1 Initiator survey.

Many compounds have been used as catalysts in bulk polymerizations of lactide including metal halides,[82,181,182] metal carboxylates,[46] metal oxides[50,78] and many kinds of organometallic compounds.[183,184] We tested a variety of catalysts for their ability to polymerize substituted glycolides. ^{1}H NMR provides a convenient method for following the polymerization reaction. As shown in **Figure 11** for ethylglycolide, the methine peak at 4.85 evolves into a broad peak at 5.05 ppm during polymerization, and thus the conversion to polymer can be calculated by integration of the two signals. **Tables 5, 6,** and **7** show results from the polymerization of ethylglycolide, isobutylglycolide and hexylglycolide respectively. As shown in **Table 5**, runs without alcohol initiators often gave near-quantitative conversion to polymer, but SnO and $SnBr_2$ gave low conversion and low molecular weights. Both SnO and $SnBr_2$ are heterogeneous systems and the poor activity is not surprising. However, the number average molecular weight obtained from soluble initiators varied greatly, ranging from 26,000 for Sn(2-ethylhexanoate)$_2$ to > 100,000 for Ph_4Sn. Given a 100:1 monomer to initiator ratio and complete participation by all initiator added to the polymerization, the M_n for these polymerization should be near 17,000. Membrane osmometry results obtained in toluene indicate that the number average molecular weight of poly(ethylglycolide) and polystyrene determined from GPC data are comparable, and thus number-average molecular weights > 17,000 are consistent with incomplete initiation. The effect of adding alcohol as

initiato

conve

polym

polym

ethylh

Thus,

of lac

initiat

contr

adde

are p

impu

poly

(Fig

are

buty

rela

The

hig

and

initiator (second row of each entry) is clear. All of initiators surveyed gave high conversions and molecular weights close to the theoretical values for M_n.

Sn(2-ethylhexanoate)$_2$ is the most efficient catalyst known for the bulk polymerization of lactide. Lactide polymerizations using this catalyst have high polymerization rates and require small catalyst loads. Also, Sn(2-ethylhexanoate)$_2$ produces high molecular weight polylactides in high yield. Thus, Sn(2-ethylhexanoate)$_2$ was our primary choice of catalyst.

Because most proposed mechanisms for solution and bulk polymerization of lactide using Sn(2-ethylhexanoate)$_2$ invoke participation of water or alcohol as initiators, we added *t*-butylbenzyl alcohol (BBA) to polymerizations to gain better control of the molecular weight and the molecular weight distribution. Without the added alcohol, the polymerization is initiated by residual moisture or alcohols that are present as impurities in the polymerization, and because the amount of such impurities vary from run to run, the initiation efficiency should also vary. The polymerization of ethylglycolide shows the importance of the added alcohol (**Figure 12**). The results from six Sn(2-ethylhexanoate)$_2$ initiated polymerizations are shown, three without an alcohol initiator, and three where one equivalent of *t*-butylbenzyl alcohol was added. Runs with added alcohol show a linear relationship between molecular weight and conversion up to >60% conversion. The data from the three runs without alcohol are more scattered, especially at high conversion, showing that added alcohol improved the efficiency of initiation and provides better control of molecular weight.

poly

mol

theo

for

one

betw

has

attrib

and

Figure 13 shows the evolution of molecular weight with conversion for the polymerization of lactide, ethylglycolide, isobutylglycolide and hexylglycolide. The molecular weight increases linearly with conversion and nearly reaches the theoretical values, 14,000 for polylactide, 17,000 for poly(ethylglycolide), 23,000 for poly(isobutylglycolide) and 28,000 for poly(hexylglycolide). These data show one characteristic expected of a living polymerization, a linear relationship between M_n and conversion. The drop in molecular weight at the end of the run has been observed previously in lactide polymerizations,[92,185] and is usually attributed to intramolecular transesterification reactions that form cyclic products and decrease the number average molecular weight.

Entr

1

2

3

4

5

[e

a

data for

([ethylgly

Table 5. Bulk Polymerization of Ethylglycolide

Entry	Catalyst	%converion[a]	$M_n \times 10^{-3}$	M_w/M_n
1	$Sn(Oct)_2$	99	26.2	2.00
		95	16.0	1.73
2	Ph_4Sn	95	114	1.33
		96	15.5	1.88
3	SnO	7	5.4	1.15
		94	14.9	1.86
4	PbO	96	31.7	1.65
		97	13.9	1.90
5	$SnBr_4$	98	37.7	1.78
		98	15.2	1.89
6	$SnBr_2$	61	13.3	1.64
		97	13.9	1.82

[ethylglycolide]:[catalyst] = 100: polymerization run at 180 °C for 2.5 hours

a. determined by ^1H NMR; top and bottom entries for each catalyst are data for polymerization with no alcohol added and with neopentyl alcohol ([ethylglycolide]/[alcohol]=100) as the initiator, respectively.

Table 6. Bulk Polymerization of Isobutylglycolide

Entry	Catalyst	%converion[a]	$M_n \times 10^{-3}$	M_w/M_n
1	$Sn(Oct)_2$	97	37.1	2.00
		96	22.2	1.65
2	Ph_4Sn	95	50.2	1.97
		96	21.3	1.88
3	SnO	45	10.9	1.23
		94	20.8	1.84
4	PbO	96	41.9	1.65
		97	22.9	1.90
5	$SnBr_4$	98	57.1	1.88
		98	20.5	1.78
6	$SnBr_2$	76	31.2	1.84
		97	21.8	1.89

[isobutylglycolide]:[catalyst] = 100: polymerization run at 180 °C for 2.5 hours

a. determined by ^1H NMR; top and bottom entries for each catalyst are data for polymerization with no alcohol added and with neopentyl alcohol ([isobutylglycolide]/[alcohol]=100) as the initiator, respectively.

Table 7. Bulk Polymerization of Hexylglycolide

Entry	Catalyst	%converion[a]	$M_n \times 10^{-3}$	M_w/M_n
1	$Sn(Oct)_2$	95	53.2	1.92
		97	26.8	1.93
2	Ph_4Sn	93	43.4	1.83
		96	25.5	1.78
3	SnO	31	13.5	1.19
		97	27.9	1.81
4	PbO	94	67.7	1.95
		98	25.9	1.82
5	$SnBr_4$	95	47.1	1.88
		99	26.9	1.89
6	$SnBr_2$	32	17.3	1.54
		96	23.2	1.87

[hexyllglycolide]:[catalyst] = 100: polymerization run at 180 °C for 2.5 hours

a. determined by ^1H NMR; top and bottom entries for each catalyst are data for polymerization with with no alcohol added and with neopentyl alcohol ([hexylglycolide]/[alcohol]=100) as the initiator, respectively.

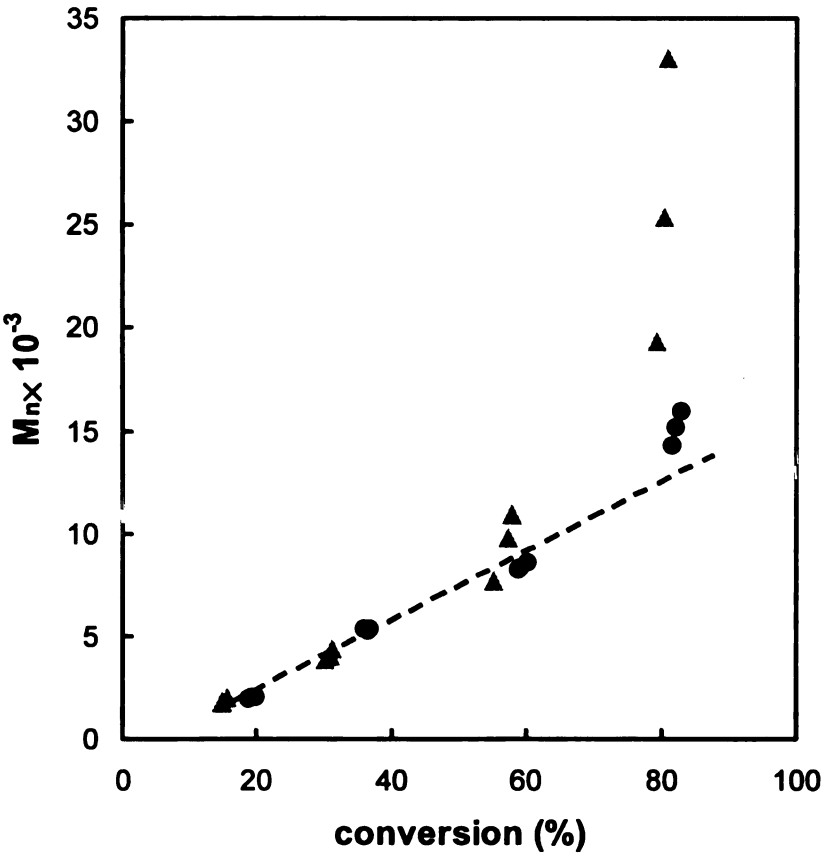

Figure 12. Bulk polymerization of ethylglycolide with (●) and without (▲) added *t*-butylbenzyl alcohol as co-initiator. Polymerization conditions: 130 °C, $[Sn(Oct)_2]/[t\text{-butylbenzyl alcohol}] = 1$, [Monomer]/[Initiator] = 100.

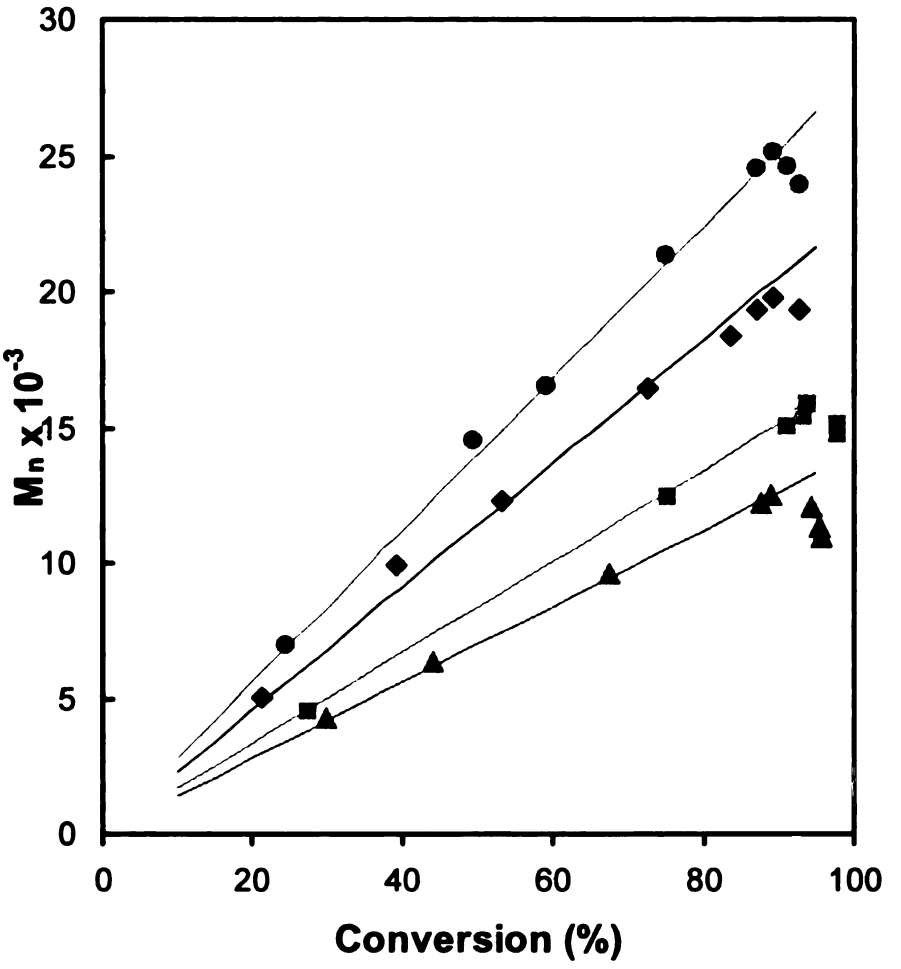

Figure 13. Molecular weight versus conversion for the bulk polymerization of substituted glycolides. (▲) lactide, (■) ethylglycolide, (●) hexylglycolide, (◆) isobutylglycolide. Polymerization condition: 130 °C, [$Sn(Oct)_2$]/[*t*-butylbenzyl alcohol] = 1, [Monomer]/[Initiator] = 100.

2.2 Kinetics of Bulk Polymerization

Ring-opening polymerizations of lactides and lactones typically follow first order kinetics that can be expressed by Eq. (1)

$$R = -\frac{d[M]}{dt} = k_p[M][I] \quad \text{.....(1)}$$

where [M] and [I] are the concentration of monomer and initiator, and k_p is the rate constant for propagation. For the case of a living polymerization, [I] is constant and integration of Eq. (1) yields:

$$-\ln(\frac{[M]_t}{[M]_0}) = k_p[I]_0 t \quad \text{.....(2)}$$

where $[M]_t$ is the concentration of the monomer at time t, $[M]_0$ is the initial monomer concentration (at t=0) and $[I]_0$ is the initial concentration of initiator. For living polymerizations, $[I]$ is constant and plots of $-ln([M]_t/[M]_0)$ vs. t are linear. **Figure 14** shows kinetic data for several substituted lactides. After a fast initial polymerization, the rate slows as the conversion exceeds 80% ($-ln([M]_t/[M]_0)$=1.6). The data for low conversions are shown in **Figure 15**, and from each data set, $k_p[I]$ values were extracted from slopes of the linear portion of the the plots. However, the data in **Figure 14** also show strong deviation from linearity at conversions above 80%, and that the conversion saturated near 97% conversion.

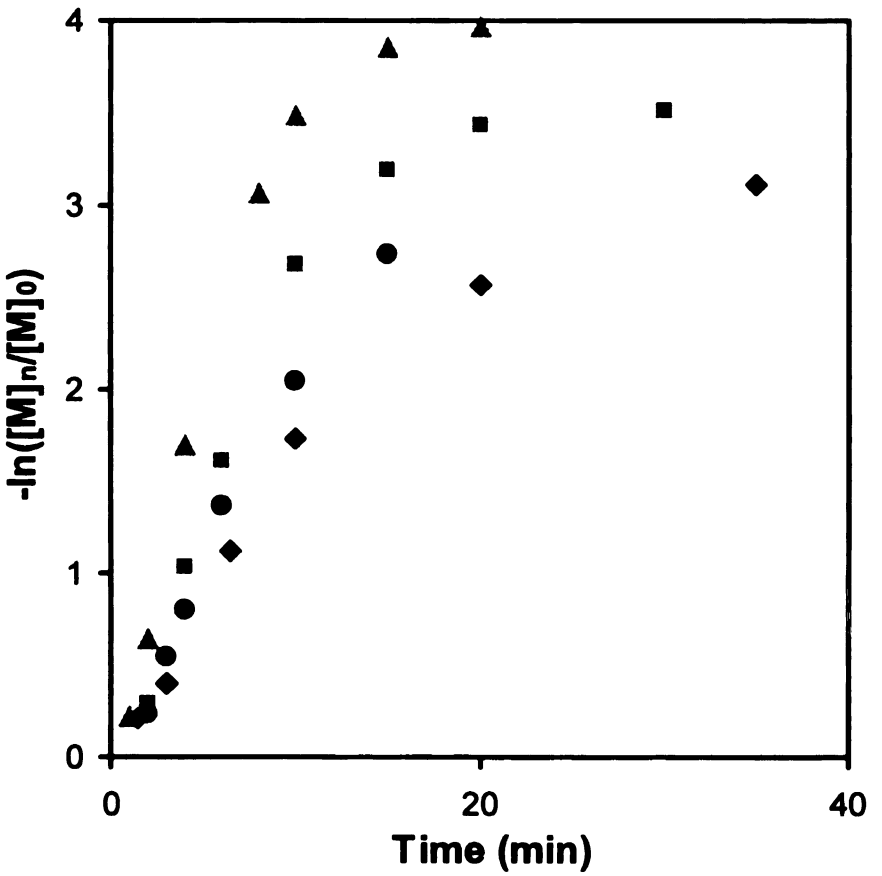

Figure 14. Kinetics of bulk polymerization of substituted glycolides. (▲) lactide, (■) ethylglycolide, (●) hexylglycolide, (◆) isobutylglycolide. Polymerization conditions: 130 °C, [$Sn(Oct)_2$]/[*t*-butylbenzyl alcohol] = 1, [Monomer]/[Initiator] = 100

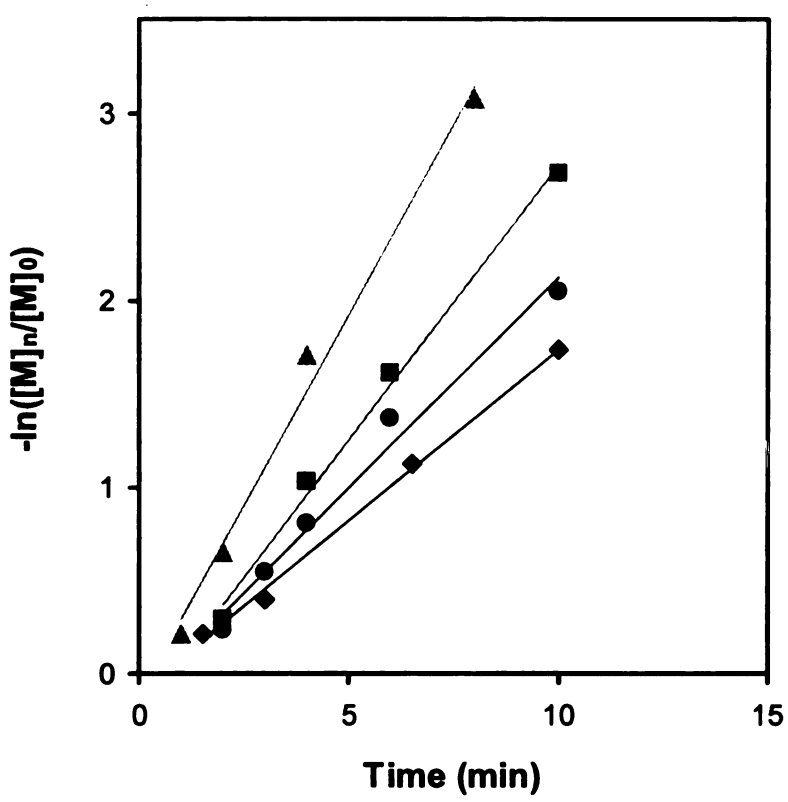

Figure 15. Kinetics of bulk polymerization of substituted glycolides at low conversion. (▲) lactide, (■) ethylglycolide, (●) hexylglycolide, (◆) isobutylglycolide. Polymerization conditions: 130 °C, $[Sn(Oct)_2]$/[*t*-butylbenzyl alcohol] = 1, [Monomer]/[Initiator] = 100

From **Figure 14** and **Figure 15**, we learned that bulk polymerizations of substituted lactides are first order in the concentration of monomer and first order in the concentration of initiator at low conversion. At high conversion, the polymerization rate begins to drop and finally polymerization stops without reaching 100% conversion. This phenomenon has been reported in the literature.[92,93] Witzke *et al.*[87] explained it using an equilibrium polymerization model. However, we think there are two possibilities that can influence the polymerization kinetics. First, the polymerization is an equilibrium reaction, second, the initiator continuously degrades during the polymerization. The possibility of catalyst decay came from the solution polymerization of ethylglycolide, where we recovered a precipitate from the polymerizations. We believe it has the structure shown in **Figure 16**. This precipitation may represent catalyst lost from the solution polymerization (discussed later).

We used these two models to fit the kinetic data that we obtained from bulk polymerization. If the polymerization is an equilibrium reaction, the kinetics of the polymerization can be expressed using following equations.[87]

$$[M]_t = [M]_{eq} + ([M]_0 - [M]_{eq})e^{-k_p[I]t} \quad \text{.....(1)}$$

$$X = (1 - \frac{[M]_{eq}}{[M]_0})(1 - e^{-k_p[I]t}) \quad \text{.....(2)}$$

where $[M]_{eq}$ is the monomer concentration at equilibrium, X is the conversion $(([M]_0-[M]_t)/[M]_0)$, and k_p is rate constant for polymerization. We fit the data using equation (2). The results shown in **Figure 17** show that the fit was good.

If the initiator continuously degrades during the polymerization, the kinetics of the polymerization can be expressed as:

$$P = -\frac{d[M]}{dt} = k_p[M][I]e^{-k_d t} \quad \text{.....(3)}$$

where k_d is the rate constant for catalyst decay. Integration of equation (3) yields

$$-\ln(\frac{[M]_t}{[M]_0}) = \frac{k_p}{k_d}[I]_0(1-e^{-k_d t}) \quad \text{.....(4)}$$

We also used equation (4) to fit the kinetic dat the result is shown in **Figure 18.** Unfortunately, the data also fits equation (4) well. Thus, we still can not decide which model correctly describes the kinetics of the lactide polymerization.

To decide which model is appropriate, we studied the depolymerization reaction. If the lactide polymerization is indeed an equilibrium reaction, depolymerization should give us the same $[M]_{eq}$ as polymerization. We scrupulously purified the polymers to remove all monomer in the polymer, and we conducted polymerization and depolymerization using the same conditions. The

results are shown in **Figure 19**. The polymerization and depolymerization indeed reached the same $[M]_{eq}$, about 3%. The white precipitate recovered from solution polymerization was tested as a catalyst for the bulk polymerization of ethylglycolide. The polymerization also reached 97% conversion. These experiments proved that the equilibrium model is the right model.

At low conversion, the polymerization is first order in monomer concentration with characteristics of a living polymerization. For a first order reaction, the kinetics can be expressed as:

$$R = -\frac{d[M]}{dt} = k_p[M][I] \quad \text{.....(5)}$$

where [M] and [I] are the concentration of monomer and initiator, and k_p is the rate constant for propagation. For the case of a living polymerization, [I] is constant and integration of Eq. (5) yields

$$-\ln(\frac{[M]_t}{[M]_0}) = k_p[I]_0 t \quad \text{.....(6)}$$

where $[M]_t$ is the concentration of the monomer at time t, $[M]_0$ is the initial monomer concentration (at t=0) and [I] is the concentration of initiator

From **Figure 15**, we know that the plot of $-ln([M]_t/[M]_0)$ vs. t is linear at low conversion. The slope is $k_p[I]$, which is the rate constant for lactide polymerization. The correct fit to the kinetic model should produce the same $k_p[I]$.

The results (**Table 8**) show that the $k_p[I]$ values obtained from the equilibrium model are consistent with those obtained from the fit to the first order reaction, and that the catalyst degradation model dramatically overestimates the $k_p[I]$. These $k_p[I]$ data indirectly support that equilibrium model as the correct model to describe the kinetics of lactide polymerization.

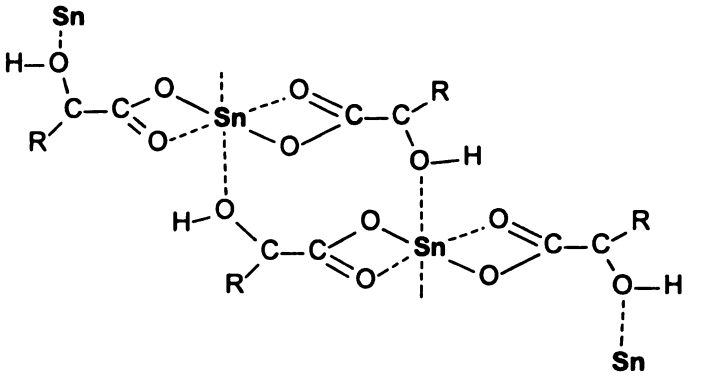

Figure 16. The structure of the white precipitate formed during the solution polymerization of ethylglycolide using $Sn(Oct)_2$/ROH as initiator

Table 8. The kinetic data for bulk polymerization of substituted lactides

	$K_p[I]$ (sec^{-1}) $\times 10^3$		
Monomer	**from conversion vs. time data**	**from fit to equilibrium model**	**from fit to catalyst degradation model**
lactide	6.2	6.7	15.1
ethylglycolide	4.8	4.7	10.8
hexylglycolide	3.7	3.7	6.7
isobutylglycolide	3.0	3.0	5.3

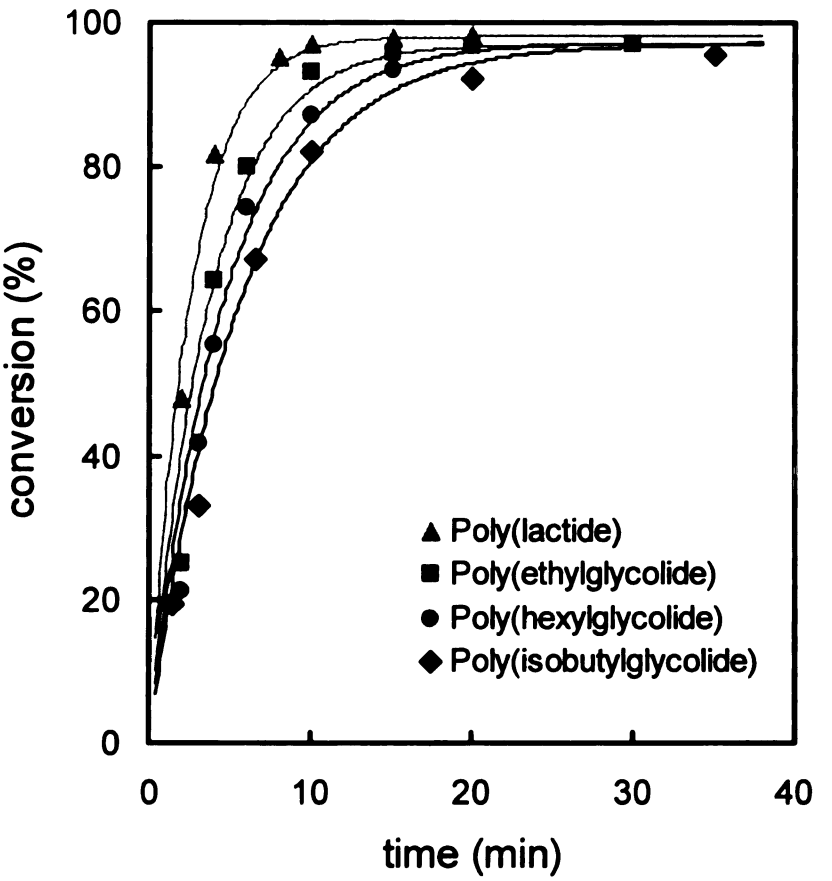

Figure 17 Kinetics of bulk polymerization of substituted glycolide. (▲) lactide, (■) ethylglycolide, (●) hexylglycolide, (◆) isobutylglycolide. Polymerization condition: 130 °C, $[Sn(Oct)_2]/[t\text{-butylbenzyl alcohol}]=1$, [Monomer]/[Initiator]=100. The data were fitted using an equilibrium model.

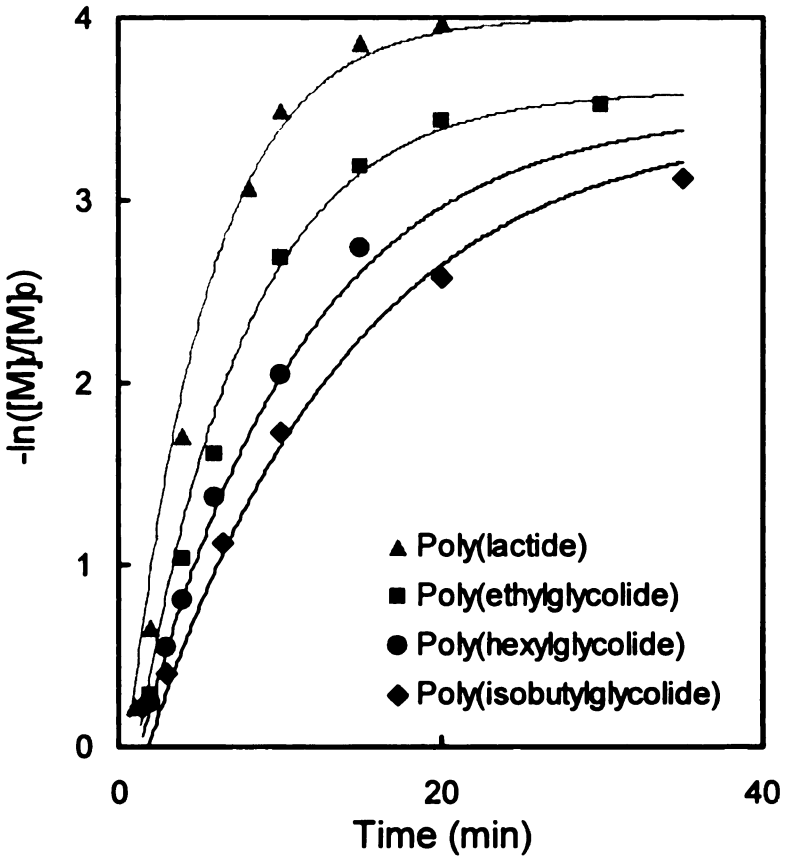

Figure 18. Kinetics of bulk polymerization of substituted glycolide. (▲) lactide, (■) ethylglycolide, (●) hexylglycolide, (◆) isobutylglycolide. Polymerization condition: 130 °C, $[Sn(Oct)_2]$/[*t*-butylbenzyl alcohol]=1, [Monomer]/[Initiator]=100. The data were fitted using the initiator degradation model.

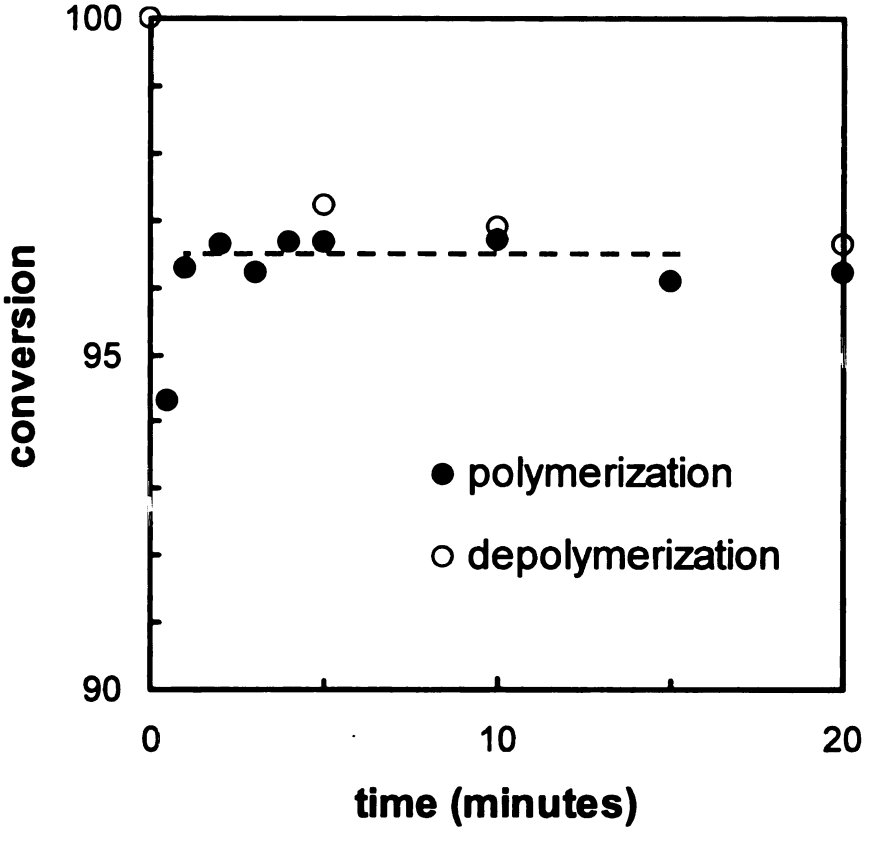

Figure 19. Polymerization/depolymerization data for the bulk polymerization of ethylglycolide. Conditions: 200 °C $[Sn(Oct)_2]$/[BBA]=1 [monomer]/[catalyst]=100

Ring opening polymerization of substituted lactides is facile, though a bit slower than lactide itself. The propagation step of glycolide polymerization is depicted in **Scheme 31**. The glycolide ring is arbitrarily drawn in a planar conformation with the R group in an equatorial position, although a more realistic representation would need to account for the boat-like conformation of the ring seen from x-ray studies and the mixture of glycolide diastereomers used in the polymerization. The polymerization rate of glycolide is faster than lactide (R = CH_3), because the steric bulk of the methyl group hinders nucleophilic attack at the ring carbonyls. Increasing the size of the ring substitutent should decrease the polymerization rate further. Returning to **Figure 15**, we see that the rates of polymerization follow the expected trend: lactide> ethylglycolide> hexylglycolide> isobutylglycolide. A survey of lactide monomers by Hall[186] showed that ring substitution plays a major role in defining the polymerizability of lactide. For example, 3,3,6,6-tetramethyl-1,4-dioxane-2,5-dione, obtained by adding two methyl groups to the lactide ring, does not undergo ring-opening polymerization. Presumably, nucleophilic attack by either the initiator or the growing polylactide chain is too hindered to lead to polymer.

Scheme 31. The propagation step for lactide polymerization using Sn(2-ethylhexanoate)$_2$ as catalyst

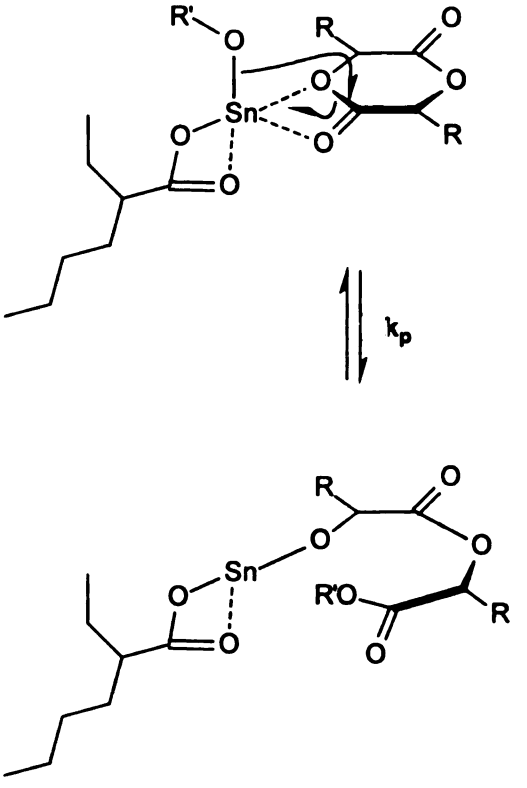

3. Solution Polymerization of Substituted Lactides

Solution polymerizations exhibit different polymerization behavior than bulk polymerizations. Because of the added solvent, the concentration of the monomer is lower and the propagation rate, $k_p[M][M^*]$, is reduced. Also, solution polymerizations are run at lower temperatures than bulk polymerization, usually lower than boiling point of the solvent. Because of the lower polymerization temperature, control of molecular weight and the molecular weight distribution is much better and there are fewer side reactions. The solvents used in solution polymerizations of lactide include toluene, THF and CH_2Cl_2. The most commonly used solvent is toluene. We choose $Al(OiPr)_3$ and Sn(2-ethylhexanoate)$_2$/alcohol as initiators since $Al(OiPr)_3$ is known to be a good initiator for solution polymerization of lactide, while the Sn(2-ethylhexanoate)$_2$/alcohol system is commonly used for bulk polymerization. We wanted to evaluate the Sn system under solution polymerization conditions, since studying the more controlled solution polymerization can help us understand more about the polymerization mechanism when Sn(2-ethylhexanoate)$_2$ is used as catalyst for bulk polymerization.

3.1 $Al(OiPr)_3$ as Initiator

$Al(OiPr)_3$ is well-known to initiate living lactide polymerization, where the molecular weight grows linearly with conversion and the polymerization follows first order kinetics. Plots of $-ln([M]_t/[M]_0)$ versus t should be linear. The

substituted lactides have structures similar to lactide, so we should expect the polymerization of substituted lactides also to be living and follow first-order kinetics. The molecular weight versus conversion data are shown in **Figure 20** and a plot of $-ln([M]_t/[M]_0)$ versus t is shown in **Figure 21**. As expected, the polymerization of substituted lactides using $Al(OiPr)_3$ is a living polymerization and follows first order kinetics. From **Figure 20** we can see that $Al(OiPr)_3$ initiates three chains. The molecular weight of polymers can be predicted from the equation:

$$M_n = \frac{[M]}{3 \times [I]} \times M_0$$

where M_n is the number-average molecular weight of polymer, *[M]* is concentration of the monomer, *[I]* is the concentration of the initiator, M_0 is molecular weight of monomer and n is the number of initiating species for the $Al(OiPr)_3$ complex. Since the observed molecular weight is one third that predicted by the [M]/[I] ratio, each isopropoxide must initiate one polymer chain.

Based on the bulk polymerization results, we expected that the rates of the polymerization should follow the order: lactide > ethylglycolide > hexylglycolide > isobutylglycolide, because the steric bulk of the ring substitutents increase in that order. However, the solution polymerization rates do not follow the expected order. Lactide, ethylglycolide and hexylglycolide do follow the expected trend, but isobutylglycolide has the bulkiest side group and the fastest polymerization rate.

To understand this phenomenon, we calculated the activation energy for solution polymerization of substituted lactides. The activation energy can be calculated from the Arrhenius equation:

$$k = Ae^{-\frac{E_a}{RT}}$$

$$\ln k = \ln A - \frac{E_a}{RT}$$

where k is the rate constant, A is a constant of integration called the frequency factor, E_a is the activation energy, R is the gas constant and T is the temperature in Kelvin. When $-ln\ k$ is plotted against $1/T$, the activation energy and frequency factor can be extracted from slope and intercept, respectively.

Polymerizations were run at three temperatures: 70 °C, 90 °C and 100 °C. The results are shown in **Figure 21, Figure 22** and **Figure 23** respectively. The rate constants are shown in **Table 9**. The activation energies were obtained from the plots shown in **Figure 24** and the results are listed in **Table 10**. The results are totally unexpected. We believed that bulkier side groups should hinder attack at the carbonyl group on the lactide ring, and lead to a higher the activation energy. Our expectation that the bulkier side groups should result in the higher activation energies is based on the assumption that the nucleophilic attack on the carbonyl group is the rate-determining step. This might not be the case. The polymerization of lactide includes several mechanistic steps: coordination, nucleophilic attack, and ring opening. Nucleophilic attack might be rate limiting

for linear alkyl substituents, but may not be the rate-determinating step for more bulky or highly substituted lactides.

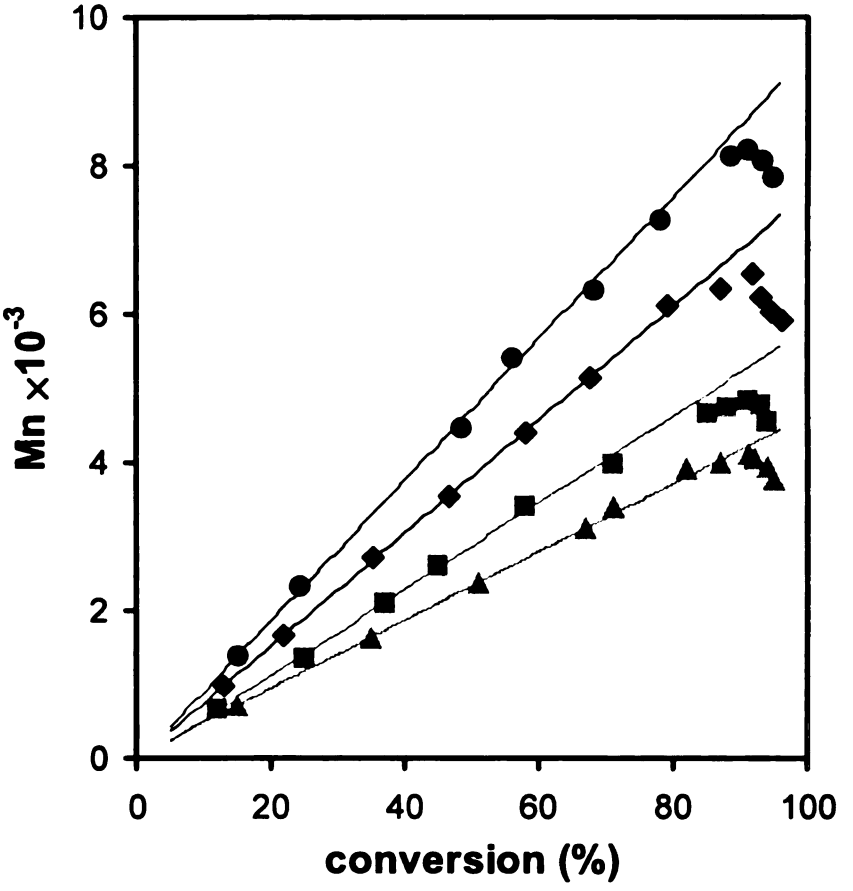

Figure 20. Molecular weight versus conversion for the solution polymerization of substituted lactides. (▲) lactide, (■) ethylglycolide, (●) hexylglycolide, (◆) isobutylglycolide. Polymerization conditions: toluene as solvent, $Al(OiPr)_3$ as initiator, 90 °C, [Monomer]/[Initiator] = 100

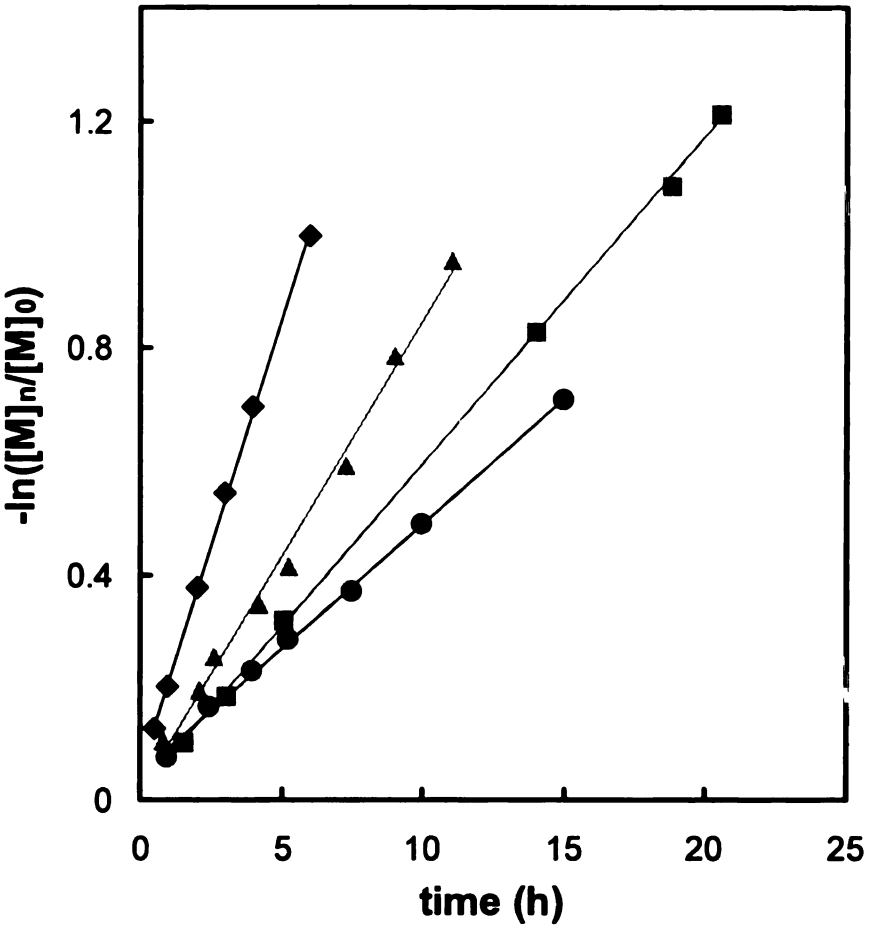

Figure 21 Kinetics for the solution polymerization of substituted lactides at 70 °C. (▲) lactide, (■) ethylglycolide, (●) hexylglycolide, (◆) isobutylglycolide. Polymerization conditions: toluene as solvent, $Al(OiPr)_3$ as initiator, [Monomer]/[Initiator] = 100

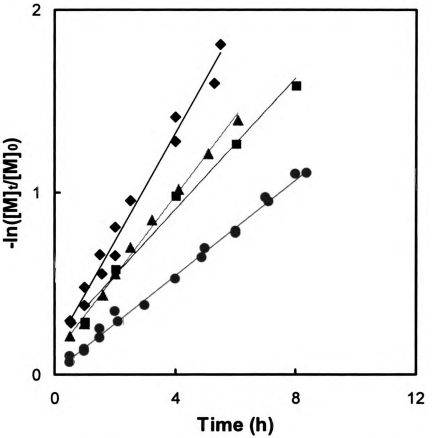

Figure 22 Kinetics for the solution polymerization of substituted lactides at 90 °C, (▲) lactide, (■) ethylglycolide, (●) hexylglycolide, (◆) isobutylglycolide. Polymerization conditions: toluene as solvent, $Al(OiPr)_3$ as initiator, [Monomer]/[Initiator] = 100

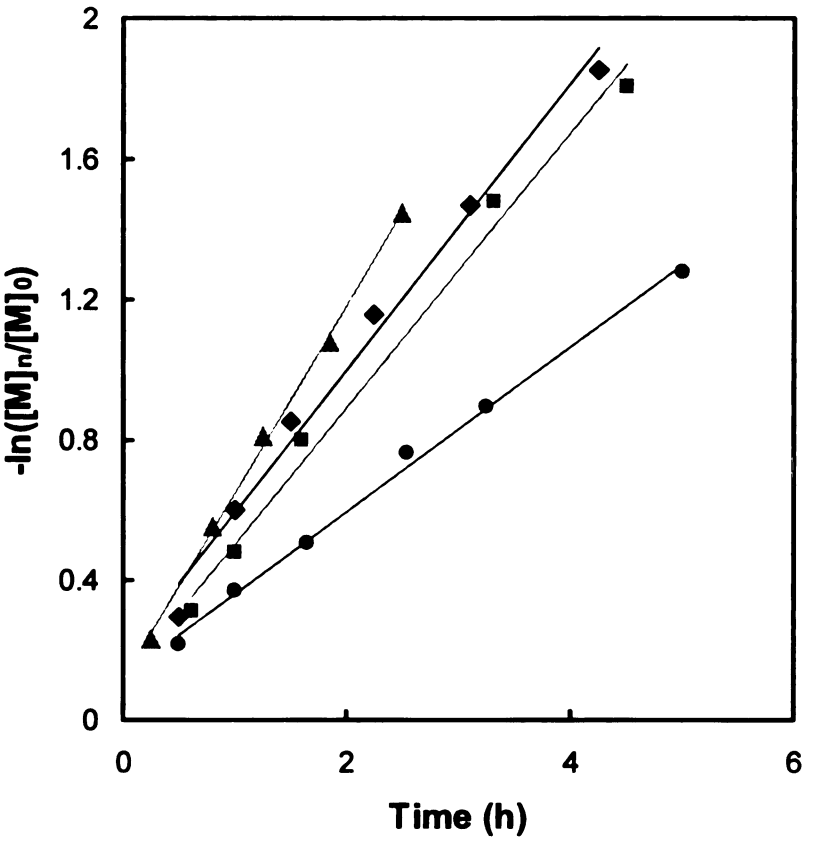

Figure 23 Kinetics for the solution polymerization of substituted lactide 100 °C. (▲) lactide, (■) ethylglycolide, (●) hexylglycolide, (◆) isobutylglycolide. Polymerization condition: toluene as solvent, $Al(OiPr)_3$ as initiator, [Monomer]/[Initiator] = 100

Table 9. Polymerization rate constants of substituted lactides

Monomers	$k_p \times 10^3$ (L/mol·s)		
	70 °C	90 °C	100 °C
lactide	10.5	38.5	73.8
ethylglycolide	8.03	25.0	54.2
hexylglycolide	6.15	18.2	32.6
isobutylglycolide	22.2	40.7	56.6

Table 10. Polymerization activation energies for substituted lactides

Monomers	E_a (kJ/mol)	lnA
lactide	68.8	21.6
ethylglycolide	66.2	20.4
hexylglycolide	58.6	17.4
isobutylglycolide	32.9	9.7

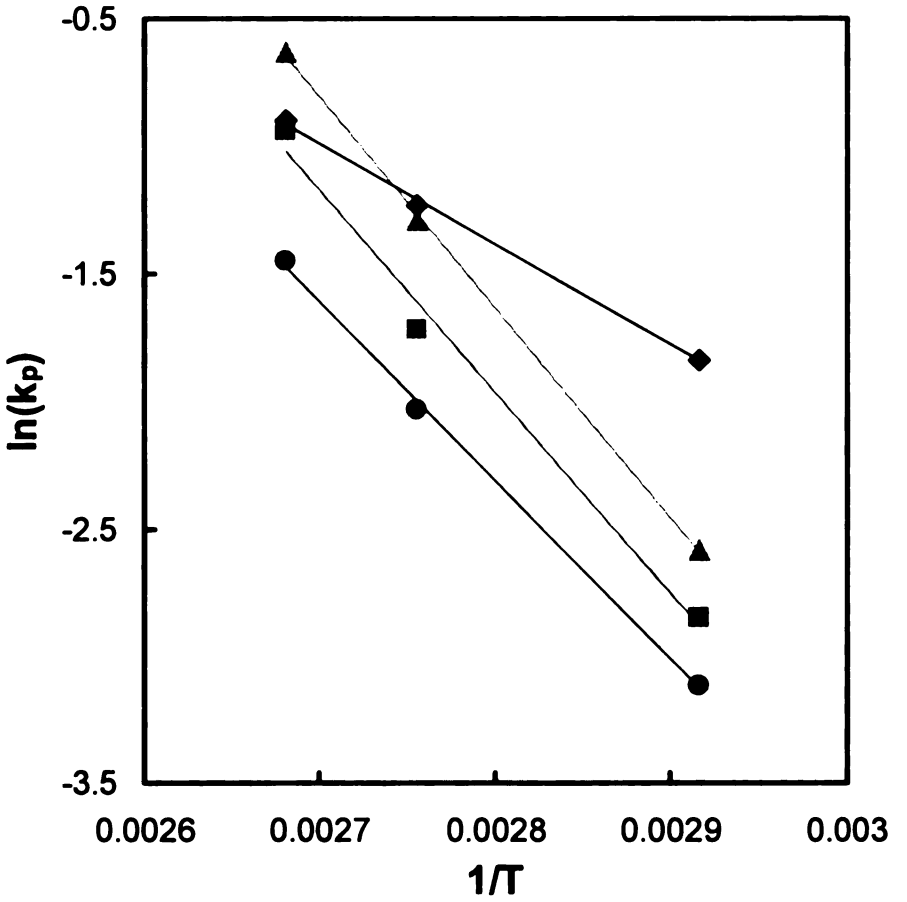

Figure 24. Activation energies for polymerization of substituted lactides

(▲) lactide, (■) ethylglycolide, (●) hexylglycolide, (◆) isobutylglycolide

3.2 $Sn(Oct)_2$/ROH as initiators

The $Sn(Oct)_2$/ROH system is a very good catalyst/initiator system for bulk polymerization, but Its use in solution polymerizations is rarely mentioned in the literature. Also, solution polymerizations have a lower polymerization rate than bulk polymerizations, so it is relatively easy to study the kinetics and mechanism of the $Sn(Oct)_2$/ROH system in solution.

That ROH is the initiator and $Sn(Oct)_2$ is the catalyst often has been claimed in the literature, but direct evidence is lacking. We compared solution polymerization of ethylglycolide initiated by $Sn(Oct)_2$ and by $Sn(Oct)_2$/ROH, where ROH is neopentyl alcohol. The results are shown in **Figure 25**. The diamonds of **Figure 25** are the data for polymerization initiated by only $Sn(Oct)_2$ where moisture and impurities have been scrupulously excluded. The rate of polymerization (slope of curve) is very low, and the polymerization barely reached 10% conversion. If moisture and impurities are not carefully excluded, polymerizations often showed appreciable conversion. The squres at the top of **Figure 25** show results for a polymerization where one equivalent of neopentyl alcohol was added as initiator. Both higher polymerization rates and conversions are routinely obtained when ROH is used. Hydroxyl-containing compounds such as ROH and H_2O are truly the initiator for the polymerization. The 10% conversion achieved in the bottom trace is likely caused by impurities. No matter how hard you try to exclude moisture and impurities, small-scale polymerizations always are affected by trace impurities. In the bottom trace, the impurities were carefully excluded, which caused the low polymerization rate and low conversion.

To further understand the role of ROH in polymerization, we ran solution polymerizations at different $Sn(Oct)_2$/ROH ratios, while keeping the concentration of ethylglycolide and $Sn(Oct)_2$ constant. The results are shown in **Figure 26** and **Figure 27**. There are two important results. The polymerization follows first order kinetics up to about 70% conversion, and the higher the ROH/$Sn(Oct)_2$ ratio, the faster the polymerization. However, as shown in **Figure 27**, the polymerization rate did not increase by five when the ROH/$Sn(Oct)_2$ ratio was increased by five, which means that the kinetics of the polymerization are not first order in ROH. We ran two solution polymerizations with ROH/$Sn(Oct)_2$=1, and [M]/[$Sn(Oct)_2$]=100 and 200, respectively. The results are shown in **Figure 28** and **Figure 29**. **Figure 29** is the linear part of **Figure 28**. The results show that when the amount of both $Sn(Oct)_2$ and ROH double, the rate of polymerization also doubles, which proves that $Sn(Oct)_2$ and ROH together decide the kinetics of the polymerization.

An explanation for the results is that the first step of the polymerization is an equilibrium between $Sn(Oct)_2$ and ROH as shown in **Scheme 32**. The true initiatior is intermediate (**A**). The concentration of (**A**) can be calculated using equation below:

$$K = \frac{[OctSnOR][HOct]}{[Sn(Oct)_2][ROH]}$$

where *K* is the equilibrium constant.

When [$Sn(Oct_2$]/[ROH]=1, the concentration of initiator (OctSnOR) can be calculated using following equation:

$$[OctSnOR] = \sqrt{K[Sn(Oct)_2][ROH]}$$

so the concentration of initiator (OctSnOR) will double if [$Sn(Oct)_2$] and [ROH] both double. If [ROH] increases, [OctSnOR] will increases, but at a level defined by equation above.

Scheme 32. The first step for lactide polymerization using $Sn(Oct)_2$/ROH

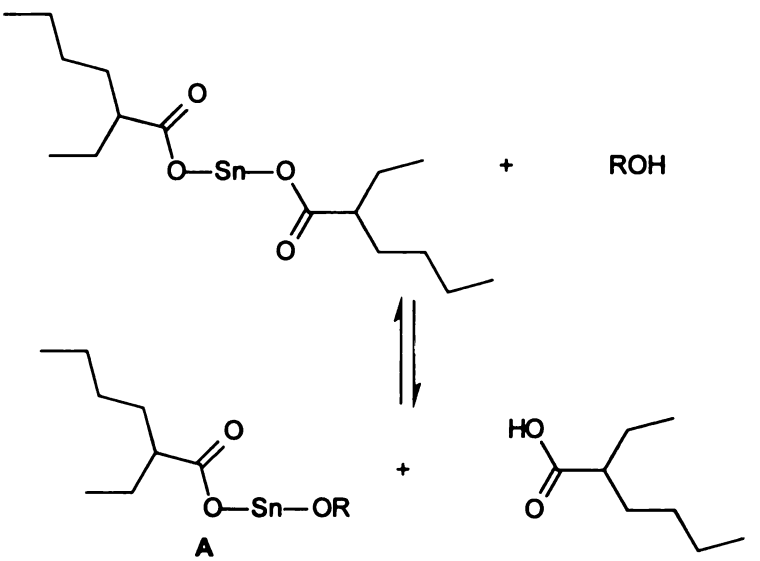

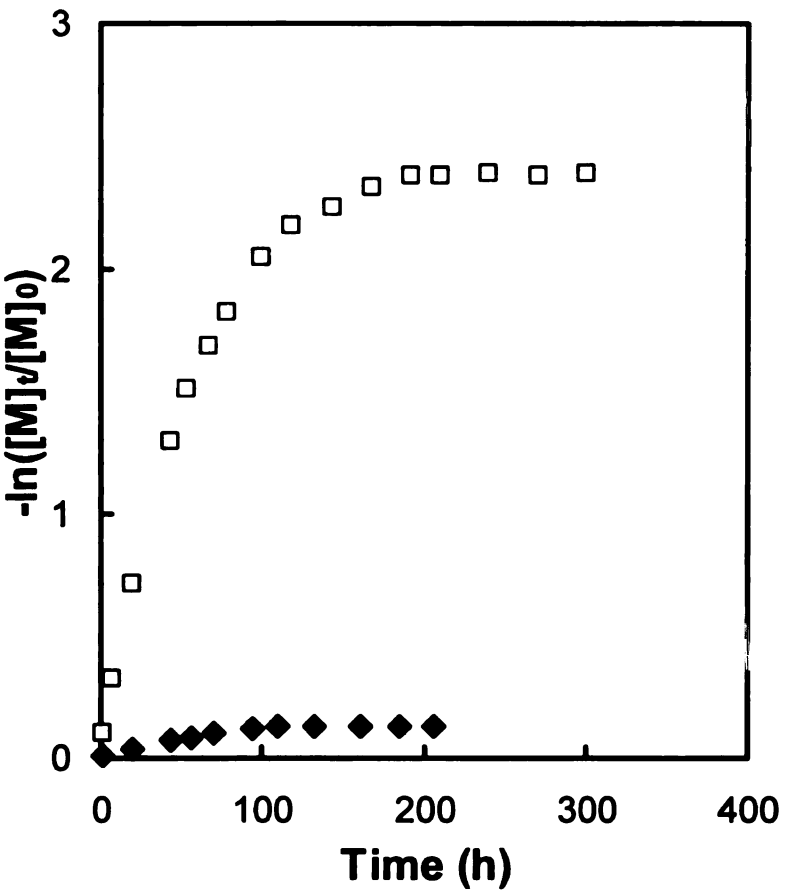

Figure 25 Kinetics for the polymerization of ethylglycolide initiated by $Sn(Oct)_2$/ROH and $Sn(Oct)_2$. (□) $Sn(Oct)_2$/neopentyl alcohol (◆) $Sn(Oct)_2$. Polymerization temperature is 90 °C. $[M]/[Sn(Oct)_2]=100$, $[ROH]/[Sn(Oct)_2]=1$

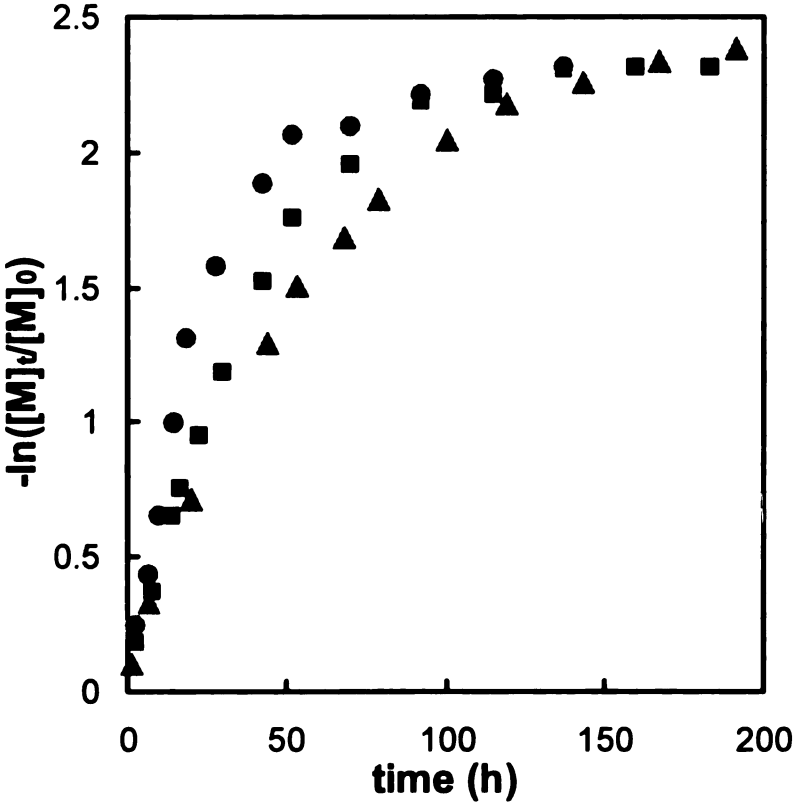

Figure 26 Solution polymerization of ethylglycolide at different $Sn(Oct_2)$/alcohol ratios. Polymerization temperature is 90 °C. (●) $[Sn(Oct_2]/[ROH]=1/10$, (■)$[Sn(Oct_2]/[ROH]=1/5$, (▲) $[Sn(Oct_2]/[ROH]=1$. ROH is neopentyl alcohol. $[M]=0.2$ mol/L, $[M]/[Sn(Oct)_2]=100$.

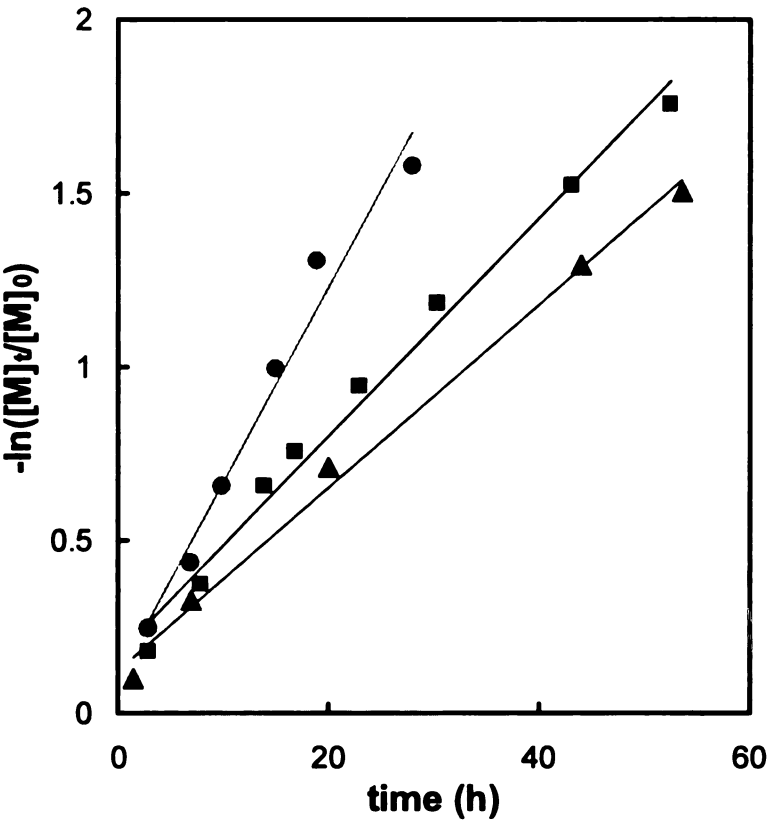

Figure 27 Solution polymerization of ethylglycolide at different $Sn(Oct_2)$/alcohol ratios. Polymerization temperature is 90 °C. (●) $[Sn(Oct_2]/[ROH]=1/10$, (■)$[Sn(Oct_2]/[ROH]=1/5$, (▲) $[Sn(Oct_2]/[ROH]=1$. ROH is neopentyl alcohol. [M]=0.2 mol/L, $[M]/[Sn(Oct)_2]=100$.

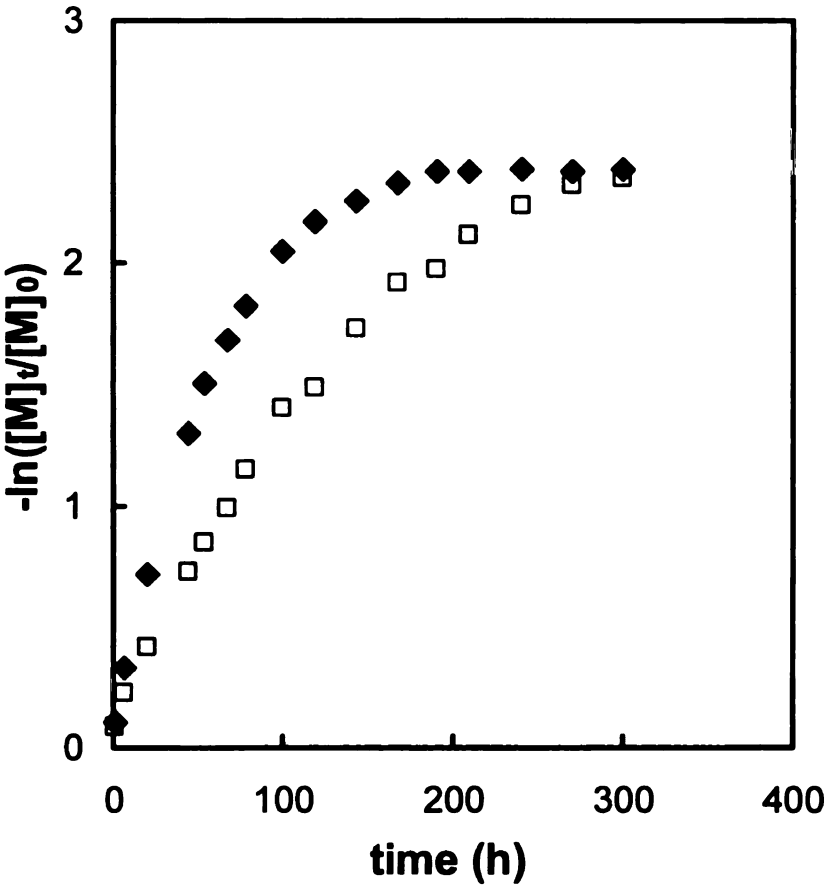

Figure 28 Solution polymerization of ethylglycolide at different monomer/initiator ratio. (□) [M]/[I]=200 (◆) [M]/[I]=100. Polymerization temperature is 90 °C [M]=0.2 mol/L, [ROH]/[$Sn(Oct)_2$]=1

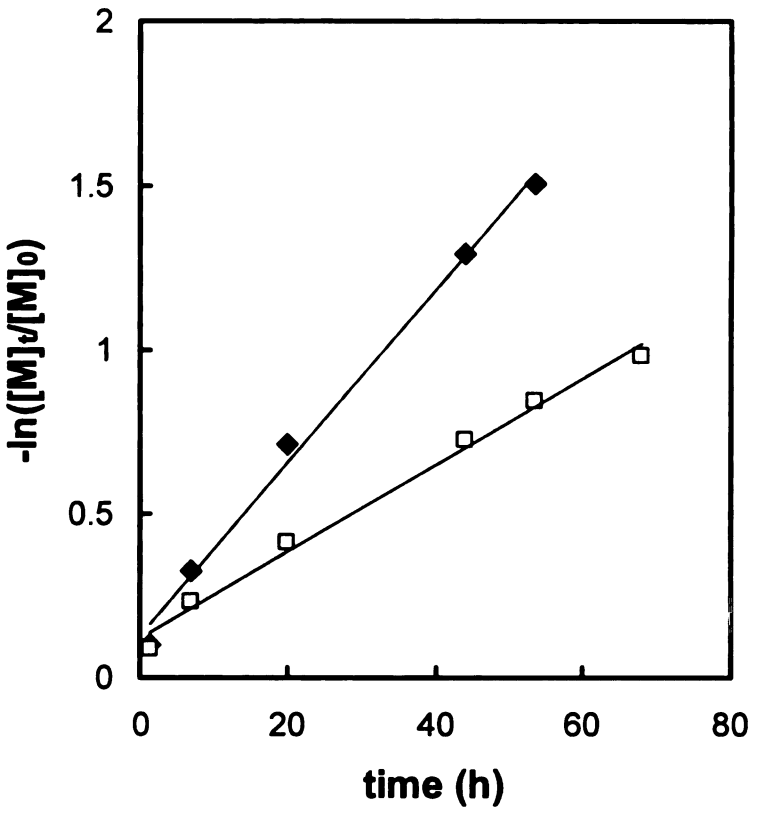

Figure 29 Solution polymerization of ethylglycolide at different monomer/initiator ratio. (❑) [M]/[I]=200 (◆) [M]/[I]=100. Polymerization temperature is 90 °C [M]=0.2 mol/L, [ROH]/[$Sn(Oct)_2$]=1

We also ran solution polymerizations of ethylglycolide at three temperatures 70 °C, 90 °C and 110 °C. The results are shown in **Figure 30** and **Figure 31**. **Figure 31** shows the linear portion of **Figure 30**. These figures provide polymerization rates for ethylglycolide initiated by $Sn(Oct)_2$/BBA at three temperatures (**Table 11**). From these rates, we calculated the activation energy for ethylglycolide polymerization (**Figure 32** and **Table 12**).

Table 11 Polymerization rates for ethylglycolide initiated by $Sn(Oct)_2$/BBA

Monomer	$k_p \times 10^3$ (mol/L•s)		
	70 °C	90 °C	110 °C
ethylglycolide	0.81	2.43	13.1

$[Sn(Oct)_2]/[BBA]=1$, BBA is *t*-butyl benzyl alcohol. $[M]/[Sn(Oct)_2]=100$

Table 12 The activation energy for ethylglycolide initiated by $Sn(Oct)_2$/BBA

monomer	E_a (KJ/mol)	lnA
ethylglycolide	75.68	21.3

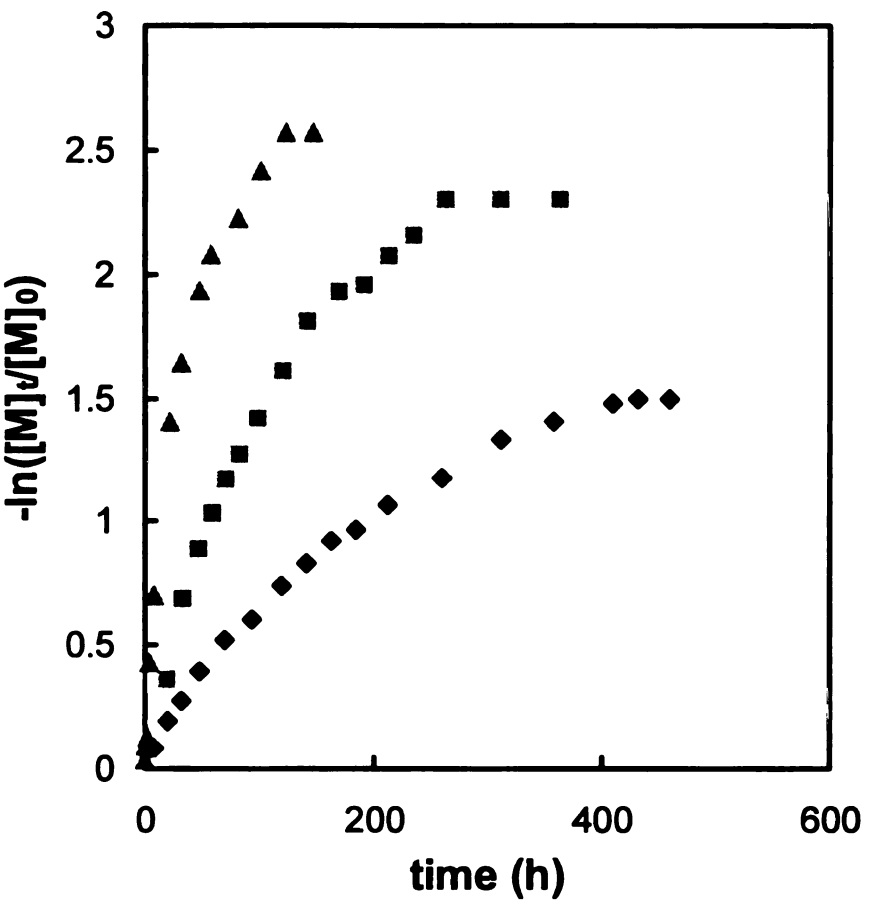

Figure 30 Solution polymerization of ethylglycolide initiated by $Sn(Oct)_2$/BBA. $[Sn(Oct)_2]/[BBA]=1$, BBA is *t*-butyl benzyl alcohol. (▲) 110 °C (■) 90 °C (◆) 70 °C $[M]/[Sn(Oct)_2]=100$

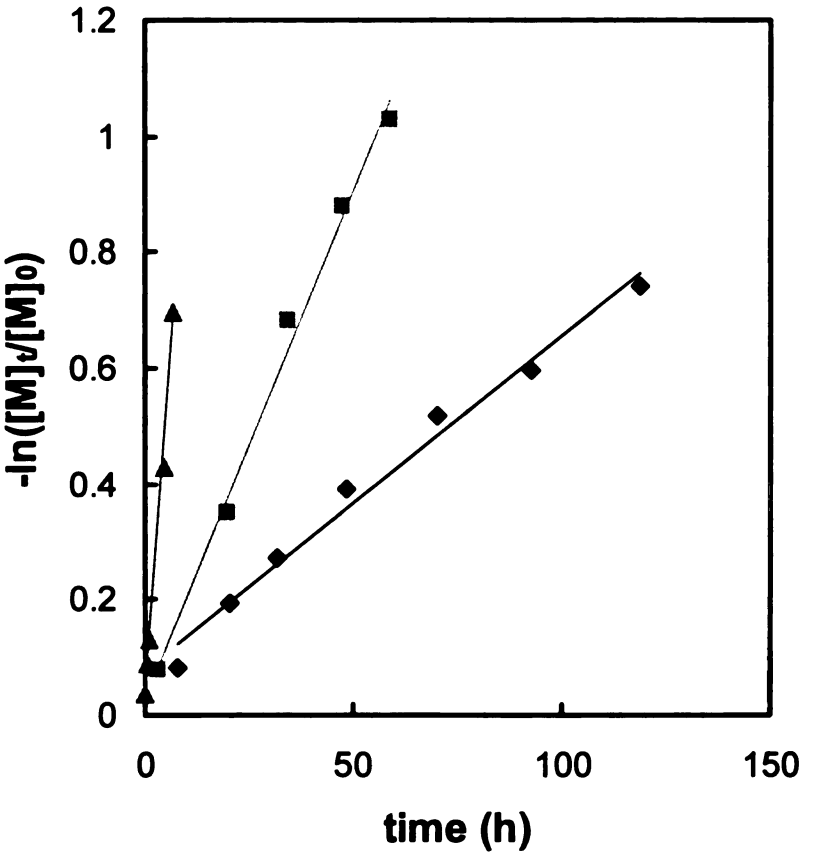

Figure 31 Solution polymerization of ethylglycolide initiated by $Sn(Oct)_2$/BBA. $[Sn(Oct)_2]/[BBA]=1$, BBA is *t*-butyl benzyl alcohol. (▲) 110 °C (■) 90 °C (◆) 70 °C $[M]/[Sn(Oct)_2]=100$

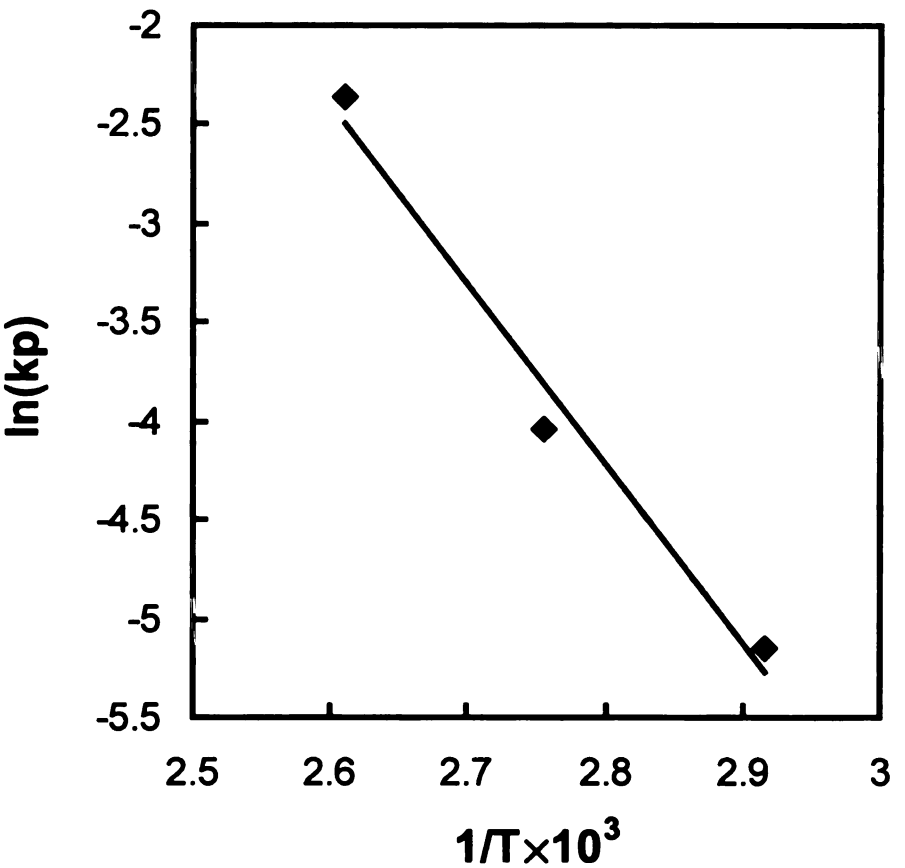

Figure 32 The activation energy of ethylglycolide initiated by $Sn(Oct)_2$/BBA

As mentioned above, we isolated a white precipitate during the solution polymerization of ethylglycolide. Vert *et al.*[89] reported a similar precipitation during polymerization of lactide using $Sn(Oct)_2$.This white precipitate does not dissolve in organic solvents, so we could not directly identify it using NMR. Indirect methods were used to identify this white precipitate. Dissolution of the precipitation in dilute HCl solution, followed by extracting with ether, gave one organic compound, 2-hydroxybutyric acid. Also, when 2-hydroxylbutyric acid was added to $Sn(Oct)_2$, a white precipitation formed instantly. These two precipitates have almost identical IR spectra (**Figure 33**).

How does this white precipitate influence the kinetics of the solution polymerizations? Is it umimportant, as was shown for bulk polymerizations, or does it remove active catalyst from the polymerization and have a significant influence on the polymerization kinetics? To answer these questions, we set up the following experiment. A solution polymerization of ethylglycolide was run until polymerization stopped. A second volume of ethyllgycolide solution equal to that initially used was added to polymerization system. If formation of the precipitate does not influence the kinetics of the solution polymerization, the polymerization should return to its equilibrium state with polymerization rate halved. If all of the catalyst has degraded to the white precipitate, and can not polymerize ethylglycolide, then the polymerization would not return to its equilibrium state and will remain near 50% conversion. The result is shown in **Figure 34**. The initial polymerization reached a plateau at 93% conversion at about 54 hours. Additional monomer solution was added, and the conversion dropped to about

50%. The polymerization then slowly retured to the plateau at >90% conversion. Thus, we can say that the polymerization is indeed an equilibrium reaction. However, we can not ignore the effect of catalyst degradation. As shown in **Figure 35**, the polymerization rate at the beginning of the polymerization and after the monomer solution was added are very different. The initial polymerization rate is almost ten times faster than the polymerization rate after the monomer was added. As mentioned before, if there is no effect from catalyst degradation, the polymerization rate after adding monomer should be half the initial polymerization rate. Since the observed rate is 5 times lower than expected, we conclude that ~80% of the catalyst had precipitated by the time the second portion of monomer was added, and does not participate in polymerization.

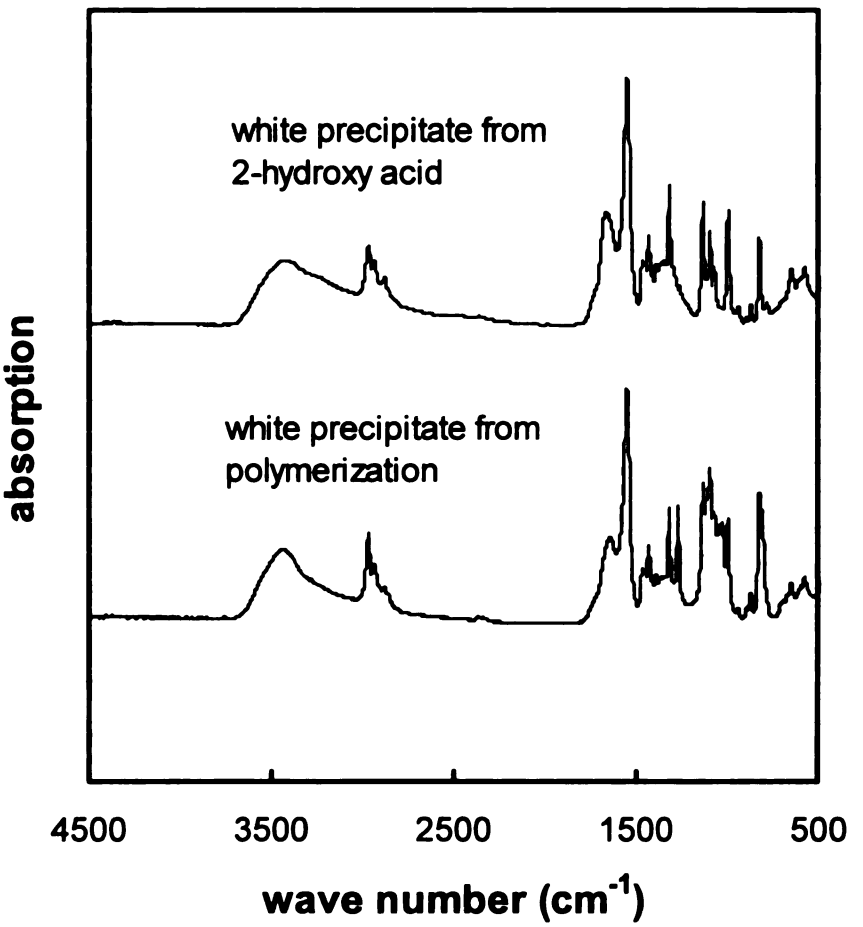

Figure 33. IR spectra for white precipitates formed during polymerization of ethylglycolide and by mixing 2-hydroxylbutyric acid and $Sn(Oct)_2$.

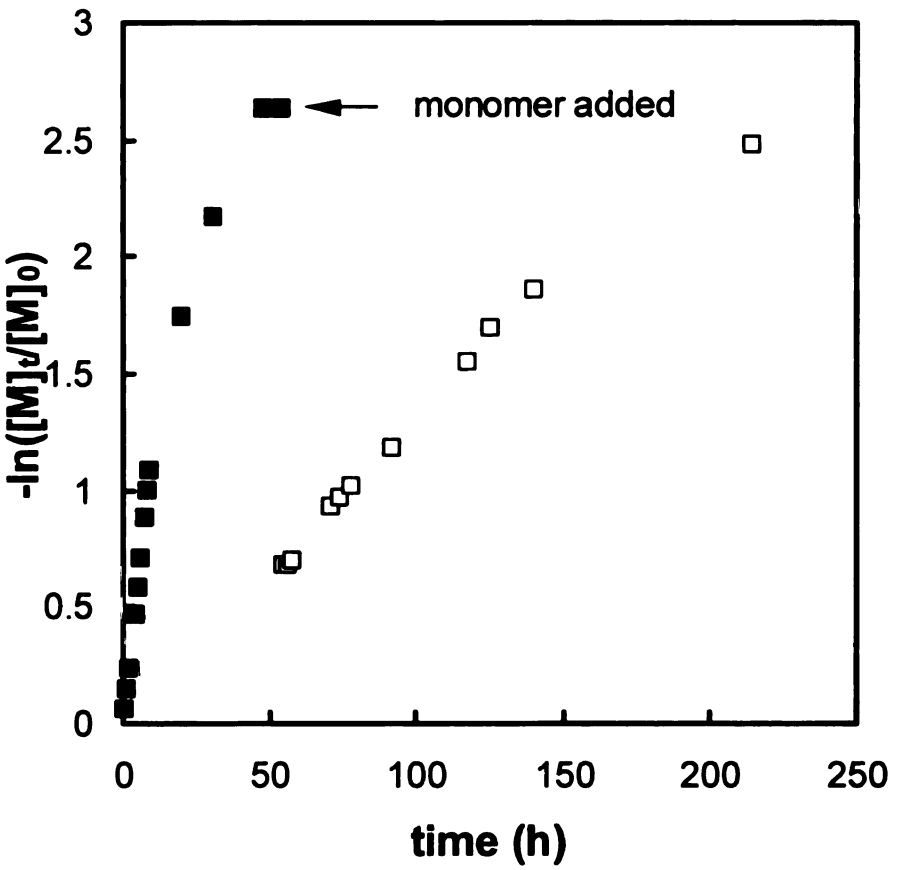

Figure 34. Kinetics of solution polymerization of ethylglycolide showing the result after adding extra monomer after the polymerization reached equilibrium. Polymerization temperature is 90 °C. $[M]/[Sn(Oct)_2]=100$, $[ROH]/[Sn(Oct)_2] = 1$

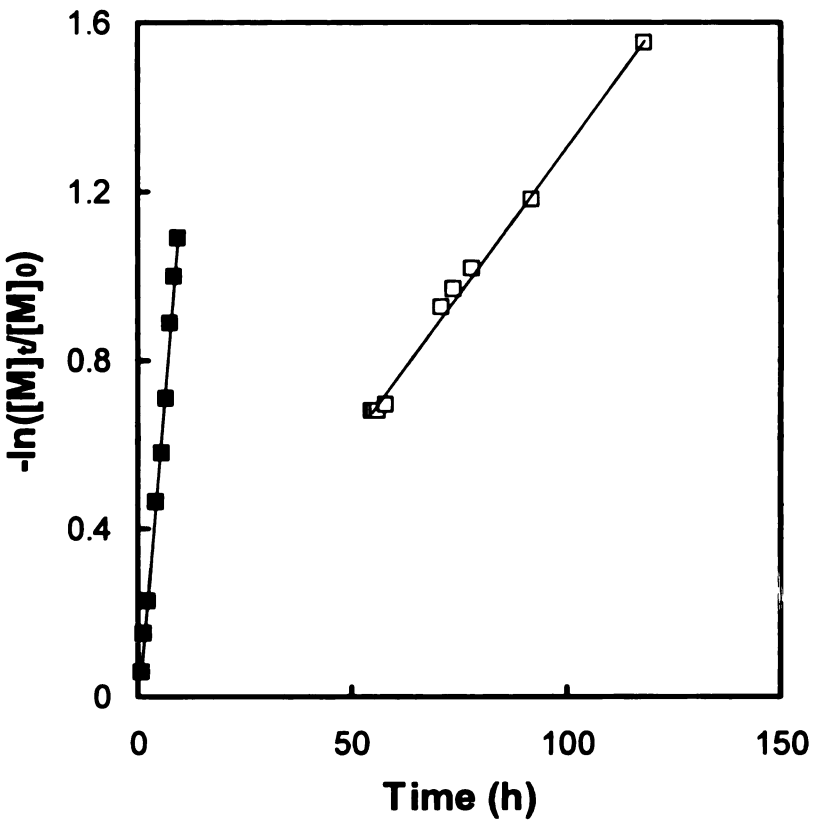

Figure 35. Initial polymerization rate for ethylglycolide and the decreased rate observed after adding addtional monomer. Polymerization temperature is 90 °C. $[M]/[Sn(Oct)_2]=100$, $[ROH]/[Sn(Oct)_2] = 1$

Earlier, we saw that for solution polymerizations using $Al(OiPr)_3$, the polymerization rates for substituted lactides did not follow the order predicted by the steric hindrance of the substituent on the glycolide ring (**Figure 21, 22 and 23**). To determine whether the effect is initiator-related, we ran solution polymerizations of substituted lactides using $Sn(Oct)_2$/BBA instead $Al(OiPr)_3$. The results are shown in **Figure 36**. The results are slightly different, but again the polymerization rates did not follow the order expected based on steric hinderance. For polymerizations using $Al(OiPr)_3$ at 90 °C, the order of the polymerization rate is isobutylglycolide > lactide > ethylglycolide >hexylglycolide, but for polymerization using $Sn(Oct)_2$/BBA, the order is lactide > isobutylglycolide > ethylglycolide > hexylglycolide. These results reflect activation energy differences for the two initiator systems.

3.3 Comparison of $Al(OiPr)_3$ and $Sn(Oct)_2$/ROH as Initiators in Solution Polymerization

$Sn(Oct)_2$/ROH is the best initiator for bulk polymerization of lactides, but it is less effective in solution polymerizations. **Figure 37** shows a comparison of the $Al(OiPr)_3$ and $Sn(Oct)_2$/ROH initiators for solution polymerization of ethylglycolide at 70 °C. The polymerization initiated by $Al(OiPr)_3$ is almost 10 times faster than the polymerization initiated by $Sn(Oct)_2$/ROH. Considering that an $Al(OiPr)_3$ molecule initiates three chains and $Sn(Oct)_2$/BBA only initiates one chain, lactide chains in the $Al(OiPr)_3$ system grow almost three times faster at 70 °C than those initiated by $Sn(Oct)_2$/BBA. **Figure 38** shows that the same rate difference holds

at 90 °C. The activation energies calculated from the solution polymerizations are shown in **Figure 39** and **Table 13**. The activation energy for $Al(OiPr)_3$ catalyzed polymerization is ~10% less than for the $Sn(Oct)_2$/BBA system. Theoretically, lnA from both initiators should be the same because lnA represent the steric factors of the monomer. The values of lnA calculated from the experiments are fairly close.

Table 13 The activation energy of ethylglycolide initiated by $Sn(Oct)_2$/BBA and $Al(OiPr)_3$

initiator	E_a (KJ/mol)	lnA
$Al(OiPr)_3$	66.2	20.4
$Sn(Oct)_2$/BBA	75.7	21.3

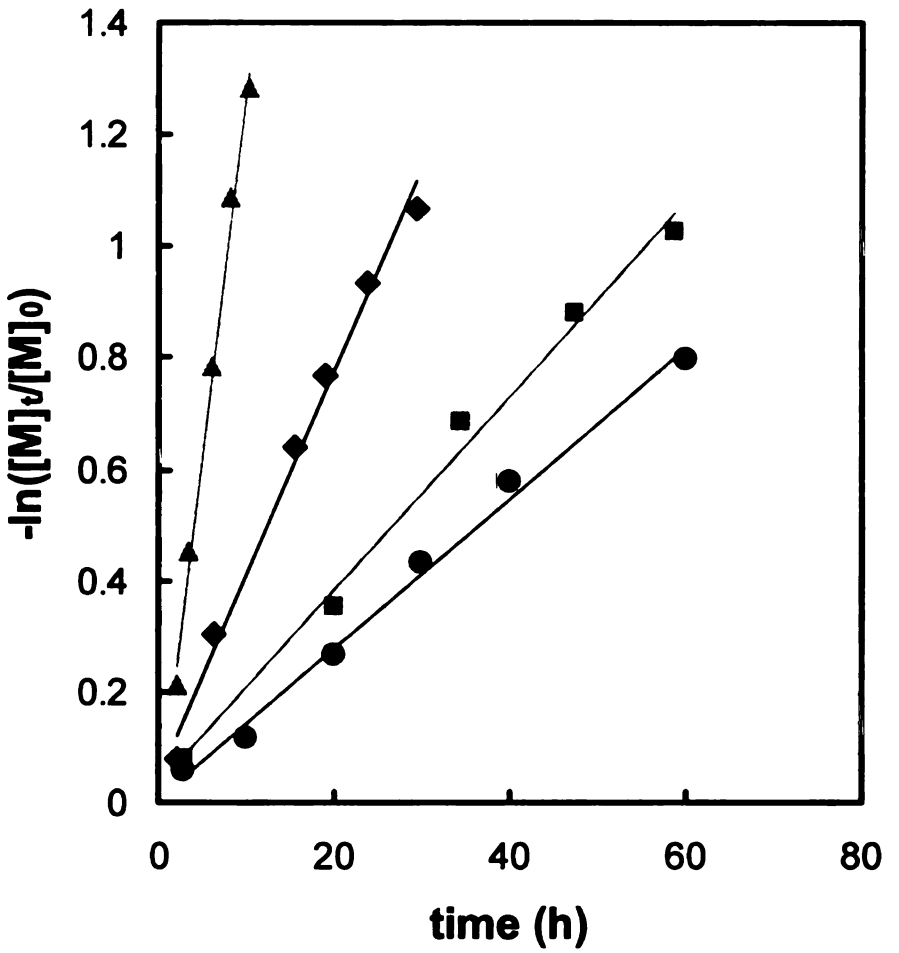

Figure 36 Solution polymerization of substituted lactides initiated by $Sn(Oct)_2$/BBA. Polymerization temperature is 90 °C, (▲) lactide, (■) ethylglycolide, (●) hexylglycolide, (◆) isobutylglycolide $[Sn(Oct)_2]/[BBA]=1$, BBA is *t*-butyl benzyl alcohol. $[M]/[Sn(Oct)_2]=100$. Toluene is the solvent.

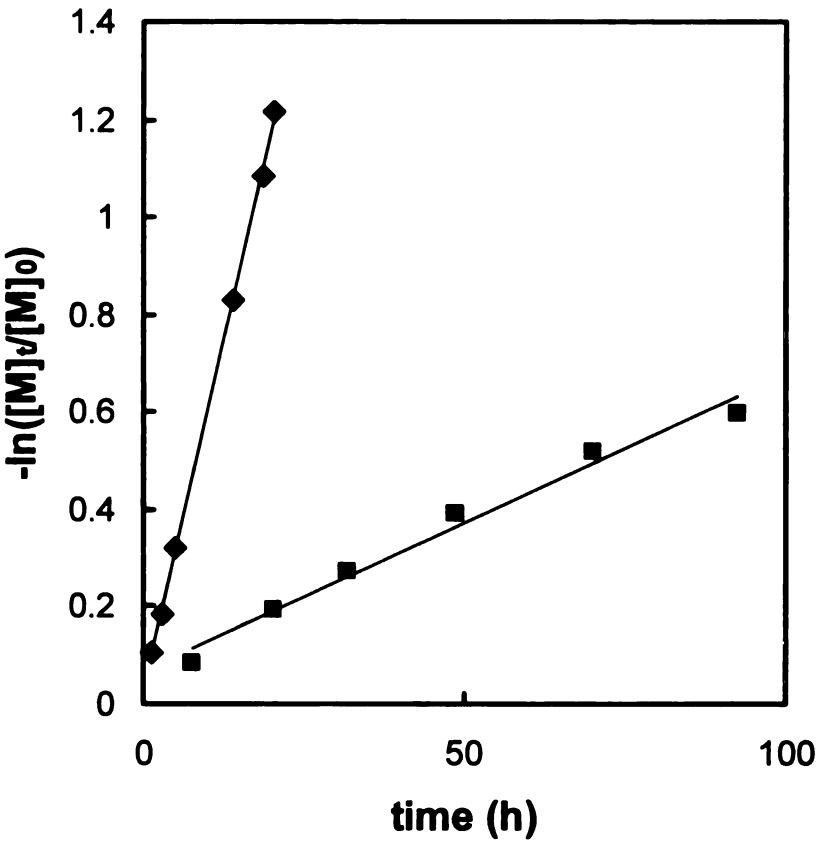

Figure 37. Solution polymerization of ethylglycolide initiated by $Al(OiPr)_3$ (◆) and $Sn(Oct)_2$/BBA (■). $[M]_0$=0.2 mol/L. [M]/[I]=100, $[Sn(Oct)_2]$/[BBA]=1 polymerization temperature is 70 °C and toluene is the solvent.

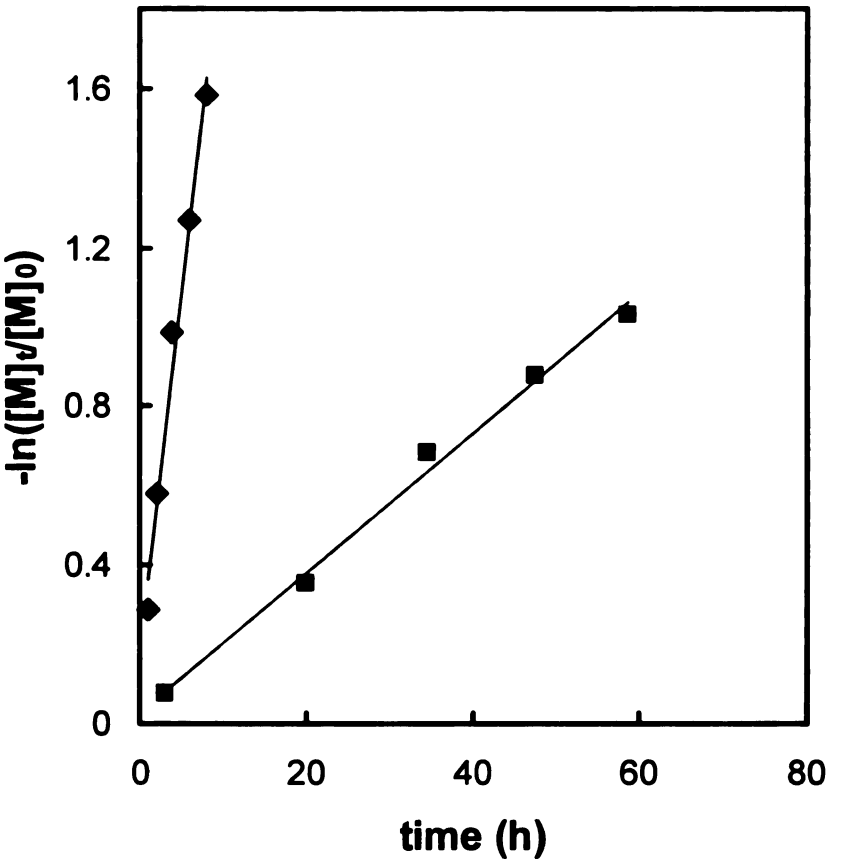

Figure 38. Solution polymerization of ethylglycolide initiated by $Al(OiPr)_3$ (◆) and $Sn(Oct)_2$/BBA (■). $[M]_0$=0.2 mol/L. [M]/[I]=100, $[Sn(Oct)_2]$/[BBA]=1 polymerization temperature is 90 °C and toluene is the solvent.

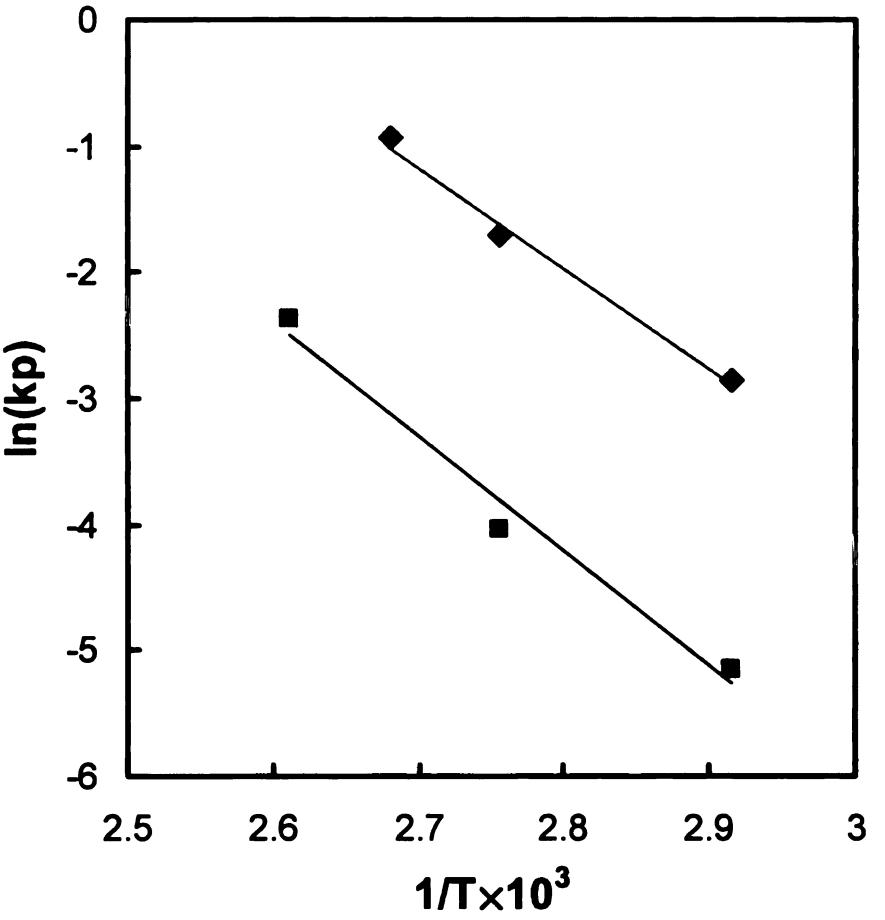

Figure 39. The activation energy for polymerization of ethylglycolide initiated by $Sn(Oct)_2$/BBA (■) and $Al(OiPr)_3$ (◆).

3.4. Polymerization Mechanism

3.4.1 $Al(OiPr)_3$ as initiator

We think there are two possible scenarios that cause abnormal kinetic behavior. First, the polymerization is a three-step process as shown in **Scheme 33**. It includes coordination (**A**), nucleophilic attack (**B**) and ring-opening (**C**). When we expect polymerization rate to drop with increasing size of substituted group, we assume that the nucleophilic attack step (**B**) is the rate-determining step. However, the nucleophilic attack step (**B**) may not be the rate-determining step and identification of the rate-determining step has not been addressed in literature. It is possible that step **B** and step **C** are rate-determining. In step **C**, the ring opens up to form a linear chain. In a ring system, the substituents on the ring and the initiator are more crowded than that on a linear chain. The larger the group, the more crowded the ring and the easier it is to open the ring. If step **C** is rate-determining, larger substituents on the ring should lead to faster polymerization. From the activation energy data from **Table 10**, we see that the activation energy decreased with increases in the size of the substituents. We believe that step **C** is the rate-determining step for isobutylglycolide polymerization. The frequency factor lnA, which represent the steric effect of the reaction, also is in the right order. The larger the size of the substituted group, the smaller the value of lnA.

Scheme 33. The mechanism for the lactide polymerization initiated by $Al(OiPr)_3$

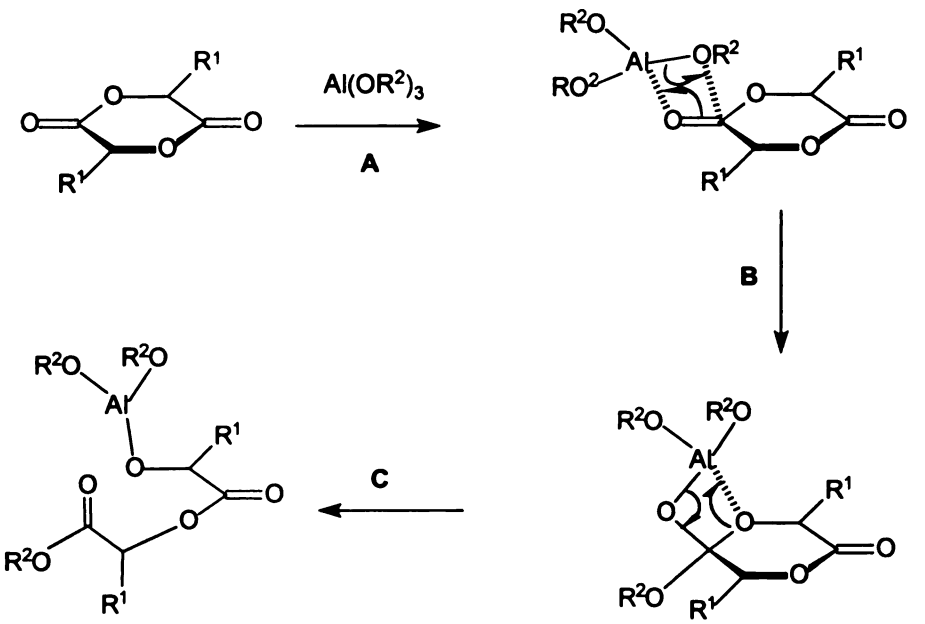

A second scenario is based on the coordination number of Al during lactide polymerization. As mentioned in the Introduction, $Al(OiPr)_3$ exists as a trimer and a tetramer (shown in **Figure 3**) in solution. During lactide polymerization, the aggregated complex is broken up by monomer to form complex (**A**) shown in **Figure 40**. The coordination number on Al is 6. During the polymerization of lactide, ethylglycolide and hexylglycolide, complex **(A)** is formed. In the case of isobutylglycolide, it is may not possible to accomodate three monomers on Al because of the large size of substituted group. It is may be possible to form the 4-coordinate complex (**B**) shown in **Figure 40**, with only one

monomer molecule coordinated to the Al atom. The 4-coordinate Al is more reactive than 6-coordinate Al, and perhaps that is why isobutylglycolide polymerized faster than lactide, ethylglycolide and hexylglycolide. However, in polymerizations of substituted lactides initiated by $Sn(Oct)_2$/ROH, the polymerization rates also do not follow the order of the size of subsitituents, and $Sn(Oct)_2$/ROH does not aggregate. Thus, it is unlikely that this hypothesis is right.

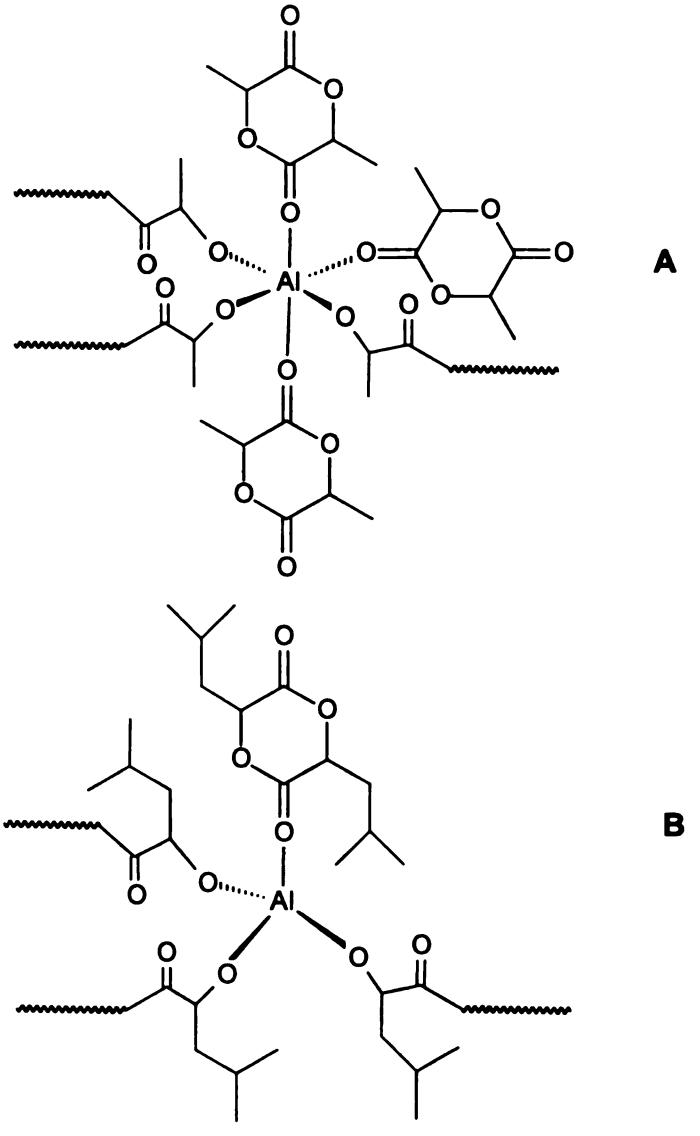

Figure 40. The structure of the transition state for polymerization of substituted lactides

3.4.2 $Sn(Oct)_2$/ROH as catalyst/initiator

Based on the kinetic data, we propose the mechanism shown in **Scheme 34**. The first step is an equilibrium between $Sn(Oct)_2$ and ROH to form RO-Sn-Oct and HOct. Because of the non-polar environment, it is unlikely that either $Sn(Oct)_2$ or ROH will dissociate appreciably. We were unable to observe the RO-Sn-Oct intermediate using low temperature NMR. One reason for our failure could be that the equilibrium favors $Sn(Oct)_2$ and thus the equilibrium concentration of RO-Sn-Oct is below the detection limits of the NMR. A different method must be developed to identify the intermediate. Recently, Penczek *et al.* reported detection of RO-Sn-Oct during polymerizaiton using MALDI Mass spectrometry.

The second step is initiation. The actual initiator is RO-Sn-Oct, a tin alkoxide. Initiation by tin alkoxides has been well documented in the literature. Though the equilibrium amount of RO-Sn-Oct is small, a fast equilibrium leads to fast initiation. We know from kinetic data that polymerizations using $Sn(Oct)_2$/ROH are living polymerizations below 80% conversion. One characteristic of living polymerization is a fast initiation reaction.

The first two steps of the polymerization are much faster than the third step of the polymerization: propagation. The propagation of lactides initiated by metal alkoxides have been well studied in systems such as $Al(OiPr)_3$ and $Sn(OMe)_4$. It is a coordination-insertion process. The fourth step of the polymerization is the regeneration of catalyst and initiator. HOct reacts with

active chains to regenerate $Sn(Oct)_2$ and a polymer chain with a hydroxyl chain end. The hydroxyl chain end can re-initiate polymerization. The last step of the polymerization is catalyst degradation. As mentioned before, $Sn(Oct)_2$ degrades to an insoluble white powder, the salt of Sn and the 2-hydroxy acid. In bulk polymerization, this white powder can also polymerize lactide, so it does not influence the kinetics of the polymerization. However, in solution polymerization, this white powder is insoluble, which means the catalyst is no longer in the polymerization system and causes the polymerization rate to drop dramatically.

This reaction mechanism is similar to atom-transfer polymerization (ATRP) (**Sheme 35**). The initiator reacts with catalyst to generate an active species, followed by initiation and propagation, and then initiator and catalyst are regenerated. ATRP is a living polymerization. Lactide polymerization initiated by $Sn(Oct)_2$/ROH is also a living polymerization at low conversion, and both have termination steps.

Scheme 34. The mechanism of lactide polymerization using $Sn(Oct)_2$/ROH as catalyst/initiator

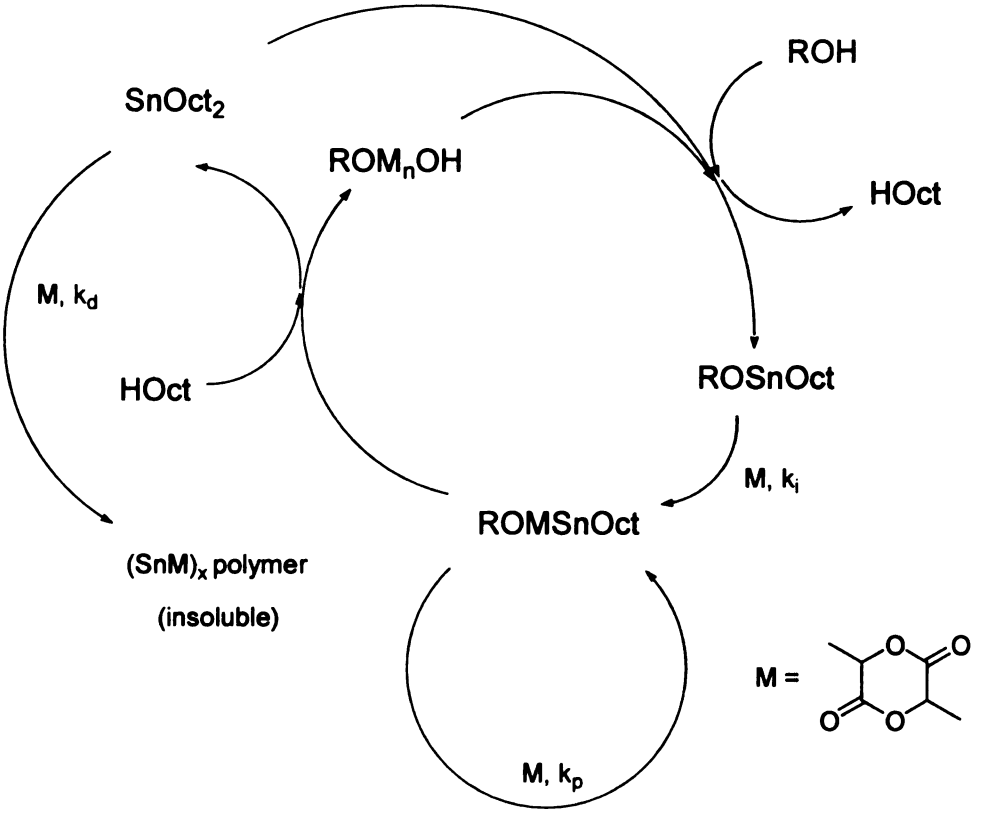

Scheme 35. The mechanism for atom-transfer radical polymerization (ATRP)

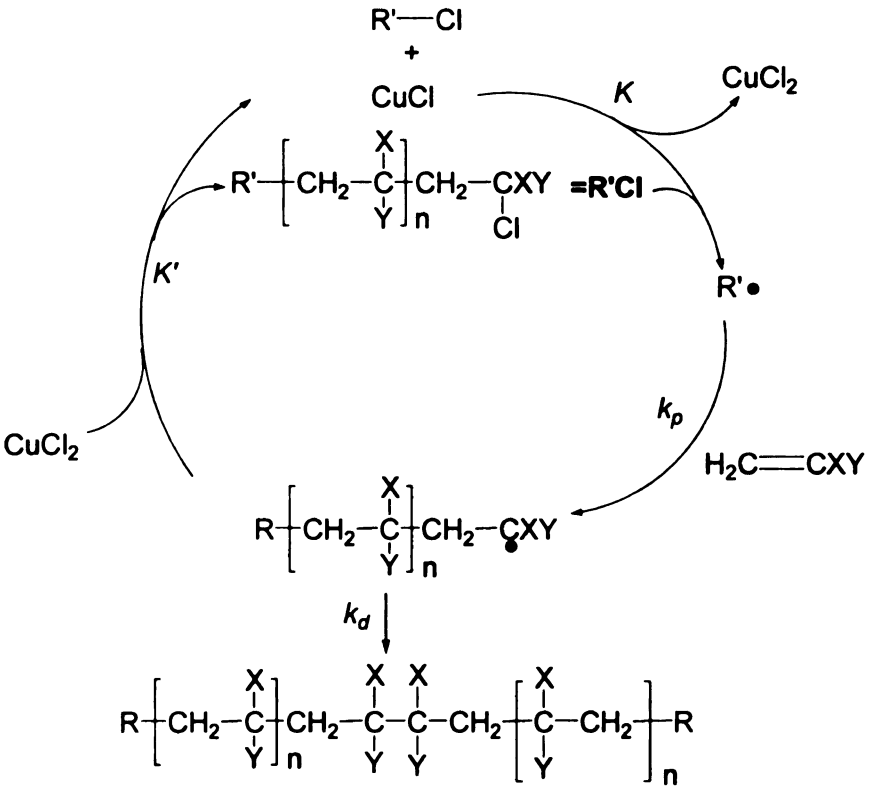

3.5. The Influence of Stereochemistry on the Kinetics of Solution Polymerization

The stereochemistry of the monomer has a big influence on the kinetics of solution polymerizations of substituted lactides. As shown in **Figure 41** and **Figure 42**, racemic lactide polymerized twice as fast as L-lactide, and racemic isobutylglycolide polymerized three times as fast as D-isobutylglycolide.

Lactide monomers have two stereocenters, so racemic lactides include an equimolar amounts of the (R,R) and (S,S) stereoisomers. As shown in **Scheme 36**, when L-lactide or D-lactide are polymerized, there is only one propagation reaction, an R active center reacting with (R,R) monomer with a rate constant $k_{p(R/R,R)}$ or an S active center reacting with (S,S) monomer with a rate constant $k_{p(S/S,S)}$. When racemic lactides polymerize, four propagation reactions must be considered, the active center with R stereochemistry reacting with (R,R) monomer with a rate constant $k_{p(R/R,R)}$, the active center with R stereochemistry reacting with (S,S) monomer with a rate constant $k_{p(R/S,S)}$, the active center with S stereochemistry reacting with (R,R) monomer with a rate constant $k_{p(S/R,R)}$ and the active center with S stereochemistry reacting with (S,S) monomer with a rate constant $k_{p(S/S,S)}$. Usually, $k_{p(R/R,R)}$ is equal to $k_{p(S/S,S)}$ and $k_{p(R/S,S)}$ is equal to $k_{p(S/R,R)}$. If $k_{p(S/R,R)}$ and $k_{p(R/S,S)} > k_{p(S/S,S)}$ and $k_{p(R/R,\ R)}$, the racemic monomer will polymerize faster than the pure D or L monomers, which is called syndiotactic preference.

Scheme 36. Stereochemistry of lactide polymerization

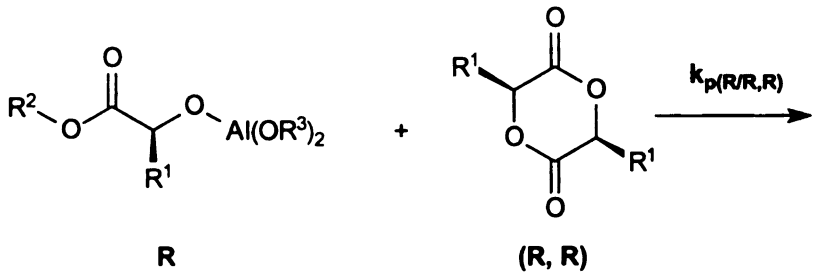

R **(R, R)**

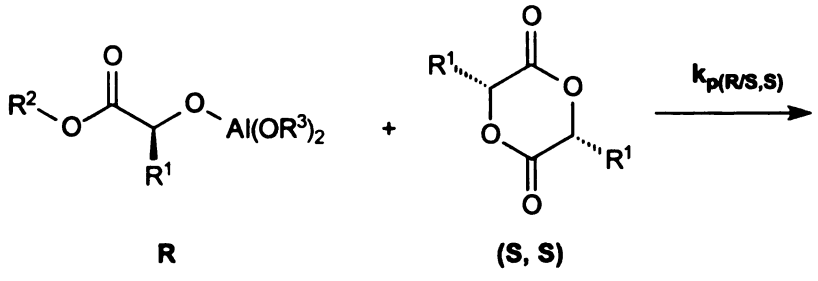

R **(S, S)**

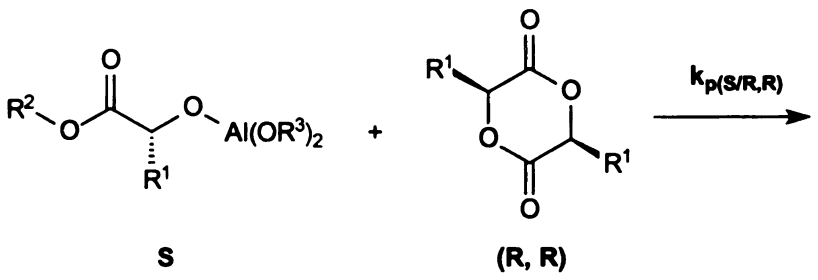

S **(R, R)**

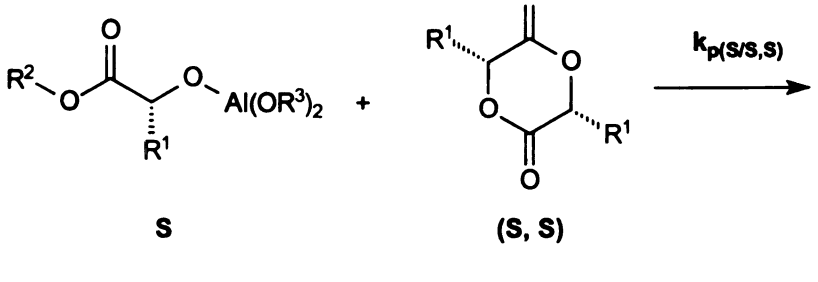

S **(S, S)**

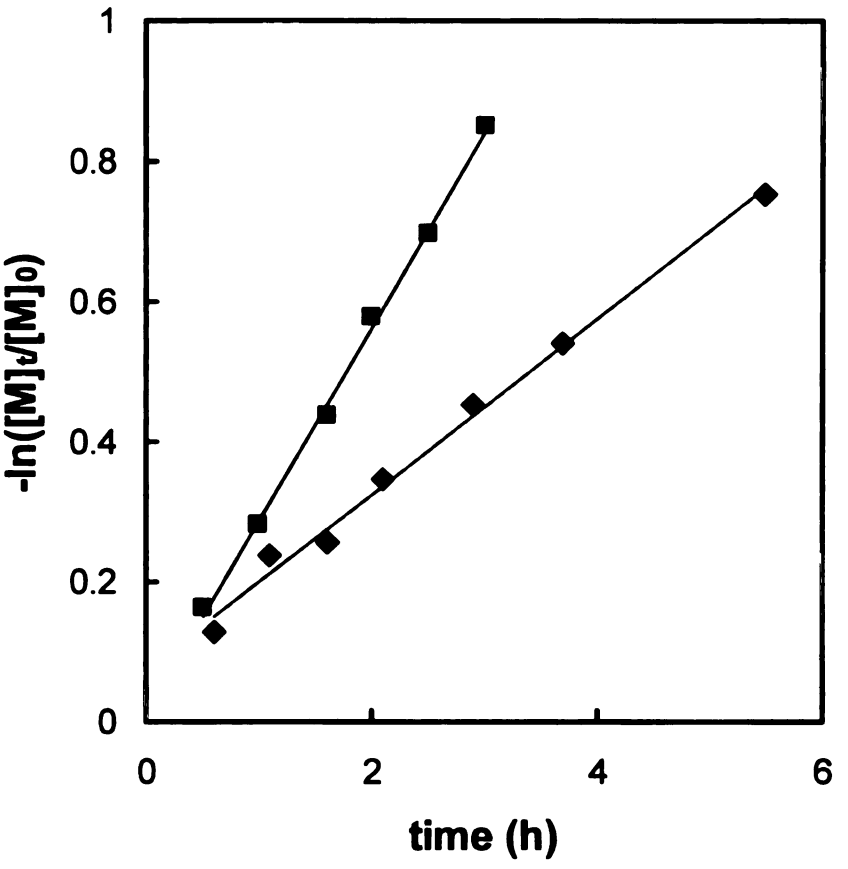

Figure 41. Polymerization of *rac*-lactide (■) and L-lactide (◆).

Polymerization temperature is 90 °C. $[M]_0$=0.2 mol/L, initiator is $Al(OiPr)_3$, [M]/[I]=100. Toluene is the solvent.

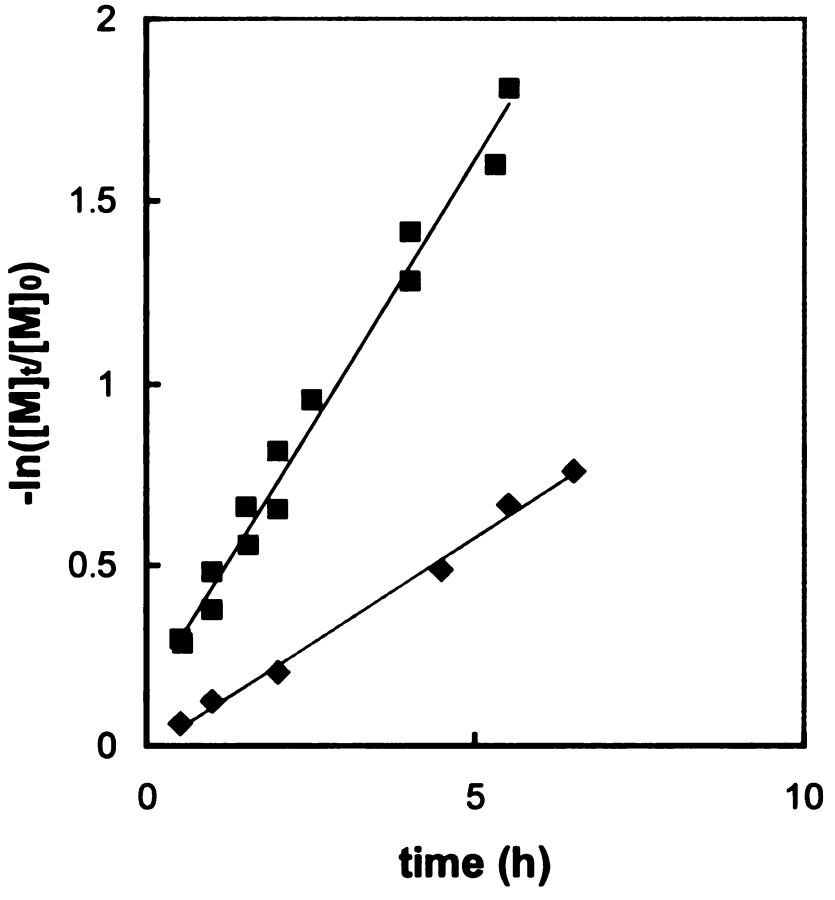

Figure 42. Polymerization of *rac*-isobutylglycolide (■) and D-isobutylglycolide (◆). Polymerization temperature is 90 °C. $[M]_0$=0.2 mol/L, initiator is $Al(OiPr)_3$, [M]/[I]=100. Toluene is the solvent.

As shown in **Figure 41** and **Figure 42**, polymerization rates of L-lactide and *rac*-lactide are different. Similar results were obtained for the polymerization rate of L-isobutylglycolide and *rac*-isobutylglycolide. Because of the stereochemistry of the monomer and the chain end, there are four different reactions during the polymerization *rac*-polylactides as shown in **Scheme 36**. The kinetics of *rac*-lactide polymerization can be expressed as shown in **Scheme 37**. Equations **A** and **C** in **Scheme 37** produce *isotactic* chains, so $k_{(S/S,S)} = k_{(R/R,R)} = k_i$, while **B** and **D** produce *syndiotactic* chains, so $k_{(S/R,R)} = k_{(R/S,S)} = k_s$. It has been found that $k_i < k_s$ in lactide polymerization, which means syndiotactic chain placement is favored in lactide polymerization. Munson *et al.*[187] found $k_i / k_s = 0.6$ for the bulk polymerization of lactide initiated by $Sn(Oct)_2$ at 180 °C and Kasperczyk[188] found $k_i / k_s = 0.32$ for solution polymerization of lactide initiated by *tert*-butoxide at 20 °C in THF. The method used to calculate k_i / k_s was monitoring ratios of stereosquences by NMR. Because the NMR assignment of the stereosquence is still a controversial topic, and the resolution of NMR is not sufficent to clearly separate all stereosquences and account for side reactions such as transesterification and racemization which will alter the stereosquence, the k_i / k_s ratio reported by Munson and Kasperczyk may not be very accurate. By studying the kinetic behavior of *rac*-lactide and L-lactide polymerization, we obtained more accurate measures of k_i / k_s.

Scheme 37. Kinetic scheme for lactide polymerization

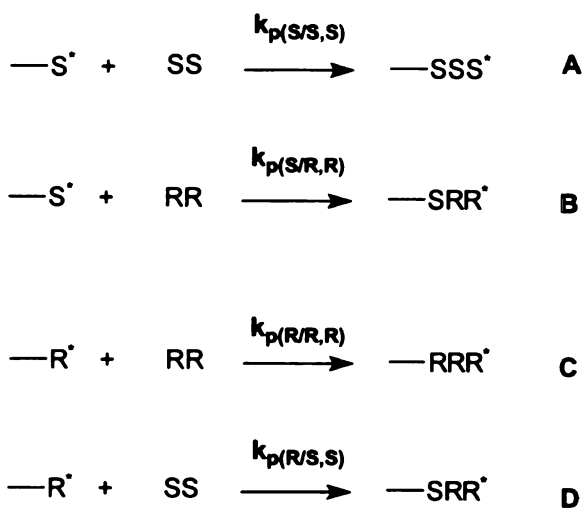

From **Scheme 37**, we can write the kinetic equation as:

$$-\frac{d[M]}{dt} = k_{(S/S,S)}[S^*][S] + k_{(S/R,R)}[S^*][R] + k_{(R/R,R)}[R^*][R] + k_{(R/S,S)}[R^*][S] \quad \text{....(7)}$$

Since

$$k_{(S/S,S)} = k_{(R/R,R)} = k_i$$
$$k_{(R/S,S)} = k_{(S/R,R)} = k_s$$

We re-write equation (7) as:

$$-\frac{d[M]}{dt} = k_i[S^*][S] + k_s[S^*][R] + k_i[R^*][R] + k_s[R^*][S] \quad \text{.....(8)}$$

In *rac*-lactide polymerization:

$$[S] = [R] = \frac{[M]}{2}$$

Equation (8) can be re-written as

$$-\frac{d[M]}{dt} = 0.5k_i[S^*][M] + 0.5k_s[S^*][M] + 0.5k_i[R^*][M] + 0.5k_s[R^*]M] \quad \text{.....(9)}$$
$$-\frac{d[M]}{dt} = 0.5k_i([S^*] + [R^*])[M] + 0.5k_s([S^*] + [R^*])[M] \quad \text{.....(10)}$$

Also:

$$[S^*] + [R^*] = [I]$$

Equation (10) can be re-written as:

$$-\frac{d[M]}{dt} = (0.5k_i + 0.5k_s)[I][M] \quad \text{.....(11)}$$

Intergration of (11) yields:

$$-\ln\frac{[M]_t}{[M]_0} = (0.5k_i + 0.5k_s)[I]t \quad \text{.....(12)}$$

Plots of $-ln([M]_t/[M]_0)$ vs t give $(0.5k_i + 0.5\ k_s)[I]$ as the slope.

In L-lactide polymerization, there is only one monomer, so the kinetics of the polymerization can expressed using equation (13):

$$-\ln\frac{[M]_t}{[M]_0} = k_i[I]t \quad \text{.....(13)}$$

$k_i\ [I]$ can be obtaied from plot of $-ln([M]_t/[M]_0)$ vs t. If a L-lactide and a *rac*-lactide polymerization is run under the same conditions, $[I]$ is the same for both polymerizations. From these two slopes, k_i/k_s can be solved. For polymerization of lactide at 90 °C, k_i/k_s = 0.29, when initiated by $Al(OiPr)_3$ in toluene, which is close to the value (0.32) reported by Kasperczyk. For polymerization of isobutylglycolide, k_i/k_s =0.24 under the same conditions. From k_i/k_s, the difference in activation energy can be calculated using the Arrhenius equation.

$$\frac{k_i}{k_s} = e^{\frac{-(\Delta E_i - \Delta E_s)}{RT}}$$

$$(\Delta E_i - \Delta E_s) = -RT \ln \frac{k_i}{k_s}$$

For polymerization of lactide, the energy difference is 3.7 KJ/mol. For polymerization of isobutylglycolide, the energy difference is 4.2 kJ/mol.

We also used semi-empirical molecular mechanics calculation to simulate lactide polymerization. The calculations were done using SPARTAN. We set up the two complexes shown in **Figure 43**. Complex **A** has a chain end with R configuration and a coordinated S,S lactide ring. Complex **B** has a chain end with an S configuration and a coordinated S,S lactide ring. Complex **A** leads to syndiotactic chain placement and complex **B** will produce isotactic chain placement. The optimized structures of complex **A** and complex **B** are shown in **Figure 44** and **Figure 45** (Images are presented in color). In **Figure 44**, the O1 and Al bond is almost perpendicular to the lactide ring, so it is in the right position for nucleophilic attack. We drove O1 close to C10 on the lactide ring until the new O1-C10 bond was formed and monitored the energy of the complex along the pathway. The transition state energy of nucleophilic attack can be obtained from this energy trajectory. From the energies of complex **A** and the transition state, the activation energy of nucleophilic attack can be calculated, which is the activation energy for syndiotactic chain placement. Using the same method, the activation energy for producing isotactic chain placement was also calculated.

betwee

close.

Ta

used

con

the

diff

is

ste

between calculated value and experimental value is shown in **Table 14**. It is fairly close.

Table 14. Experimental value and calculated value for activation energy difference.

	$\Delta E_l - \Delta E_s$ (KJ/mol)	
	lactide	**isobutyglycolide**
Experimental value	3.7	4.2
Calculated value [a]	4.5	5.1

a. Calculated using SPARTAN.

The SPARTAN calculation has strong limitations. First, the calculation is used to simulate gas phase, which is very different from actual reaction conditions. Second, since a semi-empirical method was used in the calculation, the accuracy of calculation may not be good enough to judge the small energy difference shown in **Table 14**.

The preference for syndiotactic chain placement for lactide polymerization is cause by small differences in activation energy, which is probably caused by steric hindrance at polymer growing site.

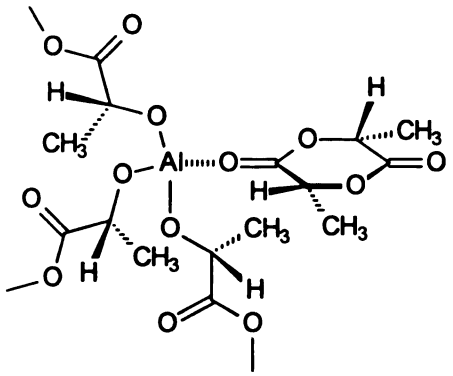

A

R chain end and S S lactide ring

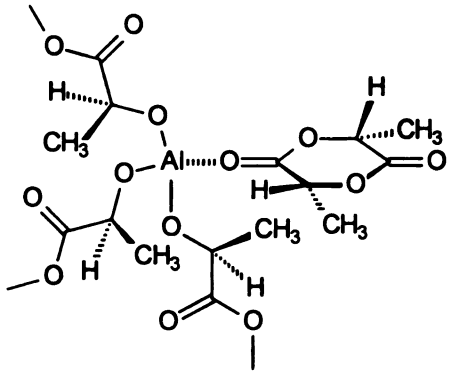

B

S chain end and S S lactide ring

Figure 43. The structure of complexes used to simulate polymer growth

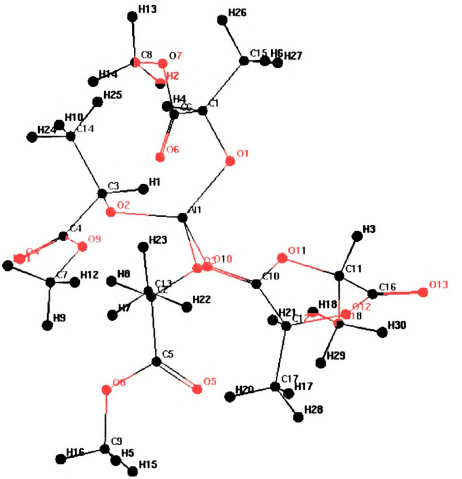

Figure 44. The calculated structure for the complex with R configuration chain end and S,S lactide ring.

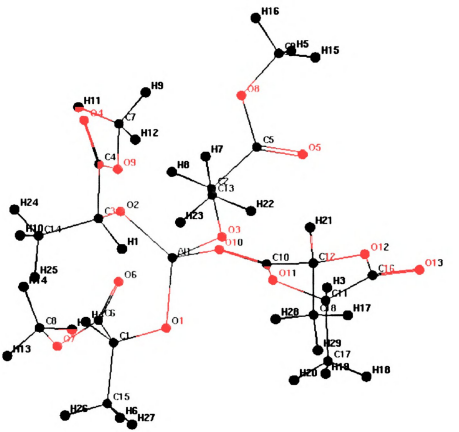

Figure 45. The calculated structure for the complex with S configuration chain end and S,S lactide ring.

4. Pol

give

purifi

obta

solu

mel

poly

wei

sh

in

of

th

a

p

a

p

lo

p

b

4. Polymer properties

To determine the properties of the polymers, polymerizations were run to give molecular weights near 50,000 g/mol (**Table 15**). The crude polymers were purified by precipitation into methanol and dried to constant weight. All polymers obtained from the polymerization of substituted glycolides are colorless, and are soluble in solvents ranging from toluene to $CHCl_3$. Flexible films can be either melt pressed at 150 °C or cast from solvent. Because of the low T_gs for the polymers, the films tend to be somewhat tacky regardless of the molecular weight, and characterization of the polymers by polarizing optical microscopy showed that none of the polymers is crystalline. Given that the monomers used in the polymerizations is a mixture of R,R, S,S, and R,S diastereomers, the lack of crystallinity is not surprising.

DSC scans were used to measure the glass transition temperatures for the polymers, and the results appear in **Figure 46** and **Table 15**. Overall, thermal analysis data show that T_gs of the substituted glycolides range from –37 °C for poly(hexylglycolide) to 66 °C for polylactide. For polymers substituted with linear alkyl groups, The T_gs decreased as length of the alkyl group increased. For these polymers, the flexible pendant group reduces T_g by acting as "internal diluent", lowering the frictional interaction between chains. Conversely, the branched pendant group of poly(isobutylglycolide) hinders rotation of the polymer backbone, resulting in a higher T_g.

We further investigated the properties of poly(ethylglycolide) using thermal and dynamic mechanical analyses. DSC runs show a T_g near 12 °C, with no sign of crystallinity. A T_g of 12 °C is lower than that of polylactide itself (66 °C), and in line with our expectation that increasing the length of the side chain should lead to a decrease in T_g. DMA runs support the T_g assignment made from DSC data. As shown in **Figure 47**, the tan δ trace for the polymer shows a peak near 12 °C which is nearly identical to the baseline inflection seen in the DSC data. In addition, the DMA probe position trace shows the expected behavior for a polymer heated to above T_g, expansion followed by penetration of the probe through the sample.

The decomposition of polymers measured using TGA define the limiting use temperature of the polymer. **Figure 48** shows the TGA plots for the decomposition of poly(ethylglycolide) in air and under N_2. The two data sets show only slight differences, an indication that the decomposition is probably dominated by depolymerization of the polymer to monomer. As shown in **Figure 49**, the TGA plots for all polymers are similar, with the onset for decomposition shifting to higher temperatures as the size of the alkyl group increases. We found that all polymers decomposed to their monomers, and thus the shift likely reflects the lower volatility of monomers that have large substituents. In trial depolymerization reactions run on 0.1 g scales, we recovered over 93% of polymer mass as monomers.

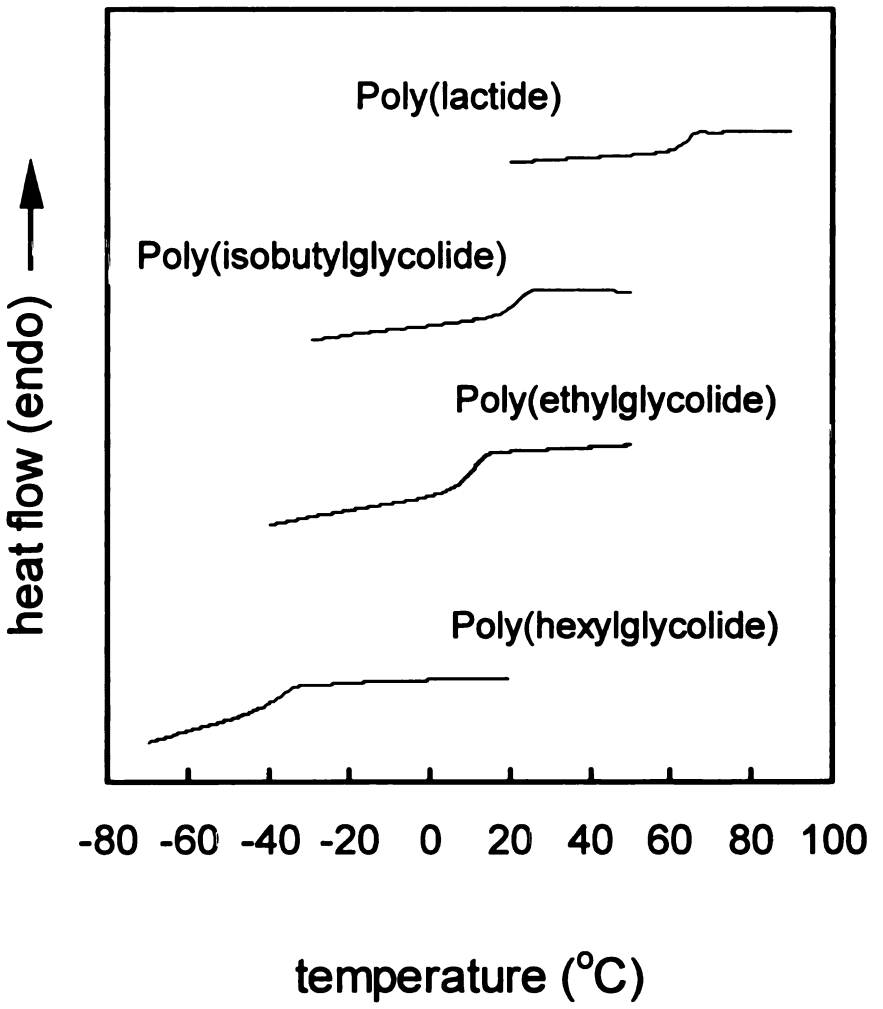

Figure 46 DSC runs (second heating after flash quenching from 100 °C) for substituted poly(glycolide)s. Heating rate: 10 °C/min under helium.

Table 15. Polymer Properties

Polymer	$M_n \times 10^{-3}$ [a]	M_w/M_n	T_g °C [b]
polylactide	35.2	1.89	22-65
Poly(ethylglycolide)	45.6	1.78	15
Poly(hexylglycolide)	43.2	1.91	-37
Poly(isobutylglycolide)	47.3	1.83	22

a. measured by GPC in THF using polystyrene as standard

b. measured by DSC under He at a rate of 10 °C/min

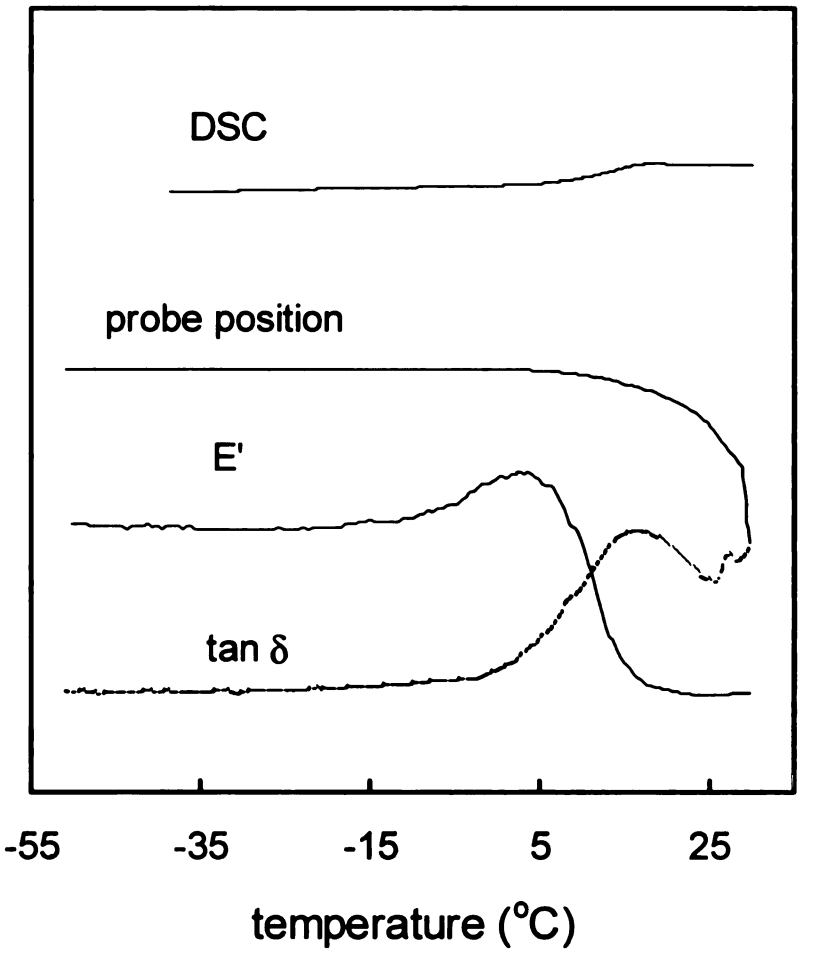

Figure 47. Thermal analysis results for poly(ethylglycolide). The bottom 3 traces are DMA results for a sample in a parallel plate geometry. Heating rate: 10 °C/min under helium (DSC) or N_2 (DMA).

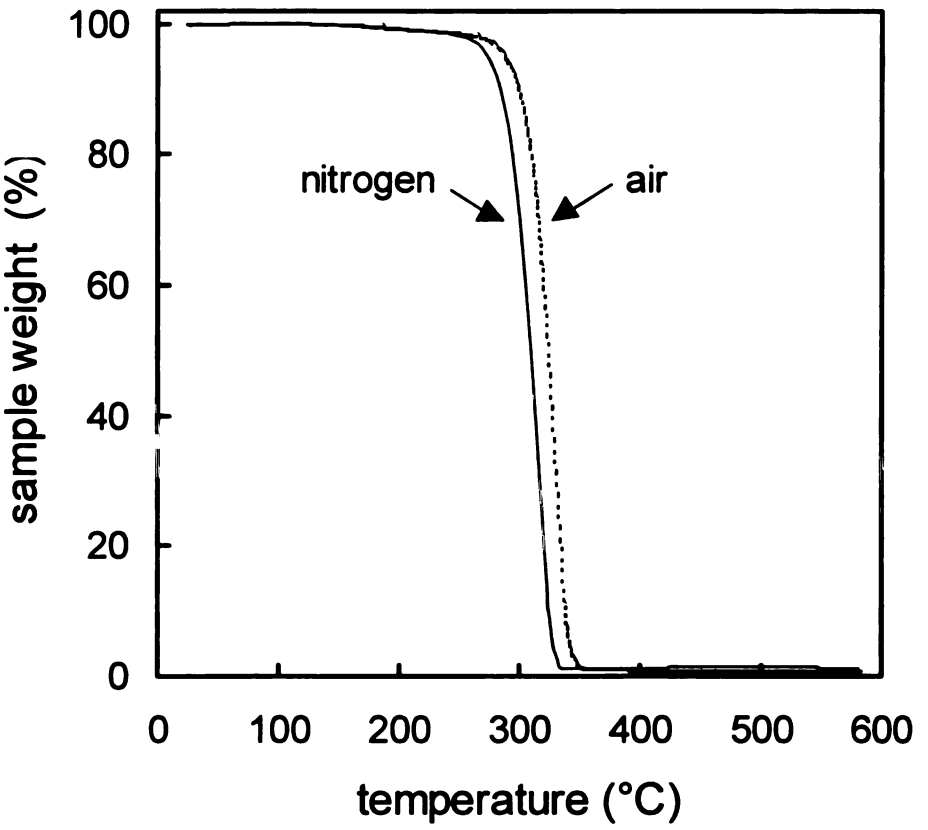

Figure 48 Thermogravimetric analysis results for poly (ethylglycolide).

Heating rate: 40 °C/min.

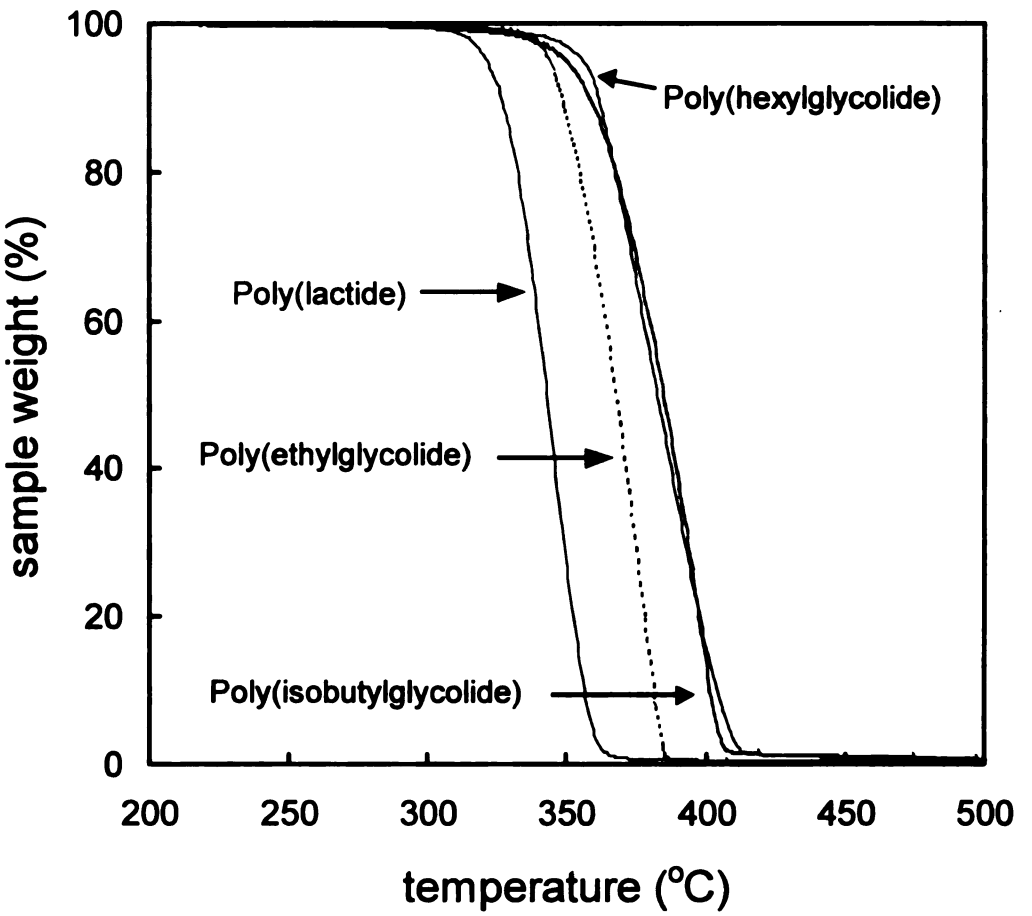

Figure 49 Thermogravimetric analysis results for substituted poly(glycolide)s run in air. Heating rate: 40 °C/min.

com

tren

chai

temp

bran

cha

from

incr

grou

dist

cha

res

sub

gro

sm

gla

the

gla

ser

gro

The glass transition temperatures of the substituted polylactides and comparable substituted polyethylenes are shown in **Table 16**. There is a similar trend in the glass transition temperature with changes in the structure of the side chain. For polymers substituted with linear alkyl groups, the glass transition temperature decreased as length of the alkyl group increases. Conversely, branched pendant groups result in higher glass transition temperatures.

The glass transition temperature is dependent on the flexibility of polymer chain and secondary forces between polymer chains. When the group changes from methyl to ethyl to hexyl group, the cross-sectional area of the group increases slightly. However, because of the linear nature of these substituted groups, they are very flexible. They act as "internal plasticizer" to increase the distance between polymer chains and lower the frictional interaction between chains. The net effect is to reduce the rotational barriers of the backbone, which results in a decrease of the glass transition temperature. For branched substituents, such as isobutyl and isopropyl, the cross sectional size of the groups is larger than the in linear counterparts, and the flexibility of the group is smaller, which result in a higher rotational barrier for the backbone and a higher glass transition temperature. Compared to isopropyl, the extra methylene unit of the isobutyl group increases the flexibility of the group, which decreases the glass transition temperature.

There is one important difference between the substituted polylactide series and the polyethylene series. Polylactides with branched substituted groups, poly(isobutylglycolide) and poly(isopropylglycolide), have lower glass

transitio

poly(isol

tempera

betwee

strong d

This int

transitio

strong,

further

isoprop

interact

poly(isc

barrier

weaker

transiti

the inte

of the

the

poly(is

polypr

transition temperatures than polylactide. In the substituted polyethylene series, poly(isobutylethylene) and poly(isopropylethylene) have higher glass transition temperatures than poly(propylene). The difference lies in the secondary forces between polymer chains in both series. Polylactides are polyesters, which have strong dipole-dipole interactions between polymer chains as shown in **Figure 50**. This interaction hinders rotation of the backbone, which increases the glass transition temperature of polymer. When R is small, the chain-chain interaction is strong, but when R is large as in the isobutyl and isopropyl cases, the chains are further separated and the interaction is weak. The larger size of isobutyl and isopropyl groups increases the rotational barrier, but the weakened secondary interaction between polymer chains decreases the rotational barrier. Thus, for poly(isopropylglycolide) and poly(isopropylglycolide), the increase in rotational barrier gained from increasing the size of the substituted group can not offset the weakened interaction between polymer chains, which results in a lower glass transition temperature than polylactide. For the substituted polyethylene series, the interaction between polymer chains is very weak because of the low polarity of the polymer backbone. The rotational barrier is mainly decided by the size of the substituted group. That is why poly(isopropyethylene) and poly(isobutylethylene) have higher glass transition temperatures than polypropylene.

Table 16. Glass transition temperature of substituted polylactides and substituted polyethylene.

polymer	T_g (°C)	polymer	T_g (°C)
polylactide	45-65	Poly(propylene)	-15 - -3
Poly(ethylglycolide)	12	Poly(1-butene)	-50
Poly(hexylglycolide)	-37	Poly(hexylethylene)	-65
Poly(isobutylglycolide)	23	Poly(isobutylethylene)	29
Poly(isopropylglycolide)	50	Poly(isopropyethylene)	50

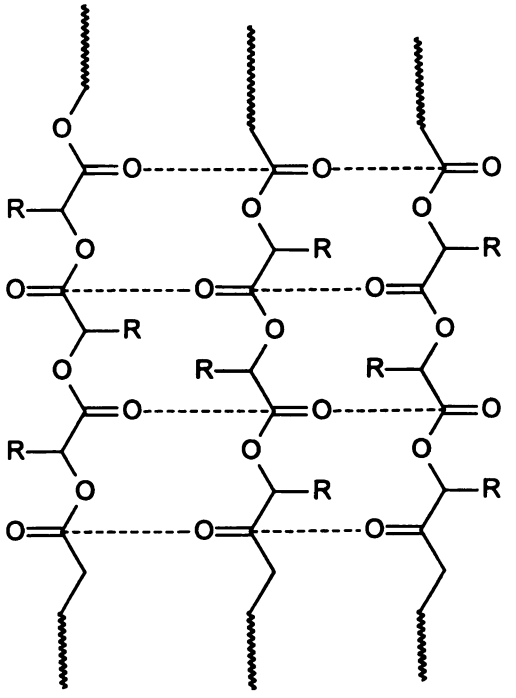

Figure 50. The secondary interaction between polyester chains

5. Copo

two ro

togeth

asymr

copol

5. Copolymerization of substituted glycolides

The copolymerization of substituted glycolides has been done using the two routes shown in **Scheme 38**. In route **1**, the two comonomers were mixed together and heated up with catalyst to make copolymers. In route **2**, the asymmetrically substituted glycolides were synthesized and polymerized to make copolymers.

Scheme 38 Copolymerization of substituted glycolides

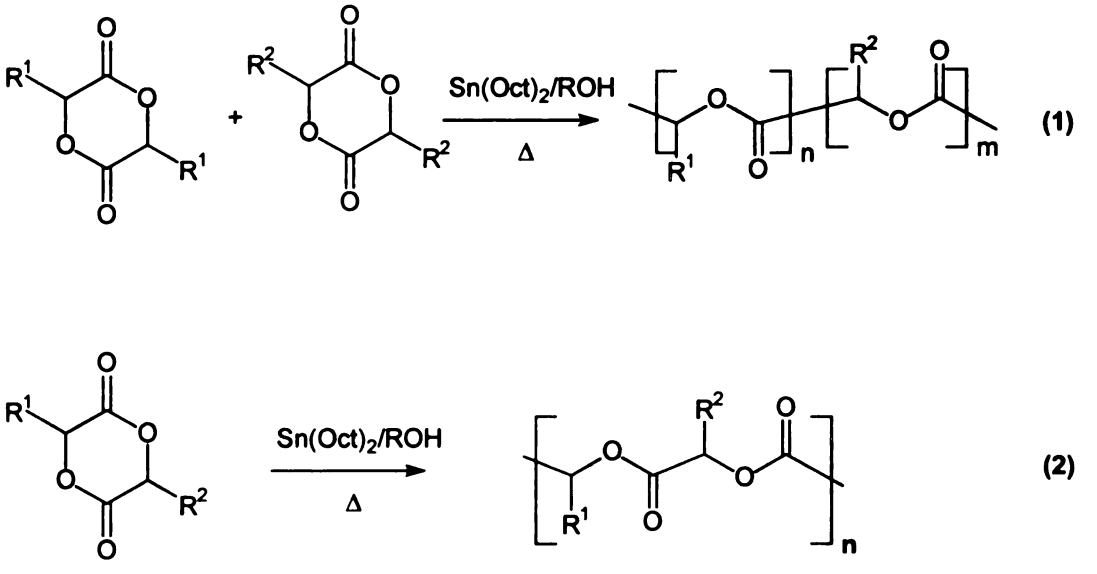

5.1.

5.1. Copolymerization through comonomers

Ethylglycolide (EG) and lactide (LA) have very similar structures. Their copolymers should retain the biodegradability, but have different physical properties than their homopolymers. A series of copolymers (EG/LA=1/5, EG/LA=1/3, EG/LA=1, EG/LA=3, EG/LA=5) were synthesized by bulk polymerization at 130 °C catalyzed by $Sn(Oct)_2$/BBA. All polymers have molecular weights >40,000 g/mol. The DSC plots are shown in **Figure 51**. The DSC runs show one glass transition temperature for each copolymer, an indication that the copolymer is not phase separated. Considering the structural similarity of the monomers, it is not surprising that copolymers are single phase. The glass transition temperatures listed in **Table 17** fall those of polylactide and poly(ethylglycolide) and increase with an increase the mole fraction of the lactide comonomer. The glass transition temperatures of copolymers can be predicted using the Fox equation:

$$\frac{1}{T_g} = \frac{w_A}{T_{gA}} + \frac{w_B}{T_{gB}}$$

where T_g, T_{gA} and T_{gB} are glass transition temperature of the copolymer, and the pure homopolymers derived from monomers A and B respectively, and w represents the mass fraction of the polymer. The Fox equation successfully predicts the glass transition temperatures of random copolymers and plasticized systems. An underlying assumption is that the polymer is homogeneous in composition, and that the comonomers are distributed randomly along the chain.

As sh

equa

or n

sens

and

far

illu

bu

str

re

H

c

As shown in **Figure 52**, the glass transition temperature of copolymers fit the Fox equation fairly well. However, whether the copolymer is truly a random copolymer or not must be defined by a characterization technique such as NMR, which is sensitive to structure at the molecule level. Based on copolymerizations of lactide and glycolide,[7,189] the distribution of monomer units in the polymers is probably far from random because differences in reactivity for the monomers. As illustrated in **Scheme 39**, these effects are likely due to differences in the steric bulk at the carbon α to the carbonyl. Lactide and glycolide share the same ring structure, but the absence of lactide's methyl groups makes glycolide far more reactive and thus "blocky" polymers are obtained from copolymerizations. However, transesterification reactions can increase the randomness of copolymers.

Table 17. Properties of copolymers

Polymers	$M_n \times 10^{-3}$ [a]	M_w/M_n	T_g °C [b]
Polylactide	35.2	1.89	66
EG/LA=1/5	41.5	1.85	42.
EG/LA=1/3	47.8	1.76	38
EG/LA=1	41.7	1.88	30
EG/LA=3	50.8	1.92	23
EG/LA=5	43.6	1.85	19
Poly(ethylglycolide)	45.6	1.78	15

a. measured by GPC in THF using polystyrene as standard

b. measured by DSC under He at a rate of 10 °C/min

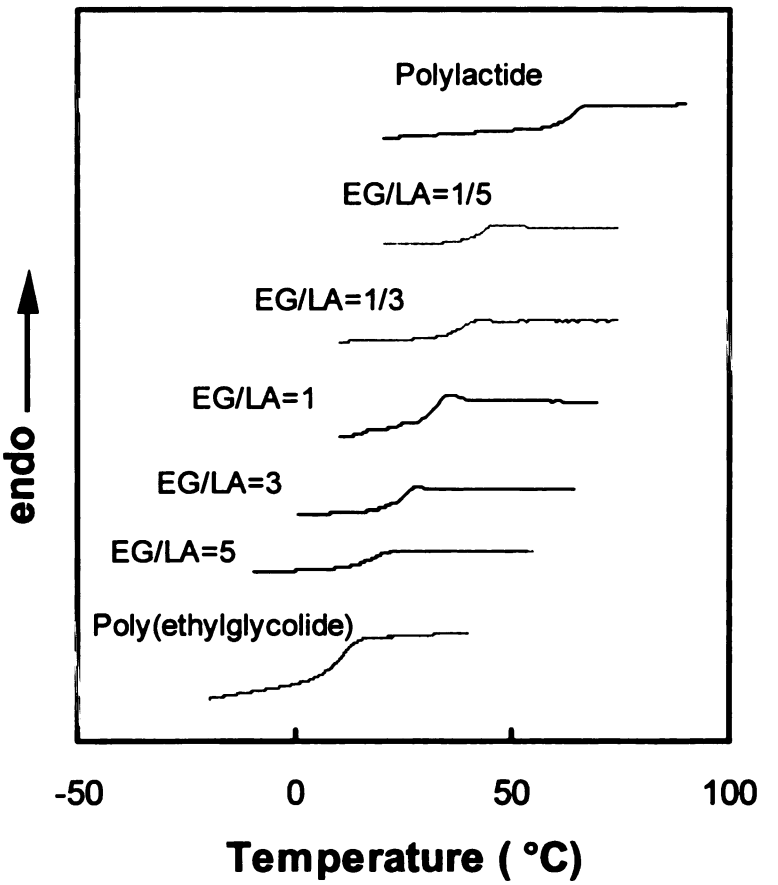

Figure 51. DSC runs (second heating after flash quenching from 100 °C) for lactide and ethylglycolide copolymers. Heating rate: 10 °C/min under helium.

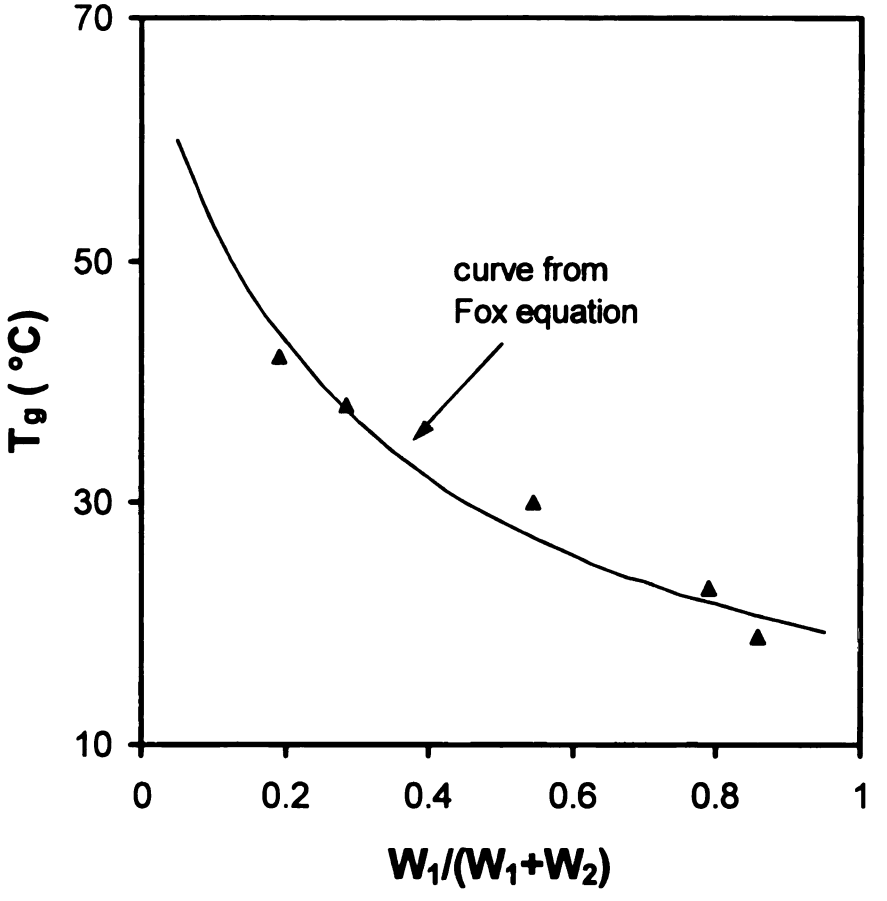

Figure 52. Glass transition temperatures of lactide and ethylglycolide copolymers.

Scheme 39. Reactivity difference leads to "blocky" copolymers.

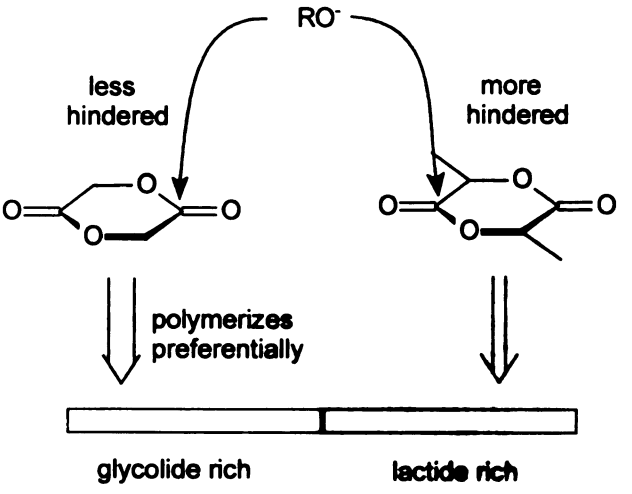

5.2

com

mis

inc

so

m

c

c

t

5.2 Copolymerization through asymmetric monomers.

Simple copolymerization has some shortcomings. If one of the comonomers is not polymerizable, the copolymer cannot be made. Also, the mismatch in reactivity between the comonomers leads to inhomogeneous incorporation of the comonomers into the polymer chain. These problems can be solved by designing the AB monomers shown in **Scheme 40**. A variety of AB monomers have been synthesized. As shown in **Scheme 41**, each monomer contains two sites for ring opening, and to a first approximation the two carbonyls of the ring can be treated independently. One site should have a reactivity similar to lactide, while the other should more closely resemble that of a substituted lactide. Thus we expect that the active end of growing lactide chain will attack the least hindered site on the AB monomer (the lactide carbonyl) at a rate somewhat slower than for lactide, and ring will open to give the substituted lactic acid residue at the growing chain end.

AB monomers also have limitations. AB monomers only produce copolymers whose composition is 50% A and 50% B. Using mixtures of comonomers can produce copolymers with any composition of A and B.

Sch

Scheme 40. The comparison between two copolymerization methods

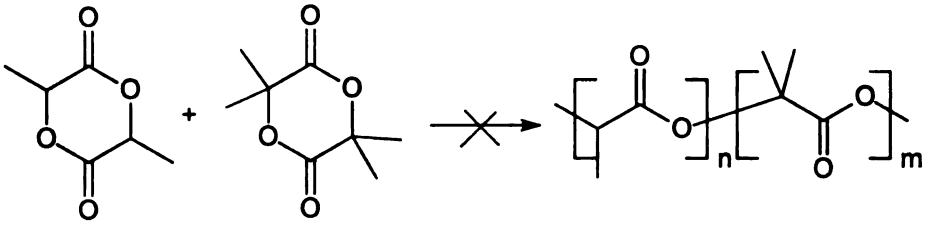

A

Because monomer **A** is not polymerizable, the compolymer can not be synthesized

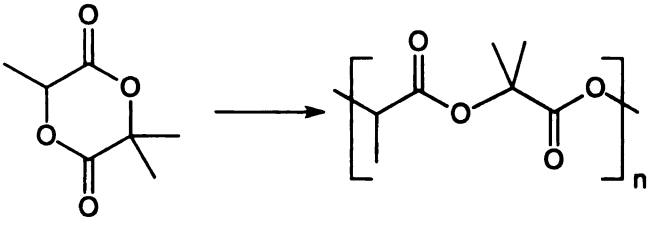

Using an AB monomer, the copolymer can be synthesized

Scheme 41. Structures of the AB monomers and reactivity of different sites

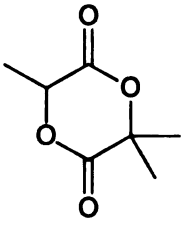

trimethylglycolide

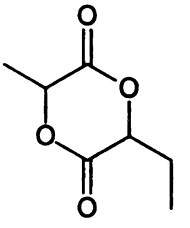

ethylmethylglycolide

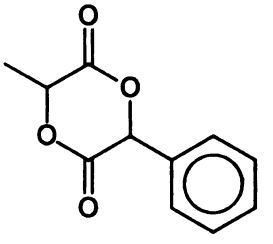

methylphenylglycolide

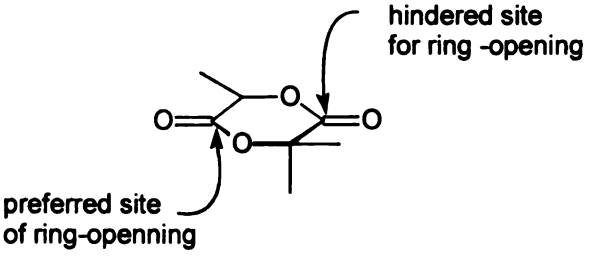

5.2.1

5.2.1. Synthesis and Polymerization of AB Monomers.

As shown in **Scheme 42**, the AB monomers were prepared by condensation of α-bromopropionyl bromide and the desired lactic acid. In this synthesis, it is important to remove all of the NEt_3 during the work-up, since even trace amounts of NEt_3 will polymerize the monomer to low molecular weight oligomers. Racemic α-bromopropionyl bromide and racemic lactic acids were used in the syntheses. As shown in **Figure 53**, the monomers are not statistical mixtures of R,R, S,S and R,S diastereomers. In the case of ethylmethylglycolide, the diastereomers form in a 3:1 ratio. For methylphenylglycolide, the selectivity is so high that the minor diastereomer is barely seen in the ^1H NMR spectrum. After recyrstallization, the pure diastereomer can be obtained. To identify the major isomer, we obtained the Nuclear Overhauser Effect (NOE) difference NMR spectra of methyphenylglycolide. As shown in **Figure 54**, methines H_a and H_b can be attached to the same side of the ring or opposite site of ring. If H_a and H_b are on the same side of ring, the signal of the H_b will be enhanced if H_a is radiated. As shown in **Figure 55**, the intensity of H_b increased when H_a was radiated. Thus, the major diastereomer is a mixture of the R,R and S,S isomers, and the minor isomer is the R,S, or S,R isomer. The kinetics of ring-closure probably favor the formation of the R,R and S,S isomers, and ring-closing competes with formation the oligomers. The selectivity can directly result from the ring closing step, or the selectivity can arise from different rates for conversion of the linear dimers to lactides or oligomers.

high

slow

know

ope

trim

poly

Ethylmethylglycolide and methylphenylglycolide can be polymerized to high molecular weight polymer easily. However, trimethylglycolide polymerizes slowly. Even after 24 hours at 180 °C, the conversion is only about 75%. It is known that the more substituents ring has, the more difficult it is for the ring to open. Lactide and other substituted lactides all are di-substituted, and trimethylglycolide is tri-substituted. One extra substituent makes it hard to polymerize.

Scheme 42. Synthesis of AB glycolide monomers

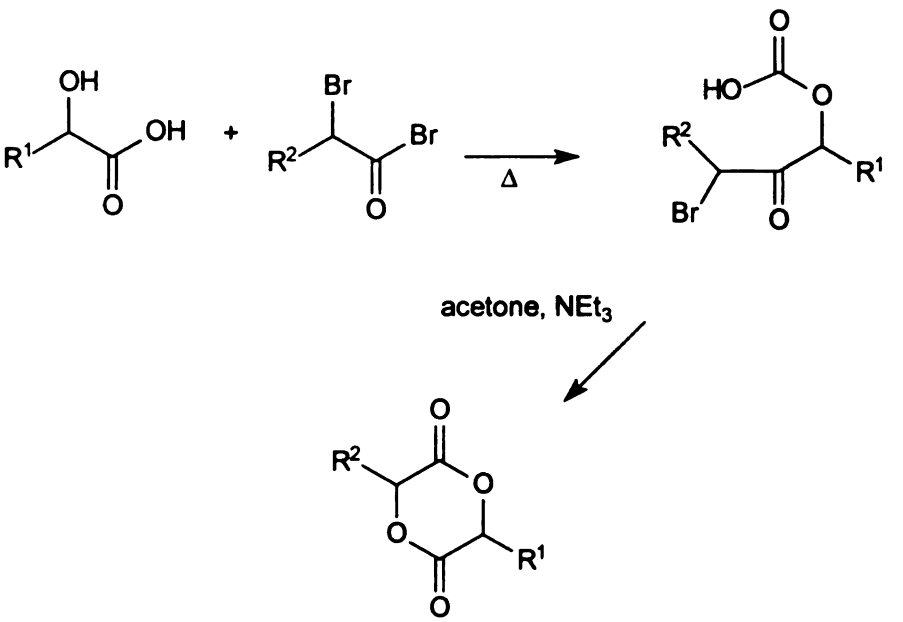

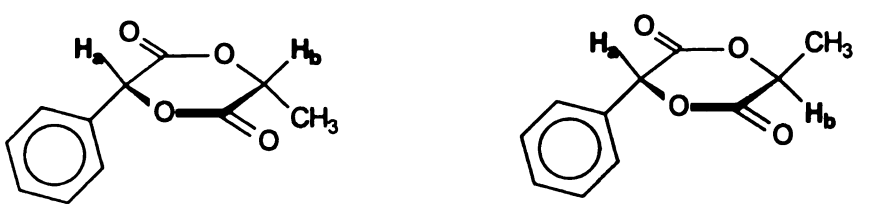

(R, R) (R, S)

Figure 54 Structure of the diastereomers of methylphenylglycolide


Minor is
5.1

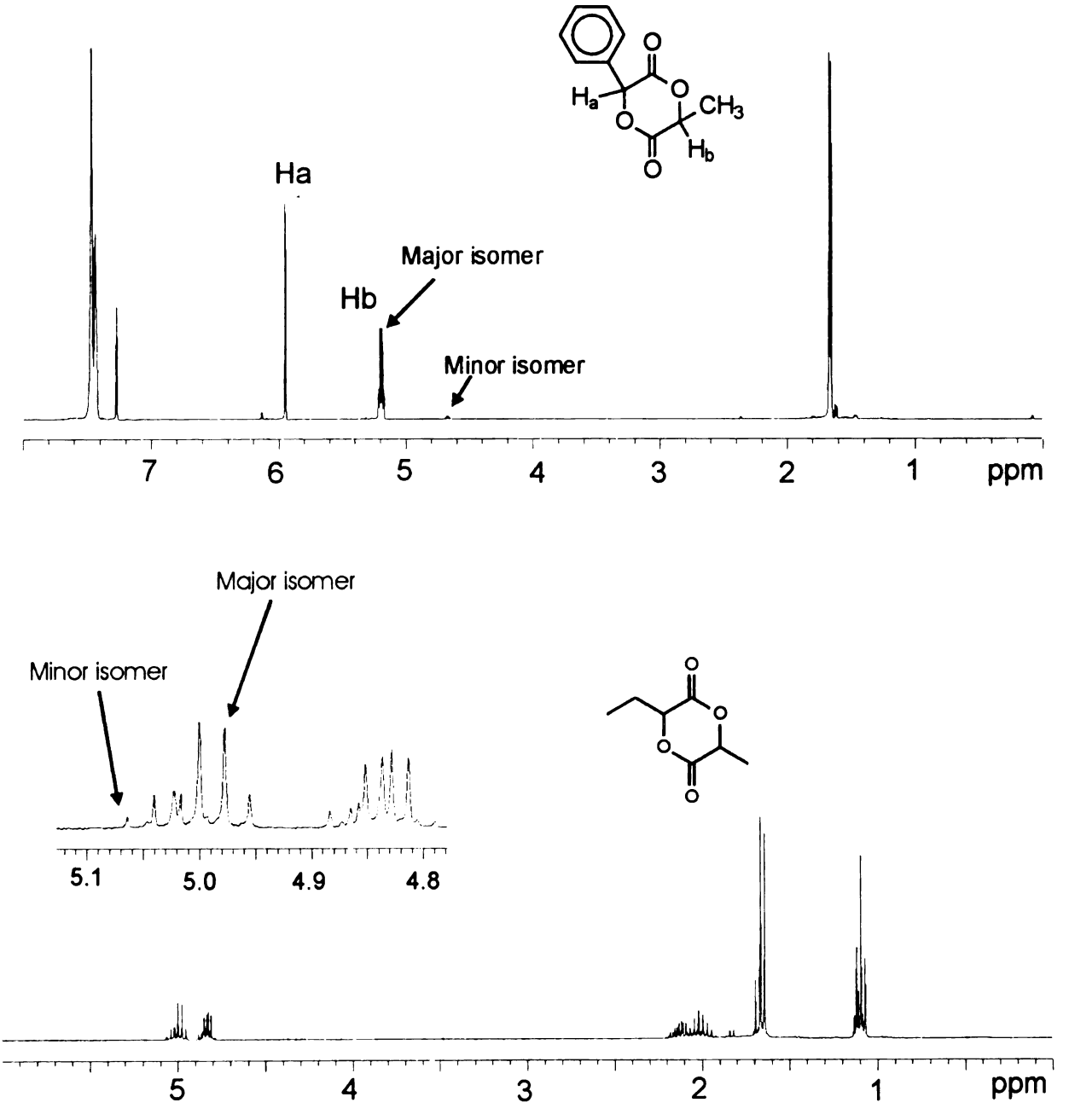

Figure 53. ^{1}H NMR spectra of ethylmethylglycolide and methylphenylglycolide

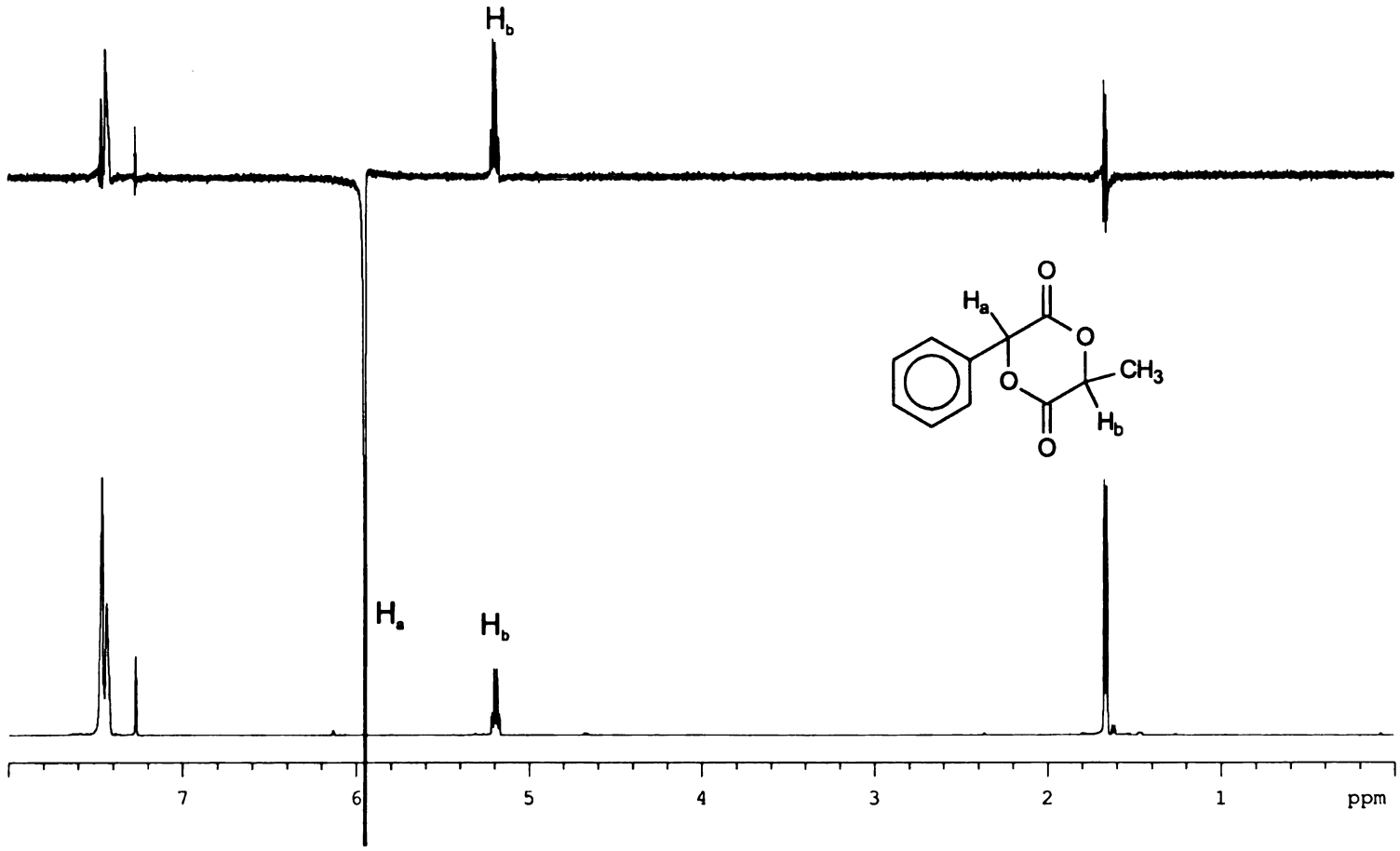

Figure 55. NOE NMR spectrum of methylphenylglycolide

5.2.2 Str

Whe

reactions a

relative siz

small, fou

copolymer

dominates

If either R

reaction

form.

Fo

is not la

know th

poly(eth

R^1 is m

group,

mande

poly(et

defect

polym

residu

5.2.2 Structure of the polymer chains.

When AB monomers polymerize, there are four possible propagation reactions as shown in as **Scheme 43**. Which reaction dominates depends on the relative size of the R^1 and R^2 side group. If the size difference of R^1 and R^2 is small, four reactions co-exist in the polymerization leading to random copolymers. If the size difference of R^1 and R^2 is large, one of the four reactions dominates, and an alternating $(AB)_n$ polymer with head to head defects will form. If either R^1 or R^2 is so large that attack from active center is totally blocked, one reaction exists in the polymerization, and a perfectly alternating copolymer will form.

For ethylmethylglycolide, R^1 is methyl and R^2 is ethyl. The size difference is not large, and from the homopolymerization of lactide and ethylglycolide, we know the reactivity difference of two monomers is not large. We expect that poly(ethylmethylglycolide) is a regio-random polymer. For methylphenylglycolide, R^1 is methyl and R^2 is phenyl. The phenyl group is much larger than the methyl group, but from studies of the polymerization of mandelide, we know that the mandelic acid residue should have some reactivity. We expect that poly(ethylmethylglycolide) is an alternating polymer with some head to head defects. For trimethylglycolide, we know that tetramethyglycolide is not polymerizable, so we expect that active center can only attack the lactic acid residue and give poly(trimethylglycolide) as a perfectly alternating polymer.

We used ^{13}C NMR to determine the chain structure of the AB copolymers. The carbonyl region of the ^{13}C NMR of AB copolymer is shown in **Figure 56**. Trace **A** is the ^{13}C NMR spectrum of poly(ethylmethylglycolide), which is very complicated. There are signals from two different carbonyl groups: one adjacent to methyl group with chemical shifts from 169 ppm to 169.8 ppm and one adjacent to the ethyl group with chemical shifts from 168.2 ppm to 169 ppm. Both carbonyl groups show multiple peaks, which are caused by the randomness of the chain structure and the stereochemistry of the chain. Trace **B** is the ^{13}C NMR spectrum of poly(trimethylglycolide), which shows a simpler pattern. Again, there are signals from two different carbonyl groups: one adjacent to the methyl group with chemical shifts from 168.7 ppm to169.6 ppm and one adjacent to the dimethyl groups with chemical shifts from 170.3 ppm to 171.3 ppm. Since tetramethylglycolide is not polymerizable, we think that the nucleophilic attack ocurred exclusively at the lactide residue and that poly(trimethylglycolide) may be a perfectly alternating polymer. Although the carbonyl resonances also show multiple peak patterns, this may be caused by the stereochemistry of the chain, because racemic monomer was used. Trace **C** is the ^{13}C NMR of poly(methylphenylglycolide). Both carbonyl groups have multiple peak patterns, although the resolution is not very good. Because the monomer used in synthesis of AB copolymers are not optically pure, the spectra contains the information of both stereochemistry of chain and structure of chain. It is very difficult to determine the structure of chains. To

una

are

Sch

unambiguously determine the structure of the chain, optically pure monomers are needed. The synthesis of optically pure monomers is still ongoing.

Scheme 43. The propagation step in the polymerization of AB monomers

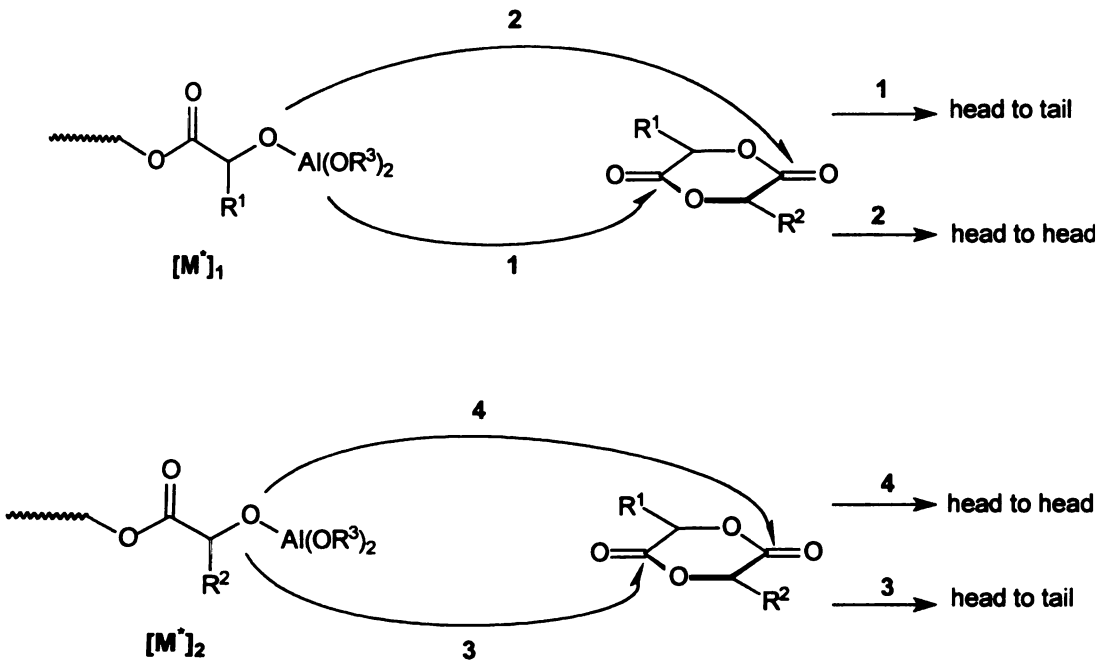

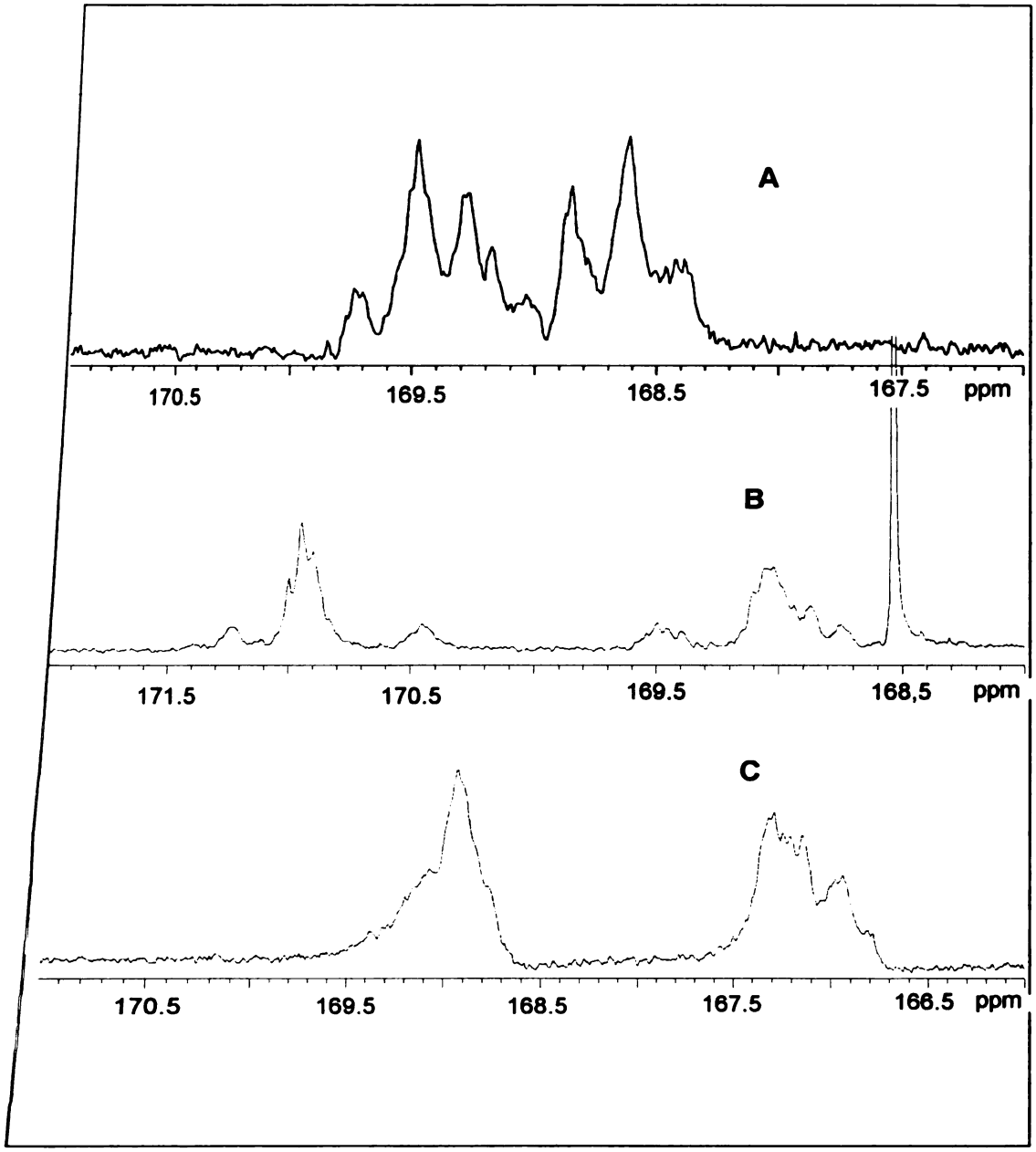

Figure 56. Carbonyl region of ^{13}C NMR of AB copolymers. **A** is poly(ethylmethylglycolide), **B** is poly(trimethylglycolide) and **C** is poly(methylphenylglycolide)

5.3 The

D

copolyr

greatly

Poly(m

Althou

its sh

4,000

transi

expe

isom

How

from

optic

the

is v

or

cry

cha

de

dif

th

Th

5.3 Thermal properties of the copolymer.

DSC was used to measure the glass transition temperatures of the copolymers. The results are shown in **Figure 57** and **Table 18**. Bulky side chains greatly increase the glass transition temperature of polymers. Poly(methylphenylglycolide) has a glass transition temperature at 85 °C. Although, poly(trimethylglycolide) shows a glass transition temperature at 50 °C, its should be higher, since the molecular weight of polymer was low (about 4,000). Polymers with molecular weights over 20,000 should have higher glass transition temperatures. None of the polymers were crystalline, which was expected, since the ethylmethylglycolide was a mixture of S,S, R,R, and R,S isomers. Trimethylglycolide and methylphenylglycolide were also racemic. However, we made (S,S)-methylphenylglycolide and (R,R)-methylphenylglycolide from L-mandelic acid and D-mandelic acid, and the copolymers from these optically pure AB monomers are still amorphous. There are two possibilities for the lack of crystallinity in these copolymers. First, the proton α to the phenyl ring is very reactive, and at high temperature, this proton may be lost to form a radical or ion. In either case, the polymers are going to be racemized, which inhibits crystallization. During bulk polymerization at 180 °C, the reaction mixture changed from colorless to dark brown very quickly. We think it was caused by the deprotonation. Second, because of transesterification and because the reactivity difference for attack at the hindered and less hindered side is not large enough, there are many head-to-head and head to tail placements in the polymer chain. Thus, the polymer chain is not ordered enough to crystallize.

The

Poly(trimet

the low m

about 6% n

the impurit

thermally s

Poly
Po
Poly

a

b

The decomposition temperatures of the polymer are shown in **Figure 58**. Poly(trimethylglycolide) has the lowest the decomposition temperature, due to the low molecular weight of the polymer. Poly(methylphenylglycolide) shows about 6% residue at 370 °C, which then disappears at 600 °C. It is not caused by the impurity such as catalyst, it is well-known that aromatic polymers often form thermally stable compounds when thermally decomposed.

Table 18. The properties of AB polymers.

Polymer	$M_n \times 10^{-3}$ [a]	M_w/M_n	T_g °C [b]
Poly(ethylmethylglycolide)	31.2	1.81	85
Poly(trimethylglycolide)	35.6	1.85	50
Poly(methylphenylglycolide)	4.2	1.25	22

a. measured by GPC in THF using polystyrene as standard
b. measured by DSC under He at rate of 10 °C/min

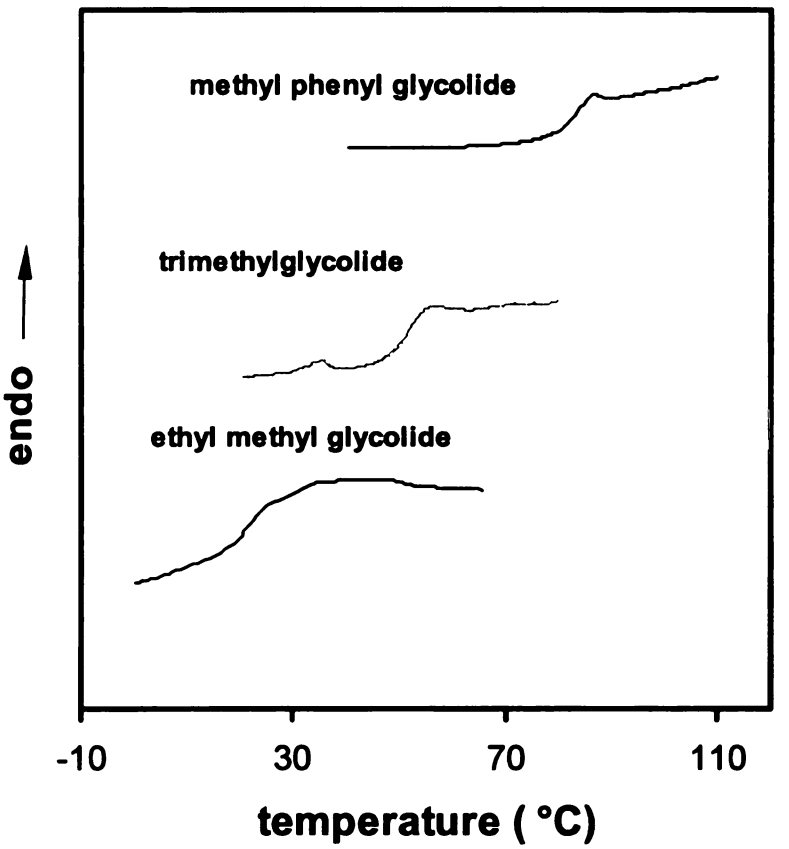

Figure 57. DSC runs (second heating after flash quenching from 100 °C) for AB polymers. Heating rate: 10 °C/min under helium.

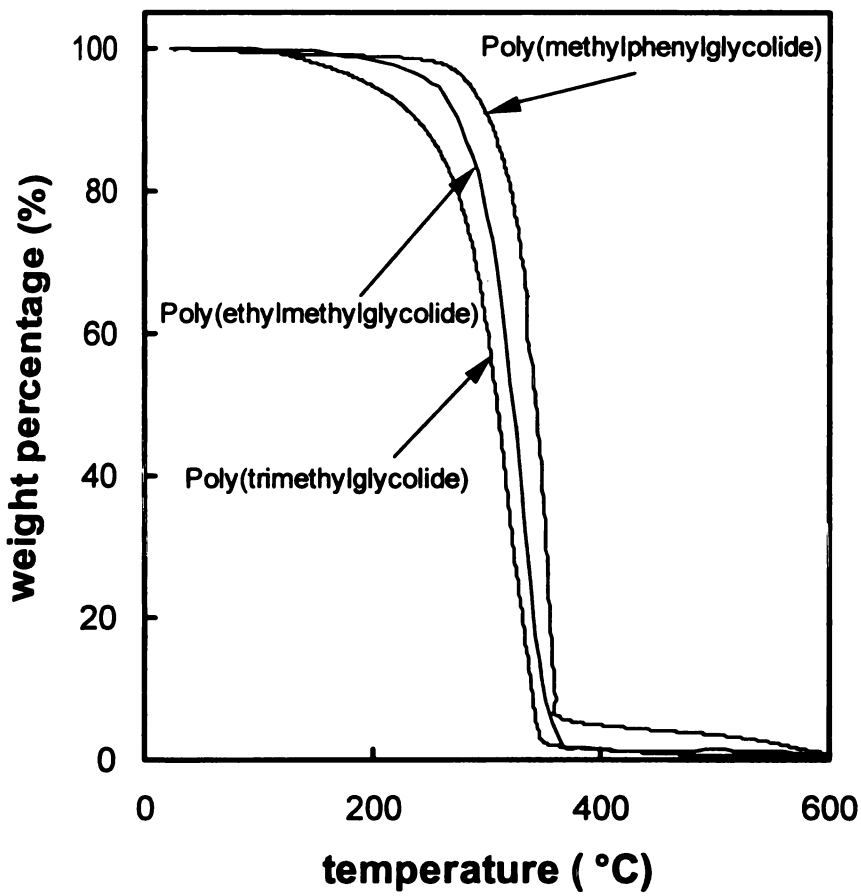

Figure 58. Thermogravimetric analysis results for AB polymers run in air. Heating rate: 40 °C/min.

6. C

6.1 Syn

A

polyme

polyme

crystal

availab

amino

optica

synth

with

This

meth

litera

foun

sepa

qua

was

lact

isop

rac

ste

6. Crystalline substituted polylactide.

6.1 Synthesis and polymerization of optical pure monomers

All of the substituted polylactides mentioned above are amorphous polymers because the monomers used to make the polymers are racemic. If we polymerize optically pure monomers, the resulting polymers should show some crystallinity. Since most optically pure 2-hydroxyacids are either not readily available or are very expensive, we prepared optically pure 2-hydroxyacids from amino acids. Optically pure amino acids are easily available and cheap, and the optically pure monomers can be obtained through simple chemical reactions. The synthesis of a monomer from valine is shown in **Scheme 44**. Valine was treated with $NaNO_2$ in acidic aqueous solution to yield the corresponding 2-hydroxyacid. This reaction proceeds with retention, and thus L-valine yields L-2-hydroxy-3-methylbutyric acid. The synthetic procedure used is a modified version of a literature preparation. The literature preparation uses HCl as the acid, but we found that about 10% of the product is the 2-chloroacid, which is very difficult to separate from the 2-hydroxyacid. Switching to dilute H_2SO_4 gave nearly quantitative yields of the 2-hydroxyacid.

The dimer of 2-hydroxy-3-methylbutyric acid is isopropylglycolide, which was synthesized using the same method used to synthesize other substituted lactides such as ethylglycolide. Because we wanted to obtain optically pure isopropylglycolide, the high temperature cracking process used in making racemic monomers is inappropriate since it leads to some epimerization of the stereocenter. 2-Hydroxy-3-methylbutyric acid was condensed in toluene using *p*-

toluenesulfonic acid as catalyst to give a mixture of the dimer and low molecular weight oligomers. The resulting glycolide was crystallized directly from toluene to give pure S-isopropylglycolide. *rac*-2-Hydroxy-3-methylbutyric acid gave a mixture of R,R, S,S and R,S isomers, and after recyrstallization from ether, only pure *rac*-isopropylglycolide (1:1 mixture of R,R and S,S isomers) was obtained.

Melt polymerizations carried out at 180 °C using $Sn(Oct)_2$/BBA as the catalyst/initiator reached 95% conversion after about one hour. At the beginning of the polymerization, the mixture was an easy to stir liquid, but after several minutes, the mixture became very viscous. After 10 minutes, the polymerization mixture solidified and was impossible to stir. The solidification was caused by crystallization of the polymer, which has a melting point >180 °C. The details of crystallization will be discussed later. The molecular weight distribution of the resulting polymer is very broad, with a polydispersity about 3, probably due to crystallization of polymer. Because of crystallization, the polymerization reaction can become diffusion controlled. If the diffusion rate of monomer is much slower than the polymerization rate, monomer is not evenly distributed in the mixture. Thus, polymerization sites have different propagation rates leading a mixture of long and short polymer chains and a broad molecular weight distribution.

NMR spectra of poly(S-isopropylglycolide) are shown in **Figure 59**. The top trace shows the methine proton region for the homo decoupled ^{1}H NMR spectrum, and the bottom trace shows the carbonyl region of the ^{13}C NMR spectrum. We conclude that there is almost no racemization during the polymerization, because only one peak is seen in both spectra.

Scheme 44. The synthesis of an optically pure substituted lactide from an amino acid precursor

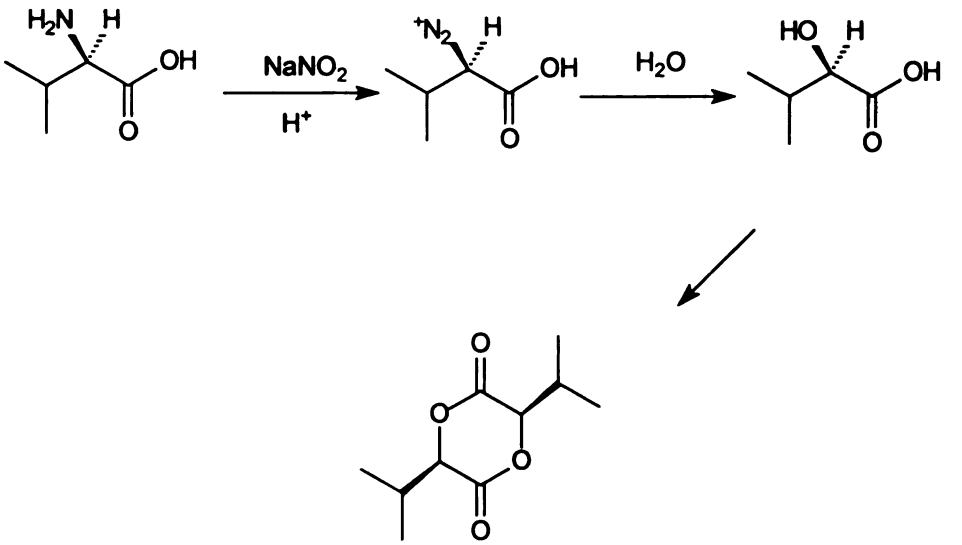

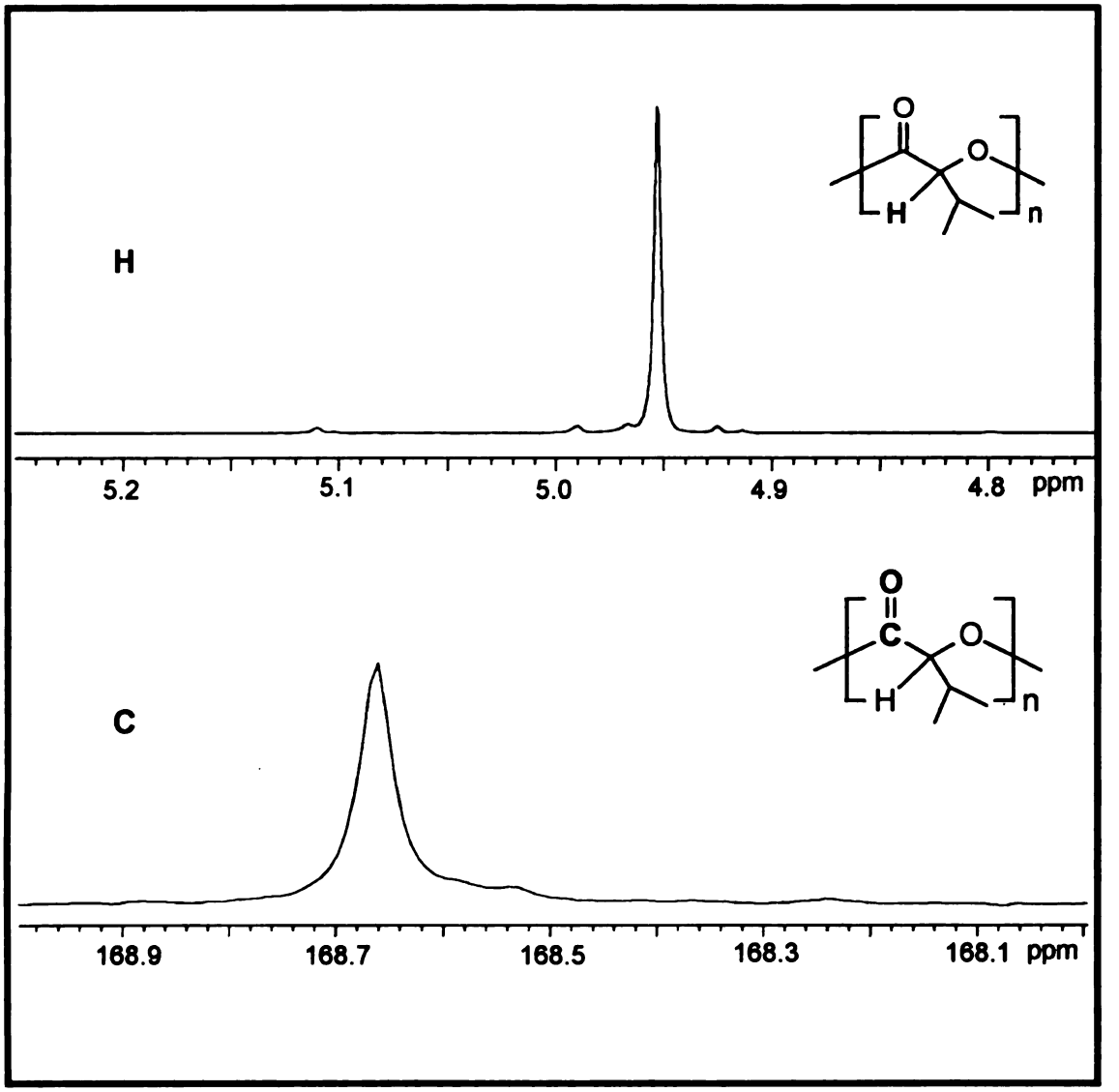

Figure 59. NMR spectra of the methine (top) and carbonyl (bottom) region of poly(S-isopropylglycolide)

6.2 The stereochemistry of the polymer chain

A number of the physical properties of poly(lactide) are linked to its stereosequence distribution in the polymer chain. For example, pure isotactic poly(L-lactide) crystallizes at faster rate and to a larger extent than when L-lactide is polymerized with small amount of either D-lactide or meso-lactide.[190] In the ^{1}H and ^{13}C NMR spectra of polylactides, the observed resonances can be assigned to various stereosequence combinations in the polymer. The assignments are designated as various combination of "i" isotactic pair-wise relationships (-RR- and –SS-) and "s" syndiotactic pair relationship (-RS- and –SR-). In the NMR spectra, the -RR- and -SS- diads and -RS- and -SR- diads are indistinguishable and have identical chemical shifts.

The assignment of resonances for polylactides up to hexads has been made by several research groups.[187,191-194] Bernoulli and first-order Markov models have been used to rationalize the assignments. In **Figure 60** are shown the building of a polymer chain by a Bernoulli and a first-order Markov process. In the Bernoulli model, the stereochemistry of chain end is not important, which means that stereochemistry of the chain end does not influence the addition of the monomer to the chain end. In the first-order Markov model, the stereochemistry, which may be *i* or *s* is strongly influenced on the adding monomers to the chain end.

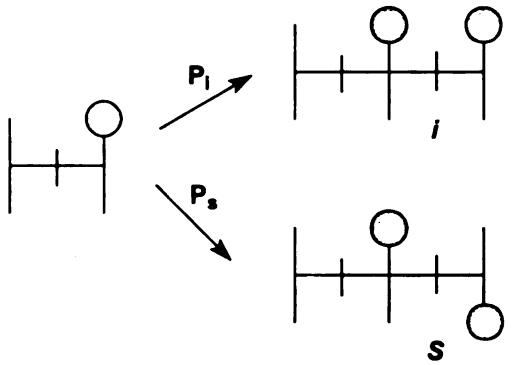

Bernoullian Model

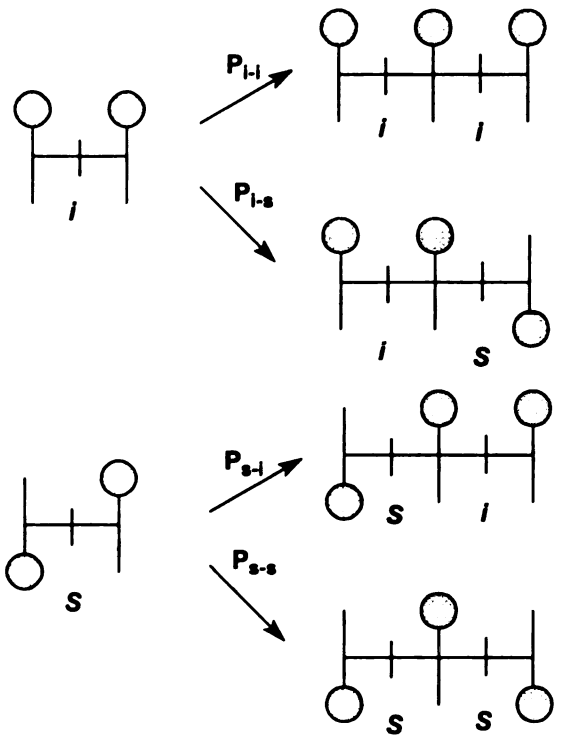

First-order Markov model

Figure 60. Schematic representation of the Bernoulli and first-order Markov model.

The physical properties of poly(isopropylgycolide) are also dependent on the stereosequence of the polymer chain. As shown in **Figure 61**, pure poly(S-isopropyglycolide) has a melting point around 230 °C. The melting point of poly(isopropyglycolide) decreases when S-isopropylglycolide is polymerized with a small amount of *rac*-isopropyglycolide. From measurements of the heat of fusion, we found that the extent of crystallization also decreased. As was done with polylactide, we would like to assign the stereosquences of poly(isopropyglycolide) to understand the relationship between the physical properties of poly(isopropyglycolide) and stereochemistry of the polymer chain.

The stereochemical assignments were made by comparing the trends observed in the spectra of a number of poly(isopropylglycolide)s to the probability distribution expected on the basis of their lactide feed composition. Shown in **Figure 62** and **Figure 63** are the carbonyl region of the ^{13}C NMR of poly(isopropyglycolide) and the methine region of ^{1}H NMR of poly(isoproplyglycolide). Trace **A** in each figure is spectrum of the polymer prepared from 100% S-isopropyglycolide. The single peak in both spectra can be identified as resulting from an *iiiii* sequence. The **B** traces are spectra for the polymers prepared from 85% R-isopropylgycolide and 15% racemic isopropyglycolide. In additon to the *iiiii* peak, several new peaks appeared. Because the amount of S-isopropyglycolide is small, probability dictates that these peaks should be *isiii* and *iiisi* sequences. By comparing the spectra from samples with different ratios of S-isopropylglycolide and *rac*-isoproylglycolide, we assigned all 11 hexads of the polymer chain. The result is shown in **Figure 64**.

Because the resolution of ^{1}H NMR spectrum is not as good as for the ^{13}C NMR, we only assigned stereosequences in the ^{13}C NMR spectrum.

The unusual intensitry of the *iiiii* hexad in the poly(*rac*-isopropyglycolide) spectrum suggests that the polymerization follows non-Bernoullian statistics and stereoselection occurs during the polymerization of *rac*-isopropyglycolide. We used the first-order Markov model to describe such a process. We assume that the probabilities for an RR monomer adding to an RR chain end and an SS monomer adding to an SS chain end are p, and the probabilities of an RR monomer adding to an SS chain end and an SS monomer adding to an RR chain end are $(1-p)$. It is possible to calculate the expected intensity values of the individual sequences as shown below:

$$iiiii = p^3 + 0.5p^2(1-p)$$

$$iiiis = siiii = iisii = 0.5p^2(1-p)$$

$$iiisi = isiii = 0.5p^2(1-p) + 0.5p(1-p)^2$$

$$iisis = siiis = sisii = 0.5p(1-p)^2$$

$$isisi = 0.5p(1-p)^2 + 0.5(1-p)^3$$

$$sisis = 0.5(1-p)^3$$

We compared the experimental values and calculated values using equation $\Sigma[(I_{cal}-I_{exp})/I_{exp}]^2$, where I_{cal} is calculated peak intensity and I_{exp} is experimental peak intensity. We found that when p=0.61, the I_{cal} is closest to I_{exp}. The result is shown in **Table 14.** It indicates a preference for addition RR

monomer to the RR chain end and SS monomer addition to SS chain end, which enhances contribution of isotactic segments in poly(isopropylglycolide). This result is very different from that obtained for polylactide, where several authors reported that the lactide polymerization favors syndiotactic chain segments (p<0.5). The reason for this difference is not clear and is still under investigation.

Table 19. Experimental and calculated values of hexad intensities in the carbonyl region of ^{13}C NMR spectra of poly(*rac*-isopropyglycolide)

	iiiii+siii i+iiiis	***iiisi***	***sisii***	***isiii+iisii +siiis***	***iisis+sisis***	***isisi***
Experimental values	46.2	11.8	4.4	22.3	7.07	8.25
Calculated values (p=0.61)	44.4	11.9	4.6	23.8	7.61	7.61

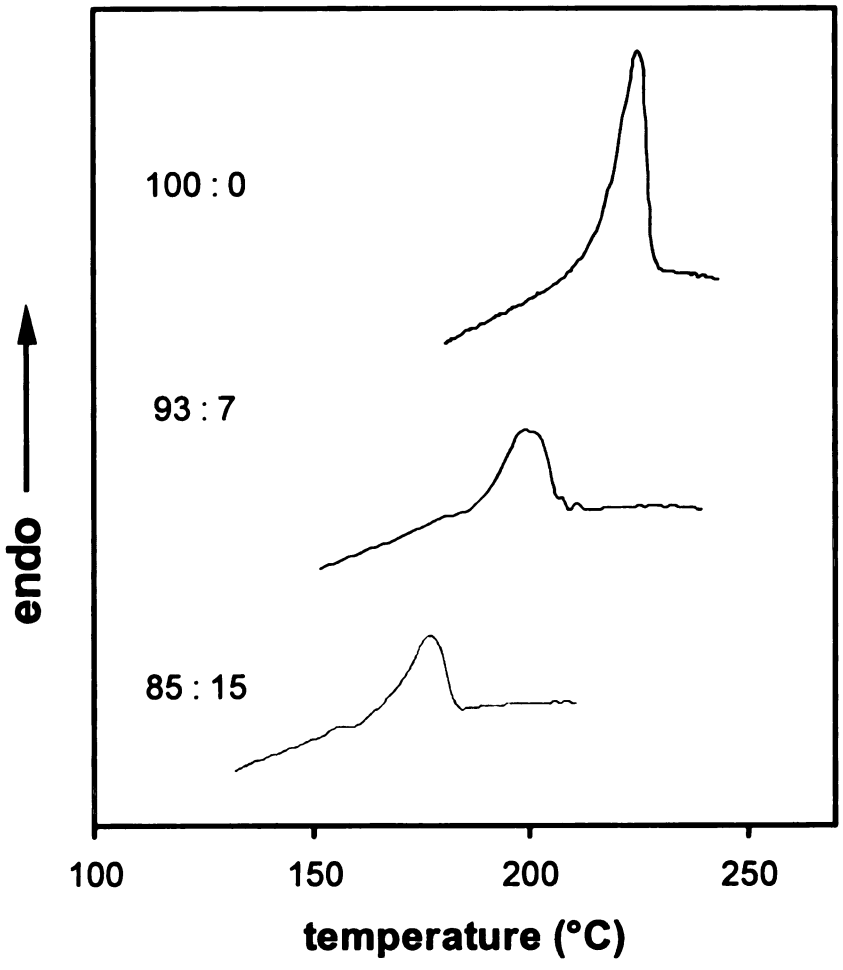

Figure 61. DSC runs showing the melting point for poly(isopropyglycolide)s prepared from S and *rac*-isoproplyglycolide. The ratios are the S:*rac* content in the polymers.

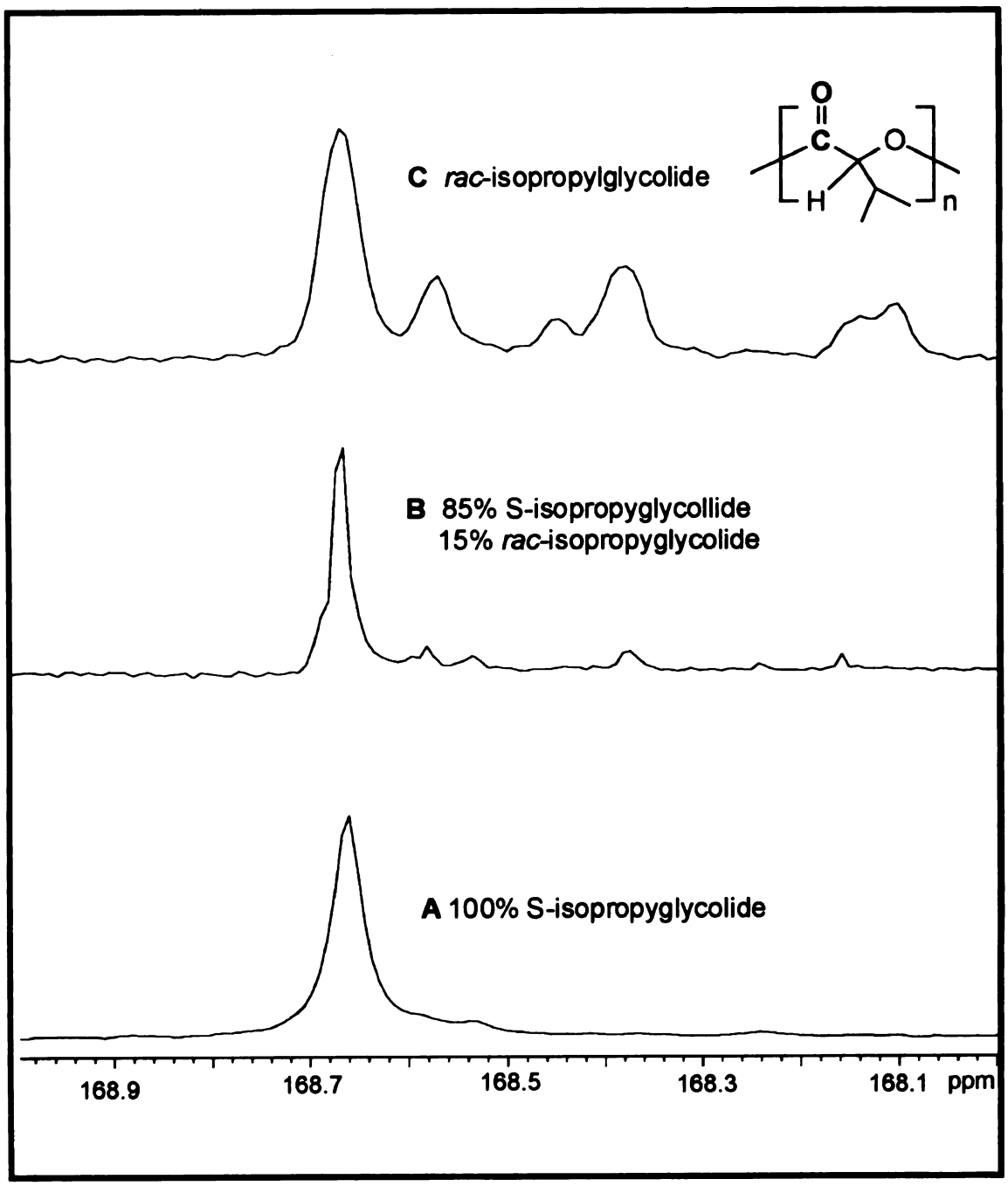

Figure 62. ^{13}C NMR of poly(isopropylglycolide)

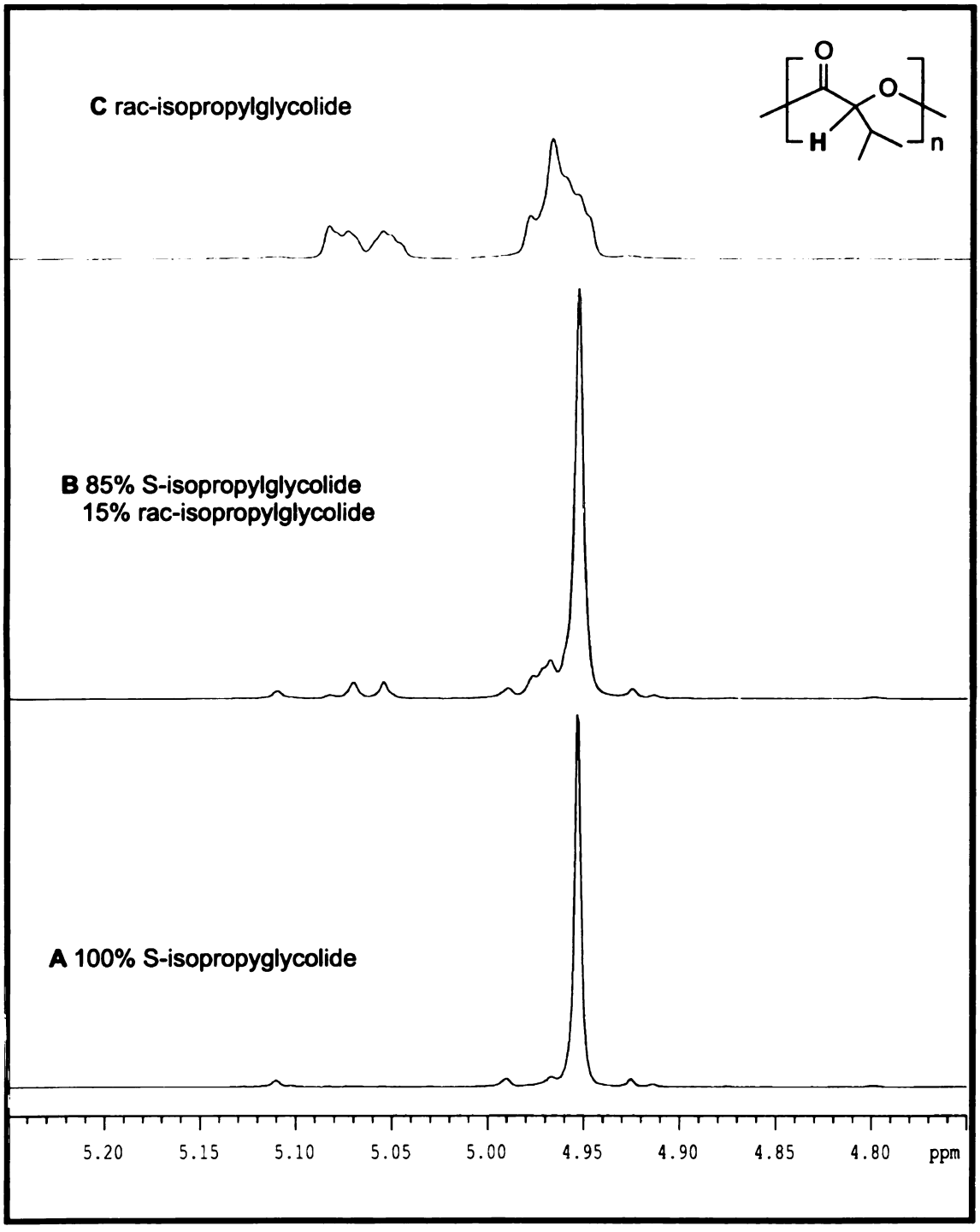

Figure 63. ^{1}H NMR of poly(isopropylglycolide)

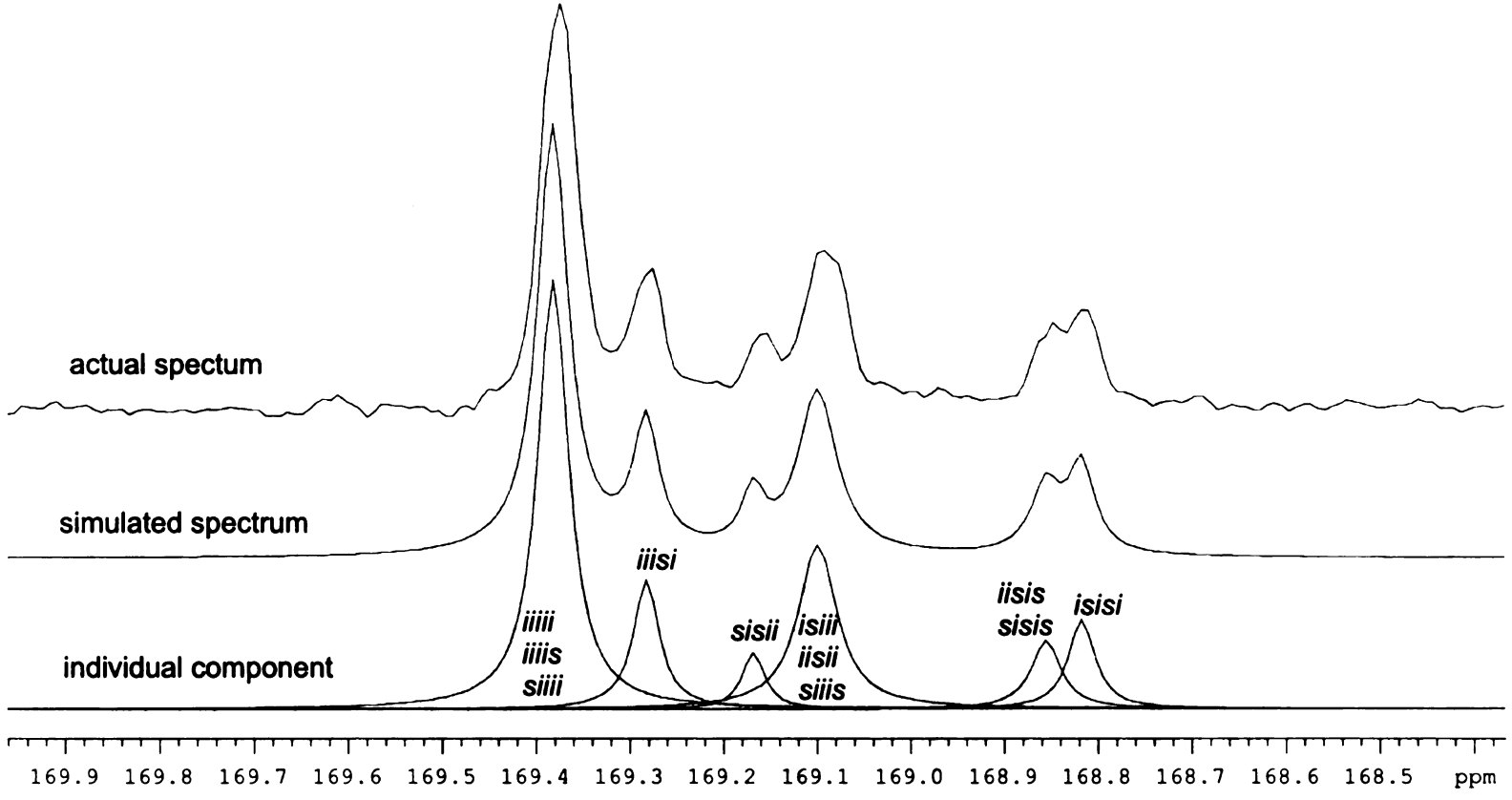

Figure 64. Stereosequence assignment for ^{13}C spectrum of poly(*rac*-isopropylglycolide)

6.3 The crystallinity of poly(isopropyglycolide)

We used X-ray diffraction to determine the crystallinity of poly(R-isopropyglycolide). This method has been used by Hermans and Weidinger to measure the crystallinity of polyethylene,[195] polypropylene,[196] and polystyrene.[197] The X-ray diffraction pattern of crystalline poly(isopropylglycolide) is shown in **Figure 65**. A valid procedure for subtracting the amorphous scattering from the total scattering is always the first and most essential step in any attempt to derive a measure of crystallinity from X-ray diffraction. However, unavoidably, it always involves certain uncontrollable assumptions. The X-ray diffraction pattern for amorphous poly(isopropyglycolide) made from *rac*-isopropyglycolide is shown in **Figure 66**. The amorphous sample shows a broad peak with maximum at about 12 degrees. We assumed that the amorphous fraction in the crystalline sample should have the same maximum and the same line-shape. To make the problem easier, we selected a 10-degree window, 6-16 degrees, for the calculation. PeakSolve software was used to deconvolute the diffraction pattern into amorphous and crystalline components. The result is shown in **Figure 67**. The area under amorphous peak is O_{am} and the area under three crystalline peaks is O_{cr}.

The degree of crystallinity is calculated by comparing the results from two or more samples of the same polymer with crystalline fraction X_1 and X_2, where X_1-X_2 is as large as possible. Then, X_1 and X_2 can be described using following equation:

$$X_1/X_2=O_{cr1}/O_{cr2}$$

$$(1-X_1)/(1-X_2)=O_{am1}/O_{am2}$$

The crystallinity of several different poly(isopropylglycolide) samples are shown in **Table 20**. We combined the crystallinity data and the heat of fusion measured using DSC to estimate the heat of fusion for a 100% crystalline sample. By plotting the heat of fusion vs. crystallinity of sample, we use data from **Figure 68** to estimate the heat of fusion for 100% crystallinity. The result, 43.6.J/g, is about half that of polylactide's 100 J/g.

Table 20. The crystallinity and heat of fusion of poly(isopropylglycolide)

Samples	Crystallinity [a] (%)	Heat of fusion (ΔH J/g)
1	46.9	22.1
2	35.2	17.9
3	27.8	14.3

a. estimated from X-ray analysis of samples

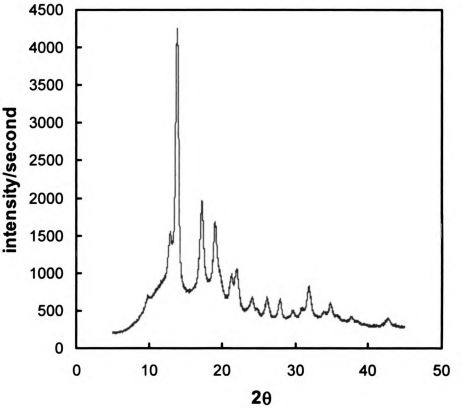

Figure 65. X-ray diffraction pattern for crystalline poly(S-isopropylglycolide)

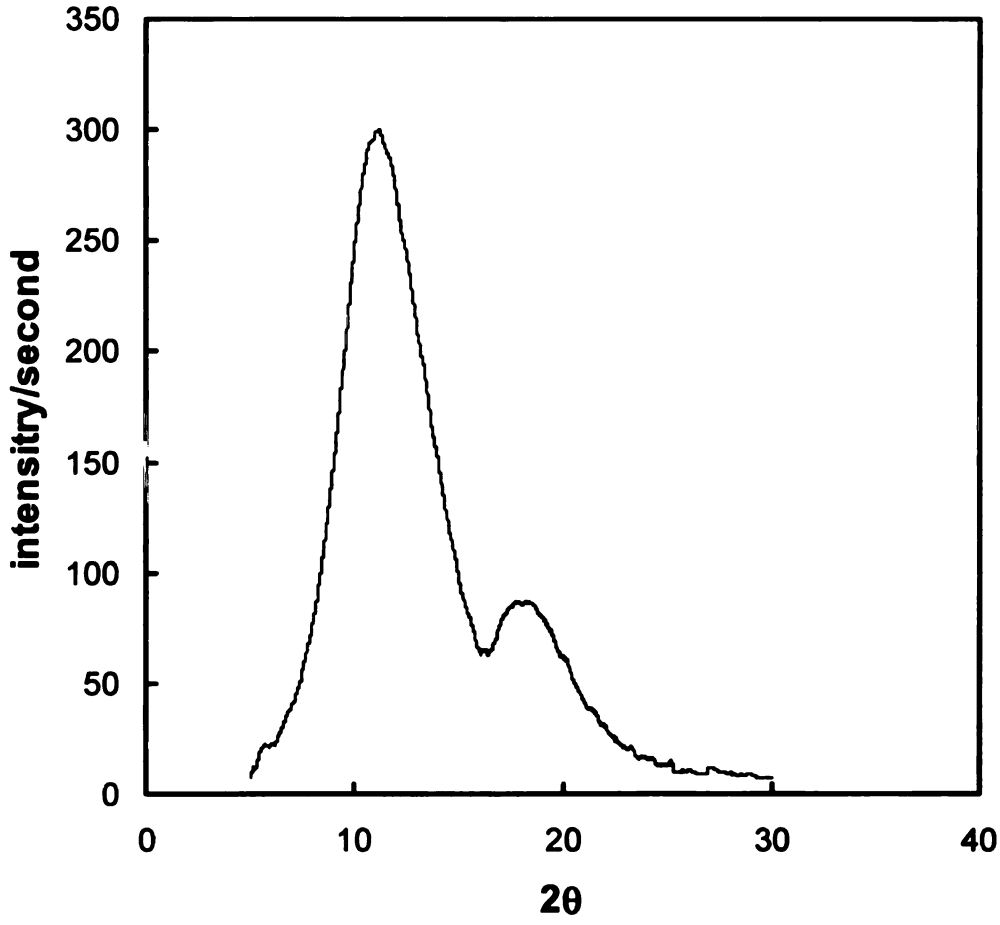

Figure 66. X-ray diffraction for amorphous poly(*rac*-isopropylglycolide)

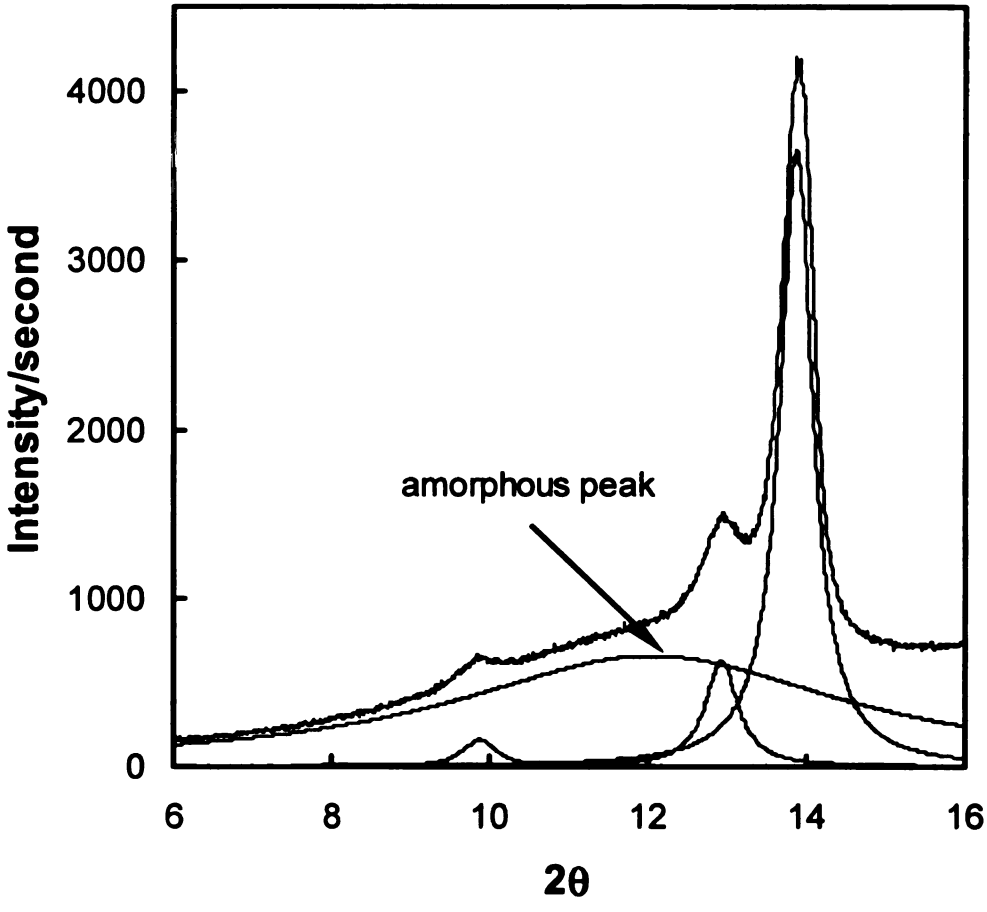

Figure 67. Peak deconvolution for crystalline poly(S-isopropylglycolide)

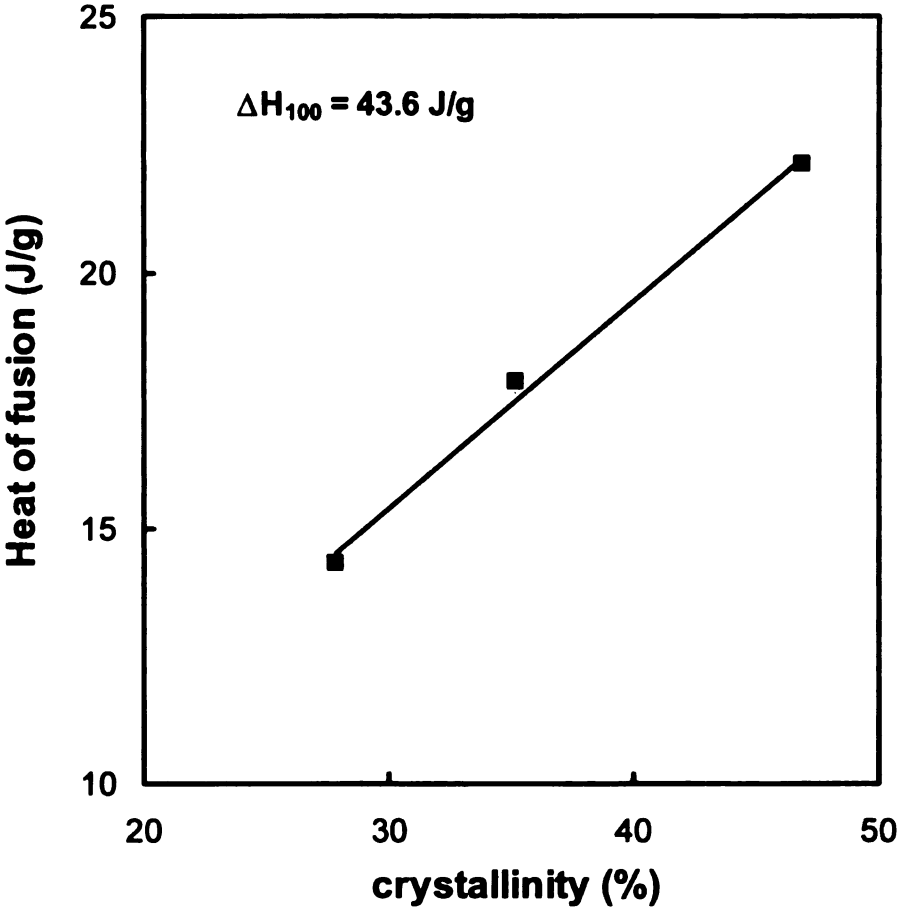

Figure 68. Determination of heat of fusion for 100% crystalline poly(isopropylglycolide)

7. The degradation of substituted polylactides

The degradability of the substituted polylactides was evaluated by hydrolytic degradation in phosphate buffer solution (0.01M KH_2PO_4/K_2HPO_4 solution, pH=7.4) at 55 °C. To exclude the influence of autocatalysis, we chopped the polymer samples into small pieces. The auotcatalytic effect is caused by the increase in acidity when the degradation products are acidic and have limited diffusion. If polymer samples are small enough, the diffusion rate of buffer solution into the bulk is higher than the polymer chain scission and the hydrolytic degradation can proceed uniformly in the bulk of the specimen. The morphology of the polymer also influences the degradation of polymer. The crystalline polymer degrades much slower than the amorphous polymer. The much tighter packing of the crystalline phase makes water much harder to penetrate into the bulk of the polymer. To study the influence of chemical structure of polymer on degradability, we have to eliminate the influence of morphology. To do that, we used amorphous substituted polylactides prepared from racemic monomers. All polymers were tested using DSC to ensure that the polymers were amorphous.

The weight loss and molecular weight decrease with degradation time are two of most important properties of biodegradable polymers. The weight and molecular weight loss versus time are shown in **Figure 69** and **Figure 70**, respectively. The sample weights were constant for a period of time, and then began to drop. The molecular weight of polymer dropped immediately once the degradation begins. These are typical behavior for hydrolytic degradation.

To calculate the degradation rate constant, we used the random scission model to fit the data. For the random scission model, the average number of bond cleavages per polymer molecule (N) was calculated according to:

$$N=[M_n(0)/M_0(t)-1]= K_d P_n(0)t$$

where $M_n(0)$ and $M_n(t)$ are the number-average molecular weights of polyesters at time 0 and time t. k_d is the rate constant for hydrolytic degradation, and $P_n(0)$ is the number-average of degree of polymerization at time 0.

K_d was obtained from plots of $[M_n(0)/M_0(t)-1]/P_n(0)$ *versus t*. The slopes of the plots are the rate constants for hydrolytic degradation. The results are shown in **Figure 71**. From the figure, we can see that polylactide degrades fastest, poly(ethylglycolide) and poly(hexylglycolide) have almost the same degradation rate and slower than poly(lactide), and poly(isobutylglycolide) degrades the slowest.

An interesting phenomenon showed up when remaining weight fraction was plotted vs. degree of polymerization, as shown in **Figure 72**. The weights of all polymers began to drop at almost the same degree of polymerization, which is about 30. We think this is critical molecular weight for entanglement. When the degree of polymerization is higher than 30, almost all of the polymer chains are entangled, so polymers will not dissipate into the water and there is almost no weight loss for the polymers. When the degree of polymerization of polymer is

lower than 30, some of polymer chains are not entangled, so these chains will dissipate into water and there is weight loss for the polymers.

How the substituent influences the degradation rate of substituted polylactides is the question we need to answer. We think there are two factors that influence the degradation rate: the glass transition temperature and the surface energy of the polymers. At the degradation temperature, the free volume will be larger in polymers with a relatively low glass transition temperature than those with high glass transition temperatures. Thus, low T_g polymers will have a higher water content, which causes the higher degradation rate. If a polymer has a very low surface energy (hydrophobic), the solubility of water will be low and the degradation rate will be low.

The glass transition temperatures of the substituted lactides are shown in **Table 21**. The order of glass transition temperature is lactide > isobutylglycolide > ethylglycolide > hexylglycolide. Based on glass transition temperature, we would expect the order of the degradation rate is hexylglycolide > ethylglycolide > isobutylglycolide > lactide. However, besides the glass transition temperature, we also need to consider the surface energy of the polymers.

We used contact angle method measurements to characterize the surface energy of the substituted polylactides. We make a series of water/methanol solutions with different water/methanol ratios. The surface tensions of these solution were measured, and then these solution were dropped on the polymer films. The contact angle between the solution and polymer film

were measured, and the surface energy of the film were calculate using the Zisman equation:

$$\cos\theta = 1 + \beta(\gamma_L - \gamma_C)$$

where θ is contact angle, γ_L is surface tension of testing solution (water/methanol solution). γ_C is the surface energy of the polymer surface, and β is constant. Values of $\cos\theta$ vs γ_L were plotted for each substituted polylactide shown in **Figure 73**, and then the lines were extend to $\cos\theta = 1$. The intercept γ_L value is the surface energy of polymer (**Table 21**).

Table 21. The degradation of substituted polylactide

polymer	Glass transition temperature(°C)	Surface energy γ (dyn/cm)	Degradation rate (day^{-1}) $\times 10^3$
polylactide	65	21.6	3.7
Poly(ethylglycolide)	15	19.9	2.6
Poly(isobutylglycolide)	23	18.5	2.4
Poly(hexylglycolide)	-37	16.2	1.0

The length of linear alkyl substituted group increases from lactide to ethylglycolide to hexylglycolide, which causes the glass transition temperature and surface energy to decrease. However, these two factors have opposite effects. Decreasing glass transition temperature increases the degradation rate, and decreasing the surface energy decrease the degradation rate. So a combination these two factors may explain the observed order of degradation For poly(isobutylglycolide), the branched the side chain gives the polymer a relatively high glass transition temperature and low surface energy; these two factors work in concert to slow the degradation rate. It is not surprising that poly(isobutylglycolide) has slowest the degradation rate.

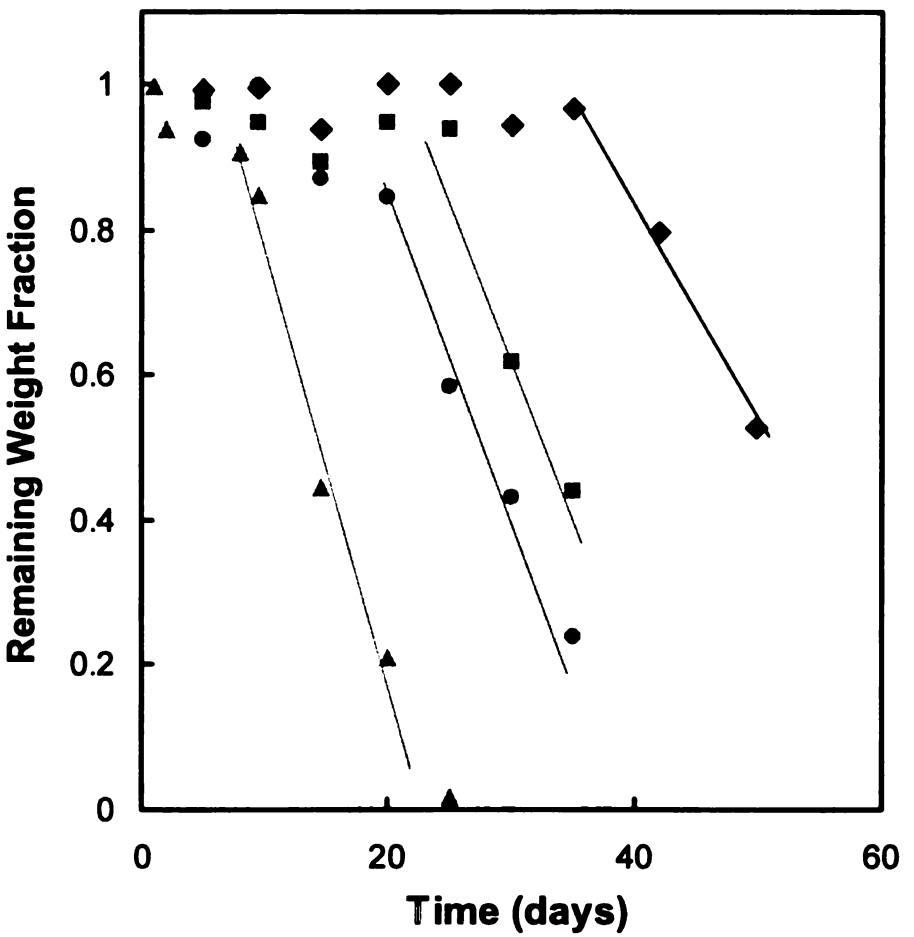

Figure 69. The weight loss of substituted glycolide during hydrolytic degradation. (▲) lactide, (■) ethylglycolide, (●) hexylglycolide, (◆) isobutylglycolide.

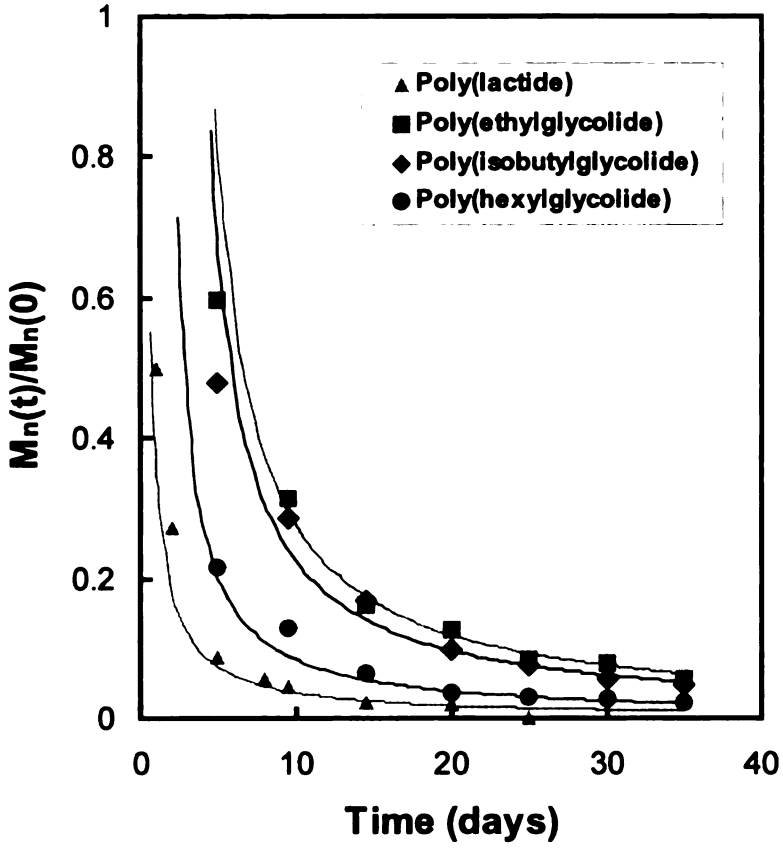

Figure 70. The molecular weight loss of substituted glycolide during hydrolytic degradation. (▲) lactide, (■) ethylglycolide, (●) hexylglycolide, (◆) isobutylglycolide.

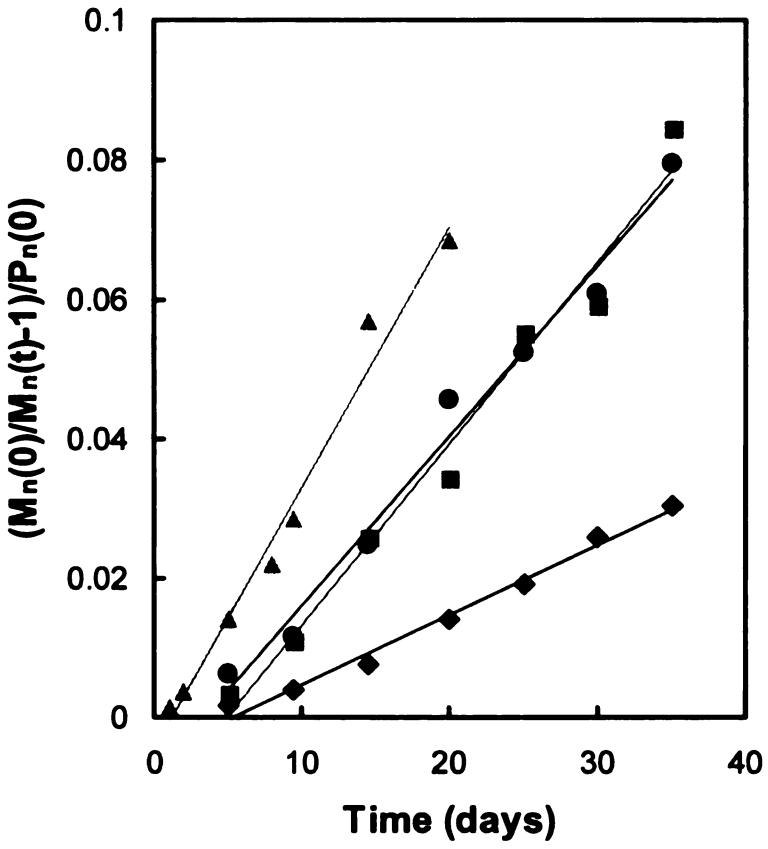

Figure 71. The molecular weight decrease of substituted lactides during hydrolytic degradation fitted to the random chain scission model. (▲) lactide, (■) ethylglycolide, (●) hexylglycolide, (◆) isobutylglycolide

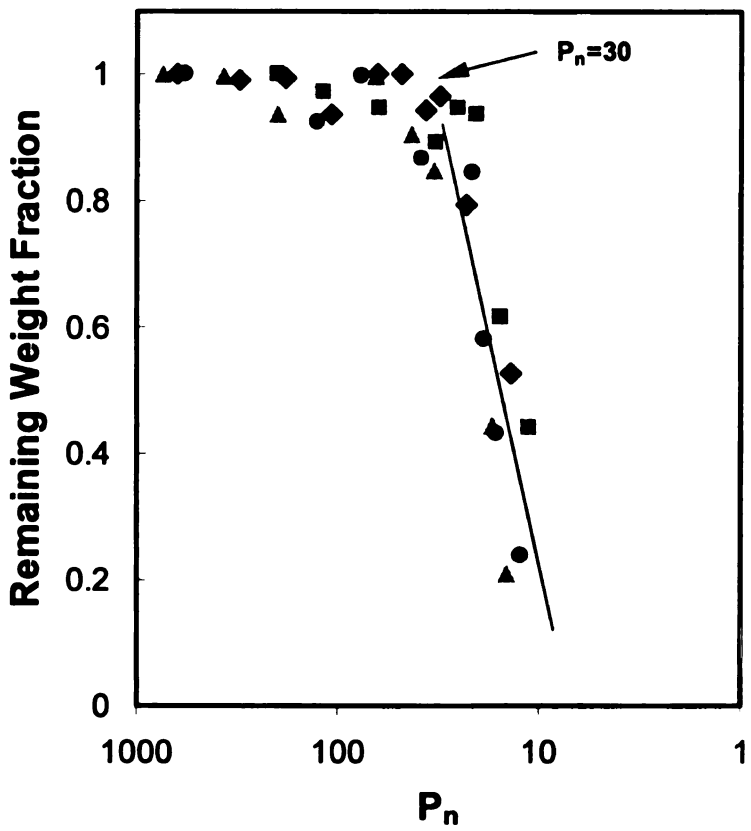

Figure 72. The decrease in the degree of polymerization of substituted lactides during hydrolytic degradation. (▲) lactide, (■) ethylglycolide, (●) hexylglycolide, (◆) isobutylglycolide

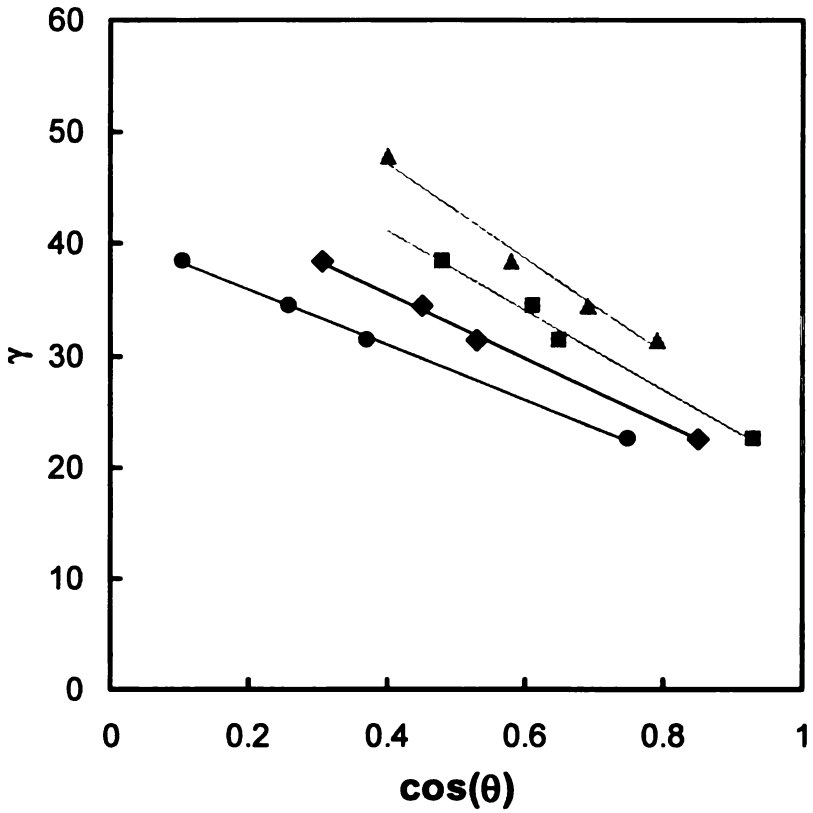

Figure 73. Contact angles on substituted polylactides plotted as γ (surface tension of water/methanol solutions) vs cos θ. (▲) lactide, (■) ethylglycolide, (●) hexylglycolide, (◆) isobutylglycolide

EXPERIMENTAL

1. General

Unless otherwise specified, ACS reagent grade starting materials and solvents were used as received from commercial suppliers without further purification. Proton nuclear magnetic resonance (^{1}H NMR) and carbon nuclear magnetic resonance (^{13}C NMR) analyses were carried out at room temperature in deuterated chloroform ($CDCl_3$) on a Varian Gemini-300 and Varian Vax-500 spectrometers with the solvent proton signals being used as chemical shift standards. Mass spectral analyses were carried out on a VG Trio-1 Benchtop GC-MS.

The molecular weights of polymers were determined by gel permeation chromatography (GPC) using a PLgel 20m Mixed A column and a Waters R401 Differential Refractometer detector at room temperature. THF was used as the eluting solvent at a flow rate 1 mL/min, and monodisperse polystyrene standards were used to calibrate the molecular weights. The concentration of the polymer solutions used for GPC measurements was 1 mg/mL. Differential scanning calorimetry (DSC) analyses of the polymers were obtained using a Perkin Elmer DSC 7. Samples were run under a helium atmosphere at a heating rate of 10 °C/min, with the temperature calibrated with an indium standard. Thermogravimetric analyses (TGA) were run in both air and under nitrogen at a heating rate of 10 °C/min using a Perkin Elmer TGA 7. Measurements of the

mechanical properties of polymer samples were made using a Perkin Elmer DMA 7 Dynamic Mechanical Analyzer at a heating rate of 10 °C/min.

X-ray Powder Diffraction (XRD) patterns were recorded on a Rigaku rotaflex 200B diffractometer equipped with a rotating anode, Cu $K_{\square}$x-ray radiation (λ= 1.541838Å) and a curved crystal graphite monochromator. The x-ray was operated at 45 KV and 100 mA. Diffraction patterns were collected at 0.01° intervals between 5 and 45° values of 2θ at a scanning rate of 0.1° per minute and DS and SS slit widths of 1/2. Powder samples were prepared by spreading solid samples on the window of the glass sample holder with a spatula, or by taping polymer film made from solvent casting on to the window of the sample holder.

2. Synthesis

Symmetric Monomer Synthesis, general procedure. (Route 1 in Scheme 3) A mixture of 10 g of the appropriate α-hydroxy acid and 0.2 g of *p*-toluenesulfonic acid in 700 mL of toluene was heated at reflux for four days, with the water removed azeotropically using a Barrett trap. The toluene solution was then cooled, washed with sat. $NaHCO_3$, and dried over $MgSO_4$. After removing the toluene, about 0.1 g of ZnO was added and the residue was distilled under reduced pressure using a Kugelrohr distillation apparatus.[19]

3,6-Diethyl-1,4-dioxane-2,5-dione (Ethylglycolide) (1). Ethylglycolide was collected at 180 °C (100 mtorr), and was dissolved in the minimum amount

of ether needed to dissolve the product. The solution was cooled to –30 °C, and petroleum ether was added drop-wise until the solution turned cloudy. The colorless crystals were collected by cold filtration and dried under vacuum to give 5.2 g (63%) of ethylglycolide as a colorless oil. ^{1}H NMR indicates that the product is a statistical mixture of diastereomers. ^{1}H NMR (300 MHz, $CDCl_3$): δ 4.88 (dd), 4.83 (dd, 1H total for the signals at 4.88 and 4.83), 2.08 (m, 2H), 1.15 (tt, 3H). ^{13}C NMR (75 MHz, $CDCl_3$) δ: 167.62, 166.58, 76.4, 75.6. mp 19.5 – 20.5 °C lit.[179] 21-22 °C; MS (EI) m/z = 173.4 (M+1). **Preparation via α-bromoacyl bromides.**[180] Under a nitrogen atmosphere, 0.90 g (8.7 mmol) of 2-hydroxybutyric acid and 2.1 g (8.7 mmol) of 2-bromobutyryl bromide were heated at 80 °C until HBr evolution ceased (0.5-2 h). The solution was cooled and 100 mL of dry acetone were added followed by the drop-wise addition of 2.2 mL (17 mmol) of triethylamine. The solution was heated to reflux for 3 h, and then cooled to room temperature. After removing the acetone under reduced pressure, the residue was washed with sat. $NaHCO_3$, extracted with ether, and the ether layer was dried over $MgSO_4$. After removing the ether, the dimer was purified by recrystallization as described above to give 0.62 g (41%) of ethylglycolide as a colorless oil. The product is approximately a 4:1 mixture of the R,R/S,S and R,S diastereomers.

3,6-Diisobutyl-1,4-dioxane-2,5-dione (isobutylgycolide) (2). Isobutylglycolide was collected at 120 °C (50 mtorr), and was recrystallized from ether. The white crystals were collected by filtration and dried under vacuum to give 6.1g (71%) of isobutylglycolide as white solid. ^{1}H NMR indicates that the

product is a statistical mixture of the R,R/S,S and R,S diastereomers. ^{1}H NMR (300 MHz, $CDCl_3$): δ 4.91 (dd), 4.89 (dd), (1H total for the signals at 4.91 and 4.89), 1.8-2.0 (m, 3H), 0.95 (m, 6H). ^{13}C NMR (75 MHz, $CDCl_3$) δ: 167.28, 166.20, 74.88, 74.09, 40.37, 38.82, 24.07, 23.84, 23.02, 22.84, 21.29, 21.25. MS (*m/q*) 229.4 (M+1); mp 167-167.5 °C (lit.[198] 169-170 °C).

3,6-Dihexyl-1,4-dioxane-2,5-dione (hexylglycolide) (3). Hexylglycolide was collected at 145 °C (50 mtorr), and was recrystallized from ether. The white crystals were collected by filtration and dried under vacuum to give 5.8 g (65%) of hexylglycolide as a white solid. ^{1}H NMR indicates that the product is a statistical mixture of the R,R/S,S and R,S diastereomers. ^{1}H NMR (300 MHz, $CDCl_3$): δ 4.88 (dd), 4.83 (dd), (1H total for the signals at 4.88 and 4.83), 2.01 (m, 2H), 1.4-1.6 (br m, 2H), 1.2-1.4 (br m, 6H), 0.85 (t, 3H). ^{13}C NMR (75 MHz, $CDCl_3$) δ: 166.95, 165.85, 76.42, 75.65, 31.99, 31.46, 31.41, 30.15, 28.74, 28.56; MS (m/z) 285.4 (M+1), mp 78-80 °C .

3,6-Diisopropyl-1,4-dioxane-2,5-dione (isopropylglycolide) (4). Isopropylglycolide was synthesized from DL-2-hydroxy-3-methyl butyric The crude product was recrystallized directly from toulene after removing of toluene. The white crystal was collected by filtration and dried under vacuum. Yield 47%. ^{1}H NMR (300 MHz, $CDCl_3$): δ 4.95 (d, 1H), 2.30 (m, 1H), 1.03 (d, 3H), 1.01 (d, 3H). ^{13}C NMR (75 MHz, $CDCl_3$) δ 166.38, 79.55, 29.36, 19.55, 15.81. MS (m/z) 201.4 (M+1), mp 137-138 °C [lit.[199] 136 °C].

3S,6S-Diisopropyl-1,4-dioxane-2,5-dione (S-isopropylglycolide) (5). S-isopropylglycolide was synthesized from L-2-hydroxy-3-methyl butyric The S-isopropylglycolide was recrystallized from toluene. The white crystals were collected by filtration and dried under vacuum. Yield 43%, $[\alpha]_{20}$ = -264.0 (c=1, THF). ^{1}H NMR (300 MHz, $CDCl_3$): δ 4.95 (d, 1H), 2.30 (m, 1H), 1.03 (d, 3H), 1.01 (d, 3H). ^{13}C NMR (75 MHz, $CDCl_3$) δ: 166.38, 79.55, 29.36, 19.55, 15.81. MS (m/z) 201.4 (M+1), mp 140-141 °C. The S-isopropylglycolide is 99% ee was determined by hydrolyzing S-isopropylglycolide to 2-hydroxy-3-methyl butyric acid and comparing the optical rotation value the acid with known value ($[\alpha]_{20}$=+19.0 c=1 $CHCl_3$) from Aldrich catalog.

2-hydroxy-3-methylbutyric acid. (6) A solution of 60 mL concentrated H_2SO_4 in 1L r water was cooled in an ice-bath. To the cooled solution was added 60 g of valine follwed by the dropwise of 144 g $NaNO_2$ dissolved in 1L water. After the solution was stirred at 0 °C for overnight, the solution was extracted with ether (6 × 300 mL), and the ether layer was dried over $MgSO_4$. After removing the ether, the product was purified by recrystallized from toluene. The white crystals were collected by filtration and dried under vacuum to give 45 g (75%) of 2-hydroxy-3-methyl butyric acid as a white solid. DL-2-hydroxy-3-methyl butyric acid was obtained from DL-valine and L-2-hydroxy-3-methyl butyric acid was prepared form L-valine. The L-2-hydroxy-3-methyl butyric acid was obtained in 99% ee based on measurement of its optical rotation ($[\alpha]_{20}$=+18.9 c=1 $CHCl_3$).

Unsymmetric Monomer synthesis, general procedure. Under a nitrogen atmosphere, one equivalent of a 2-hydroxy acid and one equivalent of a 2-bromoacyl bromide were heated at 80 °C until HBr evolution ceased (0.5-2 h.). The solution was cooled and 200 mL of dry acetone was added for each gram of acid, followed by the dropwise addition of two equivalent of triethylamine. The solution was heated to reflux for 6 h., and then was cooled. After removing the acetone, ethyl acetate was added to dissolve the residue. The solution was washed with 2N HCl, water, then washed with sat. $NaHCO_3$, and the organic layer was dried over $MgSO_4$. After removing solvent, the monomers was purified by recrystallization and distillation.

3-ethyl-6-methyl-2,5-dioxane-1,4-dione (7) was synthesized from 2-hydroxybutyric acid and 2-bromopropionyl bromide. It was purified by distillation (45 °C/50 mtorr) to give a colorless oil. Yield: 53%. ^1H NMR ($CDCl_3$) δ 5.03 (q), 4.99 (q, 1H for signal at 5.03 and 4.99 ppm), 4.86 (dd), 4.83 (dd, 1H for signal at 4.86 and 4.83), 1.90-2.20 (m, 2H), 1.69 (d), 1.66 (d, 3H for signals at 1.69 and 1.66 ppm). 1.15 (t). 1.14 (t, 3H for signals at 1.15 and 1.14ppm). ^{13}C NMR ($CDCl_3$) δ 167.6, 166.8, 166.3, 165.6, 77.7, 76.6, 72.5, 72.2, 25.3, 23.3, 17.5, 15.7, 9.1, 8.7. MS (*m/q*) 159.4 (M+1). The product is approximately a 3:1 mixture of the R,R/S,S and R,S diastereomers.

3-dimethyl-6-methyl-2,5-dioxiane-1,4-dione (8) was synthesized from 2-hydroxyisobutyric acid and 2-bromopropionyl bromide. Recrystallization from ether give white crystal. mp 66-69°C. Yield: 43%. ^1H NMR ($CDCl_3$) δ 5.07 (q, 1H),

1.68 (s, 6H). 1.65 (d, 3H). ^{13}C NMR ($CDCl_3$) δ 168.59, 166.64, 80.55,72.92, 26.25, 25.31, 17.45 MS (*m/q*) 159.4 (M+1)

3-methyl-6-phenyl-2,5-dioxane-1,4-dione (9) was synthesized by using mandelic acid and 2-bromopropyionyl bromide. Recrystallization from toluene gave white crystals. mp 153-156 °C. Yield: 33%. ^1H NMR ($CDCl_3$) δ 7.43 (m, 5H), 5.92 (s, 1H) 5.17 (q, 1H), 1.63 (d, 3H). ^{13}C NMR ($CDCl_3$) δ 166.90, 165.55, 131.24, 129.95, 128.92, 127.44, 77.74, 72.77, 16.42. MS (*m/q*) 207.4 (M+1).

***S*-3-methyl-*S*-6-phenyl-2,5-dioxiane-1,4-dione (10)** was synthesized from S-mandelic acid and 2-bromopropionyl bromide. Recrystallization from toluene gave white crystals. mp 160-163 °C, yield: 41%. $[\alpha]_{20}$ = +301.0 ^1H NMR ($CDCl_3$) δ 7.43 (m, 5H), 5.92 (s, 1H) 5.17 (q, 1H), 1.63 (d, 3H). ^{13}C NMR ($CDCl_3$) δ 166.90, 165.55, 131.24, 129.95, 128.92, 127.44, 77.74, 72.77, 16.42. MS (*m/q*) 207.4 (M+1).

***R*-3-methyl-*R*-6-phenyl-2,5-dioxiane-1,4-dione (11)** was synthesized from R-mandelic acid and 2-bromopropionyl bromide. Recrystallization from toluene gave white crystals. mp 160-163 °C, yield: 35%. $[\alpha]_{20}$ = -302.0. ^1H NMR ($CDCl_3$) δ 7.43 (m, 5H), 5.92 (s, 1H) 5.17 (q, 1H), 1.63 (d, 3H). ^{13}C NMR ($CDCl_3$) δ 166.90, 165.55, 131.24, 129.95, 128.92, 127.44, 77.74, 72.77, 16.42. MS (*m/q*) 207.4 (M+1).

3. Bulk polymerization of substituted glycolides.

Solvent-free polymerizations were carried out in sealed tubes prepared from 3/8 inch diameter glass tubing. A representative polymerization is described below. In an oxygen and moisture-free dry box, a solution of initiator in toluene (≈ 0.01 M) and 0.1g of monomer were added to the tube. The amount of initiator solution added was determined by the desired monomer/initiator ratio. For runs using initiators that are insoluble in toluene, the initiator was added directly to the tube and the walls of the tube were washed with solvent to ensure that all of the initiator was added to the monomer. The solvent was removed in vacuum, and the tube was sealed and immersed in an oil bath at 130 °C. At the end of the polymerization, the tube was cooled, opened, and the polymer was dissolved in THF. A portion of the sample was evacuated to dryness and analyzed by NMR for conversion. After removal of the solvent, the polymer was dissolved in toluene and precipitated into methanol to remove residual initiator. Typical yields of poly(ethylglycolide) were >85%. For kinetic runs, multiple tubes were prepared and individual tubes were removed from the heating bath at predetermined intervals and were cooled in ice, opened, and the contents dissolved in THF. A portion of the sample was analyzed by GPC for molecular weight, and the remainder was evacuated to dryness and analyzed by NMR for conversion. Polymerizations that used alcohols as co-initiators were set up as described above, except that the appropriate amount of alcohol was added to the toluene solution of initiator just prior to adding the initiator solution to the tube.

For insoluble initiators, tubes were first loaded with monomer and initiator, and the alcohol co-initiator was directly added to the tube as a toluene solution.

4. Solution polymerization of substituted glycolides.

The reaction flask was charged with 2 mmol of monomer and dried under vacuum (diffusion pump) at room temperature overnight. Toluene (10 mL) was added to the solvent flask through a rubber septum with a syringe, and the toluene was purified by initiating an anionic polymerization of styrene. The solvent was transferred under vacuum to the reaction flask, and the initiator $Al(OiPr)_3$ or $Sn(Oct)_2$ was added into reaction flask with a syringe through a rubber septum. The amount of initiator solution added was determined by the desired monomer/initiator ratio The polymerization was carried out at 70 °C, 90 °C and 100 °C. After the polymerization finished, the reaction was terminated with 1 mL 2NHCl solution then washed with distilled water until PH=7. The polymer was precipitated into cold methanol, filtered, and dried under vacuum. For kinetic studies, small samples were removed at predetermined times using a syringe through the rubber septum. The samples were analyzed by NMR for conversion and GPC for molecular weight.

5. The surface energy of polymers

Polymer films. The polymers were dissolved in small amount of toluene, then the solutions were spread on the clean glass slides. The glass slides were dried in air for 3 days, then dried under vacuum for one day.

Surface tension of solutions. A series of H_2O/CH_3OH solutions were made. The densities of solutions were measured using hydrometer. The surface tensions of solutions were measured using pendant drop method[200] by FTÅ 200 contact angle analyzer, which was calibrated using de-ionized water.

Surface tension of polymers. The H_2O/CH_3OH solutions were dropped on the polymer films. The contact angles between the solutions and polymer films were measured using FTÅ 200 contact angle analyzer, which was calibrated using de-ionized water. From change of contact angles with change of surface tensions of solutions, the surface energies of polymers can be calculated by Zisman equation:

$$\cos\theta = 1 + \beta(\gamma_L - \gamma_C)$$

where θ is contact angle, γ_L is surface tension of testing solution (water/methanol solution). γ_C is the surface energy of the polymer surface, and β is constant.

6. The degradation of polymers.

About 50 mg of polymer sample was accurately weighed and chopped to 1mm by 1mm pieces. The chopped sample was immersed in to 15 mL 0.1M phosphate buffer solution (pH=7.4). The degradation was carried out at 55 ± 0.1 °C. After a predetermined period of time, the sample was taken out, washed thoroughly with distill water and dried under vacuum. The sample was weighed to determine the weight loss and molecular weight loss was determined by GPC.

BIBLIOGRAPHY

BIBLIOGRAPHY

1. Zhang, X. C.; Wyss, U. P.; Pichora, D.; Goosen, M. F. A.; *J. Macromol. Sci.-Pure Appl. Chem.* **1993**, *A30*, 933-947.
2. Han, D. K.; Hubbell, J. A.; *Macromolecules* **1997**, *30*, 6077-6083.
3. Kricheldorf, H. R.; KreiserSaunders, I.; *Macromol. Symp.* **1996**, *103*, 85-102.
4. Chen, X. H.; McCarthy, S. P.; Gross, R. A.; *Macromolecules* **1997**, *30*, 4295-4301
5. Nobes, G. A. R.; Marchessault, R. H.; Maysinger, D.; *Drug Deliv.* **1998**, *5*, 167-177.
6. Fukuzaki, H.; Yoshida, M.; Asano, M.; Kumakura, M.; *Biomaterials* **1990**, *11*, 441446.
7. Breitenbach, A.; Kissel, T.; *Polymer* **1998**, *39*, 3261-3271.
8. McCoy, M.; *C&EN* **1998**, *76*, 71-72.
9. Sinclair, R. G.; *J. M. S. - Pure Appl. Chem.* **1996**, *A33*, 585-597.
10. Meinander, K.; Niemi, M.; Hakola, J. S.; Selin, J. F.; *Macromol. Symp.* **1997**, *123*, 147-153.
11. Grijpma, D. W.; Nijenhuis, A. J.; Vanwijk, P. G. T.; Pennings, A. J.; *Polym. Bull.* **1992**, *29*, 571-578.
12. Spinu, M.; Jackson, C.; Keating, M. Y.; Gardner, K. H.; *J. Macromol. Sci.-Pure Appl. Chem.* **1996**, *A33*, 1497-1530.
13. Vert, M.; Schwarch, G.; Coudane, J.; *J. Macromol. Sci.-Pure Appl. Chem.* **1995**, *A32*, 787-796.
14. Bastioli, C.; *Macromol. Symp.* **1998**, *135*, 193-204.
15. Fukuzaki, H.; Yoshida, M.; Asano, M.; Kumakura, M.; *Polymer* **1990**, *31*, 432.

16. Buchholz, B.,German patent 443,542,A2 (1991)

17. Otera, J.; Kawada, K.; Yano, T.; *Chem. Lett.* **1996**, 225-226.

18. Yamaguchi, A.; Suzuki, K.; Enomoto, K.; Ajioka, M.; *Bull. Chem. Soc. Jpn.* **1995**, *68*, 2125-2131.

19. Deane, D. D.; Hammond, E. G.; *J. Dairy Sci.* **1960**, *43*, 1421.

20. Guber, P. R.; Benson, R. D.; Iwen, M. L.,U. S. patent 5,141,023 (1992)

21. Johns, D. B.; Lenz, R. W.; Luecke, A. *Ring-Opening Polymerization*; Ivin, K. J. and Saegusa, T., Ed.; Elsevier Applied Science Publishers, 1984; Vol. 1, pp 461.

22. Odian, G. *Principle of Polymerization*; Third ed.; John Wiley & Son:, 1991.

23. Hall, H. K., Jr.; Brandt, M. K.; Mason, R. W.; *J. Am. Chem. Soc.* **1958**, *80*, 6420.

24. Carothers, W. H.; Borough, G. L.; Van Natta, R. W.; *J. Am. Chem. Soc* **1932**, *54*, 761.

25. Lundberg, R. D.; Cox, E. F. *Ring-Opening Polymerization*; Marcel Dekker: New York, 1969.

26. Kricheldorf, H. R.; Michael Jonte, J.; Dunsing, R.; *J. Macromol. Soc.* **1986**, *A23(4)*, 495.

27. Rozenberg, D.; *Makromol. Chem., Macromol. Symp.* **1990**, *32*, 267.

28. Crivello, J. V.; Lockhart, T., P.; *J. polym. Sci., Polym. Chem. Ed.* **1983**, *21*, 97.

29. Cherdron, H.; Korte, F.; *Makromol. Chem.* **1962**, *56*, 179.

30. Penczek, S.; Hofman, A.; Szymanski, R.; Slomkowski, S.; *Makromol. Chem.* **1984**, *185*, 655-667.

31. Hofman, A.; Stomkowski, S.; Penczek, S.; *Makromol. Chem.* **1987**, *188*, 2027-2040.

32. Kricheldorf, H. R.; Michael Jonte, J.; Dunsing, R.; *Makromol. Chem.* **1986**, *187*, 771-785.

33. Okamoto, Y.; *Makromol. Chem., Macromol. Symp.* **1991**, *42/43*, 117.

34. Kohn, F. E.; Van Ommen, J. G.; Feuen, J.; *European Polymer Journal* **1983**, *19*, 1081-1088.

35. Kricheldorf, H. R.; Dunsing, R.; *Makromol. Chem.* **1986**, *187*, 1611-1625.

36. Jedlinski, Z.; Kurcok, P.; Kowalczuk, M.; Matuszowicz, A.; Dubois, P.; Jerome, R.; Kricheldorf, H. R.; *Macromolecules* **1995**, *28*, 7276-7280.

37. Penczek, S.; Duda, A.; Libiszowski, J.; *Macromol. Symp.* **1998**, *128*, 241-254.

38. Kurcok, P.; Kowalczuk, M.; Hennek, K.; Jedlinski, Z.; *Macromolecules* **1992**, *25*, 2017-2020.

39. Yuan, M. L.; Xiong, C. D.; Deng, X. M.; *J. Appl. Polym. Sci.* **1998**, *67*, 1273-1276.

40. Kurcok, P.; Penczek, J.; Franek, J.; Jedlinski, Z.; *Macromolecules* **1992**, *25*, 2285-2289.

41. Kricheldorf, H. R.; Scharnagl, N.; Jedlinski, Z.; *Polymer* **1996**, *37*, 1405-1411.

42. Kricheldorf, H. R.; Kreiser-saunders, I.; *Makromol. Chem.-Macro. Chem. Phys.* **1990**, *191*, 1057-1066.

43. Jedlinski, Z.; Walach, W.; Kurcok, P.; Adamus, G.; *Makromol. Chem.-Macro. Chem. Phys.* **1991**, *192*, 2051-2057.

44. Emig, N.; Nguyen, H.; Krautscheid, H.; Reau, R.; Cazaux, J. B.; Bertrand, G.; *Organometallics* **1998**, *17*, 3599-3608.

45. Leborgne, A.; Vincens, V.; Jouglard, M.; Spassky, N.; *Makromol. Chem., Macromol. Symp* **1993**, *73*, 37-46.

46. Kowalski, A.; Duda, A.; Penczek, S.; *Macromol. Rapid Commun.* **1998**, *19*, 567-572.

47. Witzke, D. R.; Narayan, R.; *Abstr. Pap. Am. Chem. Soc.* **1998**, *216*, U11-U12.

48. Schwach, G.; Coudane, J.; Engel, R.; Vert, M.; *Polym. Int.* **1998**, *46*, 177-182.

49. Kricheldorf, H. R.; Damrau, D. O.; *Macromol. Chem. Phys.* **1997**, *198*, 1753-1766.

50. Sodergard, A.; Stolt, M.; *Macromol. Symp.* **1998**, *130*, 393-402.

51. Simic, V.; Girardon, V.; Spassky, N.; Hubert-Pfalzgraf, L. G.; Duda, A.; *Polym. Degrad. Stabil.* **1998**, *59*, 227-229.

52. McLain, S. J.; Ford, T. M.; Drysdale, N. E.; *Abstr. Pap. Am. Chem. Soc.* **1992**, *204*, 188-POLY.

53. Bero, M.; Kasperczyk, J.; Adamus, G.; *Makromol. Chem., Macromol. Symp* **1993**, *194*, 907-912.

54. Degee, P.; Dubois, P.; Jerome, R.; *Macromol. Symp.* **1997**, *123*, 67-84.

55. Dubois, P.; Jacobs, C.; Jerome, R.; Teyssie, P.; *Macromolecules* **1991**, *24*, 2266-2270.

56. Montaudo, G.; Montaudo, M. S.; Puglisi, C.; Samperi, F.; Spassky, N.; LeBorgne, A.; Wisniewski, M.; *Macromolecules* **1996**, *29*, 6461-6465.

57. Duda, A.; *Macromolecules* **1996**, *29*, 1399-1406.

58. Kowalski, A.; Duda, A.; Penczek, S.; *Macromolecules* **1998**, *31*, 2114-2122.

59. Ropson, N.; Dubois, P.; Jerome, R.; Teyssie, P.; *Macromolecules* **1993**, *26*, 6378-6385.

60. Duda, A.; Penczek, S.; *Macromolecules* **1995**, *28*, 5981-5992.

61. Duda, A.; Penczek, S.; *Macromol. Rapid Commun.* **1995**, *16*, 67-76.

62. Dubios, P.; Jerome, R.; Teyssie, P.; *Polymer Perprint* **1994**, *35*, 536-537.

63. Ropson, N.; Dubois, P.; Jerome, R.; Teyssie, P.; *Macromolecules* **1995**, *28*, 7589-7598.

64. Kricheldorf, H. R.; Boettcher, C.; Tonnes, K. U.; *Polymer* **1992**, *33*, 2817-2824.

65. Degee, P.; Dubois, P.; Jerome, R.; Teyssie, P.; *Macromolecules* **1992**, *25*, 4242-4248.

66. Dubois, P.; Jerome, R.; Teyssie, P.; *Abstr. Pap. Am. Chem. Soc.* **1990**, *199*, 16-POLY.

67. Barakat, I.; Dubois, P.; Jerome, R.; Teyssie, P.; *J. Polym. Sci. Pol. Chem.* **1993**, *31*, 505-514.

68. Tian, D.; Dubois, P.; Jerome, R.; Teyssie, P.; *Macromolecules* **1994**, *27*, 4134-4144.

69. Barakat, I.; Dubois, P.; Jerome, R.; Teyssie, P.; Goethals, E.; *J. Polym. Sci. Pol. Chem.* **1994**, *32*, 2099-3110.

70. Trofimoff, L.; Aida, T.; Inoue, S.; *Chem. Lett.* **1987**, 991-994.

71. Endo, M.; Aida, T.; Inoue, S.; *Macromolecules* **1987**, *20*, 2982-2988.

72. Isoda, M.; Sugimoto, H.; Aida, T.; Inoue, S.; *Macromolecules* **1997**, *30*, 57-62.

73. Sugimoto, H.; Aida, T.; Inoue, S.; *Macromolecules* **1990**, *23*, 2869-2875.

74. Sugimoto, H.; Kawamura, C.; Kuroki, M.; Aida, T.; Inoue, S.; *Macromolecules* **1994**, *27*, 2013-2028.

75. sugimoto, H.; Aida, T.; Inoue, S.; *Macromolecules* **1993**, *26*, 4751-4755.

76. Mogstad, A. L.; Waymouth, R. M.; *Macromolecules* **1994**, *27*, 2313-2315.

77. Kricheldorf, H. R.; Boettcher, C.; *Makromol. Chem.-Macro. Chem. Phys.* **1993**, *194*, 463-473.

78. Kricheldorf, H. R.; Meierhaack, J.; *Makromol. Chem.-Macro. Chem. Phys.* **1993**, *194*, 715-725.

79. Sandner, B.; Steurich, S.; Gopp, U.; *Polymer* **1997**, *38*, 2515-2522.

80. Kricheldorf, H. R.; Sumbel, M.; *Eur. Polym. J.* **1989**, *25*, 585-591.

81. Kricheldorf, H. R.; Mahler, A.; *Polymer* **1996**, *37*, 4383-4388.

82. Kricheldorf, H. R.; WeegenSchulz, B.; *Polymer* **1995**, *36*, 4997-5003.

83. Kricheldorf, H. R.; Lee, S. R.; Scharnagl, N.; *Macromolecules* **1994**, *27*, 3139-3146.

84. Kricheldorf, H. R.; Sumbel, M. V.; Kreisersaunders, I.; *Macromolecules* **1991**, *24*, 1944-1949.

85. Kricheldorf, H. R.; Eggerstedt, S.; *Macromolecules* **1997**, *30*, 5693-5697.

86. Kricheldorf, H. R.; Lee, S. R.; *Macromolecules* **1995**, *28*, 6718-6725.

87. Witzke, D. R.; Narayan, R.; Kolstad, J. J.; *Macromolecules* **1997**, *30*, 7075-7085.

88. Leenslag, J. W.; Pennings, A. J.; *Makromol. Chem.-Macro. Chem. Phys.* **1987**, *188*, 1809-1814.

89. Schwach, G.; Coudane, J.; Engel, R.; Vert, M.; *J. Polym. Sci. Pol. Chem.* **1997**, *35*, 3431-3440.

90. Kricheldorf, H. R.; Boettcher, C.; *J. Macromol. Sci.-Pure Appl. Chem.* **1993**, *A30*, 441-448.

91. Kricheldorf, H. R.; Damrau, D. O.; *J. Macromol. Sci.-Pure Appl. Chem.* **1998**, *A35*, 1875-1887.

92. Nijenhuis, A. J.; Grijpma, D. W.; Pennings, A. J.; *Macromolecules* **1992**, *25*, 6419-6424.

93. Du, Y. J.; Lemstra, P. J.; Nijenhuis, A. J.; Vanaert, H. A. M.; Bastiaansen, C.; *Macromolecules* **1995**, *28*, 2124-2132.

94. Kricheldorf, H. R.; Kreisersaunders, I.; Boettcher, C.; *Polymer* **1995**, *36*, 1253-1259.

95. Kowalski, A.; Duda, A.; Penczek, S.; *Macromolecules* **2000**, *33*, 689-695.

96. Yasuda, H.; Ihara, E.; In *Advances in Polymer Science*; Advances in Polymer Science 133, 1997.

97. Yasuda, H.; Ihara, E.; *Bull. Chem. Soc. Jpn.* **1997**, *70*, 1745-1767.

98. Yamashita, M.; Takemoto, Y.; Ihara, E.; Yasuda, H.; *Macromolecules* **1996**, *29*, 1798-1806.

99. Stevels, W. M.; Ankone, M. J. K.; Dijkstra, P. J.; Feijen, J.; *Macromolecules* **1996**, *29*, 8296-9303.

100. Stevels, W. M.; Ankone, M. J. K.; Dijkstra, P. L.; Feijen, J.; *Macromol. Chem. Phys.* **1995**, *196*, 1153-1161.

101. Huang, Q. H.; Shen, Z. Q.; Zhang, Y. F.; Shen, Y. Q.; Shen, L. F.; Yuan, H. Z.; *Polym. J.* **1998**, *30*, 168-170.

102. Shen, Y. Q.; Zhu, K. J.; Shen, Z. Q.; Yao, K. M.; *J. Polym. Sci. Pol. Chem.* **1996**, *34*, 1799-1805.

103. Shen, Y. Q.; Shen, Z. Q.; Zhang, F. Y.; Zhang, Y. F.; *Polym. J.* **1995**, *27*, 59-64.

104. Shen, Y. Q.; Shen, Z. Q.; Zhang, Y. F.; Yao, K. M.; *Macromolecules* **1996**, *29*, 8289-8295.

105. Shen, Y. Q.; Shen, Z. Q.; Shen, J. L.; Zhang, Y., F.; Yao, K. M.; *Macromolecules* **1996**, *29*, 3441-3446.

106. Shen, Y. Q.; Shen, Z. Q.; Zhang, Y. F.; Hang, G. H.; *J. Polym. Sci. Pol. Chem.* **1997**, *35*, 1339-1352.

107. Ohse, H.; Cherdron, H.; Korte, F.; *Makromol. Chem.* **1965**, *86*, 312.

108. Saotome, K.; Kodaira, Y.; *Makromol. Chem.* **1965**, *82*, 41.

109. Wilson, D. R.; Beaman, R. G.; *J. Polym. Sci., Part A-1* **1970**, *8*, 2161.

110. Perego, G.; Cella, G. D.; Bastioli, C.; *J. Appl. Polym. Sci.* **1996**, *59*, 37-43.

111. Macdonald, R. T.; McCarthy, S. P.; Gross, R. A.; *Macromolecules* **1996**, *29*, 7356-7361.

112. Grijpma, D. W.; Pennings, A. J.; *Macromol. Chem. Phys.* **1994**, *195*, 1633-1647.

113. Tsuji, H.; Horii, F.; Hyon, S. H.; Ikada, Y.; *Macromolecules* **1991**, *24*, 2719-2724.

114. Ikada, Y.; Tsuji, H.; *Macromolecules* **1993**, *26*, 6918-6926.

115. Ikada, Y.; Hyon, S. H.; Tsuji, H.; *Macromolecules* **1991**, *24*, 5651-5656.

116. Tsuji, H.; Ikada, Y.; *J. Appl. Polym. Sci.* **1994**, *53*, 1061-1071.

117. Tsuji, H.; Ikada, Y.; Hyon, S. H.; Kimura, Y.; Kitao, T.; *J. Appl. Polym. Sci.* **1994**, *51*, 337-344.

118. Tsuji, H.; Ikada, Y.; *Macromolecules* **1993**, *26*, 6918-6926.

119. Tsuji, H.; Ikada, Y.; *Macromolecules* **1992**, *25*, 5719-5723.

120. Tsuji, H.; Hyon, S. H.; Ikada, Y.; *Macromolecules* **1992**, *25*, 2940-2946.

121. Tsuji, H.; Hyon, S. H.; Ikada, Y.; *Macromolecules* **1991**, *24*, 5651-5656.

122. Tsuji, H.; Hyon, S. H.; Ikada, Y.; *Macromolecules* **1991**, *24*, 5657-5662.

123. HiljanenVainio, M. P.; Orava, P. A.; Seppala, J. V.; *J. Biomed. Mater. Res.* **1997**, *34*, 39-46.

124. Lostocco, M. R.; Huang, S. J.; *Abstr. Pap. Am. Chem. Soc.* **1996**, *212*, 245-PMSE.

125. Stevels, W. M.; Ankone, M. J. K.; Dijkstra, P. J.; Feijen, J.; *Macromol. Symp.* **1996**, *102*, 107-113.

126. Veld, P.; Velner, E. M.; VanDeWitte, P.; Hamhuis, J.; Dijkstra, P. J.; Feijen, J.; *J. Polym. Sci. Pol. Chem.* **1997**, *35*, 219-226.

127. Duda, A.; Biela, T.; Libiszowski, J.; Penczek, S.; Dubois, P.; Mecerreyes, D.; Jerome, R.; *Polym. Degrad. Stabil.* **1998**, *59*, 215-222.

128. Gallardo, A.; Roman, J.; Dijkstra, P. J.; Feijen, J.; *Macromolecules* **1998**, *31*, 7187-7194.

129. King, E.; Cameron, R. E.; *Polym. Int.* **1998**, *45*, 313-320.

130. Storey, R. F.; Herring, K. R.; Hoffman, D. C.; *J. Polym. Sci. Pol. Chem.* **1991**, *29*, 1759-1777.

131. Nakayama, A.; Kawasaki, N.; Maeda, Y.; Arvanitoyannis, I.; Aiba, S.; Yamamoto, N.; *J. Appl. Polym. Sci.* **1997**, *66*, 741-748.

132. Cai, J.; Zhu, K. J.; Yang, S. L.; *Polymer* **1998**, *39*, 4409-4415.

133. Ruckenstein, E.; Yuan, Y. M.; *J. Appl. Polym. Sci.* **1998**, *69*, 1429-1434.

134. Kim, Y. J.; Adamson, D. H.; *Abstr. Pap. Am. Chem. Soc.* **1998**, *216*, U24-U24.

135. Lee, D. S.; Choi, S. W.; Jeon, B. M.; Kim, S. W.; *Abstr. Pap. Am. Chem. Soc.* **1998**, *216*, U878-U878.

136. Li, S. M.; Anjard, S.; Rashkov, I.; Vert, M.; *Polymer* **1998**, *39*, 5421-5430.

137. Song, C. X.; Feng, X. D.; *Macromolecules* **1984**, *17*, 2764-2767.

138. Choi, Y. R.; Bae, Y. H.; Kim, S. W.; *Macromolecules* **1998**, *31*, 8766-8774.

139. Grijpma, D. W.; Joziasse, C. A. P.; Pennings, A. J.; *Macromol. Rapid Commun.* **1993**, *14*, 155-161.

140. Joziasse, C. A. P.; Veenstra, H.; Topp, M. D. C.; Grijpma, D. W.; Pennings, A. J.; *Polymer* **1998**, *39*, 467-474.

141. Li, Y. X.; Kissel, T.; *Polymer* **1998**, *39*, 4421-4427.

142. Eguiburu, J. L.; Berridi, M. J. F.; Sanroman, J.; *Polymer* **1995**, *36*, 173-179.

143. Jerome, R.; Mecerreyes, D.; Tian, D.; Dubois, P.; Hawker, C. J.; Trollsas, M.; Hedrick, J. L.; *Macromol. Symp.* **1998**, *132*, 385-403.

144. Jacobs, C.; Dubois, P.; Jerome, R.; Teyssie, P.; *Macromolecules* **1991**, *24*, 3027-3034.

145. Vanhoorne, P.; Dubois, P.; Jerome, R.; Teyssie, P.; *Macromolecules* **1992**, *25*, 37-44.

146. Reeve, M. S.; McCarthy, S. P.; Gross, R. A.; *Macromolecules* **1993**, *26*, 888-894.

147. Xiong, C. D.; Cheng, L. M.; Xu, R. P.; Deng, X. M.; *J. Appl. Polym. Sci.* **1995**, *55*, 865-869.

148. Tortosa, K.; Miola, C.; Hamaide, T.; *J. Appl. Polym. Sci.* **1997**, *65*, 2357-2372.

149. Wang, H.; Dong, J. H.; Qiu, K. Y.; *J. Polym. Sci. Pol. Chem.* **1998**, *36*, 695-702.

150. Huang, S. J.; Onyari, J. M.; Nicolais, L.; DelNobile, S.; Mensitieri, G.; Ambrosio, L.; *Abstr. Pap. Am. Chem. Soc.* **1997**, *213*, 126-CELL.

151. Ohya, Y.; Maruhashi, S.; Ouchi, T.; *Macromolecules* **1998**, *31*, 4662-4665.

152. Ohya, Y.; Maruhashi, S.; Ouchi, T.; *Macromol. Chem. Phys.* **1998**, *199*, 2017-2022.

153. Nijenhuis, A. J.; Grijpma, D. W.; Pennings, A. J.; *Polymer* **1996**, *37*, 2783-2791.

154. Aoyagi, T.; Miyata, F.; Nagase, Y.; *J. Control. Release* **1994**, *32*, 87-96.

155. Grijpma, D. W.; Kroeze, E.; Nijenhuis, A. J.; Pennings, A. J.; *Polymer* **1993**, *34*, 1496-1503.

156. Sandner, B.; Steurich, S.; Wartewig, S.; *Macromol. Symp.* **1996**, *103*, 149-162.

157. Storey, R. F.; Warren, S. C.; Allison, C. J.; Puckett, A. D.; *Polymer* **1997**, *38*, 6295-6301.

158. Grijpma, D. W.; Pennings, A. J.; *Macromol. Chem. Phys.* **1994**, *195*, 1649-1663.

159. Cook, A. D.; Pajvani, U. B.; Hrkach, J. S.; Cannizzaro, S. M.; Langer, R.; *Biomaterials* **1997**, *18*, 1417-1424.

160. Eguiburu, J. L.; Iruin, J. J.; Fernandez-Berridi, M. J.; Roman, J. S.; *Polymer* **1998**, *39*, 6891-6897.

161. Lostocco, M. R.; Borzacchiello, A.; Huang, S. J.; *Macromol. Symp.* **1998**, *130*, 151-160.

162. Yang, J. M.; Chen, H. L.; You, J. W.; Hwang, J. C.; *Polym. J.* **1997**, *29*, 657-662.

163. Tsuji, H.; Ikada, Y.; *J. Appl. Polym. Sci.* **1996**, *60*, 2367-2375.

164. Blumm, E.; Owen, A. J.; *Polymer* **1995**, *36*, 4077-4081.

165. Liu, X.; Dever, M.; Fair, N.; Benson, R. S.; *J. Environ. Polym. Degrad.* **1997**, *5*, 225-235.

166. Wachsen, O.; Platkowski, K.; Reichert, K. H.; *Polym. Degrad. Stabil.* **1997**, *57*, 87-94.

167. Albertsson, A. C.; Sjoling, M.; *J. Macromol. Sci.-Pure Appl. Chem.* **1992**, *29*, 43-54.

168. Zhang, X. C.; Wyss, U. P.; Pichora, D.; Goosen, M. F. A.; *Polym. Bull.* **1992**, *27*, 623-629.

169. Sodergard, A.; Nasman, J. H.; *Polym. Degrad. Stabil.* **1994**, *46*, 25-30.

170. Albertsson, A. C.; Palmgren, R.; *J. Macromol. Sci.-Pure Appl. Chem.* **1993**, *A30*, 919-931.

171. Wachsen, O.; Reichert, K. H.; Kruger, R. P.; Much, H.; Schulz, G.; *Polym. Degrad. Stabil.* **1997**, *55*, 225-231.

172. Kopinke, F. D.; Mackenzie, K.; *J. Anal. Appl. Pyrolysis* **1997**, *40-1*, 43-53.

173. Li, S. M.; McCarthy, S.; *Biomaterials* **1999**, *20*, 35-44.

174. Hyon, S. H.; *Sen-I Gakkaishi* **1998**, *54*, 527-531.

175. Li, S. M.; Garreau, H.; Vert, M.; Petrova, T.; Manolova, N.; Rashkov, I.; *J. Appl. Polym. Sci.* **1998**, *68*, 989-998.

176. Iwata, T.; Doi, Y.; *Macromolecules* **1998**, *31*, 2461-2467.

177. Abe, H.; Doi, Y.; Hori, Y.; Hagiwara, T.; *Polymer* **1998**, *39*, 59-67.

178. Gajria, A. M.; Dave, V.; Gross, R. A.; McCarthy, S. P.; *Polymer* **1996**, *37*, 437-444.

179. Bischoff, C. A.; Walden, P.; *Chem. Ber.* **1893**, *26*, 262-264.

180. Schollkopf, V. U.; Hartwig, W.; Sprotte., U.; *Angew. Chem* **1979**, 91.

181. Kricheldorf, H. R.; Weegenschulz, B.; *J. Polym. Sci. Pol. Chem.* **1995**, *33*, 2193-2201.

182. Albertsson, A. C.; Eklund, M.; *J. Polym. Sci. Pol. Chem.* **1994**, *32*, 265-279.

183. Deng, X. M.; Zhu, Z. X.; Xiong, C. D.; Zhang, L. L.; *J. Appl. Polym. Sci.* **1997**, *64*, 1295-1299.

184. Kricheldorf, H. R.; Lee, S. R.; *Macromolecules* **1996**, *29*, 8689-8695.

185. Kasperczyk, J.; Bero, M.; *Makromol. Chem.-Macro. Chem. Phys.* **1993**, *194*, 913-925.

186. Hall, H. K.; Schneider, A. K.; *J. Am. Chem. Soc.* **1958**, *80*, 6409-6412.

187. Thakur, K. A. M.; Kean, R. T.; Hall, E. S.; Kolstad, J. J.; Munson, E. J.; *Macromolecules* **1998**, *31*, 1487-1494.

188. Kasperczyk, J. E.; *Macromolecules* **1995**, *28*, 3937-3939.

189. Liu, G.; Fang, Y. E.; Shi, T. Y.; *Chem. J. Chin. Univ.-Chin.* **1997**, *18*, 486-488.

190. Huang, J.; Lisowski, M. S.; Runt, J.; Hall, E. S.; Kean, R. T.; Buehler, N.; Lin, J. S.; *Macromolecules* **1998**, *31*, 2593-2599.

191. Thakur, K. A. M.; Kean, R. T.; Zell, M. T.; Padden, B. E.; Munson, E. J.; *Chem. Commun.* **1998**, 1913-1914.

192. Zell, M. T.; Padden, B. E.; Paterick, A. J.; Hillmyer, M. A.; Munson, E. J.; Thakur, K. A. M.; Kean, R. T.; *Abstr. Pap. Am. Chem. Soc.* **1998**, *215*, U310-U310.

193. Thakur, K. A. M.; Kean, R. T.; Hall, E. S.; Doscotch, M. A.; Munson, E. J.; *Anal. Chem.* **1997**, *69*, 4303-4309.

194. Thakur, K. A. M.; Kean, R. T.; Zupfer, J. M.; Buehler, N. U.; Doscotch, M. A.; Munson, E. J.; *Macromolecules* **1996**, *29*, 8844-8851.

195. Weidinger, A.; Hermans, P. H.; *Makromol. Chem.* **1961**, *44-46*, 24.

196. Weidinger, A.; Hermans, P. H.; *Makromol. Chem.* **1961**, *50*, 98.

197. Weidinger, A.; Hermans, P. H.; *Makromol. Chem.* **1962**, *52*, 169.

198. Takayama, Y.; *Bull. Chem. Soc. Jpn.* **1933**, *8*, 173-176.

199. Schmidt, E.; Sachtleben, R.; *Justus Liebigs Ann. Chem.* **1878**, *193*, 112.

200. Adamson A. G., *Physical Chemistry of Surfaces*; Fifth ed.; John Wiley & Son:, 1990. 28-30.